THE UNIVERSITY *of* EDINBURGH

Potassium channel expression and function in the N9 murine microglial cell line

Geng Pan B.Sc, M.Sc

Thesis Presented for the Degree of Doctor of Philosophy

The University of Edinburgh

August 2012

Declaration

The composition of the work and this thesis is my own. The work presented here has not been submitted for any other degree or professional qualification

Geng Pan

August 2012

Acknowledgements

I'd like to thank my supervisor Mike for all his guidance and advice throughout my four year PhD and thesis write-up. I also would like to thank Heather, Lie Chen for their support on molecular biology. Finally I'd like to thank Lijun Tian for her support on electrophysiology and her kindly facilitation on my live in Edinburgh.

Abstract

Microglia are immunocompetent cells in the central nervous system that have many similarities with macrophages of peripheral tissues. Their activation protects local cells from foreign microbial infection in the CNS. However, “over-activated“ microglia become a “Double-edged sword” which show neuronal toxicity and are implicated in a variety of neurodegenerative diseases. Previous studies have suggested that potassium channels play a role in regulating microglial activation, migration and proliferation. However what kinds of potassium channel subunits are expressed in microglia, whether their expression changes after microglial activation and the functional role of most potassium channels expressed in microglia are still not fully characterized.

To address these questions, we used the N9 mouse microglial cell line as a cell model for experiments *in vitro*. We first optimized the cell culture and lipopolysaccharide (LPS), the endotoxin of gram-negative bacteria, mediated stimulation of microglial activation that results in subsequent nitric oxide (NO) release. Using qRT-PCR, we analyzed mRNA expression of >80 potassium channel pore-forming subunits and their regulatory subunits in both LPS-treated (1μg/ml, 24hr) and untreated microglia. The subunits which displayed the highest mRNA expression in resting N9 cells included Kcnma1 ($K_{Ca}1.1$), Kcnk6 ($K_{2p}6.1$), Kcnc3 ($K_v3.3$) and Abcc8 (SUR1). In addition, N9 cells also expressed the mRNAs for other channel subunits previously reported in microglia such as Kcnn4 ($K_{Ca}3.1$), Kcna3 ($K_v1.3$) and Kcna5 ($K_v1.5$) subunits. Of these channel subunits LPS had no significant effect on mRNA expression except for Kcnk6 which was significantly reduced.

We then examined whether pharmacological manipulation of these channels controlled LPS-induced NO release. It was found out that the $K_{Ca}3.1$ selective blocker Tram34 and the $K_v1.5$ inhibitor propafenone (PPF) significantly decreased LPS-induced NO in agreement with data in primary microglia. Ba^{2+} that inhibits

inwardly rectifying potassium channels as well as $K_{2p}6.1$ also significantly attenuated LPS-induced microglial activation. Inhibition or activation of $K_{Ca}1.1$ channels by paxilline and NS1619 respectively had no significant effect. However, paxilline significantly attenuated the effect of Tram34, PPF and Ba^{2+} to control LPS-induced NO release while NS1619 significantly facilitated the effect of Tram34 and PPF.

To investigate the major ionic currents expressed in N9 microglia with and without LPS application, we examined whole-cell ionic currents using the patch-clamp technique. Resting N9 cells display a small outward current at positive potentials but a large inwardly rectifying component at negative potentials in physiological potassium gradients. The outward current was dramatically increased by LPS application that was dependent upon the intracellular free calcium concentration. Paxilline or Tram34 was then applied to acutely block this apparent outward K_{Ca} current. The result indicated that the LPS triggered K_{Ca} current was mainly paxilline sensitive supporting a role for an LPS-induced increase in $K_{Ca}1.1$ channel current. In addition, by using current clamp the mean resting membrane potential of N9 cells was -50.6±6.6mV (N=7) determined in the presence of 1μM $[Ca^{2+}]_i$ and -59.4±8.5mV (N=10) with 10nM $[Ca^{2+}]_i$. N9 cells did not display any spontaneous action potentials and the resting membrane potential was not significantly affected by LPS.

To conclude, the work presented in this thesis extends the current knowledge regarding potassium channel mRNA expression in microglia and their function in microglial NO release. What is more, it was found that $K_{Ca}1.1$ current expression was increased in LPS-activated N9 cells and revealed $K_{Ca}1.1$ channels as a modulator of NO release by activated microglia.

Table of contents

List of Figures

Chapter 5

List of Tables

Abbreviations

$[Ca^{2+}]_i$	intracellular Ca^{2+} concentration
4-AP	4-aminopyridine
β-MET	β-mercaptoethanol
Aβ	amyloid beta
ACM	astrocyte conditioned medium
AD	Alzheimer's disease
AgTX-2	agitoxin-2
AO	antisense oligonucleotides
AP-1	activator protein 1
ATP	adenosine triphosphate
Ba^{2+}	barium
BBB	blood brain barrier
BECF	brain extracellular fluid
BK	large conductance Ca^{2+}-sensitive and voltage-activated K^+ channels
cAMP	cyclic adenosine monophosphate
CaMKII	Ca^{2+}/calmodulin-dependent protein kinase II
Ca^{2+}	calcium
CD	cluster of differentiation molecule
Cl^-	chloride
CNS	central nervous system
CO_2	carbon dioxide
CREB	cAMP response element-binding protein
CSF	cerebrospinal fluid
CSF1R	colony stimulating factor 1 receptor
DA	dopamine

DAMPs	damage associated molecular patterns
DEPC	diethylpyrocarbonate
DMEM	Dulbecco's Modified Eagle Medium
DMSO	dimethyl sulfoxide
E	embryonic day
E. coli	*Escherichia coli*
EAE	experimental autoimmune encephalomyelitis
EC_{50}	half maximal effective concentration
EGF	epidermal growth factor
Elk1	ETS-like transcription factor 1
EMR1	EGF-like module-containing mucin-like hormone receptor-like 1
eNOS	neuronal NOS
ER	endoplasmic reticulum
ERK	extracellular-signal-regulated kinase
FAD	flavin adenine dinucleotide
FasL	Fas ligand
FcR	Fc receptor
FCS	fetal calf serum
GABA	γ-aminobutyric acid
GBC	glibenclamide
GFAP	glial fibrillary acidic protein
GIRKs	G protein-coupled inwardly-rectifying K^+ channels
GLX	glutamine
GTPγS	guanosine 5'-O-(3-thiotriphosphate)
H^+	proton
HBSS	Hanks balanced salt solution
HERG	human ether-a-go-go-related gene
HGNC	HUGO Gene Nomenclature Committee

HIF-1α	hypoxia inducible factor 1alfa
HSCs	hematopoietic stem cells
IC_{50}	half-maximal inhibition concentration
IDO	indoleamine 2,3-dioxygenase
IFN-γ	interferon gama
IK	intermediate conductance Ca^{2+}-activated K^+ channels
IKKs	IκB kinases
IL	interleukin
IMDM	Iscove's modified Dulbecco's medium
iNOS	inducible nitric oxide synthase
$InsP_3$	inositol trisphosphate
IRF	interferon regulatory factor
IUPHAR	international Union of Pharmacology
JNKs	c-Jun N-terminal kinases
K^+	potassium
K_{2p}	tandem pore domain K^+ channel
K_{ATP}	ATP-sensitive K^+ channel
K_{Ca}	calcium-activated K^+ channel
KDO	keto-deoxyoctulosonate
K_{DR}	delayed outward rectifying K^+ channels
K_{ir}	inwardly rectifying K^+ channel
K_v	voltage-gated K^+ channel
LBP	LPS-binding protein
LPC	lysophosphatidylcholine
LPS	lipopolysaccharide
MAPKs	mitogen-activated protein kinases
MCP-1	monocyte chemotactic protein-1
MD2	lymphocyte antigen 96

MEM	minimum essential media
MgTX	margatoxin
MHC	major histocompatibility complex
MMP	matrix metalloproteinase
MS	multiple sclerosis
MTS	[3-(4,5-dimethylthiazol-2-yl)-5-(3-carboxymethoxyphenyl)-2-(4-sulfophenyl)-2H-tetrazolium
MyD88	myeloid differentiation primary response gene 88
n	the number of replicate
N	the number of individual experiment
Na^+	sodium
NADP+	nicotinamide adenine dinucleotide phosphate
NCX	Na^+/Ca^{2+} exchanger
NED	N-1-napthylethylenediamine dihydrochloride
NFκB	nuclear factor kappa-light-chain-enhancer of activated B cells
NK cells	Natural killer cells
NMDAR	N-methyl D-aspartate receptor
nNOS	endothelial NOS
NO	nitric oxide
NO_2^-	nitrite
NO_3^-	nitrate
NOS	NO synthase
O_2	oxygen
O_2^-	superoxide anion
P	postnatal day
PAMPs	pathogen-associated molecular patterns
PCR	polymerase chain reaction
PD	Parkinson's disease

PEN	penicillin
PKA	protein kinase A
PKC	protein kinase C
PMA	phorbol 12-myristate 13-acetate
PNS	peripheral nervous system
PPF	propafenone
PRRs	pattern recognition receptors
PTX	pertussis toxin
qRT	quantitative reverse transcription
RCK 2	regulator of conductance for K^+ 2
RNS	reactive nitrogen species
ROS	reactive oxygen species
RPMI	Roswell Park Memorial Institute medium
SK	small conductance Ca^{2+}-activated K^+ channels
SOD	superoxide dismutase
STREP	streptomycin
SUR	sulfonylurea receptor
TEA	tetraethylammonium
TGFβ	transforming growth factor beta
TIRAP	TIR domain-containing adaptor protein
TLR	Toll-like receptor
TNFα	tumor necrosis factor alfa
TRAM	TRIF-related adaptor molecule
Tram34	triarylmethane34
TRIF	TIR domain-containing adaptor
TRP	transient receptor potential channel

CHAPTER ONE

Introduction

1.1 The central nervous system

The nervous system is composed of the peripheral nervous system (PNS) and the central nervous system (CNS). The CNS is of ectodermal origin and it exists in all bilateral animals. It consists of the brain and the spinal cord which are covered by meninges and contained in the dorsal cavity (Maton, 1993). CNS receives signals from the body and sends out major commands to control animal behavior. However, neurons are not the main cell type in the CNS (Allen & Barres, 2009; Azevedo *et al.*, 2009; Hawkins & Olszewski, 1957; Pfrieger & Barres, 1995). In the human brain, there are about 86.1±8.1 billion neurons (Azevedo *et al.*, 2009) and the remainder are 84.6±9.8 billion nonneuronal cells described in the following paragraphs. The number of neurons or nonneuronal cells is location-dependent. There is about 69.0±6.7 billion neurons and about 16.0±2.2 billion nonneuronal cells in the cerebellum while about 16.3±2.2 billion neurons and about 60.8±7.0 billion nonneuronal cells in the cerebral cortex (including white matter and grey matter). In the rest of the brain (including basal ganglia, diencephalon, mesencephalon and pons) there are 0.7±0.1 billion neurons and 7.7±1.5 billion nonneuronal cells (Azevedo *et al.*, 2009).

1.1.1 Neuroglia

There are several types of nonneuronal cells which regulate the chemical environment or give physical support to neurons. These cells are called neuroglia, or glia in short (Hawkins & Olszewski, 1957; Pfrieger & Barres, 1995). Neuroglia are classified into two types, microglia and macroglia. Macroglia are composed of astrocytes (CNS), oligodendrocytes (CNS), ependymal cells (CNS), radial glia (CNS), Schwann cells (PNS), satellite cells (PNS) and enteric glial cells (PNS) (Table 1-1). Each of them have specific functions in either the CNS or the PNS. In different animals, the ratio between neurons and neuroglia in the brain is associated with the size of the brain (Allen & Barres, 2009). For example, there are 25%

	Subfamily	Cell names	Location	Function
Glia	Macroglia	Astrocytes	CNS	regulate chemical environment of neurons
		Oligodendrocytes		form myelin sheath
		Ependymal cells		form walls of ventricles and secrete cerebrospinal fluid
		Radial glia		neuronal progenitors and the scaffold for newborn neurons to migrate
		Schwann cells	PNS	form myelination in PNS
		Satellite cells		regulate chemical environment in PNS
		Enteric glial cells		play roles in digestive processes
	Microglia		CNS	immune cells in CNS

Table 1-1. Members of glial family and their general functions. Glia include two groups: macroglia and microglia. There are totally eight types of cells in either CNS or PNS. CNS: central nervous system; PNS: peripheral nervous system.

neuroglia in the fruit fly brain, 65% neuroglia in the mouse brain and 97% neuroglia in the elephant brain (Allen & Barres, 2009). For the human brain, it is not less than 50% (Azevedo *et al.*, 2009; Allen & Barres, 2009). In the human cerebral cortex, the neuroglia are composed of 75.6% oligodendrocytes, 17.3% astrocytes and 6.5% microglia (Pelvig *et al.*, 2008). However, compared to other primates, the human brain is considered unique (Jerison, 1973; Marino, 1998) as other primates have less neuroglia in the brain (Doetsch, 2003; Nishiyama *et al.*, 2005; Ullian *et al.*, 2001).

1.1.1.1 Astrocytes

Astrocytes are star shaped cells in the CNS. The identification of astrocytes is often approached by staining for glial fibrillary acidic protein (GFAP). GFAP is expressed almost exclusively by astrocytes and it is commonly used *in vitro* for glial cell identification (Conrad *et al.*, 2009; Jiang *et al.*, 2008; Paintlia *et al.*, 2008; Calderón-Garcidueñas *et al.*, 2009). However, it was pointed out that GFAP is also expressed by other glial cells like ependymal cells (Roessmann *et al.*, 1980) and radial glial cells (Shapiro *et al.*, 2005; Middeldorp *et al.*, 2010) in the CNS. Astrocytes provide structural support to the neurons with their processes enveloping synapses. Previous consideration was that astrocytes only offer physical support to neurons in the CNS. However, astrocytes are actually very important in maintaining the environment of the CNS as they play roles in secretion of nutrients for neurons, the promotion of myelination and forming of the glial scar during injury of the CNS. Recent discoveries indicate that astrocytes communicate with neurons by secreting glutamate (Santello & Volterra, 2009; Fiacco *et al.*, 2009) and adenosine triphosphate (ATP) (Santello & Volterra, 2009). The release of neurotransmitter by astrocytes is calcium (Ca^{2+})-dependent (Santello & Volterra, 2009) except for astrocytes in the hippocampus (Agulhon *et al.*, 2010). Another mechanism that astrocytes regulate is the uptake of neural transmitters (Tan *et al.*, 1997; Chatton *et al.*, 2003) and potassium (K^+) in the CNS as astrocytes express K^+ channels and transporters for several neurotransmitters (Kettenmann & Ransom, 2005), such as ATP, γ-

aminobutyric acid (GABA) and glutamate on the membrane. In addition, astrocytes also propagate intracellular Ca^{2+} for a long distance (Ca^{2+} wave) (Newman, 2001) in response to stimulation of the presynaptic cell, the postsynaptic cell and the astrocytes at the site of synapses (Araque *et al.*, 1999). The Ca^{2+} wave generated in astrocytes may transfer to neighbouring neurons through gap junction channels during the developing but not mature CNS (Scemes & Giaume, 2006). Ca^{2+} wave induced gliotransmitter release and regulate the activity of synapse (Fellin & Carmignoto, 2004; Haydon, 2001; Volterra & Meldolesi, 2005). Besides communication between astrocytes and neurons, the processes of astrocytes are also connected to the endothelial cells at the blood brain barrier (BBB) and blood vessels. Astrocytes are important for maintaining the BBB and regulating neurovascular coupling in the brain (Haydon & Carmignoto, 2006; Parri & Crunelli, 2003).

1.1.1.2 Oligodendrocyte

In some vertebrates, the main function of oligodendrocytes is the formation of the myelin sheath and this process is called myelination. Because neurons propagate electrical signals along axons, the myelin sheath can offer insulation of axons. It prevents ion leakage and increases the propagation speed due to the nodes of Ranvier between different myelin sheath (Baumann & Pham-Dinh, 2001). Every oligodendrocyte can provide myelin sheath to about 50 axons. This is different from the Schwann cells which form the myelin sheath in the PNS as each Schwann cell can only envelope one axon. In addition, there is another kind of oligodendrocyte called satellite oligodendrocytes that do not form a sheath but regulate the neural environment (Baumann & Pham-Dinh, 2001).

1.1.1.3 Ependymal cells and radial glia

Ependymal cells are a kind of neuroglia and cuboidal shaped cells which form the ependyma lining along the wall of ventricles in the CNS. Ependyma together with capillaries constitute the choroid plexus which filters the blood to produce cerebrospinal fluid (CSF) for the ventricles. Cilia on the apical surfaces of ependymal cells facilitate the flow of the CSF. What is more, with their microvilli on the membrane surface ependymal cells can also absorb CSF. Radial glial cells play a pivotal role during the development of the CNS. They are precursors for neurons, and they also regulate the migration of neurons (Noctor *et al.*, 2001; Campbell & Götz, 2002; Merkle *et al.*, 2004). In the mature brain, they exist in the cerebellum and retina maintaining synapses and facilitate the signal transduction of neurons.

1.1.1.4 Microglia

Microglia are macrophage-like immune cells in the CNS which protect the CNS from infection and regulate the neuronal environment. The detail of microglia is introduced in Chapter 1.2.

1.1.2 The blood brain barrier

The CNS is isolated from the blood circulation by the BBB which protects neurons and neuroglia by preventing large size molecules, including peptides, to enter into the CNS. The BBB was first observed by Paul Ehrlich and his student Edwin Goldmann. When they tried to stain organs of animals, they observed a compartmentalization between the brain and the rest of the body which prevented dyes to pass through. The compartmentalization was in fact the BBB. Later in 1921, the concept of the BBB was formally introduced by Lina Stern. The BBB is formed by the tight junctions of endothelial cells along the capillaries. The layer of

endothelial cells is covered by the basement membrane and connected by the end-feet of astrocytes. In this case, the BBB separates the brain extracellular fluid (BECF) of the CNS from the the blood circulation. Due the existence of the BBB, it is not easy for external microbes such as bacteria, large molecules and hydrophilic molecules to get into the CNS, but not for the smaller hydrophobic molecules like oxygen (O_2), carbon dioxide (CO_2) and small peptides (Kastin *et al.*, 1999; Banks & Kastin, 1996), which can pass through the BBB. Endothelial cells can form such tight junction because they express proteins which bind as dimers expressed by another endothelial cell, for example claudins (Furuse *et al.*, 1998), occludin (Furuse *et al.*, 1993) and junctional adhesion molecule (Martìn-Padura *et al.*, 1998). A healthy BBB is required for preventing bacterial infections. However, during pathological conditions, like meningitis, which can be caused by lipopolysaccharide (LPS) (Beam & Allen, 1977), the BBB becomes more permeable as the junction becomes less tight when exposed to molecules like tumor necrosis factor alfa (TNFα), interleukin (IL)-1β, interferon gamma (IFN-γ), or LPS. This allows bacteria, viruses and phagocytes in the PNS to pass through. For example during the CNS disease experimental autoimmune encephalomyelitis (EAE), the circulating monocytes are sometimes observed crossing the BBB (Mildner *et al.*, 2009; King *et al.*, 2009).

1.2 Microglia

1.2.1 History of microglia

Microglia were first stained together with other CNS cells in 1880s by Franz Nissl using Nissl staining. The concept of microglia was formally developed by Pio del Rio-Hortega in the seminal work "*Section X - Microglia*" of the book "*Cytology and Cellular Pathology of the Nervous System*" in 1932 before which other synonyms of microglia were used, for example mesoglia (microglia & oligodendrocyte) (Rezaie & Male, 2002) or Hortegaglia. Later, after the "Second World War" the term microglia was accepted and confirmed in "*Neuroglia Morphology and Function*" by Paul Glees 1955 and the book "*Biology of Neuroglia*" by William Frederick Windle in 1958 (Kettenmann *et al.*, 2011). Most of the properties and concepts of microglia postulated by Pio del Rio-Hortega in the beginning of the 20th century are still agreed by scientists nowadays (Kettenmann *et al.*, 2011). For example, microglia originate from the mesoderm and display amoeboid morphology during development. Under resting conditions, microglia present a typical ramified morphology. Under pathological conditions, microglia transform into an amoeboid morphology and display phagocytosis and antigen presenting abilities.

1.2.2 Origin of microglia

During embryonic development, most macroglia cells are derived from ectoderm. The origin of microglia had been a debate for a long time until the most accepted consensus that microglia, during development, are derived from hematopoietic stem cells (HSCs) in the bone marrow (Vitry *et al.*, 2003; Eglitis & Mezey, 1997) which is of mesodermal origin (Hatai, 1902; Chan *et al.*, 2007; Kaur *et al.*, 2001; Boya *et al.*, 1979). HSCs are located in the bone marrow and are the source of all types of blood cells. During proliferation, HSCs are able to self-renew and derive into two kinds of progenitor cells: common myeloid progenitor cells and common lymphoid

progenitor cells. The common lymphoid progenitor cells further differentiate into lymphocytes including natural killer (NK) cells, B lymphocytes and T lymphocytes (Zech, 2004) while the common myeloid progenitor cells differentiate into basophils, neutrophils, eosinophils, monocytes/macrophages, platelets, red blood cells and mast cells (Figure 1-1) (Zech, 2004). Here, the basophils, neutrophils and eosinophils are granulocytes while B cells, T cells and monocytes/macrophages are agranulocytes.

1.2.2.1 Relationship between microglia and macrophages

Microglia are one of the special members of leukocytes which are permanently resident in the CNS. Besides microglia (CNS), other location specific members include langerhans cells (epidermis), osteoclasts (bone) and kuppfer cells (liver). All of these cell types arise from monocyte/macrophage migration. The view that microglia originated from bone marrow derived cells was first published in 1988 (Hickey & Kimura, 1988; Eglitis & Mezey, 1997; Priller *et al.*, 2001; Block *et al.*, 2007; Ritter *et al.*, 2006). Several pieces of evidence show that microglia have a close relationship to macrophages. Both microglia and macrophages share a number of markers, for example cluster of differentiation molecule (CD)11b (Tanaka *et al.*, 2003), CD14, EGF-like module-containing mucin-like hormone receptor-like 1 (EMR1) and colony stimulating factor 1 receptor (CSF1R) (Beers *et al.*, 2006; Saijo & Glass, 2011; Kettenmann *et al.*, 2011). They also express similar ion channels like K^+, sodium (Na^+), proton (H^+), Ca^{2+} and chloride (Cl^-) channels on the plasma membrane (Färber & Kettenmann, 2005; Eder, 2005). In addition, the differentiation factor of lymphoid and myeloid cells, PU.1, is required for the generation of microglia (Beers *et al.*, 2006) and bone marrow transplants into $PU.1^{-/-}$ mice results in the recovery of microglial expression (Beers *et al.*, 2006). By using genome-wide microarray analysis on different primary hematopoietic cell lineages and microglia from wild type mice, microglia were discovered to have a close relationship with bone marrow derived and thioglycollate elicited macrophages (Figure 1-2) (Saijo & Glass, 2011). However, in the immune system, macrophages belong to the innate

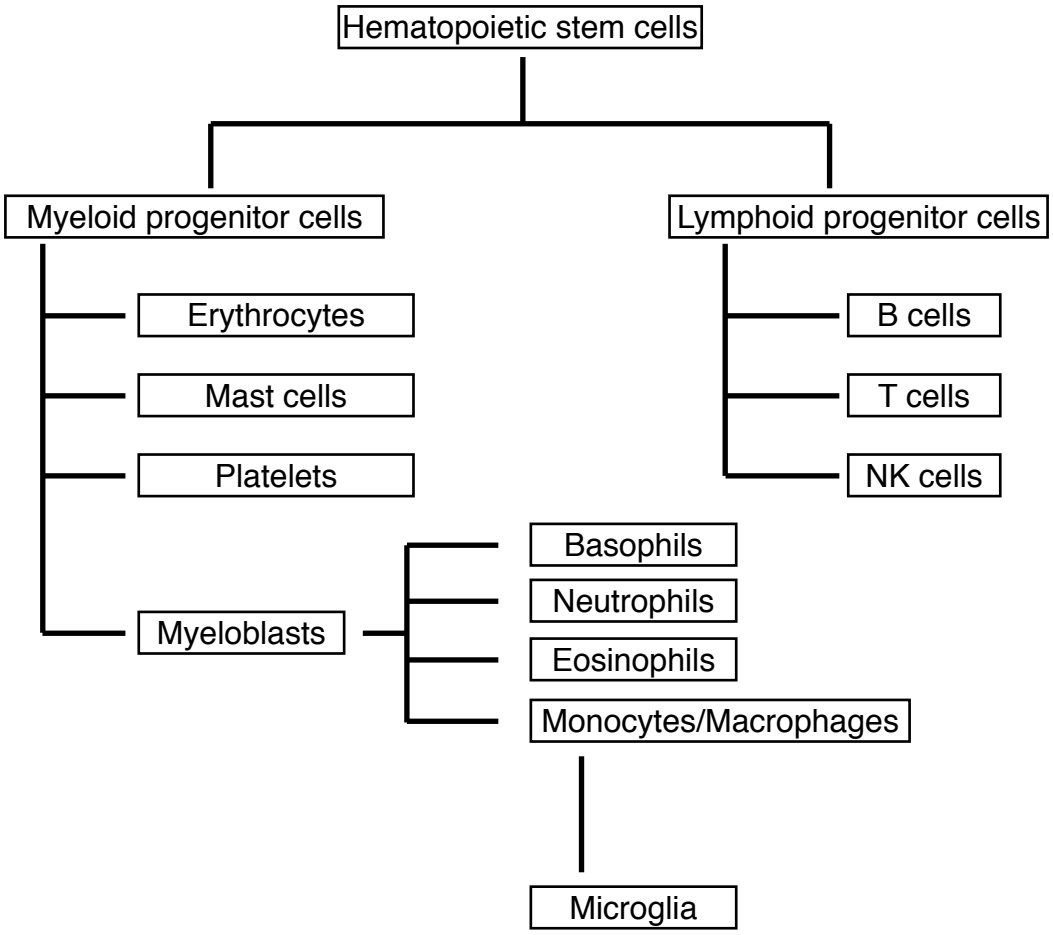

Figure 1-1. Origin of microglia during haematopoiesis. The diagram displays the differentiation of blood cell from hematopoietic stem cells. During development, monocytes/macrophages migrate into the CNS and differentiate into microglia. NK cells: natural killer cells.

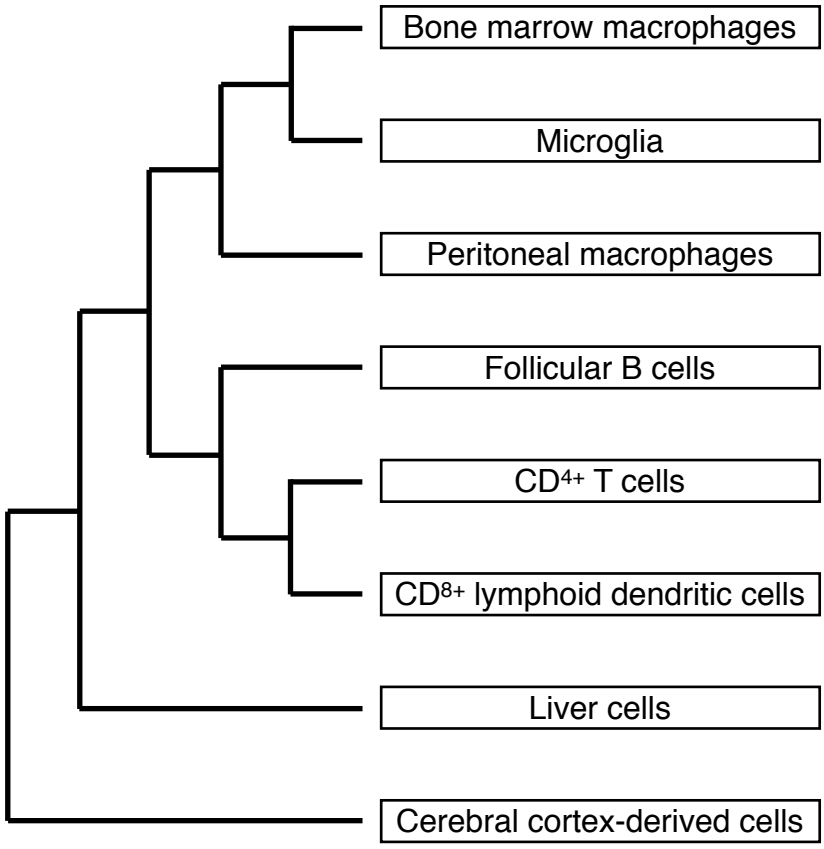

Figure 1-2. Relationship between microglia and other cells. Genome-wide microarray analysis of primary cells isolated from C57BL/6 mice revealed that microglia displayed a close gene expression pattern to bone marrow macrophages. Figure is adapted from (Saijo & Glass, 2011). The microarray data cluster analysis were from BioGPS data set of the Genomics Institute of the Novartis Research Foundation.

immune system while microglia belong to both the innate and adaptive immune systems.

1.2.2.2 Origin of fetal and adult microglia is controversial

The origins of microglia in the CNS remains controversial. The previous observation indicated that the peripheral macrophages and microglia were observed at embryonic day (E)9.5 in the fetal yolk sac of mouse (Ginhoux *et al.*, 2010; Saijo & Glass, 2011). The macrophage progenitors begin to migrate into the CNS between E8.5 to E9.5 through the embryo vascular system, and microglial migration into the CNS was observed at E10.5 (Saijo & Glass, 2011; Ginhoux *et al.*, 2010). However, during the postnatal period microglial homeostasis was not significantly regulated by peripheral hematopoietic derived cells (Ginhoux *et al.*, 2010). During development, in the healthy mature brain, hematopoietic cells from bone marrow are able to cross the BBB and then these cells contribute to the microglial and other glial transformations (Eglitis & Mezey, 1997; Priller *et al.*, 2001; Hickey & Kimura, 1988). Under pathological conditions of mature brain, like ischemia and Alzheimer's Disease (AD), bone marrow derived microglia/macrophages were observed migrating into the CNS, and this process was facilitated by brain irradiation (Tanaka *et al.*, 2003; Mildner *et al.*, 2011). In addition, under ischemic conditions, myeloid progenitors transform into microglia by migrating into the retina through the blood system (Ritter *et al.*, 2006). However, recent reports based on parabiosis experiments indicated that in adult brain during neurodegenerative diseases, the population of microglia are mainly increased by self-renewal (Ransohoff, 2007; Ajami *et al.*, 2007; Mildner *et al.*, 2007).

1.2.3 Types of microglia

Microglia are categorized into seven types: amoeboid microglia, ramified microglia, activated non-phagocytic microglia, activated phagocytic microglia, gitter cells, perivascular and juxtavascular. These types are classified due to either microglial morphology, microglial location or microglial activation status (Figure 1-3).

1.2.3.1 Amoeboid microglia

Amoeboid microglia are considered precursors of mature microglia (Penfield, 1965; Imamoto & Leblond, 1978; Tseng *et al.*, 1983). They exist during the development of the CNS which was first described by Del Rio-Hortega (Penfield, 1965). They can be selectively stained by the silver carbonate method compared to other types of neuroglia. Amoeboid microglia present a large soma which is either a round or flattened shape with short processes. In rats, amoeboid microglia can be found in the forebrain from E11 (Ashwell, 1991). From E13 to E17 amoeboid microglia concentrate at the site of the diencephalic vesicle and the telencephalic vesicle. From E15 amoeboid microglia locate at the site of the future hippocampus until the development of the corpus callosum which happens after E19 (Ashwell, 1991). This kind of microglia display the mobility and phagocytosis, but they do not have antigen presenting and other inflammatory abilities which are properties of activated microglia (Gehrmann *et al.*, 1995; Christensen *et al.*, 2006; Ferrer *et al.*, 1990).

1.2.3.2 Ramified microglia

Ramified microglia, also called “resting microglia”, are microglia in the quiescent state. They mainly localize throughout the healthy CNS in the absence of infection or cellular death (Christensen *et al.*, 2006; Aloisi, 2001). Microglia constitute about 5%~15% of the rodent brain. In the adult mouse brain, the estimated number of

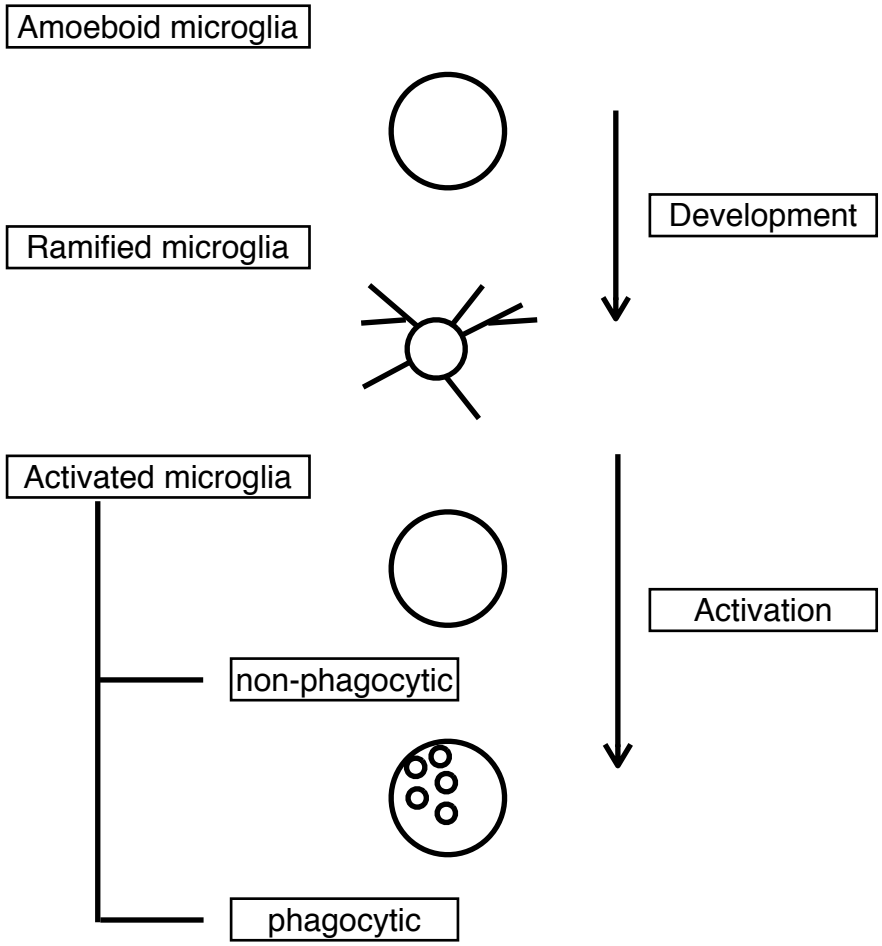

Figure 1-3. The morphology of different types of microglia. The figure illustrates microglia cell of types: amoeboid microglia, ramified, activated microglia (phagocytic and non-phagocytic microglia). Amoeboid microglia display mobility, phagocytosis but no antigen presenting and other inflammatory abilities. Ramified microglia display several primary processes without having phagocytosis, antigen presenting or inflammatory abilities. Activated microglia have the ability of antigen presenting, pro-inflammatory cytokines release.They first transform into a non-phagocytic type after which they transform into phagocytic microglia with intracellular phagosomes. Figure was adapted from (Kreutzberg, 1996). In addition, microglia have three more special types. Gitter cells: microglia reached limit amount of phagocytosis. Perivascular: microglia specifically inside the basement membrane under the endothelium. Juxtavascular: microglia connecting to the basement membrane on the endothelium.

microglia is 3.5×10^6 (Lawson *et al.*, 1990) and the density varies over five fold depending on brain region (Lawson *et al.*, 1990). Microglia mainly concentrate in the hippocampal region, the substantia nigra, the basal ganglia and the olfactory telencephalon of both rodent (Lawson *et al.*, 1990) and adult human (Block *et al.*, 2007). In contrast, the cerebellum, fibre tracts and brainstem have low density of microglia (Lawson *et al.*, 1990).

Resting microglial morphology has been investigated *in vitro* using isolated primary rat microglia and N9 murine microglial cell line (Xiang *et al.*, 2006). Microglia in *in vitro* culture display a small and round soma whose diameter is about 20~50μm with zero to five primary processes and these processes can further branch up to 6 times (Xiang *et al.*, 2006). Microglia begin to form their processes 30min after plating (Xiang *et al.*, 2006) and their length reaches a plateau after 24~48hr (Xiang *et al.*, 2006) and can reach to 150μm in length and 0.2~1.5μm in diameter. Between 16~24hr, N9 microglia form a network of processes (Xiang *et al.*, 2006). There is no difference in length of processes between N9 microglia and cultured rat microglia under the same culture period. Using dye coupling assays (Lucifer Yellow injection) there appeared to be no direct communication between microglia through their processes (Xiang *et al.*, 2006).

Ramified microglia do not display either phagocytosis, inflammation or antigen presenting abilities (Gehrmann *et al.*, 1995), but that actually does not mean they are dormant in the brain. Although their cell bodies are not motive their long branching processes are randomly and constantly scanning the microenvironment for any physiological changes (Hanisch & Kettenmann, 2007). The normal role of ramified microglia is to detect and prepare rapid responses to external invading infection or neuronal cell death (Hanisch & Kettenmann, 2007). Microglia achieve this sensitivity through a variety of ions channels, neurotransmitter receptors, chemokine receptors, pattern recognition receptors (PRRs) and purinoreceptors (Kettenmann *et al.*, 2011; Hanisch & Kettenmann, 2007).

1.2.3.3 Activated microglia

One pivotal property of microglia is that they are highly plastic and possess many structural changes associated with the status of their activation (Xiang *et al.*, 2006). Under pathological conditions, resting microglia can be rapidly activated and undergo morphological change (Aloisi, 2001). Compared to resting microglia activated microglia display a higher proliferation rate (Streit *et al.*, 1999), more mobility, inflammatory and antigen presenting abilities. Activated microglia release reactive nitrogen species (RNS), reactive oxygen species (ROS), pro-inflammatory cytokines like TNFα, transforming growth factor beta (TGFβ), IL-1, IL-6 and chemokines like monocyte chemotactic protein-1 (MCP-1). They also present cytokine receptors and major histocompatibility complex (MHC) proteins on the membrane.

Microglial activation involves two steps. They first become non-phagocytic microglia which represent a transitive status before become fully activated into phagocytic microglia (Figure 1-3) (Gehrmann *et al.*, 1995; Kreutzberg, 1996) which can be induced by conditions like cell death or neuronal terminal degeneration. The morphology between activated microglia and amoeboid microglia are similar except that fully activated phagocytic microglia display a larger round cell-body with phagosomes (Kreutzberg, 1996; Streit & Kreutzberg, 1988; Rieske *et al.*, 1989). The functional difference between non-phagocytic microglia and phagocytic microglia is indicated by their names. Phagocytic microglia are able to phagocytose external microbes while non-phagocytic microglia do not. There is also cooperation between activated microglia and other neuroglia, for example astrocytes cooperate with microglia in defending against external infection in the CNS (Gehrmann *et al.*, 1995; Aloisi, 2001).

1.2.3.4 Gitter cells, perivascular microglia and juxtavascular microglia

Besides the categorization by the activation status, there are three specific types of microglia which were categorized depending on their location or whether reaching the limit of phagocytosis. Gitter cells are a type of phagocytic microglia that have reached their limit amount of phagocytosis. Perivascular microglia are microglia specifically located inside the basement membrane under the endothelium, which facilitate the maintenance of the BBB. Juxtavascular microglia are microglia connecting to the basement membrane under the endothelium. Both perivascular and juxtavascular microglia express MHCII proteins which are required for antigen presentation. Different from all other types of microglia, perivascular microglia are regularly replaced by myeloid precursor cells (Gehrmann *et al.*, 1995).

1.2.3.5 Microglial cell lines used in *in vitro* studies

Studies on microglia *in vitro* use either isolated primary cells or immortalised cell lines. These two methods have their pros and cons. It is often considered that isolated primary microglia may represent more similar properties to microglia *in vivo* compared to cell line. However, microglial cell lines can avoid the difficulties of purifying primary microglia and offer large amount of cells. They also offer 100% purity of cells which is important for molecular approaches, like PCR. Among several microglial cell lines, BV-2 and N9 are the two most well characterized and commonly used murine microglial cell lines in the last dozen of years.

The N9 microglial cell line was derived from the brain of outbred ICR/CD1 mice (E13), using the v-myc oncogene of 3RV retrovirus (Righi *et al.*, 1989). The BV-2 microglial cell line was derived from newborn inbred C57BL/6 mice, using the J2 retrovirus containing the v-raf and v-myc oncogenes (Blasi *et al.*, 1990).

N9 microglial cells express similar membrane clusters to primary microglia such as Mac-1, Mac-2, vimentin, EMR1, Fc receptor (FcR) (Corradin *et al.*, 1993) and have been commonly applied in the investigation of microglial activation and microglial neurotoxicity (Zhang *et al.*, 2010). Similar to primary microglia, N9 cells respond to stimuli like IFN-γ, LPS or TNFα with nitric oxide (NO) release, chemokine release, activation of the nuclear factor kappa-light-chain-enhancer of activated B cells (NFκB) pathway, activation of the intracellular mitogen-activated protein kinases (MAPKs) family (Liu *et al.*, 2010; Zhao *et al.*, 2011; Chang *et al.*, 2008; Meng *et al.*, 2008; Wu *et al.*, 2007; Hou *et al.*, 2006; Bi *et al.*, 2005; Suuronen *et al.*, 2006; Nuutinen *et al.*, 2005; Suuronen *et al.*, 2003; Meda *et al.*, 1995; Bonaiuto *et al.*, 1997). In addition, N9 microglial phagocytosis is similar to primary microglia, including the phagocytosis of latex beads (Bruce-Keller *et al.*, 2001), *E. coli* bioparticles (Stefano *et al.*, 2009). BV-2 microglia show similar morphology and function to primary microglia such as the response to IFN-γ. This cell line also represents similar gene upregulation to primary microglia in response to LPS stimulation although normally the upregulation is less pronounced to primary microglia (Lund *et al.*, 2006). In addition, BV-2 cells were used in the *in vitro* electrophysiological investigations while little electrophysiological work was done using N9 cells. However, a recent investigation compared both primary microglia and immortalised cell lines from outbred ICR/CD1 mice (N9 cell line) and inbred C57Bl/6 mice (BV-2 cell line) in response to LPS stimulation. Under the same LPS stimulation, N9 or microglia from ICR/CD1 mice had a stronger response, including iNOS, than BV-2 and microglia from C57Bl/6 mice. This process was not due to expression change of toll-like receptor (TLR) 4/CD14 or proliferation change of cells but may be due to inbreeding depression (Nikodemova & Watters, 2011).

The use of immortalised cell lines provide a convenient way for studies *in vitro*. However, it is hard to conclude which cell line better than the other one as no evidence that either of them 100% represents the properties of microglia *in vivo*. Both of these cell lines were commonly used in the investigation of microglial NO

release, as little is known about the electrophysiological properties of N9 cell line while it is a well established model for investigations on LPS-induced NO release. N9 murine microglial cell line will be used in this thesis.

1.2.4 PAMPs and DAMPs

Microglia can be activated by multiple signals from either external infection or cell damage because microglia express PRRs on their membrane which recognize pathogen-associated molecular patterns (PAMPs) (Aloisi, 2001) and damage associated molecular patterns (DAMPs) (Gehrmann *et al.*, 1991; Morioka *et al.*, 1992). PAMPs are small molecules associated with pathogens (Medzhitov & Janeway, 2000) such as LPS. DAMPs are intracellular components released by damaged cells such as ATP (Ciccarelli *et al.*, 2001).

DAMPs- or PAMPs-induced activation can lead to different microglial responses. ATP is able to activate microglia (Xiang *et al.*, 2006; Inoue, 2002) through binding to purinoceptors (Bianco *et al.*, 2005; Xiang & Burnstock, 2005) like P_2Y (Honda *et al.*, 2001; Davalos *et al.*, 2005) or P_2X (Monif *et al.*, 2009) receptors. Microglia activated by ATP increased the intracellular concentration of Ca^{2+} (McLarnon *et al.*, 1999) and became amoeboid with retracted processes which become bulbs near the roots of the processes (Inoue, 2002). Longer treatment made the soma smaller, the processes shorter and bulbs larger until all the microglia finally floated in the supernatant. However the floating microglia were proven still alive since it was a reversible process after the ATP was removed (Xiang *et al.*, 2006). On the other hand, microglia activated by LPS underwent morphological change as well but did not float (Meng *et al.*, 2008; Wu *et al.*, 2007; Hou *et al.*, 2006; Bi *et al.*, 2005; Cavaliere *et al.*, 2005; Nuutinen *et al.*, 2005; Suuronen *et al.*, 2003; Chang *et al.*, 2008; Bianco *et al.*, 2005; McKimmie & Fazakerley, 2005).

Microglial receptors for PAMPs play a pivotal role in immune defence in the CNS. They are proteins on the membrane belonging to the innate immune system and their expression is increased in the activated microglia (Aloisi, 2001). The PRRs elevated in microglia for PAMPs include TLR2, TLR4, TLR9, CD14, the mannose receptor, FcR and complement receptors. TLR2 recognizes peptidoglycans and lipoteichoic acids of the gram-positive bacteria (Schwandner *et al.*, 1999; Yoshimura *et al.*, 1999; Block *et al.*, 2007). TLR4 and CD14 is specific for recognizing LPS (Horvath *et al.*, 2008; Poltorak *et al.*, 1998; Qureshi *et al.*, 1999; Wright *et al.*, 1990; Haziot *et al.*, 1996), and they are implicated in microglial activation in response to endotoxemia. TLR9 recognizes bacterial DNA (Hemmi *et al.*, 2000). Mannose receptor recognies pathogen-specific oligosaccharides (Linehan *et al.*, 2000). FcR (Aloisi, 2001) and complement receptors (Aloisi, 2001; Ehlers, 2000) recognise pathogens mediated by immunoglobulins or complement.

LPS, an endotoxin of gram-negative bacteria such as *Escherichia coli* (*E. coli*), is the prototypical member of PAMPs (Henderson *et al.*, 1996). It has been regularly used as a microglial activator *in vivo* and *in vitro* (Horvath *et al.*, 2008; Kaushal & Schlichter, 2008; Suuronen *et al.*, 2006; Suuronen *et al.*, 2005; Jianmin Zhang *et al.*, 2003; Khanna *et al.*, 2001; Fischer *et al.*, 1995; Nörenberg *et al.*, 1994; Corradin *et al.*, 1993). LPS exists on the outer membrane of bacteria (Rietschel *et al.*, 1994) and there is several nanograms of LPS in every million gram-negative bacteria (Troelstra *et al.*, 1999). LPS consists of O polysaccharide, core oligosaccharide, and lipid A (Figure 1-4) (Rietschel *et al.*, 1994). The lipid A plays a key role in activating microglia, but it is not exposed on *E. coli* (Sivagnanam *et al.*, 2010; Rietschel *et al.*, 1994) unless the bacterium is phagocytosed or lysed. Once LPS is fully exposed, it can stimulate microglial phagocytosis (Rietschel *et al.*, 1994) and stimulate release of pro-inflammatory cytokines, RNS, ROS or protease (Colton *et al.*, 1993). In addition, LPS also modulates the expression of ion channels including K^+ channels (Stock *et al.*, 2006). LPS is not directly toxic to neurons only when microglia are present as a result of the release of neurotoxic chemicals by microglia (Gibbons &

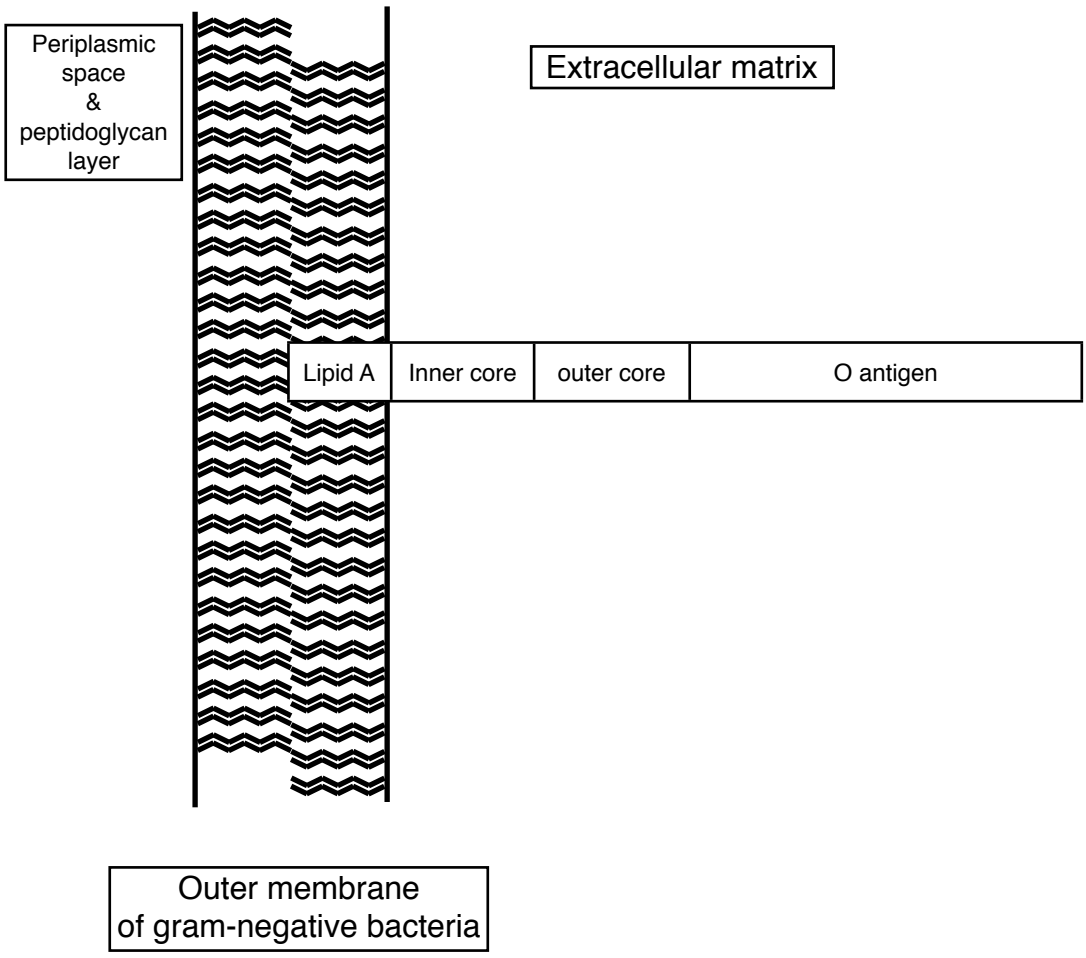

Figure 1-4. The structure of LPS. Lipopolysaccharide (LPS) is constituted of lipid A, core oligosaccharide (inner core/outer core) and O antigen (O polysaccharide). O antigen is the target of antibodies and it varies among different strains. LPS with full length O chains is smooth LPS, with reduction of O chains or no O chains is rough LPS. Bacteria with rough LPS display less tolerance to hydrophobic antibiotics (Tsujimoto *et al.*, 1999). The core oligosaccharide contains sugars, keto-deoxyoctulosonate (KDO) or other components like phosphate. Core oligosaccharide directly connects to the lipid A. Lipid A is toxic to the host cells.

Dragunow, 2006). Over-activated microglia rarely return to the ramified state unless they are treated with de-activating molecules (Block *et al.*, 2007), for example TGFβ, astrocytes conditioned medium (ACM), IL-10, IL-4 and IL-13.

To activate microglia, LPS binds to the TLR4 receptor (Poltorak *et al.*, 1998; Qureshi *et al.*, 1999) in association with CD14 (Wright *et al.*, 1990; Haziot *et al.*, 1996), lymphocyte antigen 96 (MD2) protein (Shimazu *et al.*, 1999) and LPS-binding protein (LBP) (Tobias *et al.*, 1989; Schumann *et al.*, 1990). The TLR4 signal is mediated by either myeloid differentiation primary response gene 88 (MyD88) or TIR domain-containing adaptor (TRIF) dependent pathways. The adaptors that link MyD88 or TRIF to TLR4 receptor are TIR domain-containing adaptor protein (TIRAP) and TRIF-related adaptor molecule (TRAM) separately. Both the MyD88-dependent and TRIF-dependent pathway stimulate the activation of NFκB and activator protein 1 (AP-1) through the activation of MAPKs and IκB kinases (IKKs) (Oh *et al.*, 2010; Lu *et al.*, 2008). Specifically the MyD88-dependent pathway regulates the activation of IκB and interferon regulatory factor (IRF)5 which regulate the expression of IL-6, TNFα, IL-12 (Yamamoto *et al.*, 2004) while the TRIF-dependent pathway regulates the activity of IRF3 (Lu *et al.*, 2008). Besides the activation of MAPKs and several transcription factors, the LPS-stimulated pathway also involves the activation of protein kinase C (PKC), protein kinase A (PKA), Ca^{2+}/ calmodulin-dependent protein kinase II (CaMKII) (Regenhard *et al.*, 2001) and calcineurin (Figure 1-5) (Suzuki *et al.*, 2007).

1.2.5 The release profile of microglia

Microglia regulate the CNS environment by releasing pro-inflammatory cytokines (Prinz & Hanisch, 1999; Suzumura *et al.*, 1998; Chen & Goeddel, 2002; Conti *et al.*, 1999; S. C. Lee *et al.*, 1993; Becher *et al.*, 1996), anti-inflammatory molecules (Kitamura *et al.*, 2000; Constam *et al.*, 1992; Hanisch *et al.*, 1997), chemokines (Aloisi, 2001; Hanisch, 2002), Fas ligand (FasL) (Spanaus *et al.*, 1998; White *et al.*,

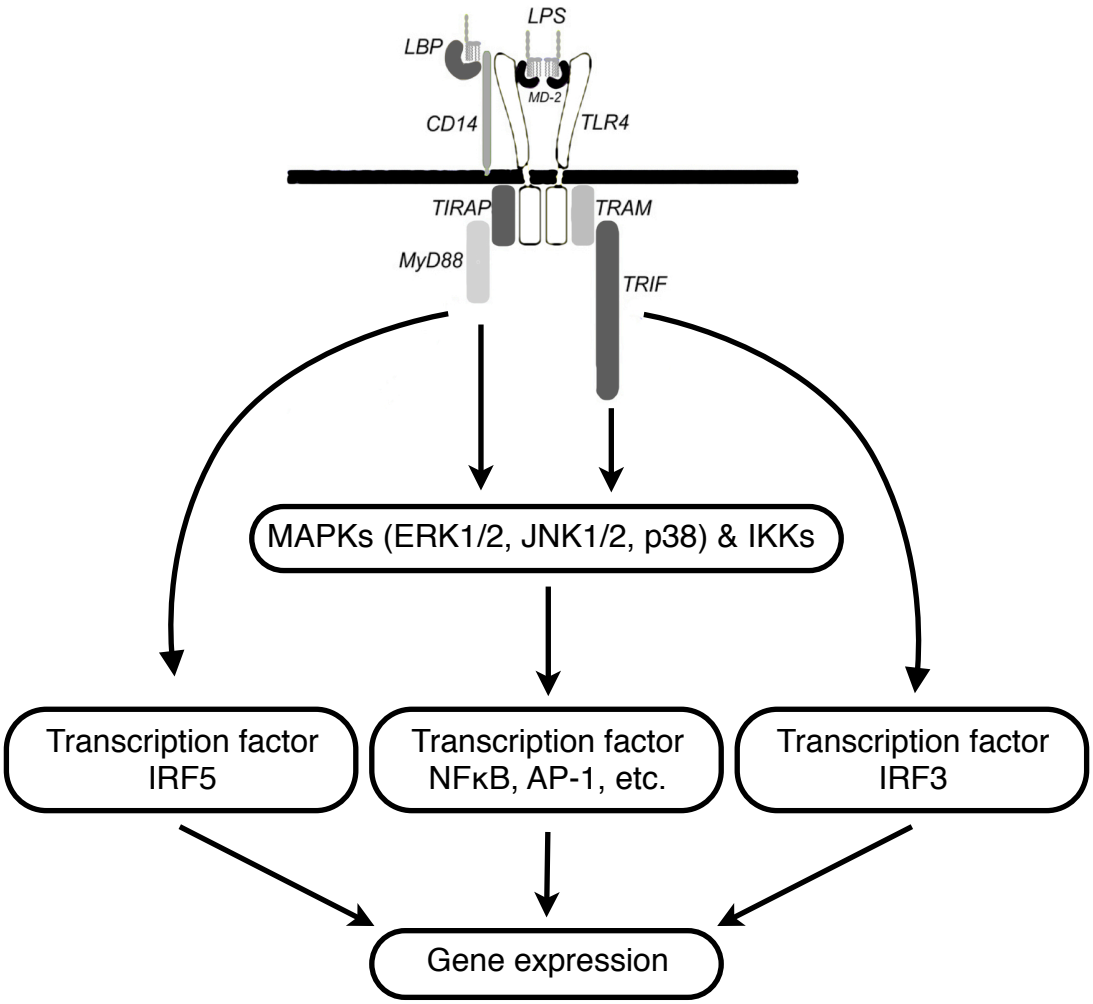

Figure 1-5. Schematic of LPS-activated TRL4/CD14 pathway. LPS activates microglia by binding to the TLR4/CD14 receptor under facilitation of LBP and MD2. The downstream mainly distributes into MyD88-dependent and MyD88-independent (TRIF-dependent) pathways. These pathways regulate transcription factors activity through a complex mechanism involving the activity of MAPKs. Several other pathways are implicated as well such as CaMKII, calcineurin, PKC and PKA. Figure is adapted from (Lu *et al.*, 2008). LBP: LPS-binding protein; TLR4: Toll-like receptor 4; CD14: Cluster of differentiation molecule 14; MD2: lymphocyte antigen 96; TIRAP: TIR domain-containing adaptor protein; TRAM: TRIF-related adaptor molecule; MyD88: Myeloid differentiation primary response gene 88; TRIF: TIR domain-containing adaptor; ERK: extracellular-signal-regulated kinase; JNK: c-Jun N-terminal kinases; PKC: Protein kinase C; PKA: Protein kinase A; MAPK: Mitogen-activated protein kinase; IKKs: IκB kinases; NFκB: nuclear factor kappa-light-chain-enhancer of activated B cells; IRF: interferon regulatory factor; AP-1: activator protein 1.

1998; Terrazzino *et al.*, 2002; Dowling *et al.*, 1996; Bechmann *et al.*, 1999; Frigerio *et al.*, 2000; Taylor *et al.*, 2005), glutamate, prostanoids (Minghetti & Levi, 1995; Giulian *et al.*, 1996; Hoozemans *et al.*, 2002; Mohri *et al.*, 2006; Jian Zhang *et al.*, 2006; Kim *et al.*, 2008), cathepsins, matrix metalloproteinase (MMP) (Petanceska *et al.*, 1996; Liuzzo *et al.*, 1999; Kingham & Pocock, 2001; Gan *et al.*, 2004; Kim *et al.*, 2007; Sakamoto *et al.*, 2008; Cross & Woodroofe, 1999; Kauppinen & Swanson, 2005; Liuzzi *et al.*, 2007; Milner *et al.*, 2007; Crocker *et al.*, 2008), ROS and RNS. Some of these molecules allow microglia to kill and phagocytose external microbes to clear the infection and resultant inflammation. However, they are also toxic to neurons which paradoxically make microglia a "Double-edged sword". The following paragraphs introduce RNS and ROS, two important molecular groups participating in microglia-induced defence and neurotoxicity.

1.2.5.1 NO and NOS

NO release has been routinely used as a marker of microglial activation. NO reacts with ROS forming the peroxynitrites which kill the phagocytosed microbes. Although controversial, NO was observed to recover the tight junction between endothelial cells after exposure to cytokines like TNFa, IL-1β (Wong *et al.*, 2004). However, over-accumulated NO can disturb normal DNA formation by activating the DNA damage p53 pathway, inhibit the respiratory mechanism by influencing mitochondrial function which leads to apoptosis and facilitate bacteria to cross the BBB by weakening the junction of endothelial cells (Buster *et al.*, 1995; Thiel & Audus, 2001). High levels of NO can also inhibit indoleamine 2,3-dioxygenase (IDO) which is a modulator of the proliferation of both tumor and immune cells (Wang *et al.*, 2010). It was reported that in p53-deficient microglia, NO release also activates the endoplasmic reticulum (ER) stress response which is normally activated during cellular stress to protect the cell (Kawahara *et al.*, 2001).

NO is catalyzed from L-arginine by NO synthase (NOS) (Moncada *et al.*, 1989). NOS is a group of enzymes with three isoforms, neuronal NOS (nNOS), inducible NOS (iNOS) and endothelial NOS (eNOS). iNOS is specifically implicated in the immune response and is primarily expressed by astrocytes and microglia (Wen *et al.*, 2011). iNOS can be induced by LPS which is mediated by the MAPKs signaling pathways. During hypoxia, iNOS/NO release is regulated by the PI3-kinase/Akt/ mTOR pathway, activation of hypoxia inducible factor 1alfa (HIF-1α) (Lu *et al.*, 2006), N-methyl D-aspartate receptor (NMDAR) and NFκB (Murugan *et al.*, 2011). iNOS has been implicated in the pathogenesis of Parkinson Disease (Broom *et al.*, 2011).

1.2.5.2 Reactive oxygen species

ROS is another important molecule released by activated microglia and their highly reactive property is due to the unpaired valence electrons (Devasagayam *et al.*, 2004). During the redox reaction ROS are in the intermediate state and can either be oxidant or reducing agents depending on what the other reactant is. Examples include singlet oxygen, hydrogen peroxide, hydroxyl radical, superoxide anion, peroxides and hypochlorous acid. They help to clear invading microbes but also threaten the survival of host cells (Rada & Leto, 2008; Conner *et al.*, 2002). During biological metabolism, ROS are produced by two main mechanisms: (1) They are by products during cellular respiration (Benzie, 2003). (2) They are produced by specific enzymes, such as nicotinamide adenine dinucleotide phosphate ($NADP^+$) oxidase. In all phagocytic cells including activated microglia, NADPH oxidase regulates ROS production (El-Benna *et al.*, 2008), except for neutrophils which have additional myeloperoxidase to produce ROS. In addition, exogenous mechanism, such as ionizing radiation, can produce ROS as well.

The core reaction sites of the NADPH oxidase complex include p22phox and gp91phox/NOX2. These two proteins are the only parts anchored on the cell

membrane. The complex of p22phox and gp91phox is called cytochrome b558 as their characteristic absorption is at 558nm. NAPDH also includes three cytosolic proteins p48phox, p67phox, p40phox and one small GTPase (either Rac1 or Rac2). Rac1 is expressed in monocytes while Rac2 is mainly expressed in neutrophils. These cytosolic components bind to the b558 during cell activation (El-Benna *et al.*, 2008). NADPH oxidase is an electron pump. During activation gp91phox binds to the electron acceptor flavin adenine dinucleotide (FAD), NADPH and two hemes (El-Benna *et al.*, 2008). Electrons are removed from NADPH by the catalytic process and forwarded to the oxygen forming molecules of superoxide anion (O_2^-) which are the precursor of other ROS. The process of NADPH oxidase activation includes: (1) The phosphorylation of p47phox. (2) GTPase activation. (3) The binding of the cytosolic components with the cytochrome b558 after phosphorylation (Quinn & Gauss, 2004; Groemping & Rittinger, 2005; El-Benna *et al.*, 2008).

NADPH has three states of activity: resting status, priming status and activated status which depends on the status of microglia. Under normal circumstances, host cells including microglia have tolerance to ROS with the help of enzymes and antioxidants, for example superoxide dismutase (SOD) and vitamin C (Rada & Leto, 2008; Conner *et al.*, 2002). SOD exists in almost all types of cells. There are three types of SOD including SOD1 (cytoplasmic), SOD2 (mitochondrial) and SOD3 (extracellular). The superoxide is catalyzed into hydrogen peroxide and oxygen by SOD. Hydrogen peroxide can be further catalyzed into water by catalase, glutathione peroxidase and peroxiredoxins. In over-activated microglia, hyperactivated NADPH oxidase damages host cells because large amounts of toxic ROS are produced (El-Benna *et al.*, 2008).

1.2.6 Microglia and disease

Due to the variety of potential cytotoxic molecules released by microglia, microglia play an important role in neurodegenerative diseases in the CNS like AD (Mrak &

Griffin, 2005), Parkinson's disease (PD) and multiple sclerosis (MS) (Dheen *et al.*, 2007). For example, one hallmark of AD is the accumulation of amyloid beta (Aβ) which activates microglia (Schilling & Eder, 2011). Activated microglia during AD release abundant cytokines including IL-1 which further induce more neural injury (Mrak & Griffin, 2005). In addition, microglia activated by LPS caused the loss of dopamine (DA) neurons which is the hallmark of PD (Block *et al.*, 2007). Microglia also have a role following viral, bacterial and parasitic infections (Rock *et al.*, 2004). For example, during the streptococcus infection-induced meningitis, microglia are activated by streptococcus through the activation of TLR2 receptor. The activated microglia response to the infection by releasing pro-inflammatory cytokines and NO which is toxic to neurons and may induce intracerebral edema (Rock *et al.*, 2004).

1.3 Ion channels and microglia

Ion channels are protein pores which allow ions to pass down their electrochemical gradient. Microglia express a variety of ion channels including sodium (Na^+) channels, Ca^{2+} channels, K^+ channels, chloride (Cl^-) channels and proton (H^+) channels (Färber & Kettenmann, 2005; Eder, 2005; Kettenmann *et al.*, 2011). Channels play a pivotal role in regulating microglial properties including membrane potential, intracellular homeostasis, RNS and ROS release, cytokine release, cellular migration and proliferation. The activities of microglial K^+ channels are tightly related to the maintenance of ionic homeostasis for many cellular processes including regulating membrane currents, microglial resting membrane potential, intracellular ion homeostasis, cell migration, change in morphology, proliferation and pro-inflammatory cytokine release. Investigation of the function of K^+ channels in microglia may reveal a potential therapeutic approach to treat microglial-related CNS diseases.

1.3.1 Introduction to K^+ channels

K^+ channels are one of the largest families of ion channels with more than 80 genes in the human genome. K^+ channels can be found in most types of cells. In excitable cells, such as neurons, and cardiac muscle, they contribute to the falling phase of the action potential. In pathological conditions, K^+ channels are implicated in neurological disorders, the control of cardio vascular tone, blood pressure and hormone release, etc. For non-excitable cells, K^+ channels control the resting membrane potential. For example, the transfection of $K_v1.3$ channels reset the membrane potential of Chinese hamster ovary cells (Defarias *et al.*, 1995).

K^+ channels are categorized into four main types: Ca^{2+}-activated K^+ channel (K_{Ca}), inwardly rectifying K^+ channel (K_{ir}), tandem pore domain K^+ channel (K_{2p}) and voltage-gated K^+ channel (K_v) (Figure 1-6).

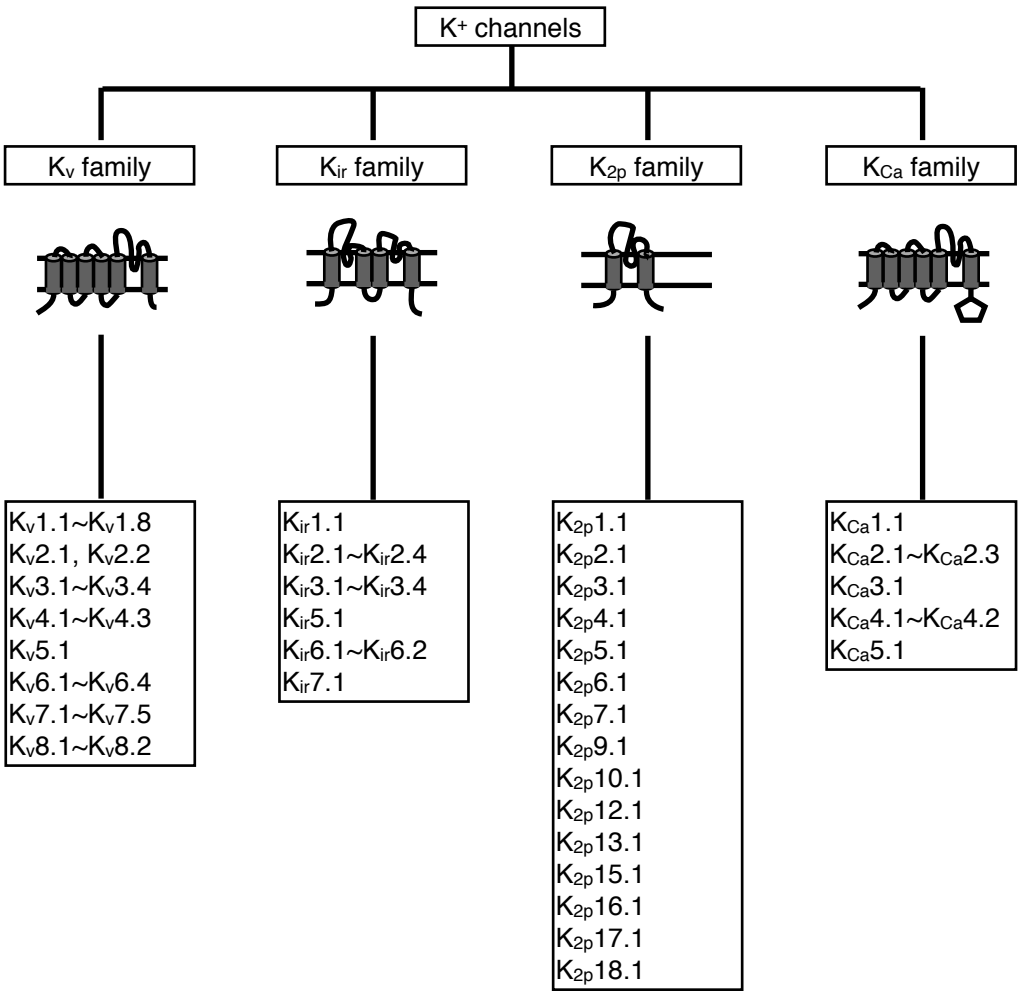

Figure 1-6. The family of K^+ channels. Potassium (K^+) channel family is composed of four groups: voltage-gated K^+ channel (K_v), inwardly rectifying K^+ channel (K_{ir}), tandem pore domain K^+ channel (K_{2p}), Ca^{2+}-activated K^+ channel (K_{Ca}). (1) The K_v channels have six transmembrane domains and one pore-forming loop. They are sensitive to voltage across the membrane. (2) The K_{ir} channels have two transmembrane domains and one pore-forming loop. (3) The K_{2p} channels have four transmembrane domains and two pore-forming loops. They are constitutively opened channels which allow K^+ ions to diffuse into the extracellular compartment and facilitate keeping the negative intracellular potential. (4) K_{Ca} channels have six transmembrane domains, one pore-forming loop and are regulated by intracellular cations. The only exception is large conductance Ca^{2+}-activated K^+ channels ($K_{Ca}1.1$) channels which have seven transmembrane domains and are sensitive to both intracellular Ca^{2+} and membrane depolarization.

1.3.2 K^+ channel expression and function in microglia

K^+ channels participate in microglial pro-inflammatory cytokine release, ROS and NO/iNOS production and proliferation. For example, the application 4-aminopyridine (4-AP) or agitoxin-2 (AgTX-2) diminished the microglial proliferation rate (Kotecha & Schlichter, 1999). Ramified microglia in acute rat brain slices expressed very little K^+ current compared to isolated microglia (Boucsein *et al.*, 2000) which is suggested as the hall mark for resting microglia. However, microglia *in vitro* displayed large inward K^+ current. The evidence indicated that isolated rat primary microglia lacked significant outward current but expressed an inwardly rectifying K^+ current as determined by blockade using barium (Ba^{2+}) and tetraethylammonium (TEA) (Kettenmann *et al.*, 1990). In addition, both resting and LPS-treated microglia *in vitro* expressed an inwardly rectifying current while only LPS-activated microglia evoked a large outwardly rectifying current. After activation under pathological conditions, microglia in acute brain slices displayed inwardly rectifying K^+ current followed by an outwardly rectifying K^+ current after 24hr (Boucsein *et al.*, 2000). These currents reversal potential was close to K^+ reversal potential calculated by the Nernst Equation suggesting that they were K^+ currents (Nörenberg *et al.*, 1992; Nörenberg *et al.*, 1994). Thus the outward K^+ currents may be a hallmark of activated microglia. It was further pointed out that the amplitude of the microglial inward rectifier currents increased after treatment by LPS (100ng/ml, 24hr) (Nörenberg *et al.*, 1992).

The magnitude of resting membrane potential of microglia is still controversial because it may differ from microglia in brain slices or isolated primary microglia *in vitro* culture, resting or activated microglia, developing or mature microglia. This may relate to the expression of outward and inward K^+ currents (Chung *et al.*, 1999).

In rat: (1) Microglia in brain slices: Microglia in the rat brain slices have their membrane potential mainly distributed at about -10~-20mV using the conventional whole-cell patch-clamp with physiological K^+ gradient (Boucsein *et al.*, 2000). This

type of microglia displayed little K^+ current either inward or outward type (Boucsein *et al.*, 2000) while mouse microglia in brain slices also had similar low K^+ current properties (Boucsein *et al.*, 2003). (2) Isolated microglia *in vitro*: Resting microglia displayed a potential at -26.2±4.4mV (Chung *et al.*, 1998) while after LPS activation, microglial membrane potential hyperpolarized to -48.2±6.1mV (Chung *et al.*, 1998). What is more, microglial membrane potential displayed a bimodal distribution phenomenon. Resting isolated rat microglia displayed two different membrane potentials at about -33mV and -73mV (Visentin *et al.*, 1995). After LPS activation, these values were reported as −45mV and -70mV (Chung *et al.*, 1999) or -35mV and -70mV (Nörenberg *et al.*, 1994). In addition, whole-cell current clamp (I=0) on a single LPS-activated microglia indicated that the resting membrane potential unusually switched between -35mV and -70mV during the recording which happened within 2~3mins (Nörenberg *et al.*, 1994).

In mouse: (1) Microglia in brain slices: Microglia have been reported to have a range of membrane potential. One report indicated their membrane potentials were at -23mV and -52mV (Boucsein *et al.*, 2003). However, such bimodal distribution was not observed by another report with the mean value at -38±2.2mV (Schilling & Eder, 2007). The membrane potential changed along with the culture duration of brain slices. Microglial membrane potential in acute brain slices was at -38±2.2mV while in cultured brain slices hyperpolarized to -41.8±2.9 mV (Schilling & Eder, 2007). Here microglia in briefly cultured brain slices may become activated (Schilling & Eder, 2007). Such hyperpolarization was similar to the one observed in isolated rat microglia (Chung *et al.*, 1998). (2) Isolated microglia *in vitro*: Isolated microglia displayed two more hyperpolarized membrane potentials which were at -29mV and -61mV (Boucsein *et al.*, 2003) compared to -23mV and -52mV of microglia in brain slices. What is more, isolated microglia displayed extra inward current which does not exist in the resting microglia in brain slices (Boucsein *et al.*, 2003; Kettenmann *et al.*, 1990). (3) Microglia in brain slices of different age animals: Microglia from 6~8 weeks old mice display -23mV and -52mV of membrane potential (Boucsein *et al.*,

2003) while microglia from postnatal day (P)6~P9 have membrane potentials at -10mV and -70mV (Brockhaus *et al.*, 1993).

Thus, in rat compared to in mice: (1) Microglia in brain slices: Due to limited evidence, microglia displaying single membrane potential was compared. The membrane potential of rat microglia was -15mV (Boucsein *et al.*, 2000) while the one of mice microglia was more hyperpolarized -38±2.2mV (Schilling & Eder, 2007). However, there is not enough data to conclude whether this is a common difference between rat and mice microglia. (2) Isolated microglia: Rat microglia have membrane potentials at -33mV and -73mV (Visentin *et al.*, 1995) while it was -29mV and -61mV of mice microglia (Boucsein *et al.*, 2003).

1.3.2.1 Inward rectifier K^+ channels in microglia

Inward rectifier K^+ currents were first found in isolated primary rat microglia through the discovery of a 30pS conductance channel (Kettenmann *et al.*, 1990) and this was followed by reports suggesting similar microglial currents in different species (Eder, 1998; McLarnon *et al.*, 1995; Visentin *et al.*, 2006). Inward rectifier K^+ currents have been observed in almost every microglial preparation studied, including primary rat microglia (Kettenmann *et al.*, 1990; Korotzer & Cotman, 1992; Schlichter *et al.*, 1996; Nörenberg *et al.*, 1993; Nörenberg *et al.*, 1992; Nörenberg *et al.*, 1994; Sievers *et al.*, 1994; Schmidtmayer *et al.*, 1994; Visentin *et al.*, 1995; Visentin & Levi, 1997), primary murine microglia (Eder *et al.*, 1995; Fischer *et al.*, 1995; Ilschner *et al.*, 1996; Ilschner *et al.*, 1995), BV-2 murine microglia cell line (Bocchini *et al.*, 1992), bovine microglia (McLarnon *et al.*, 1995) and human microglia (McLarnon *et al.*, 1997). They can be elicited by hyperpolarization and blocked by extracellular Ba^{2+}, Cs^+, TEA or quinine in microglia (Nörenberg *et al.*, 1994). It has been suggested that the inward K^+ currents are a pre-marker of microglial activation (Kettenmann *et al.*, 1993). For example, the inward K^+ current is present in microglia under pathological conditions like stroke (Lyons *et al.*, 2000).

In brain slices, microglia exhibited an inward rectifier current after axotomy and after a short period of time this current disappeared (Boucsein *et al.*, 2000; Schilling & Eder, 2007). They are also expressed in cultured microglia *in vitro.* However, the inward K^+ current may not be a marker for activated microglia cultured *in vitro*. TGFβ, which can deactivate microglia, did not influence the inward rectifier K^+ current (Schilling *et al.*, 2000). The maintenance of microglial resting membrane potential is related to this type of current. As indicated previously, isolated rat microglia had membrane potentials mainly at either around -35mV or -70mV. Cells with resting membrane potential at -70mV were depolarized to -45mV by extracellular Ba^{2+} (Chung *et al.*, 1999). The inward rectifier currents were also suggested to contribute to microglial $[Ca^{2+}]_i$ modulation. Current blockade using external Ba^{2+} caused a decrease of $[Ca^{2+}]_i$ in primary rat microglia (Franchini *et al.*, 2004).

It was postulated that the inward K^+ currents are composed of $K_{ir}2.1$ channels (Schilling *et al.*, 2000) because their characteristic properties are similar to the ones in macrophages (Kubo *et al.*, 1993) and monocytes (DeCoursey *et al.*, 1996) and $K_{ir}2.1$ mRNA was discovered in mouse microglia (Schilling *et al.*, 2000). However, due to the lack of a $K_{ir}2.1$ channel selective blocker there is still no direct pharmacological evidence supporting this assumption.

The finding of $K_{ir}2.1$, several other K_{ir} channels were found expressing in microglia as well. Adenosine A_{2a}-receptor activation, using CGS 21680, enhanced mRNA expression of $K_{ir}1.1$ and increased cyclic adenosine monophosphate (cAMP) in isolated rat primary microglia (Küst *et al.*, 1999). This effect was in turn inhibited by adenosine A_{2a}-receptor antagonists. However, elevation of cAMP decreased expression of $K_{ir}1.1$ gene levels rather than increased it (Küst *et al.*, 1999). Thus, it was postulated that the A_{2a}-receptor regulates $K_{ir}1.1$ expression through the activation of PKC rather than cAMP pathway (Küst *et al.*, 1999).

Outward current generated by G protein-coupled inwardly-rectifying K^+ channels (GIRKs) was reported in primary mouse microglia (Ilschner *et al.*, 1996; Ilschner *et al.*, 1995). By activating metabotropic receptors, which leads to activation of G proteins, the K^+ current was observed (Ilschner *et al.*, 1995). The current was elicited by intracellular guanosine 5'-O-(3-thiotriphosphate) (GTPγS), or extracellular ATP, TNFα, epidermal growth factor (EGF) or complement factor C5a (Ilschner *et al.*, 1996; Ilschner *et al.*, 1995). Forty percent of these current amplitudes was reduced by 4-AP (Ilschner *et al.*, 1995) and blocked by pretreatment with pertussis toxin (PTX). Previous studies suggested GIRKs are composed of the pore-forming subunits from K_{ir}3.x members which include Kcnj3 (K_{ir}3.1), Kcnj6 (K_{ir}3.2), Kcnj9 (K_{ir}3.3) and Kcnj5 (K_{ir}3.4). For example, the GIRK family I_{KACh} channels, which generate >60% of outward current in heart (Shi *et al.*, 2004), are composed of two Kcnj3 (K_{ir}3.1) subunits and two Kcnj9 (K_{ir}3.3) subunits (Krapivinsky *et al.*, 1995; Corey *et al.*, 1998). However, it has not been clarified yet what subunits form G protein-gated outward K^+ currents in microglia.

In addition, ATP-sensitive K^+ channel (K_{ATP}) channels were also found in murine microglia (Ortega *et al.*, 2012). These channels consist of pore-forming subunits including Kcnj8 (K_{ir}6.1) and Kcnj11 (K_{ir}6.2) with regulatory subunits, SUR1 and SUR2. Expression of both mRNA and protein of K_{ir}6.1, K_{ir}6.2 and SUR1 but not SUR2 were detected in BV-2 microglia and their expression was elevated by LPS +IFN-γ treatment (Ortega *et al.*, 2012). Protein expression of SUR1, SUR2B and K_{ir}6.2 was detected in rat brain slices during stroke (Ortega *et al.*, 2012). The blockade of K_{ATP} channels using glibenclamide (GBC) facilitated LPS+IFN-γ mediated BV-2 microglial activation, phagocytosis and TNFα release and it also protected neurons against stroke in the brain slices (Ortega *et al.*, 2012).

1.3.2.2 The delayed outwardly rectifying K^+ channels

The delayed outwardly rectifying K^+ channels (K_{DR}) belong to K_v family. Most of the channels display a slow inactivation or non-inactivation property. This group of K^+ channels include members from $K_v1.x$, $K_v2.x$, $K_v3.x$, $K_v7.x$ and $K_v10.x$.

The K_{DR} current is one of most studied K^+ currents in microglia which was observed in activated microglia in 1992 (Nörenberg *et al.*, 1992). It can be elevated by stimulation with the cell wall of gram-positive bacteria (Draheim *et al.*, 1999), LPS, IFN-γ, hydrophobic teflon or pathological conditions like ischemia and is eliminated by the protein synthesis blocker, cycloheximide (Nörenberg *et al.*, 1992). The elevation of K_{DR} current differs between different microglia activators. For example, gram-positive bacterial cell wall only triggered K_{DR} in mature microglia while LPS elevated K_{DR} expression in both amoeboid and postnatal microglia (Draheim *et al.*, 1999). However, microglia conditioned by astrocyte conditioned medium (ACM), a solution used for microglial de-activation (Shih *et al.*, 2006) also express K_{DR} currents (Eder, 1998). What is more, the K_{DR} current is regulated by extracellular pH. In an alkaline environment the threshold of K_{DR} currents became more hyperpolarized (Eder & Heinemann, 1996).

Similar to K_{ir} currents, K_{DR} currents also participate in setting microglial membrane potential. It was reported that 4-AP, a blocker of the outward K^+ current, depolarized the resting membrane potential. For example, 2mM of 4-AP depolarized the resting potential of LPS-activated rat microglia from about -45mV to -25mV within 30s (Chung *et al.*, 1998). In addition, study on cultured primary microglia of newborn (P1 to P3) rats indicated that LPS-activated microglia hyperpolarized the higher value of resting membrane potential from -32.2mV to -44.3mV while inward K^+ current blocker, Ba^{2+}, was not able to reverse this process (Chung *et al.*, 1999). The membrane potential K_{DR} also regulated microglial NO release (Pyo *et al.*, 1997) and IL-1 synthesis (Sanz & Di Virgilio, 2000).

To date, members of the K_{DR} channels found in microglia include $K_v1.1$ (Wu *et al.*, 2009), $K_v1.2$ (Li *et al.*, 2008a; Fordyce *et al.*, 2005; Kotecha & Schlichter, 1999), $K_v1.3$ (Kotecha & Schlichter, 1999; Fordyce *et al.*, 2005; Khanna *et al.*, 2001; Pannasch *et al.*, 2006; Küst *et al.*, 1999; Schilling *et al.*, 2000), $K_v1.5$ (Pannasch *et al.*, 2006; Khanna *et al.*, 2001) and $K_v1.6$ (Kotecha & Schlichter, 1999) which are introduced below.

$K_v1.1$ channels were expressed in amoeboid microglia at early postnatal days and their expression was gradually reduced during maturation of the brain. Using rat brain slices from P1 to P10, $K_v1.1$ channels were found in the cytoplasm excluding the nucleus of amoeboid microglia using immunohistological staining approaches and after microglia transformation into mature ramified microglia, the expression progressively decreased and became completely undetectable at P14 and P21 (Wu *et al.*, 2009). However, different result indicated that the mRNA expression of $K_v1.1$ was not detected in isolated primary microglia from rat of P5 to P14 (Kotecha & Schlichter, 1999). Expression of $K_v1.1$ was elevated in activated microglia. Hypoxia exposure recovered the $K_v1.1$ expression in the mature (P21) brain slices (Wu *et al.*, 2009) and longer exposure led to more $K_v1.1$ being expressed. Using the BV-2 microglial cell line, LPS treatment or hypoxia increased both the mRNA and protein expression of $K_v1.1$ channels while it was decreased by dexamethasone, an immunosuppressant steroid (Wu *et al.*, 2009). In addition, $K_v1.1$ regulated LPS-activated microglial pro-inflammatory mediator. Neutralization of $K_v1.1$ using a $K_v1.1$ antibody suppressed the release of TNFα, IL-1β and NO in the BV-2 cell line (Wu *et al.*, 2009). Thus $K_v1.1$ channels may play a role in the microglial immune response and regulate the activated microglial release profile.

In previous studies, expression of $K_v1.1$ in the brain was closely associated with the expression of $K_v1.2$ sharing similar localization and distribution (Wang *et al.*, 1994; Chung *et al.*, 2001b; Yang *et al.*, 2007). $K_v1.2$ together with $K_v1.1$ is expressed in microglia as well. Similar to $K_v1.1$, protein of $K_v1.2$ channels is expressed in rat

brain slices during development of microglia until P14 while at P21 it was not detectable (Li *et al.*, 2008a). The absence of $K_v1.2$ channels was recovered by hypoxia exposure. Using BV-2 cells, similar results indicated that mRNA of $K_v1.2$ was detected which was upregulated by hypoxia exposure, extracellular ATP or LPS application (Li *et al.*, 2008a). In cultured primary microglia from rat of P2 to P3 (Fordyce *et al.*, 2005) or P5 to P14 (Kotecha & Schlichter, 1999), either the mRNA or protein of $K_v1.2$ was detected but their expression was not changed using phorbol 12-myristate 13-acetate (PMA) and LPS stimulation (Fordyce *et al.*, 2005). This is different with $K_v1.1$. The reason may be due to different age, different cell culture conditions or the different activation method applied to the cells (Li *et al.*, 2008a; Fordyce *et al.*, 2005; Kotecha & Schlichter, 1999). Similar to $K_v1.1$, blocking $K_v1.2$ suppressed the release of IL-1β, TNFα and ROS.

$K_v1.3$ is the most studied K_v channel in microglia (Kotecha & Schlichter, 1999; Fordyce *et al.*, 2005; Khanna *et al.*, 2001; Pannasch *et al.*, 2006; Küst *et al.*, 1999; Schilling *et al.*, 2000; Jou *et al.*, 1998; Schilling & Eder, 2007; Chung *et al.*, 2001a; Visentin *et al.*, 2001; Cayabyab *et al.*, 2000; Koeberle & Schlichter, 2010). However, the expression of $K_v1.3$ in microglia and whether their expression is elevated after microglial activation are still under debate. It was reported that $K_v1.3$ protein was hardly detectable in rat brain slices and injection of LPS near the hippocampal region did not elevate its expression (Jou *et al.*, 1998). TGFβ increased gene expression of $K_v1.3$ in the BV-2 cell line (Schilling *et al.*, 2000). Different results indicated that $K_v1.3$ mRNA was increased in cultured primary rat microglia after LPS or PMA stimulation (Fordyce *et al.*, 2005). Elevation of cAMP, which is downstream of LPS, increased the mRNA expression of $K_v1.3$ channels and activation of the A_{2a}-receptor also enhanced $K_v1.3$ mRNA and protein expression (Küst *et al.*, 1999). In addition, $K_v1.3$-like currents in activated microglia in brain slices was over five times larger in amplitude than those in resting microglia (Schilling & Eder, 2007). LPS treatment enhanced $K_v1.3$ current in cultured primary mouse microglia (Pannasch *et al.*, 2006). Aβ, a marker of AD, induced the expression of $K_v1.3$-type current in isolated rat

primary microglia (Chung *et al.*, 2001a). Activation of cultured primary rat microglia using Tat, a HIV-1 regulatory protein, also increased the expression of $K_v1.3$ current and this pathway was confirmed to be mediated through the NFκB transcription factor (Visentin *et al.*, 2001). Although the $K_v1.3$ current expression is associated with microglial activation, this may not involve changes in protein expression. For example, LPS and PMA treatment did not influence protein expression of $K_v1.3$ channels in cultured primary rat microglia (Fordyce *et al.*, 2005). The reason may be the translation of $K_v1.3$ protein in cells is not associated with their mRNA expression level. Finally, as various activation methods induced different $K_v1.3$ expression, the expression of $K_v1.3$ may be regulated by several different pathways. Functionally, the $K_v1.3$ selective blocker AgTX-2 diminished neuronal cell death evoked by LPS-activated microglia (Fordyce *et al.*, 2005). The effect of $K_v1.3$ was not through the NO release. Deletion of $K_v1.3$ by antisense oligonucleotides (Pannasch *et al.*, 2006), or blockade of $K_v1.3$ channels using AgTX-2 (Fordyce *et al.*, 2005), did not change microglial NO release. This process was proposed to be through ROS regulation. Blocking $K_v1.3$ using margatoxin (MgTX) attenuated Aβ-induced ROS release (Schilling & Eder, 2011) and reduced LPS- (Fordyce *et al.*, 2005) or PMA- (Khanna *et al.*, 2001) induced microglial respiratory burst. Although how $K_v1.3$ regulates ROS release is not fully clarified yet, blockade of $K_v1.3$ channels did not influence p38 MAPK activation (Fordyce *et al.*, 2005). In turn, accumulation of oxidative products may decrease the expression of $K_v1.3$ through phosphorylation by protein tyrosine kinase (Cayabyab *et al.*, 2000). In addition, $K_v1.3$ channel expression was associated with microglial proliferation. During the proliferation of rat primary microglia, $K_v1.3$ replaced $K_v1.5$ on the plasma membrane as determined by patch-clamping and immunostaining methods (Kotecha & Schlichter, 1999).

Like $K_v1.3$ channels, the mRNA (Pannasch *et al.*, 2006; Fordyce *et al.*, 2005), protein (Fordyce *et al.*, 2005) or current (Pannasch *et al.*, 2006) expression of $K_v1.5$ channels have been reported in microglia (Jou *et al.*, 1998; Khanna *et al.*, 2001; Kotecha & Schlichter, 1999). The protein and current expression of $K_v1.5$ were

enhanced during microglial activation. For example, $K_v1.5$ protein found in the rat brain *in vivo* was elevated by LPS injection near the hippocampus (Jou *et al.*, 1998). In addition, Aβ triggered an outward current in cultured rat primary microglia and this current was removed by antisense deoxyoligonucleotides against $K_v1.5$ (Chung *et al.*, 2001a). BV-2 microglia treated by TGFβ did not express $K_v1.5$ channels (Schilling *et al.*, 2000). The expression of $K_v1.5$, especially current expression, may be cell species dependent. For instance, the transcripts and protein of $K_v1.5$ channels were detected, but their current expression was not detectable in cultured primary rat microglia (Fordyce *et al.*, 2005) while the current was found in cultured primary mouse microglia and upregulated by LPS (100ng/ml, 24hr) stimulation (Pannasch *et al.*, 2006). One more reason for different current expression may be that the culture condition led to different distribution of channels (Kotecha & Schlichter, 1999) during which the proteins of $K_v1.5$ were subcellular localized so that their current was not expressed (Khanna *et al.*, 2001). However, unlike the protein and current expression, mRNA expression of $K_v1.5$ in primary cultured mouse microglia displayed a decrease after LPS treatment (Pannasch *et al.*, 2006). Functionally, $K_v1.5$ regulated microglial NO release. In $K_v1.5$ knockout mice (Pannasch *et al.*, 2006), or deletion of $K_v1.5$ using antisense oligonucleotides (AO) in rat microglia, LPS-induced microglial NO release was reduced (Pannasch *et al.*, 2006).

In addition, $K_v1.6$ mRNA was reported at a very low level in cultured primary rat microglia (Kotecha & Schlichter, 1999) but little is known about its function in microglia.

1.3.2.3 HERG channels

This channel, also known as $K_v11.1$, is encoded by human ether-a-go-go-related gene (HERG). They can be opened under high $[K^+]_o$ with hyperpolarization from 0mV and are sensitive to external E-4031 but less sensitive to the universal K^+ current blockers Ba^{2+} and Cs^+ (Eder, 1998). The current of HERG channels was discovered

in rat MSL-9 microglia cell line (Zhou *et al.*, 1998). Little is known about their distribution *in situ* and function in microglia.

1.3.2.4 The Ca^{2+}-dependent K^+ channels

Ca^{2+}-dependent K^+ channels found in microglia include large conductance Ca^{2+}-sensitive and voltage-activated K^+ channels (BK) channels (McLarnon *et al.*, 1995; McLarnon *et al.*, 1997; Schilling *et al.*, 2002; Schilling & Eder, 2007), intermediate conductance Ca^{2+}-activated K^+ channels (IK) channels (Kaushal *et al.*, 2007; Schlichter *et al.*, 2010), small conductance Ca^{2+}-activated K^+ channels (SK)2 and SK3 channels (Schlichter *et al.*, 2010). BK-type currents have been reported in microglia from adult bovine, human and mice. Using inside-out patches with a symmetrical K^+ solution in bovine microglia, a Ca^{2+}-activated K^+ current was detected whose conductance was 240pS (McLarnon *et al.*, 1995). In microglia from a human fetus using physiological ion gradients, a single channel current with conductance of 106pS was detected (McLarnon *et al.*, 1997). In addition, both of these single channel currents increased their mean open times in response to depolarization which is predicted for BK channels. In microglia from juvenile mouse hippocampal slices, a BK-type current was elicited with conductance about 164pS (Schilling & Eder, 2007). Recent studies indicated that blocking BK current using paxilline did not attenuate Aβ-induced ROS release (Schilling & Eder, 2011). Further investigation on the function of BK channels is still required.

It was reported the expression of SK2 (Khanna *et al.*, 2001), SK3 (Khanna *et al.*, 2001) and IK (Kaushal *et al.*, 2007) were detected in rodent microglia. Respiratory burst, a key reaction by microglia which plays an important role in killing neurons, was neutralized by blocking SK current using apamin (Khanna *et al.*, 2001). A recent study suggested that SK3 was expressed in the rat striatum and the expression was elevated by LPS activation in culture microglia or hypoxia exposure in rat striatum (Schlichter *et al.*, 2010). Functionally, blocking either SK3 or IK reduced microglial

neurotoxicity (Schlichter *et al.*, 2010; Kaushal *et al.*, 2007). In addition, this effect of IK may be through the regulation of microglial NO release and MAPKs activity but not ROS synthesis as Tram34 did not influence Aβ-induced ROS release (Kaushal *et al.*, 2007; Schilling & Eder, 2011).

1.3.3 K^+ channels in microglia need further investigation

As introduced above, it is clear that K^+ channels play important roles in microglia. However, the expression and function of most K^+ family members are still not known in microglia. The mechanisms by which K^+ regulate microglial activation are still not fully understood. The cross talk between microglia and other cells in the CNS, e.g. astrocytes, neurons, may require the activation of K^+ channels. Importantly, there is a lack of systematic determination of K^+ channel expression in microglia and how their expression may change during microglial activation.

1.4 The primary aims of the thesis

Microglia play an important role in maintaining environment in the CNS, participate in both the native and adaptive immune response, generate acute and chronic neuroinflammation, and are implicated in the process of neurodegeneration. Microglia are either neuronal protective or neurotoxic depending on the release of mediators by activated microglia under acute status or chronic status.

K^+ channels play important roles in microglial proliferation (Kotecha & Schlichter, 1999), activation (Fordyce *et al.*, 2005; Khanna *et al.*, 2001; Schilling & Eder, 2011) and microglial neuronal toxicity (Fordyce *et al.*, 2005). However, to date the expression of K^+ channels in microglia has not been fully characterized and for those discovered expressions are still controversial (Küst *et al.*, 1999; Fordyce *et al.*, 2005; Pannasch *et al.*, 2006). LPS-induced microglial NO release plays an important role in microglia-induced CNS defense and neuronal toxicity. K^+ channels that regulate microglial NO release may be important for generation of new therapies for microglia-related CNS disease in the future (Schlichter *et al.*, 2010; Kaushal *et al.*, 2007). Thus a systematic screen of K^+ channels in microglia is necessary to be performed and understanding of their roles in microglial activity also needs to be examined. In addition, K^+ current expression is reported associating with microglial status (Boucsein *et al.*, 2000; Kettenmann *et al.*, 1990; Boucsein *et al.*, 2000; Nörenberg *et al.*, 1992). Thus it is important to know which K^+ channel currents are expressed in microglia and whether LPS regulates these channels.

As described in section 1.2.3.5, N9 murine microglial cell line will be used to address these aims. This cell line has been widely used in the *in vitro* investigation of microglial activation. However, the culture conditions used for N9 microglia varied significantly among different previous experiments (Suuronen *et al.*, 2006; Nuutinen *et al.*, 2005; Suuronen *et al.*, 2003; McKimmie & Fazakerley, 2005; Bianco *et al.*, 2005; Garg & Chang, 2006; Chang *et al.*, 2008). Microglia are very sensitive to the

environment and this may determine the expression change of K^+ channels. Thus an optimized maintenance and activation method needs to be confirmed.

In summary, in this thesis the overall hypothesis that N9 murine microglia express multiple K^+ channels and that K^+ channels regulate LPS-induced microglial NO release is tested.

Each chapter involves the following investigations:

(1) Chapter 3: Optimization of N9 microglial regular maintenance and LPS-induced N9 microglial activation.

(2) Chapter 4: What K^+ channels are expressed in N9 microglia and how their mRNA expressions are changed by LPS treatment.

(3) Chapter 5: What the functional roles of K^+ channels are in N9 microglia, including their roles in LPS-induced microglial NO release and their current expression in resting and activated N9 microglia.

CHAPTER TWO

Materials & Methods

2.1 Methods

2.1.1 Preparation of cells

2.1.1.1 N9 murine microglial cell line

N9 microglia cell line was a kind gift from Prof. Alun Williams and Dr. Clive Bate (the Royal Veterinary College, London, UK). It is one of the most commonly used models of primary microglia in culture. The cell line is similar to primary microglia in morphology and offers similar response to activating stimulation (Corradin *et al.*, 1993; Meda *et al.*, 1995; Bonaiuto *et al.*, 1997; Xiang *et al.*, 2006). Especially it provides pronounced NO release in response to lipopolysaccharide (LPS) stimulation (Nikodemova & Watters, 2011). The murine N9 microglial cell line which has been commonly used to investigate microglial nitric oxide (NO) release *in vitro* was used for studies of the thesis.

2.1.1.2 Regular passaging of N9 cells

The N9 cells were cultured in Iscove's modified Dulbecco's medium (IMDM) with 5% fetal calf serum (FCS), 100U/ml penicillin (PEN), 100μg/ml streptomycin (STREP) and 50μM β-mercaptoethanol (β-MET), and maintained at 37°C in 5% (v/v) CO_2.

During general passaging, N9 cells were cultured in 25cm^2 flasks (CELLSTAR, Greiner Bio-one). The supernatant was removed and cells were washed twice using Hanks balanced salt solution (HBSS). After which cells were incubated with 0.05% Trypsin-EDTA (0.5ml for 25cm^2 flask) at 37°C in 5% (v/v) CO_2 for 5~10mins. Cells were detached by gently tapping the flask. At this stage, 1ml growth medium was added to stop the reaction of Trypsin-EDTA. Cells were resuspended thoroughly and further diluted by adding 13ml of growth medium to every 0.5ml of cell suspension of which 5ml was plated into a new 25cm^2 flask. Cells were harvested 2~3 times a

week and were typically used 48hr after seeding, over a passage ranging from 7 to 40. Within this range, the N9 microglia gave a constant NO release to LPS stimulation.

2.1.1.3 N9 cell seeding density for experiments

During experimental preparation, cells were counted using a haemocytometer (#BS. 748, Hawksley) and a tally counter. Unless indicated separately, for Griess reagent assays (Promega) the seeding density was: 3×10^4 cells/well on 96 well plate, 5×10^4 cells/well on 24 well plate, $2\sim3\times10^5$ cells/well on 6 well plate. These were within the range of $2.5\times10^4\sim2\times10^5$ cells/well (24 well plate) which was confirmed in Chapter 3. For electrophysiology the seeding density was: $2\sim3\times10^5$ cells/well (6 well plate). For quantitative reverse transcription polymerase chain reaction (qRT-PCR) the seeding amount was 3×10^5 cells/well (6 well plate) (Table 2-1).

2.1.1.4 Optimization of growth medium for N9 cells

2.1.1.4.1 Components of growth medium

In previous studies growth medium used for N9 microglia varied from each other, thus their effect on N9 cell morphology, proliferation and even activation was examined. Initially three different recipes of growth medium were generated based on previous publications (Table 2-2) (Chang *et al.*, 2008; Meng *et al.*, 2008; Wu *et al.*, 2007; Hou *et al.*, 2006; Bi *et al.*, 2005; Cavaliere *et al.*, 2005; Wang *et al.*, 2008; Garg & Chang, 2006; Nuutinen *et al.*, 2005; Suuronen *et al.*, 2003; Suuronen *et al.*, 2006; McKimmie & Fazakerley, 2005; Bianco *et al.*, 2005), namely GM[0], GM[1] and GM[2]. The components of GM[0] included: Dulbecco's Modified Eagle Medium (DMEM) (no glutamine (GLX)) with 5% FCS, 100U/ml PEN, 100µg/ml STREP, 50µM β-MET. The components of GM[1] included: IMDM (including 4mM GLX) with 5% FCS, 100U/ml PEN, 100µg/ml STREP, 50µM β-MET. The

culture vessel	cells/well	surface area (cm^2)	density (cells/cm^2)	total volume of medium (ml)
96 well plate	3×10^4	0.3	1×10^5	0.2~0.25
24 well plate	5×10^4	1.9	2.6×10^4	1
6 well plate	$2\sim3\times10^5$	9.4	$2.1\sim3.2\times10^4$	2~3
25 cm^2 flask	$2.5\sim7\times10^5$	25	$1\sim2.8\times10^4$	6~10

Table 2-1. Seeding density in each culture vessel. The density was confirmed based on the optimized N9 microglial activation method as described in Chapter 3.

Media	FCS (%)	GLX (mM)	PEN (U/ml)	STREP (μg/ml)	β-MET (μM)	References
IMDM	5		100	100	50	(Chang *et al.*, 2008)
IMDM	5	2	100	100	50	(Meng *et al.*, 2008; Wu *et al.*, 2007; Hou *et al.*, 2006; Bi *et al.*, 2005; Cavaliere *et al.*, 2005)
DMEM	10	2			50	(Wang *et al.*, 2008)
MEM	5	1.4				(Garg & Chang, 2006)
IMDM	5					(Suuronen *et al.*, 2006; Nuutinen *et al.*, 2005; Suuronen *et al.*, 2003)
RPMI	5	2	100	100		(McKimmie & Fazakerley, 2005)
IMDM	5		100	10	50	(Bianco *et al.*, 2005)

Table 2-2. Different growth media used for N9 microglia culture. Here lists recipes of growth media for N9 cells culture *in vitro* used in previous studies. Based on the these studies, components in the culture medium mainly included: Iscove's modified Dulbecco's medium (IMDM), glutamine (GLX), fetal calf serum (FCS), penicillin (PEN), streptomycin (STREP) and β-mercaptoethanol (β-MET). In addition, Roswell Park Memorial Institute (RPMI) medium, minimum essential media (MEM) and Dulbecco's Modified Eagle Medium (DMEM) were also used for growth of N9 microglial culture as well.

components of GM[2] included: IMDM (including 4mM GLX) with 5% FCS, 100U/ml PEN, 100μg/ml STREP (Table 2-3).

2.1.1.4.2 Cell imaging

N9 cells were plated at the density of 2.5×10^5 cells in three $25cm^2$ flasks with 10ml of growth medium: GM[0], GM[1] or GM[2] separately and cultured for up to 120hr without replacing the culture medium. After each 24hr of culture, the morphology of cells from six different locations of each $25cm^2$ flask was captured using a digital camera (FX7, Panasonic) together with optical microscope (AE20, Motic). 10x eyepieces with 4x or 10x objective lens were used. The images were prepared for the following length measurement and cell number counting approaches.

2.1.1.4.3 Measurement of microglial morphology

At 24hr after seeding, the longest process of each microglia was obtained by measuring the linear length from the center of cell soma (amoeboid) to the end of the process. If microglial soma displayed an oval shape, radius of soma was applied as half of the diameter which was the average of the transverse and longitudinal axes. According to the study which examined length of process and soma of primary microglia (Kozlowski & Weimer, 2012), the ratio between the length of process and the diameter of soma of resting microglia is not less than two. Thus the proportion of microglia with long process equal or more than twice the diameter of soma was calculated. Scale was obtained using a transparent flat lens with ruler engraved (Zeiss) during cell imaging assays. All measurement was processed using Photoshop CS4.

	Medium	FCS (%)	PEN (U/ml)	STREP (µg/ml)	β-MET (µM)
GM[0]	DMEM (Excl. GLX)	5	100	100	50
GM[1]	IMDM (Incl. 4mM GLX)	5	100	100	50
GM[2]	IMDM (Incl. 4mM GLX)	5	100	100	

Table 2-3. Components of GM[0], GM[1] and GM[2] culture media. The basal medium of GM[0] was DMEM while the other two used IMDM. The difference between GM[1] and GM[2] was β-MET component in GM[1] while GM[2] did not contain it.

2.1.1.4.4 Cell number

At 72hr after seeding, the cell number in each growth medium was counted and the density was obtained by normalizing cell numbers to the area (mm^2).

2.1.1.4.5 Measurement of NO_2^- concentration in each growth medium

The microglial NO release under each growth medium condition was examined. The supernatant after 120hr of culture was collected and the nitrite (NO_2^-) concentration was measured using the Griess reagent assay. Procedure of Griess reagent reaction is described below (section 2.1.1.6).

2.1.1.5 Optimization of N9 microglial activation

2.1.1.5.1 Examination of time course and dose dependence of LPS treatment

LPS from the endotoxin of gram-negative bacteria *Escherichia coli* (*E. coli*) induces the immunoresponse of mammals and it has been commonly used for the external stimulation of microglial activation *in vitro*. The previous dose of LPS used on microglia varied a lot between publications. The concentration of LPS ranged from 1ng/ml to 10μg/ml and the LPS challenge duration ranged from 6hr to 48hr (Chang *et al.*, 2008; Meng *et al.*, 2008; Wu *et al.*, 2007; Hou *et al.*, 2006; Bi *et al.*, 2005; Cavaliere *et al.*, 2005; Wang *et al.*, 2008; Garg & Chang, 2006; Nuutinen *et al.*, 2005; Suuronen *et al.*, 2003; Suuronen *et al.*, 2006; McKimmie & Fazakerley, 2005; Bianco *et al.*, 2005). It is required to confirm a proper LPS activation method before processing the following experiments.

To investigate the effect of different concentrations of LPS, 0.01μg/ml, 0.1μg/ml and 1μg/ml of LPS were applied in parallel. For general procedure, five groups of N9

cells were cultured at the density of 5×10^4 cells/well on 24 well plate for totally 48hr. Group one was cultured with three different concentrations of LPS for 48hr. Group two was challenged by LPS at 36hr after plating and cultured with LPS for 12hr. Group three was challenged by LPS at 24hr after plating and cultured with LPS for 24hr. Group four was challenged by LPS at 12hr after plating and cultured with LPS for 36hr. The final group was cultured without LPS for 48hr as a negative control. After 48hr of culture, the supernatant of each sample was collected and used for NO detection by Griess reagent reaction.

2.1.1.5.2 Optimized N9 microglial activation

To stimulate N9 microglial activation, first cells were cultured for 24hr after which LPS was added into the supernatant to reach the final concentration of 1μg/ml and cells were co-cultured with LPS for another 24hr after which cells were activated and ready for the following approaches. During the activation, cells without the LPS treatment were established in parallel as a control. This activation protocol by LPS (1μg/ml, 24hr) was based on the result of Chapter 3.

2.1.1.6 Griess reagent reaction

As described in section 1.2.5.2, activated microglia release NO which was produced from L-arginine by inducible nitric oxide synthase (iNOS) (Moncada *et al.*, 1989). NO is reactive and can be oxidized to the stable form NO_2^-. In the culture medium, this chemical reaction formula is:

Formula 2.1:

$$4NO+O_2+2H_2O\rightarrow4HNO_2$$

It was pointed out part of the NO_2^- in the supernatant will be further oxidized to nitrate (NO_3^-) (Marletta *et al.*, 1988), but such effect was offset as all the samples including control were prepared in the same condition during microglial activation.

The detection of microglial NO release was then examined by measurement of the NO_2^- concentration in the culture medium by the Griess reagent assay (Green *et al.*, 1982) which was originally described by Griess in 1879. This method is based on the reaction of NO_2^-, sulfanilamide and N-1-napthylethylenediamine dihydrochloride (NED) (Figure 2-1) following the manual of the manufacturer (Griess Reagent System, Promega). The limit of detection for this assay is 0.1μM of NO_2^- in the supernatant.

For general protocol, after the activation of microglia the supernatants were transferred to fresh 1.5ml Eppendorf tube and stored at -20°C until measurement. During the Griess reaction, 50μl of each sample was added in a 96 well plate. 50μl of the sulfanilamide was following added to each sample/well by an electronic multichannel pipette and the mixture at room temperature for 5~10min during which plates were protected from light. Finally, 50μl NED was added to each well and incubated the mixture at room temperature for another 5~10min, protected from light. A pink color will form and its absorbance was measured at 550nm within 30min using a plate reader (PowerWave XS, BioTEK). Meanwhile, a standard curve was generated by dissolving sodium nitrite in culture medium at concentration ranging from 0~100μM in a two-fold series dilution. All samples were run in or more than triplicate. Data analysis was processed using KCjunior 1.41.8 (BioTEK).

2.1.1.7 Cell viability assay

To avoid the possible effect of blocking or activating K^+ channels on cell viability, LPS-induced NO release was normalized to cell number determined by MTS assay. In many previous studies, such pharmacological effect on microglial proliferation has

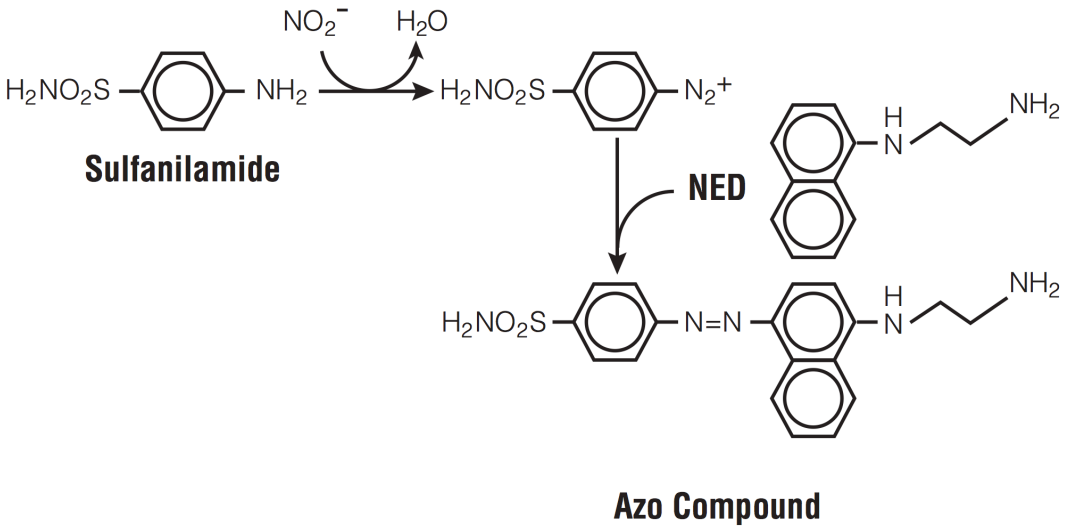

Figure 2-1. Reaction of Griess reagent assay. Sulfanilamide and N-1-napthylethylenediamine dihydrochloride (NED) react with nitrite (NO_2^-) forming Azo compound which has high absorbance at 530~550nm. Figure is adapted from manual of the manufacturer (Griess reagent System, Promega).

not been routinely examined. However, an assumption of the MTS approach to reliably measure cell number is that the pharmacological manipulation does not dramatically affect the mitochondrial function and further work should also explore other cell counting methods.

To examine the pharmacological effect on cell viability, the influence of cell number under different culture conditions using [3-(4,5-dimethylthiazol-2-yl)-5-(3-carboxymethoxyphenyl)-2-(4-sulfophenyl)-2H-tetrazolium (MTS) technique was determined. The yellow MTS reacts with dehydrogenases at the site of mitochondria and transfers into purple formazan (Figure 2-2). As this process only occurs in live cell, the amount of formazan in the supernatant is an indicator of cells numbers.

The procedure was following the manual of the manufacturer (CellTiter 96 AQ_{ueous} One Solution Cell Proliferation Assay, Promega). For general protocol on 96 well plate, cells were cultured in the microplates. 100µl of growth medium was left in each well and then 20µl of "CellTiter 96 AQ_{ueous} One Solution reagent" which contains MTS was added to each well. Cells were incubated under the condition of 37°C with humidified 5% (v/v) CO_2 atmosphere for 1hr. After that the plate was processed for absorbance measuring at 490nm using a plate reader (PowerWave XS, BioTEK). According to the manual, the change of cell numbers was represented by the direct comparison between the absorbance of sample and control. Background was measured and subtracted using samples without cells. Data analysis was processed using KCjunior (BioTEK).

2.1.2 Molecular protocols

The investigation on the expression of potassium (K^+) channel mRNAs was based on qRT-PCR.

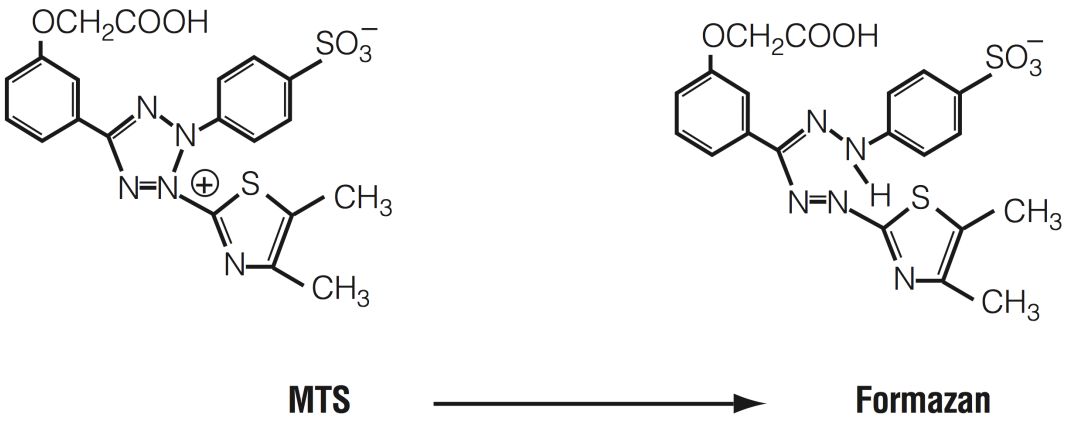

Figure 2-2. Reaction of cell viability. Yellow MTS is converted by dehydrogenases at the site of cellular mitochondria into purple formazan. The absorbance was then measured at 490nM and used as indicator for live cell number. Figure is adapted from manual of the manufacturer (CellTiter 96 Aqueous One Solution Cell Proliferation Assay kit, Promega). MTS: [3-(4,5-dimethylthiazol-2-yl)-5-(3-carboxymethoxyphenyl)-2-(4-sulfophenyl)-2H-tetrazolium.

2.1.2.1 RNA purification

The total RNA was obtained according to the manual of RNeasy Mini Kit (QIAGEN) which technology was based on the selective binding properties between RNA (>200 bases) and silica-based membrane. For the general protocols, cells were prepared in 6 well plate with cell number no more than 1×10^6 cells/well (6 well plate) in advance. Prior to lysis of cells, the bench was cleaned with RNaseZap (Invitrogen). Cells were first lysed by the RNeasy lysis buffer containing guanidine thiocyanate which inactivates the RNase. This step also aimed to release all the RNA of the cells by disrupting the membranes of cells and organelles. After the lysis of cells, the lysates were homogenized by being passed through a needle of 0.8mm diameter for 30 times. This step reduced the viscosity of the lysates aiming to increase the efficiency of binding of RNA to the silica-based membrane. After this step, same volume of 70% ethanol was added to the lysates. Total RNA of the lysates was bound to the membrane of the RNeasy spin column by centrifugation. The membrane was washed by centrifuging with the wash buffer provided following the protocol of the manufacturer. Finally, RNA was eluted by centrifuging the RNeasy spin column with the RNase free water.

2.1.2.2 Analysis of RNA integrity

The RNA integrity was checked by running the samples in gel electrophoresis. Samples were denatured by being heated at 65°C for 10min and put on ice for 5min before running the gel (10% agarose). Two bands (28S and 18S) representing ribosomal RNA should appear (Figure 2-3A).

A

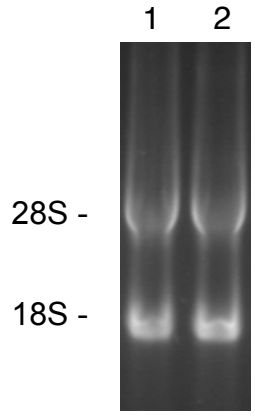

B

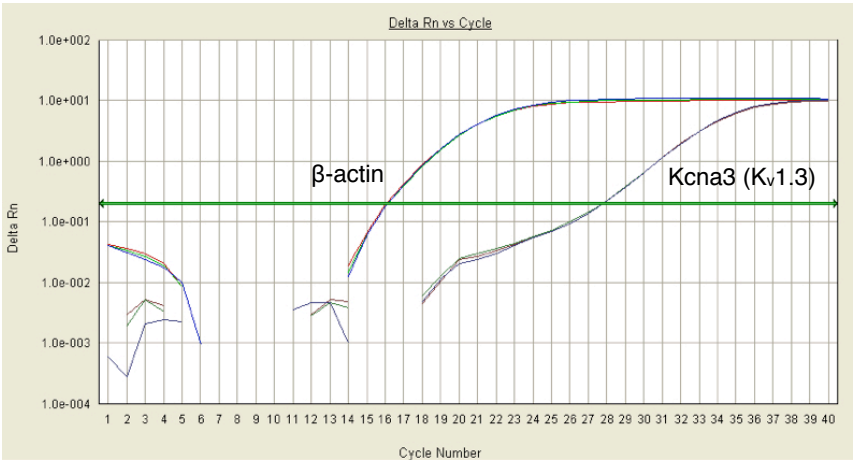

Figure 2-3. Representative samples for RNA integrity and qRT-PCR. (**A**) A sample for the reproducible total RNA isolation from direct lysis of N9 microglia. The 28S and 18S ribosomal RNA are distinguishable. Lane 1 is from resting microglia and lane 2 is from LPS-activated microglia. (**B**) A representative trace for qRT-PCR (Delta Rn vs. cycle number). Data presented is β-actin and Kcna3 (K_v1.3) (Triplicate). The baseline was set from cycle 3 to cycle 10 and threshold was 0.2. Rn is the ratio of fluorescence emission intensity of reporter dye to the passive reference dye. Delta Rn is Rn value subtracting the baseline. Ct is cycle number at which the fluorescence passes the threshold. qRT-PCR: quantitative reverse transcription polymerase chain reaction; K_v: voltage-gated K^+ channel.

2.1.2.3 Reverse transcription

The reverse transcription was performed using the Transcriptor High Fidelity cDNA Synthesis Kit (Roche). First 3~4μg of total RNA with 0.5μl anchored-oligo$(dT)_{18}$ Primer and 1μl Random Hexamer Primer were made up to 11.4μl by adding the appropriated volume of RNAse free H_2O. The mixture was denatured by being heated at 65°C for 10min in a thermocycler (#2720, Applied Biosystems) during which the secondary structure of RNA was diminished and immediately the template-primer mixture was cooled on ice to prevent the formation of secondary structure. The following components were added into the denatured template-primer mixture: 4μl Reaction buffer (5× conc.), 0.5μ RNase Inhibitor (40U/μl), 2μl Deoxynucleotide (10mM), 1.1μl RNase-free water and 1.1μl reverse transcriptase. The final volume was then 20μl. The reaction started by heating the mixture at 50°C for 30min followed by the incubation at 85°C for 5min to inactivate the reverse transcriptase. Finally the reaction was stopped by putting the mixture on ice. cDNA was then used for following experiment or stored at -20°C for later use. During this procedure, the non-template control, which did not contain RNA, and the non-enzyme control which did not contain the reverse transcriptase were prepared.

2.1.2.4 Quantitation of RNA and cDNA

The purity was calculated by the ratio of OD_{260}/OD_{280}. For pure cDNA the ratio is ~1.8 while for pure RNA the ratio is ~2.0 (Barbas *et al.*, 2007). All samples displayed no contamination. The RNA or cDNA was diluted with H_2O by 200 times and the absorbance of the mixture was measured by a spectrophotometer (Biomate 3, Thermo Co.). The equations to calculate cDNA and RNA concentrations (Barbas *et al.*, 2007) are :

Equation 2.1:

$$\text{ssDNA concentration} = 33\mu g/ml \times OD_{260} \times \text{dilution factor}$$

Equation 2.2:

$$\text{RNA concentration} = 40\mu g/ml \times OD_{260} \times \text{dilution factor}$$

2.1.2.5 Quantitative reverse transcription polymerase chain reaction

The SYBR Green based qRT-PCR was carried out using ABI PRISM 7000 Sequence Detection System (Applied Biosystems). Over 80 K^+ channel subunits were examined. For the general procedure, 25µl of mixture containing 1µl forward primer (5µM), 1µl reverse primer (5µM) of each subunits (Table 2-4 to Table 2-9), 12.5µl SYBR Green reagent (including the internal reference dye), 2.5µl cDNA template and 8µl diethylpyrocarbonate (DEPC) water was prepared for each sample. All samples were run in triplicate and the cycling parameter was: 50°C for 2min (1 cycle), 95°C for 10min (1 cycle), 95°C for 15sec to 60°C for 1min (40 cycles) followed by the dissociation stage which was: 95°C for 15sec to 60°C for 20sec to 95°C for 15sec (1 cycle). Data was collected at step of 95°C for 15sec to 60°C for 1min (40 cycles) using ABI PRISM 7000 System (Applied Biosystems). Representative traces are presented (Figure 2-3B). The Ct threshold was 0.2 and baseline was from start cycle 3 to end cycle 10. K^+ channel mRNAs expression were normalised to the expression of β-actin. All primers were designed by SIGMA and validated before use.

2.1.2.6 Examination of the effect of LPS on β-actin expression

Each Ct value of β-actin was normalised to the concentration of the template (cDNA). Normalised Ct values of resting microglia and LPS-activated microglia were compared.

Name		GeneBank #	Primer Sequence (5'-3')
K_{ir}1.1	Kcnj1	NM_01965925	f: TGGTCTCCTGTGGTATGTCGTAGC r: ATCCGTAACCTATGGTCACTTGGG
K_{ir}2.1	Kcnj2	NM_008425	f: GAGAACCAACCGCTACAGCATCG r: TCCTGCACTGTTGTCGGGTATGG
K_{ir}2.3	Kcnj4	NM_008427	f: GCAACCGCTTTGTCAAGAAGAACG r: AGAAGAGCCAGGAAACGAGGAAGG
K_{ir}2.4	Kcnj14	NM_145963	f: ACTGATCGCATCTTCCTCGTCTCC r: CAACCATACCTTCAAGAATGACCACCAG
K_{ir}3.1	Kcnj3	NM_008426	f: ATCTGGCTCGCCCCTCCGTATTATG r: GAAGTGGTCACTACCTGGTAATCGTC
K_{ir}3.2	Kcnj6	NM_001025584	f: TGTTTCCTCCTTTTCTTGTATTTTCTTCCC r: TTCACTCCATCCTGATCGCCTCTC
K_{ir}3.3	Kcnj9	NM_008429	f: AGGAGAAACAGCAGTGTC r: GAGAAGAGTAGCCAGCAG
K_{ir}3.4	Kcnj5	NM_010605	f: CCACTCTGCCACCGCCTCTC r: GACTCCTATCTCCATGTCTTGATTCATAGC
K_{ir}4.1	Kcnj10	NM_001039484	f: CTCCGCTCGCCGCTCCTG r: CGTCATCTTGGCTCGAAGGTGAAG
K_{ir}4.2	Kcnj15	NM_001039056	f: TCTGAGAAACTTGACTTCCAAAGGC r: ACTCACTCTGTAGGTCAGGAATCTTC
K_{ir}5.1	Kcnj16	NM_010604	f: CCTCCCTGTGGAAGAGTGAATGAAG r:TCAGAGGAGTCCGATGTCAGTTAAAAG
K_{ir}6.1	Kcnj8	NM_008428	f: TGGCCTGGAGTCCGCTGTC r: GTTGATGATCAGACCCACGATGTTC
K_{ir}6.2	Kcnj11	NM_010602	f: GGGGCGGTGGAGGAGAGC r: GCTGGGTTCTGCTTCTCTTTATACTAC

Table 2-4. Primers for K_{ir} channels used in qRT-PCR. Both International Union of Pharmacology (IUPHAR) and HUGO Gene Nomenclature Committee (HGNC) names of each gene are shown. K_{ir}: inwardly rectifying K^+ channel

Name		GeneBank #	Primer Sequence (5'-3')
K_v1.1	Kcna1	NM_010595	f: TTGCGTCGGACCTGACCATCTC r: TTGTCATTCAGTTCCCATCCTTGCC
K_v1.2	Kcna2	NM_008417	f: CACCCAGGAACATGGAGGCTCTG r: CGCACCACGACTTGAGGAGGAG
K_v1.3	Kcna3	NM_008418	f: ATTGTGTCAGTGCTGGTCATTCTCATC r: ACAAGGTCTCCACCACGAAGAAGG
K_v1.4	Kcna4	NM_021275	f: TGGGATGGATACTGGAGAAGGAATGC r: GGGCTGGGAACGGAAGTCAAGG
K_v1.5	Kcna5	NM_145983	f: CAAGAGCCATTGCCATCGTGTCG r: CAGGCAGAGTCTCCAAGCAGAAGG
K_v1.6	Kcna6	NM_013568	f: TCGTCTCAGTATTGGTCATCCTCATCTC r: TCATCTTCTTCCTCGTGGCTCCTG
K_v1.7	Kcna7	NM_010596	f: CCTCCCCGACAGCCCTTCAAC r: GCCACCAGACGCACCAGCAG
K_v2.1	Kcnb1	NM_008420	f: CGTGCTGTGCTGAGAAGAGGAAG r: TGACAGGGCAATGGTGGAGAGG
K_v2.2	Kcnb2	NM_001098528	f: GAAACTTTGGGACTTGCTGGAGAAAC r: AATGGTGGAAAGAACGATGAACAGG
K_v3.1	Kcnc1	NM_001112739	f: ACTCCCTTCCTCCCTCCCTCTTTAC r: CAGGCAGGTGCGGGTCCAG
K_v3.2	Kcnc2	NM_001025581	f: ACAGAGATGGGCAAGATCGAGAGC r: TGAGGTTCAGAGGAGGCAAGAAGG
K_v3.3	Kcnc3	NM_008422	f: CACACGAGGGCTTCATCCACATC r: AGGTCAAGAAGGGTTCCGTCTCC
K_v3.4	Kcnc4	NM_145922	f: CTGGAGGTGGGATTGAGTGGTTTG r: GCCAAGAAGATGATAAGCAACAGGAAC
K_v4.1	Kcnd1	NM_008423	f: TGAGAAGGGCACGAGCAAGACC r: AGACACCGCTAAGTGAGCAGATGG
K_v4.2	Kcnd2	NM_019697	f: GCCGCAGCACCTAGTCGTTAC r: TTGTCTGTCATCACCAGCCCAATG
K_v4.3	Kcnd3	NM_001039347	f: TCCGTTGTGTGCTTAACTTCTACCG r: CTGGTTGTTTTCAGAGTCATTGTCATCC
K_v5.1	Kcnf1	NM_201531	f: TCTTGGACGACCTGGGTGTTGAC r: GACCACGGAGGAGACAAGGATGAG

Table 2-5. Primers for K_v channels used in qRT-PCR (Part 1). Both IUPHAR and HGNC names of each gene are shown.

Name		GeneBank #	Primer Sequence (5'-3')
K_v7.1	Kcnq1	NM_008434	f: ACCACTTCACCGTCTTCCTCATTG r: TCTGTCCCAAAGAACACCACAAGG
K_v7.2	Kcnq2	NM_010611	f: GTGACTATCGTGGTATTCGGTGTTGAG r: CCAGCAGCCAGCACAGCAATG
K_v7.3	Kcnq3	NM_152923	f: CACTCATCCTTTCTTCATTTCTTGTCTACC r: CTCAAACTCCTCCTTCATTTCCTCTCC
K_v7.4	Kcnq4	NM_001081142	f: AACTTGCCAACGAGTGTCTCCTTATC r: GTCCCTGCCATCCTCTGTAGCG
K_v7.5	Kcnq5	NM_023872	f: TTCTCCTTGTGTTTGGTTGCTTGATTTTG r: TCAGTCTTCCTTGCCATCCTCTATAACG
K_v8.1	Kcnv1	NM_026200	f: GCTCTGGGATATTCTGGAGAAACCTG r: GCCATGTTGACGATGGACACTGC
K_v8.2	Kcnv2	NM_183179	f: TGGACCGAGGGCAACTACAATTACTAC r: TTCACTTTCAGCGTGGACATTTGGG
K_v9.1	Kcns1	NM_008435	f: TGGAGACCAATACAGTTGTAGGTAATAAGC r: GGAGTGATGGGATGGTGGGATGG
K_v9.2	Kcns2	NM_181317	f: CGAGCAGAGTGACCAGGAAAGC r: CGAACTTGGAAGCATCATTATAGAAGGC
K_v9.3	Kcns3	NM_173417	f: TGGGACCAGAAAAGCAACGATGTG r: TCAAACTTCTCCAGCTCTTTCTCAAACAG
K_v10.1	Kcnh1	NM_001038607	f: TCTACACAGCCATCTTGGTCCCTTAC r: CGTCTTCAGGTAGTTCATGCGGATAAG
K_v11.1	Kcnh2	NM_013569	f: GCTTCCTGTGTCTGGTGGATGTG r: ACCATGTCCTTCTCCATCACTACTTC
K_v11.2	Kcnh6	NM_001037712	f: ACGCCCTACTCTGCTGCCTTTC r: TCGGAAGTTGATGACAATATCCACCAC
K_v11.3	Kcnh7	NM_133207	f: AAGCAGATGATACGAAAGCCTTGATACAG r: GGTCCAGAGGTCCTGATATGTTCACTAAG
K_v12.1	Kcnh8	NM_001031811	f: CCACTCGGAGCACAACGGTCAG r: ATACAGGAGGTCAAAGGGCAAGGC
K_v12.2	Kcnh3	NM_010601	f: CAATAAGGGAGTGTTTGGAGAGAAGCC r: CCACAGTGCAGCAGGATAAAGGG

Table 2-6. Primers for K_v channels used in qRT-PCR (Part 2). Both IUPHAR and HGNC names of each gene are shown.

Name		GeneBank #	Primer Sequence (5'-3')
K_{2P}1.1	Kcnk1	NM_008430	f: CCTCGGGAAATTGGAATTGGGACTTC r: GAGGAGGGTGAACGGGATGCC
K_{2P}2.1	Kcnk2	NM_010607	f: GATTTTCCTGGTGGTCGTCCTCTAC r: AAGGTCTGCTTCTGGATCACAATGG
K_{2P}3.1	Kcnk3	NM_010608	f: CCATCGGCTTCGGCGACTATG r: GCAGCACCACGAGGTTGAGG
K_{2P}4.1	Kcnk4	NM_008431	f: TGACTCTCACCACTGTAGGCTTTG r: ACTGAGGCGAAGTAGGCTAGGC
K_{2P}5.1	Kcnk5	NM_021542	f: TCTGGTGATCCCGCCCTTTGTG r: TGGAGATGGTGATGAAGGAATAGTAGAGG
K_{2P}6.1	Kcnk6	NM_001033525	f: CTGCTTCATCTCTCTGTCCACCATTG r: GGAAACACGGCGGAAAGTCTGC
K_{2P}7.1	Kcnk7	NM_010609	f: ACCCCAGCCTCAGTATCAGAACATC r: CCTTGGTGCCTCCCGCTCAG
K_{2P}9.1	Kcnk9	NM_001033876	f: TTGCTGGAAATCCAAGAAGAGTGTCTG r; CCAGGGAAGCAGAGATAGCACAGG
K_{2P}12.1	Kcnk12	NM_199251	f: GACGCCGCCAGCTCAATTATAGG r: AGCAGGGTGAACCGTAGAGTCC
K_{2P}13.1	Kcnk13	NM_146037	f: CCAGCCACAACGGGAGGGAAG r: AAGGTTGAAGAAGAGGATGGTACTTGC
K_{2P}18.1	Kcnk18	NM_207261	f: AATCCCTCTAATGTTCCTGGTCCTCAC r: CCGACTGTAAGCCCTGGATAAGATGG

Table 2-7. Primers for K_{2p} channels used in qRT-PCR. Both IUPHAR and HGNC names of each gene are shown. K_{2p}: tandem pore domain K^+ channel.

Name		GeneBank #	Primer Sequence (5'-3')
K_{Ca}1.1	Kcnma1	NM_010610	f: CTCCAATGAAATGTACACAGAATATCTC r: CTATCATCAGGAGCTTAAGCTTCACA
K_{Ca}2.1	Kcnn1	NM_032397	f: CATCAGCCTGTCCACTGTCATCTTG r: GTCGTCGGCACCATTGTCCAC
K_{Ca}2.2	Kcnn2	NM_080465	f: ATCTTCGGCATGTTCGGCATCG r: ATCGTGGAGAGACTGATAAGGCATTTC
K_{Ca}2.3	Kcnn3	NM_080466	f: GCTTGTCCATCCTGGTCTGTTGC r: ATGGCGGTAGAGTTGGCTGAAGTG
K_{Ca}3.1	Kcnn4	NM_008433	f: ATTCCGATCACATTCCTGACCATTGG r: TGTTTCTCCGCCTTGTTGAACTCC
K_{Ca}4.1	Kcnt1	NM_175462	f: CTGCCCTTCATCATCACGGTCTTC r: GCTGACTGTGTGCGTAGGATGG
K_{Ca}4.2	Kcnt2	NM_001081027	f: ATCCGTGTGTTGCTTGAGAAACCG r: CAATGCCACTGAGACCTGTAAACCC
K_{Ca}5.1	Kcnu1	NM_008432	f: AGACAAGATCAAGTTCTGGTTGGAGATG r: AATAATAAGAAATAAAGGTTGGCGGGATGG

Table 2-8. Primers of K_{Ca} channels used in qRT-PCR. Both IUPHAR and HGNC names of each gene are shown. K_{Ca}: calcium-activated K^+ channel.

Name		GeneBank #	Primer Sequence (5'-3')
$K_v\beta1$	Kcnab1	NM_010597	f: GCCGACCGCCTGTGTTGTG r: CGAGCGATGATAGCGACAGTGC
$K_v\beta2$	Kcnab2	NM_010598	f: GGGGTGCTAAAGTCGCAAGGG r: GTCTGCCGCAGGGAGAGTCG
$K_v\beta3$	Kcnab3	NM_010599	f: CTTGAGTCGCAAACACATCATTGAAGG r: CATAGGACTATTAGGATCTGAACGATTGGC
minK	Kcne1	NM_008424	f: TGATGGGAGACATGGGCATGATGAG r: ACAGGGAGGATGAAGAGCACACAC
MiRP1	Kcne2	NM_134110	f: CCCACTTGTGCTTGCTCAGAAGAC r: ACCCCAACAGGCTCACCTAAACC
MiRP2	Kcne3	NM_020574	f: GCCTTCCTGGTCGTAATGACAACTC r: ACATCAGATCATAGACACACGGTTCTTG
MiRP3	Kcne4	NM_021342	f: TGGAGCCTCTGAACAGCACATACC r: AGGAAAACGCCATAGAAGGACATAACG
slo$\beta1$	Kcnmb1	NM_031169	f: GCTGTATCACACGGAAGACACTCG r: CGCTGGTCTCGTTGACTTGAGG
slo$\beta2$	Kcnmb2	NM_028231	f: TGCCTGTCACTCCTATTGTCCTTCC r: CATTGATGTCACACCCTCGCTAACTC
slo$\beta3$	Kcnmb3	XM_001475546	f: CCACTCGGGACAGAAAGTGCTTC r: AGGGGAAAGTTCCATTGTTGTGATCG
slo$\beta4$	Kcnmb4	NM_021452	f: GTGCTCCTATATCCCGCCCTGTAAG r: GCAAGTGAATGGCTGGGAACCG
SUR1	Abcc8	NM_011510	f: ACTATCACAACATTGAGACCTCTAACTTCC r: TCCACCAGCAGCAGCATCCC
SUR2	Abcc9	NM_001044720	f: CTTCCTGCTGTTTATCACCTTTCCAATAC r: AACGATGCCTTCCGCTATCTCAC
KChIP1	Kcnip1	NM_027398	f: CCGATTTCTTTTCAGGGGAGGGAAG r: GGGTCGCCTTTGTTTGGTCTGC
KChIP2	Kcnip2	NM_030716	f: ACAAACCAAGTTCACACGCAGAGAG r: TTGACAATTCCGCTGGGACATTCG
KChIP3	Kcnip3	NM_019789	f: GCATACCACTGAGCAAGAGGGAAAG r: CCACTTGATTAAGCAGCAACGCATC
KChIP4	Kcnip4	NM_030265	f: CGACCGAAGAGGCAAATGTGAACG r: GGTGACATGGATGCAGATTTGTAACTGG

Table 2-9. Primers of regulatory subunits used in qRT-PCR. Both IUPHAR and HGNC names of each gene are shown. SUR: sulfonylurea receptor.

2.1.3 Electrophysiology assays

2.1.3.1 General procedures

The voltage clamp and current clamp recording was carried out in the conventional whole-cell configuration, at room temperature (15~25°C). For voltage clamp, cells were clamped at -50mV and whole-cell current was evoked by steps from -140mV to +100mV in 10mV increment for 200ms. Current was detected at 20ms after the stimulation of each voltage step. For current clamp, cells were held at I=0. Membrane potential was recorded after cells were stabilized for 5min. During recordings filter was 2kHz and sampling was 100μs.

Cells were plated in 6 well plate with glass coverslips at $2\sim3\times10^5$ cells/well. The culture duration and LPS activation method were described in section 2.1.1.5.2. Coverslips were then transferred to the recording chamber which was attached to an inverted microscope (Diaphot 300, Nikon). Patching was performed using ×40 phase contrast objective. The fine manipulation of the pipette was operated by using the mechanical and hydraulic manipulators (model MHW-3, Narishige International, Japan) which was mounted on the microscope stage. Whole-cell signal was obtained using an Axopatch-200A patch clamp amplifier (Axon Instruments, USA), a digitizer (Digidata 1320, Axon Instruments) and a computer with pClamp (v8) installed. Pipettes were pulled by a Flaming/Brown type micropipette puller (P-97, SUTTER instrument CO.) and fire polished (home-made fire polisher) every day and subsequently mounted to the headstage (CV201A, Axon instruments). To investigate the sensitivity of whole-cell current to pharmacological manipulation, cells were incubated with bath solution containing channel modulators in the electrophysiological chamber for >5min before the patching.

2.1.3.2 Solutions

Pipette and bath solutions were modified from (Pannasch *et al.*, 2006) in which the physiological K^+ gradient was applied. Bath solution (mM): 150 NaCl, 5.4 KCl, 2 $CaCl_2$, 1 $MgCl_2$, 5 HEPES (pH=7.4) and 10 D-glucose; Pipette solution (mM): 130 KCl, 2 $MgCl_2$, 2 K_2-ATP, 10 HEPES (pH=7.3), with intracellular free Ca^{2+} buffered to 10nM or 1μM by 1mM BAPTA. Osmolarity for each solution was adjusted at 290~310mosM with the pipette solution normally 10 lower than bath solution using sucrose (Kotecha & Schlichter, 1999).

2.1.3.3 Low sealing success rate on N9 cells & glass capillaries

Before performing whole-cell patching assay, optimization of cell sealing was performed. The following glasses were tested:

Borosilicate glass capillaries with filament, GC150F-7.5 (Harvard Apparatus)
Borosilicate glass capillaries with filament, GC150TF-7.5 (Harvard Apparatus)
Borosilicate glass capillaries no filament, #1409250 (Hilgenberg)
Borosilicate glass capillaries no filament, #1409249 (Hilgenberg)
Borosilicate glass capillaries no filament, #EN-1 (Garner Glass Co.)

Here either Hilgenberg (#1409250) or Harvard (GC150TF-7.5) was most suitable for N9 microglia patching. The optimal resistance of patch electrodes was 2.7±0.3MΩ. However, the optimized sealing rate was not above 7.5%.

2.1.4 Data analysis

Data statistics was processed using GraphPad Prism v5 (GraphPad Software, Inc). Statistical analysis was carried out using either Student's t-test or Anova with post-

hoc comparison test as indicated in each figure legend. Significant difference was indicated by p values of *p<0.05, **p<0.01 and ***p<0.001.

2.2 Reagents

Cell culture reagents: DMEM (#41965, GIBCO); IMDM (#21980, GIBCO); FCS (#10270, GIBCO); HBSS (#14175, GIBCO); 0.05% Trypsin-EDTA (#25300, GIBCO); PEN & STREP (#15140, GIBCO); β-MET (#3135, GIBCO).

Pharmacological reagents: LPS (vehicle H_2O, from *E. coli* 055:B5, #L6529, SIGMA); Tram34 (vehicle dimethyl sulfoxide (DMSO), #T6700, SIGMA); $BaCl_2$ (vehicle H_2O; #342920, SIGMA); GBC (vehicle DMSO, #G0639, SIGMA); PPF-hydrochloride (vehicle DMSO, #P4670, SIGMA); MgTX (vehicle DMSO, M8437, SIGMA); paxilline (vehicle DMSO, from Penicillium paxilli, #P2928, SIGMA); NS1619 (vehicle ethanol, #N170, SIGMA); NS309 (vehicle DMSO, #N8161, SIGMA); Griess reagent (#G2930, SIGMA); CellTiter 96 Aqueous One Solution Cell Proliferation Assay kit (#G3580, Promega).

Molecular reagents: RNeasy Mini Kit (#74104, QIAGEN); Transcriptor High Fidelity cDNA Synthesis Kit (#05081963001, Roche); RNAse Zap (#AM9780, Ambion); FastStart Universal SYBR Green Master (Rox) (#04813750001, Roche); primers for qRT-PCR (SIGMA)

Electrophysiological reagent: BAPTA (#196418, Calbiochem); 1M $CaCl_2$ (#190464K, BDH)

CHAPTER THREE

Optimizing Maintenance of N9 Microglial Cell Line & LPS-induced Nitric Oxide Release

3.1 Chapter introduction

3.1.1 Microglia play an important role in the CNS

As the guardian in the central nervous system (CNS), microglia regulate their environment by interacting with neighboring cells like neurons and astrocytes. During pathological conditions like external infection, microglia undergo activation and protect the CNS by releasing pro-inflammatory cytokines, recognizing and phagocytosing the invading material. As over-activated microglia may become harmful to the native cells in the CNS, they are implicated in a variety of CNS diseases like Alzheimer's disease (AD), Parkinson's disease (PD) and multiple sclerosis (MS) (Mrak & Griffin, 2005; Dheen *et al.*, 2007). Thus, microglia are an important cellular component for understanding CNS diseases.

3.1.2 N9 murine microglia cell line

The difficulties in purifying primary microglia and their maintenance of the resting state to allow systematic gene expression and functional studies led us to explore the N9 murine microglial cell line as a suitable model.

N9 murine microglia cell line has been used in >110 published studies in NCBI PubMed in the last 10 years. This cell line was constructed from the brain of embryonic day (E)13 CBA mice using the 3RV retrovirus containing an active v-myc oncogene (Righi *et al.*, 1989). As discussed in section 1.2.3.5, N9 microglia have been often utilised in the investigation of microglial activation and nitric oxide (NO) release (Zhao *et al.*, 2011; Chang *et al.*, 2008; Meng *et al.*, 2008; Wu *et al.*, 2007; Hou *et al.*, 2006; Bi *et al.*, 2005; Suuronen *et al.*, 2006; Nuutinen *et al.*, 2005; Suuronen *et al.*, 2003). However, to date electrophysiological analysis in ion channel expression in N9 microglia and their functional role have not been fully clarified.

3.1.3 Optimizing N9 microglia culture conditions

For culture *in vitro*, as microglia are very sensitive to the environment, a suitable growth medium is important to keep them in resting status. In previous studies, several different media for N9 microglial growth were used (Table 2-2). However, whether they are all suitable for keeping N9 in the resting state or there are differences in N9 properties between them is not clear. The media frequently used included the following materials: Iscove's modified Dulbecco's medium (IMDM), fetal calf serum (FCS), glutamine (GLX), penicillin (PEN), streptomycin (STREP) and β-mercaptoethanol (β-MET). PEN and STREP are both bactericidal antibiotics used to kill bacteria in the growth medium.

To determine an optimal growth medium for the subsequent research, three different growth media with components based on previous studies were examined (Table 2-3). The validation of each growth medium was determined by three steps: (1) The proliferation rate of microglia measured using cell counting. (2) The ramified level of microglia determined by comparing the length of the longest process to the diameter of cell soma. (3) The microglial NO release under each culture condition determined by the Griess reagent assay.

3.1.4 Optimizing LPS-induced activation of N9 microglia

Lipopolysaccharide (LPS) challenge has been commonly used in studies investigating N9 microglial activation (Or *et al.*, 2011; Chang *et al.*, 2008; Chang *et al.*, 2008; Wang *et al.*, 2004; Qin *et al.*, 2005; Qin *et al.*, 2004; Roy *et al.*, 2008; Huo *et al.*, 2011; Zhao *et al.*, 2011; Chang *et al.*, 2008; Meng *et al.*, 2008; Wu *et al.*, 2007; Hou *et al.*, 2006; Bi *et al.*, 2005; Suuronen *et al.*, 2006; Nuutinen *et al.*, 2005; Suuronen *et al.*, 2003). However, the dose and duration of LPS exposure as well as N9 seeding density varied widely in previous studies (Zhao *et al.*, 2011; Chang *et al.*, 2008; Meng *et al.*, 2008; Wu *et al.*, 2007; Hou *et al.*, 2006; Bi *et al.*, 2005; Suuronen

et al., 2006; Nuutinen *et al.*, 2005; Suuronen *et al.*, 2003). For example, the concentration LPS ranged from 1ng/ml to 10μg/ml, the duration of LPS challenge ranged from 6hr to 48hr and the seeding density ranged from $4\times10^4/cm^2$ to $2.7\times10^5/cm^2$ (Table 3-1). In addition, it is noteworthy that the results under some LPS challenge conditions are contradictory. For example, the use of 10μg/ml LPS has been reported several times without causing death of microglia (Suuronen *et al.*, 2006; Nuutinen *et al.*, 2005; Suuronen *et al.*, 2003), but other studies revealed that this concentration was toxic to microglia (Sivagnanam *et al.*, 2010; Zahn *et al.*, 1997). These findings indicate that although LPS has been usually used to trigger N9 activation, the microglial activation by LPS is in need of systematic analysis. There have been a limited number of publications addressing this. For instance, 0.001~10μg/ml of LPS has been tested on N9 for 18hr at seeding concentration of 8×10^4 cells/well in 96 well plate after which only 1μg/ml and 10μg/ml stimulate detectable nitrite (NO_2^-) in the supernatant (Chang *et al.*, 2008). N9 cells treated by 5μg/ml LPS for 6hr, 12hr and 24hr induced about 2μM, 5μM and 15μM NO_2^- in the supernatant (Suuronen *et al.*, 2006) while 10μg/ml LPS treated N9 cells for 12hr and 24hr and induced about 2μM and 18μM NO_2^- (Suuronen *et al.*, 2003). However, when examining the relationship between LPS treatment and NO release it is necessary to consider the cell seeding density, LPS concentration and LPS challenge duration at the same time. Thus the relationship between these three elements on N9 microglial NO release was tested aiming to generate a consistent activation protocol for the following experiments.

3.1.5 Working hypothesis

In this chapter, the hypothesis that microglial NO release depends on LPS concentration, LPS treatment duration and N9 microglial seeding density will be tested.

Con.	Time	Seeding density (cells/well)	References
1~10ng/ml	18hr	8×10^4; 96 well plate	(Chang *et al.*, 2008)
1μg/ml	24hr or 48hr	5×10^4; 96 well plate	(Zhao *et al.*, 2011)
1μg/ml	24hr	3×10^4; 96 well plate	(Hou *et al.*, 2006; Bi *et al.*, 2005)
1μg/ml	48hr	3×10^4; 96 well plate	(Wu *et al.*, 2007)
1μg/ml	48hr	5×10^4; 96 well plate	(Meng *et al.*, 2008)
10μg/ml	6hr 12hr or 24hr	2×10^5; 24 well plate	(Suuronen *et al.*, 2006)
10μg/ml	12hr or 24hr	4×10^4 cells/cm^2	(Suuronen *et al.*, 2003)
10μg/ml	24hr	2×10^5; 12 well plate	(Nuutinen *et al.*, 2005)

Table 3-1. A variety of N9 microglial activation methods by LPS. The concentration (1ng/ml~10μg/ml), culture duration (6~48hr) and the N9 cell seeding density varied considerably among different *in vitro* studies.

3.1.6 Aims to be addressed in this chapter

3.1.6.1 What is the status of N9 cells in different growth media?

Based on previous studies, three growth media were created and analyzed, namely, GM[0], GM[1] and GM[2] (Table 2-3). The basal medium for GM[0] is Dulbecco's Modified Eagle Medium (DMEM) while GM[1] and GM[2] are IMDM. In addition, GM[1] includes extra β-MET compared to GM[2]. The morphology of N9 cells were examined by comparing the length of the longest process to the diameter of soma as resting microglia have long process and small soma. In addition it was questioned whether the proliferation rate of N9 cells was different in different growth media. This was measured using cell counting. Besides morphology and proliferation, it was investigated whether N9 cells were activated in these growth media in the absence of LPS. The NO released by microglia was measured as NO_2^- concentration in the supernatant using the Griess reagent assay.

3.1.6.2 What is the relationship between LPS exposure and microglial status?

In previous studies, LPS-induced microglial NO release was widely used as a microglial activation model. However, the relationship between LPS concentration, culture duration, microglial seeding density and NO release has not been fully examined. To examine this question, a series of LPS challenge conditions was applied. LPS concentration ranged from 10ng/ml to 1μg/ml. LPS culture time ranged from 12hr to 48hr. In addition, a series of microglial seeding density was applied.

3.2 Results

3.2.1 Cell proliferation under three different growth media

N9 cells were seeded into 25cm^2 flasks at the same density (2.5×10^5 cells/flask) using different growth media of same volume: GM[0], GM[1] and GM[2] (Table 2-3) and cells were cultured for up to 120hr without replacing the growth medium. Details of the procedure are described in Chapter 2. Cell confluency increased under different growth media and was different after 72hr of culture and this difference became more obvious at 120hr of culture (Figure 3-1).

After 72hr of culture, cells at six locations of each 25cm^2 flask were counted. Cells in GM[0] displayed a significant reduction which was ~36.8% of the cell number compared to GM[1] and GM[2]. The cell number of N9 cells cultured in GM[1] and GM[2] displayed no difference with each other (Figure 3-2).

3.2.2 Morphology of N9 cells in three different growth media

Activated microglia display amoeboid morphology while resting microglia display ramified morphology. To determine the status of microglia in these growth media, the morphology of cells was analyzed first.

To avoid cell contact which can influence cell morphology, the measurement was performed at 24hr of culture. No latter than this stage, cells in each growth medium began to form long processes while part of them still displayed round soma with short processes (Figure 3-3A). The mean diameter of soma and length of the longest process of each cell were them measured (Figure 3-3). The result indicated that cells in GM[0] and GM[1] displayed similar diameter of soma which were 17.5±0.2μm and 17.2±0.2μm. Cells in GM[2] growth medium displayed significantly smaller soma at 16.7±0.2μm compared to GM[0]. For the length of process, cells in GM[1]

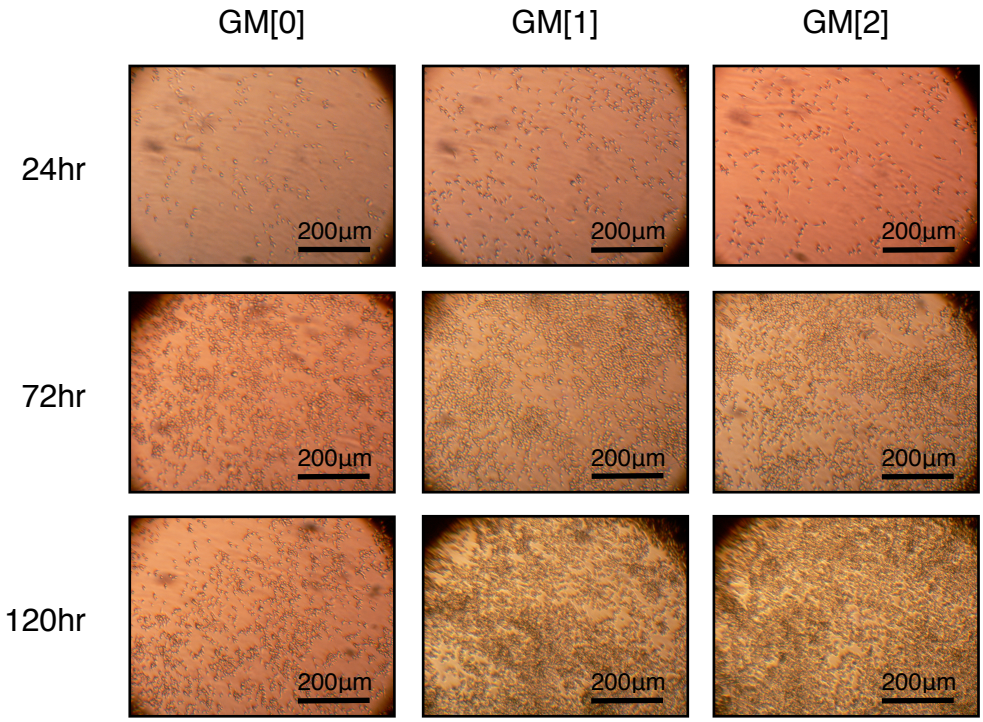

Figure 3-1. Representative photographs of N9 cells cultured in different growth media for 24hr~120hr. Same amount (2.5×10^5 cells/flask) of N9 cells were seeded into three 25cm^2 flask cultured in same volume of GM[0], GM[1] and GM[2] for up to 120hr without replacing the growth medium. The proliferation rate in GM[0] was slower than in GM[1] and GM[2].

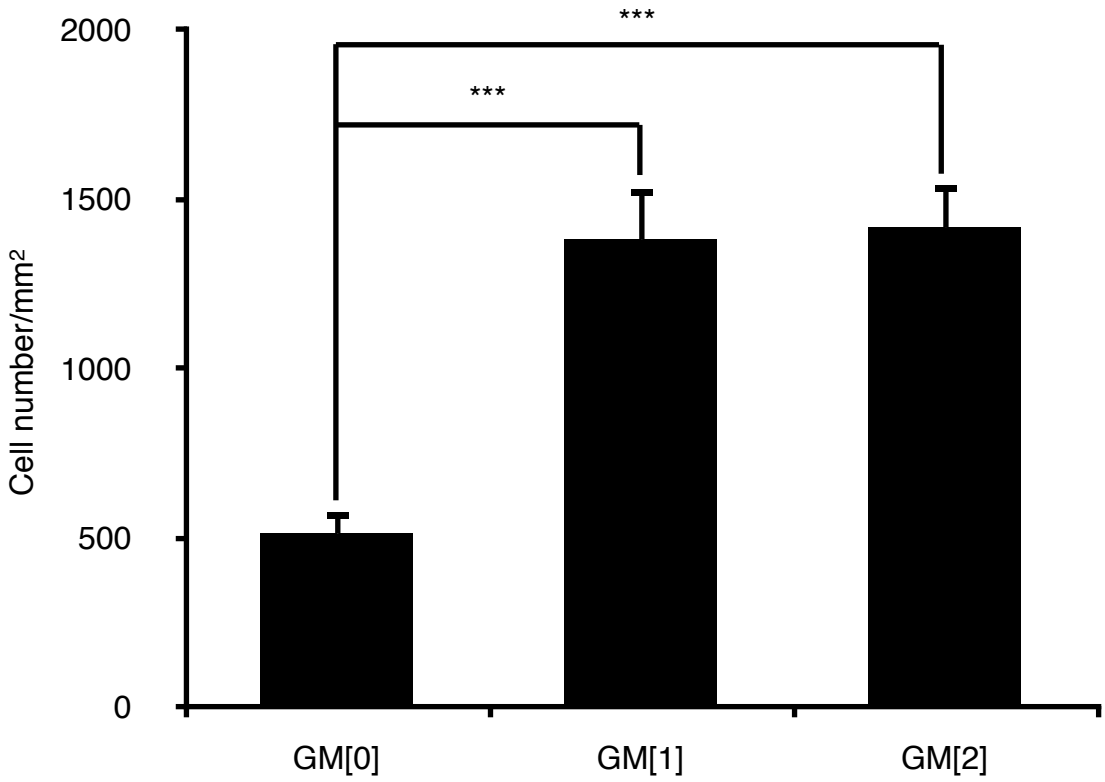

Figure 3-2. Quantification of cell number at 72hr after seeding. On day 3 (72hr) cell density of each culture condition was: GM[0] 515±63.9/mm^2, GM[1] 1381±150.8/mm^2 and GM[2] 1416±133.0/mm^2. N9 cells in GM[0] proliferated slower than GM[1] and GM[2] while GM[1] and GM[2] had no difference on the N9 microglial proliferation rate. Data are given as mean ±SEM. ***$p<0.001$ to GM[0], by ANOVA with Tukey post hoc test. (n=6)

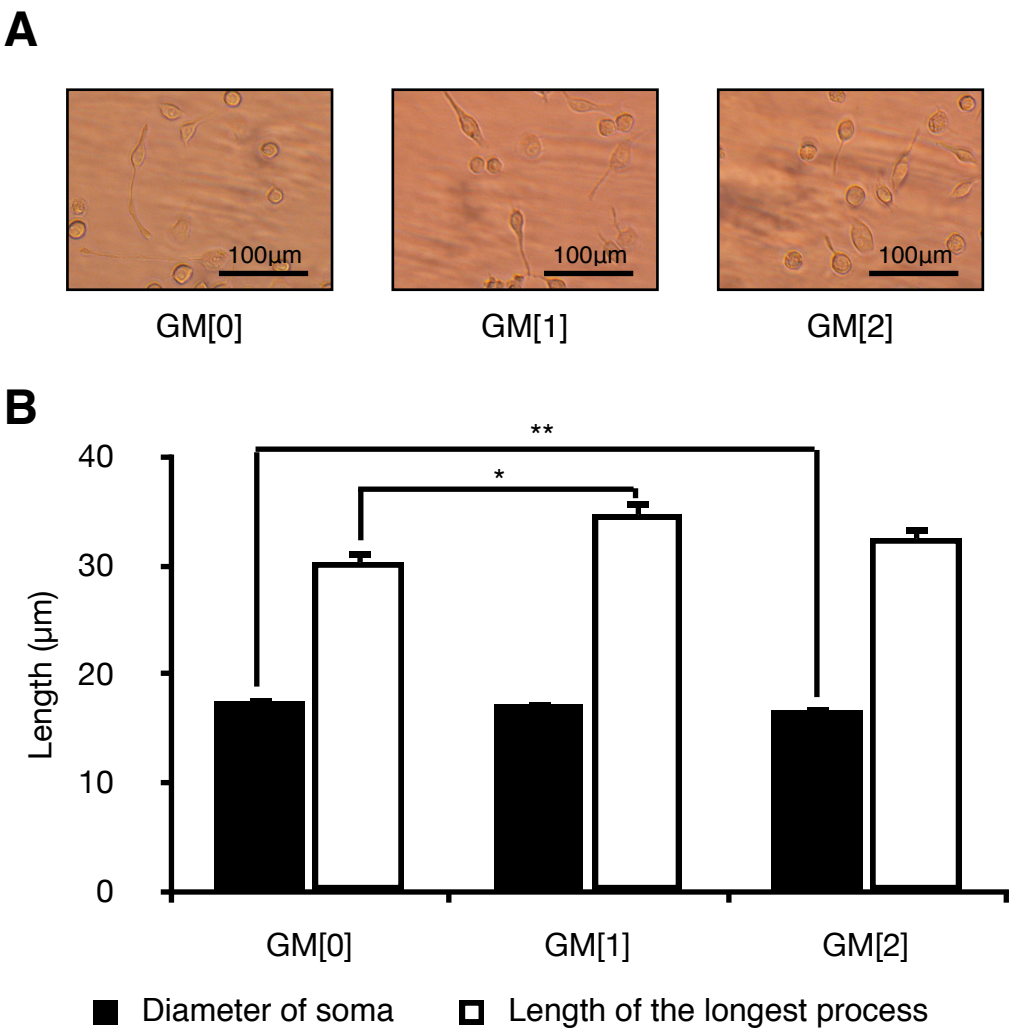

Figure 3-3. Microglial morphology in different growth media. (**A**) Images of N9 cells at 24hr of culture in three different growth media. Cells began to expand by extending their processes no latter than this stage. (**B**) At this stage, the diameter of soma and length of the longest process of each cells were measured. The diameters of cell soma in each growth medium were: GM[0]=17.5±0.2µm, GM[1]=17.2±0.2µm and GM[2]=16.7±0.2µm. The lengths of the of process were: GM[0] 30.3±1.1µm, GM[1]: 34.7±1.3µm and GM[2]: 32.5±1.0µm. Cells in GM[0] had the larger soma and shorter process while there was no difference between cell morphology in GM[1] and GM[2]. Data are given as mean±SEM. *p<0.05, **p<0.01, by ANOVA with Tukey post hoc test. ($n_{GM[0]}$=300, $n_{GM[1]}$=296, $n_{GM[2]}$=407)

and GM[2] had similar length processes at 34.7±1.3μm and 32.5±1.0μm while cells in GM[0] had significantly shorter processes at 30.3±1.1μm compared to GM[1] (Figure 3-3B).

As the proportion of ramified microglia may be different in each growth medium, the ratio between the length of the longest process and the diameter of soma of each cell was then determined. Cells in GM[0] displayed the smallest ratio while GM[1] and GM[2] were similar (Figure 3-4). To obtain a more direct understanding on the proportion of ramified microglia in the culture, the proportion whose process was two times longer than or equal to the diameter of the soma were calculated (Kozlowski & Weimer, 2012) of which cells in GM[1] displayed the highest value of 38.5% and cells in GM[0] displayed the lowest at 30.0% (Figure 3-4).

3.2.3 The microglial NO release in three different growth media

Besides the morphological examination, microglial resting status in different growth media was also compared through the microglial NO release. At 120hr of culture, the supernatant was collected for Griess reagent assay. None of the supernatant had detectable NO_2^- level which meant N9 cells in any growth medium did not release significant NO during the whole culture process (data not shown).

3.2.4 Seeding amount and microglial NO release

Cells in GM[0] displayed most larger cell soma and most shorter process (Figure 3-3), GM[0] was not suitable for N9 microglial maintenance. GM[1] and GM[2] did not display much difference from each other. Because GM[1] was more commonly used in previous publications (Table 2-2) (Meng *et al.*, 2008; Wu *et al.*, 2007; Hou *et al.*, 2006; Bi *et al.*, 2005; Cavaliere *et al.*, 2005), it was used for the subsequent assays. The relationship between cell number and LPS-induced microglial NO

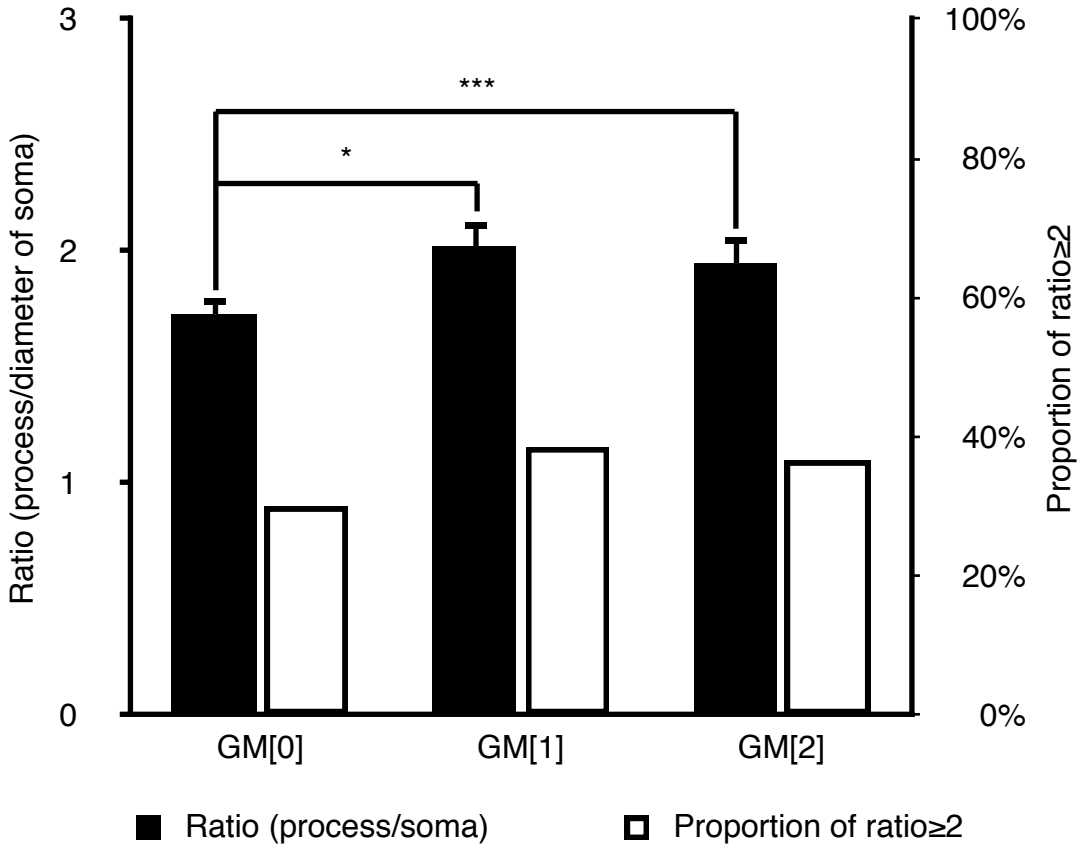

Figure 3-4. The ratio of process/soma and the proportion of ramified cells in three growth media. At 24hr after plating, the ratios of process vs. diameter of soma for cells in different growth medium were: GM[0]=1.7±0.1, GM[1]=2.0±0.1 and GM[2]=2.0±0.1. The proportion of cells whose process were not less than twice the diameter of soma were: GM[0]=30%, GM[1]=39% and GM[2]=37%. Data are given as mean±SEM. *p<0.05, ***p<0.001, by ANOVA with Tukey post hoc test. ($n_{GM[0]}$=300, $n_{GM[1]}$=296, $n_{GM[2]}$=407)

release was first examined. Serial dilutions of N9 cells (0~2×10^5 cells/well; 24 well plate) were seeded and cells were cultured for 24hr before LPS was applied (1μg/ml; 24hr). NO release increased dramatically above the seeding density of 2.5×10^4 cells/ well after which the NO release and the cell density displayed a near linear relationship (Figure 3-5). Thus the seeding density in the range from 2.5×10^4 cells/ well to 2×10^5 cells/well on 24 well plate was suitable for the N9 microglial NO release. The detail of seeding density on different culture vessels is indicated in Table 2-1.

3.2.5 Time course and dose response of LPS-induced NO release

The cells were cultured for up to 48hr. At 0hr, 12hr, 24hr, 36hr, 48hr after seeding, LPS with different concentrations (0ng/ml, 10ng/ml, 100ng/ml, 1μg/ml) were applied.

The results indicated that following LPS application, the NO_2^- concentration in the supernatant increased in the first 12hr, reached a plateau within 12hr~36hr, and displayed a dropping phase after 36hr of LPS challenge until 48hr (Figure 3-6).

In addition, NO was released in a dose-dependent manner by LPS. Under any LPS challenge duration, 1μg/ml LPS always triggered the most NO released while 10ng/ml of LPS always induced the least NO release (Figure 3-6 and Figure 3-7). Using 1μg/ml of LPS, the peak value appeared between 24hr or 36hr (Figure 3-7). There was no significant difference between these two values, (Figure 3-6), thus 1μg/ml for 24hr of LPS was chosen for N9 microglial activation.

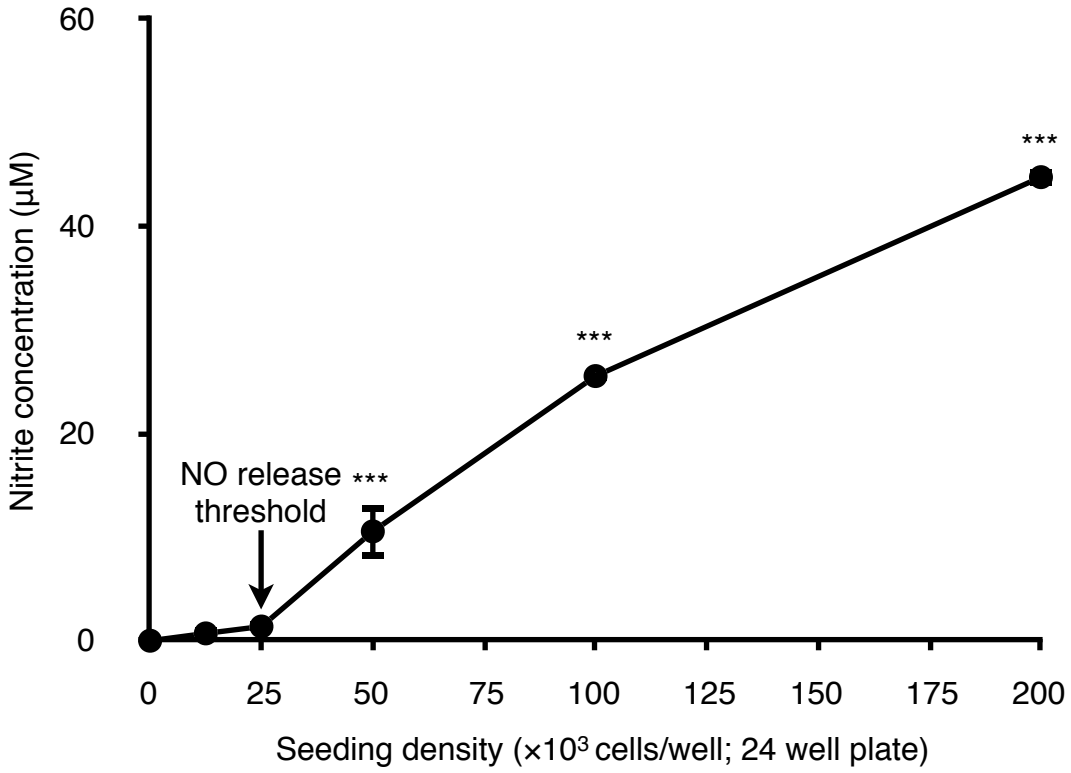

Figure 3-5. The seeding density of N9 cells and LPS-induced microglial NO release. Cells were cultured in 24 well plate for 24hr before the application of 1μg/ml LPS for another 24hr. There was a threshold of 2.5×10^4 cells/well before the detectable nitric oxide (NO) release. When seeding density was over this threshold the nitrite (NO_2^-) concentration, they displayed a near linear relationship with seeding density. Data are given as mean±SEM. ***$p<0.001$ vs. the preceding value, by ANOVA with Tukey post hoc test. Error bars are within the symbol unless otherwise shown. (N=4)

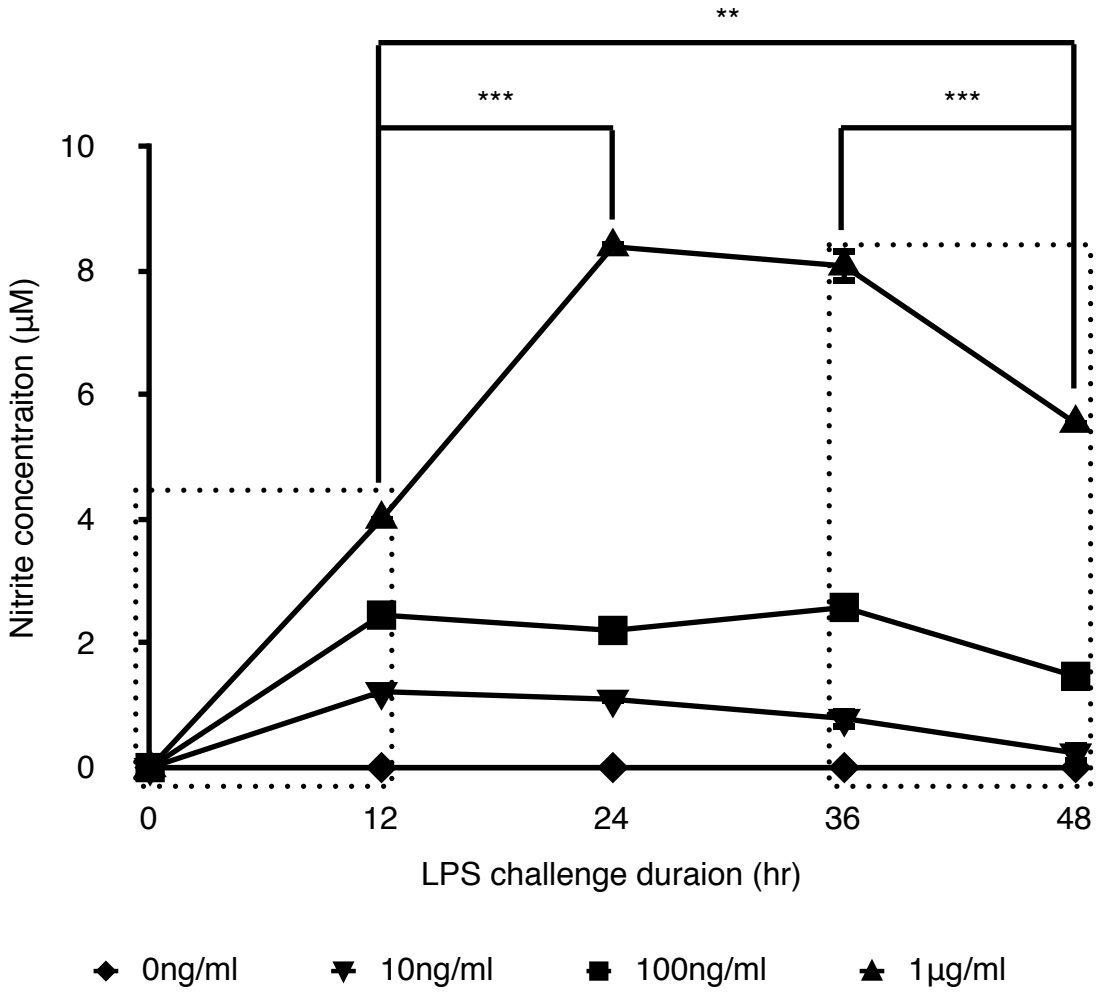

Figure 3-6. Time course of LPS challenge on N9 microglial NO release. Same amount of cells were challenged with different concentrations of LPS (0~1μg/ml) and duration (0~48hr). Nitrite began to accumulate in the supernatant during the first 12hr of LPS challenge (left dotted rectangle). The application of 1μg/ml LPS always induced the most abundant nitrite in the supernatant and there was a plateau at around 24hr to 36hr culture duration. The nitrite concentration began to decrease after around 36hr of culture (right dot rectangle). Data are given as mean±SEM. **p<0.01, ***p<0.001, by ANOVA with Tukey post hoc test. Error bars are within the symbol unless otherwise shown. (n=3)

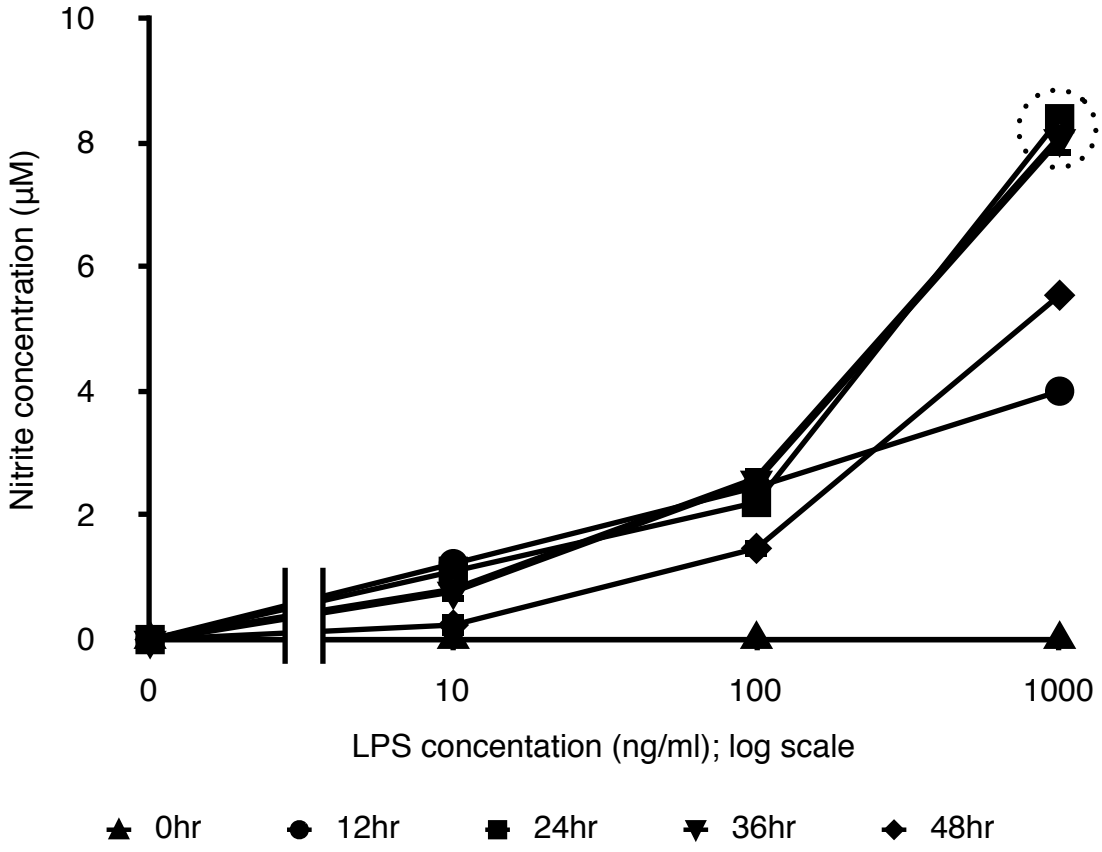

Figure 3-7. Dose-dependent effect of LPS on microglial NO release. Data presented in Figure 3-6 are re-plotted to reveal the dose-dependent effect of LPS-induced microglial NO release. 24hr and 36hr of 1μg/ml LPS stimulation induced peak nitrite concentration in the supernatant (dotted circle). Data are given as mean±SEM. Error bars are within the symbol unless otherwise shown. (n=3)

3.3 Discussion

3.3.1 N9 cells displayed higher proliferation rate in IMDM than DMEM

As indicated by the result the cells in GM[0] proliferate slower than ones cultured in either GM[1] or GM[2] while cells in GM[1] and GM[2] have the same growth rate. The main difference between GM[0], GM[1] and GM[2] is the basal medium. As indicated in the introduction, the basal medium used was DMEM (excl. GLX) for GM[0], and IMDM (incl. GLX) for GM[1] and GM[2]. Thus the difference probably results from the basal medium.

IMDM was originally designed for the culture of lymphocytes (Iscove & Melchers, 1978) which in addition was suitable for cell proliferation in *in vitro* cultures. Compared to DMEM, IMDM contains extra selenium, sodium pyruvate and other components like amino acids and vitamins. Here selenium may provide an essential trace element to N9 cells and incorporate into enzymes which then display antioxidant functions and protect cells against harmful oxidative damage from peroxides such as organic hydroperoxides and peroxynitrites in the growth medium. Sodium pyruvate is commonly used as an energy source in the culture medium and similar to selenium it also provides an antioxidant effect (Giandomenico *et al.*, 1997). GLX included in the IMDM medium is one non-essential amino acid (Fürst & Stehle, 2004) and it is also the only amino acid which can directly cross the blood-brain barrier (BBB) (Reeds, 2000). Including GLX in the medium may thus mimic the CNS environment to the microglia culture *in vitro*. In addition, GLX also participates in DNA synthesis, protein synthesis, division of immune cells and energy support to the brain. The advantage of IMDM compared to DMEM for N9 cell proliferation may thus come from these elements which protected and facilitated the microglial growth in the culture.

3.3.2 N9 cells in DMEM displayed reduced ramified morphology

Cells in DMEM not only displayed a low proliferation rate but also a less ramified morphology with larger soma and shorter processes. Only 30% cells in GM[0] displayed long process as twice the diameter of soma compared to 39% in GM[1] and 37% in GM[2]. As indicate above, the extra components in IMDM, such as selenium protected cells from reactive oxygen species (ROS) damage. Cells cultured in medium without such protected mechanism may display a more activated status, but this was not a fully activated status due to there was no NO_2^- detected in any growth medium. Microglial status is associated with their morphology and this may explain why there were fewer ramified cells cultured in DMEM than the ones in IMDM. As keeping microglia in a resting status during *in vitr*o culture was the aim of the experiment, the medium GM[0] and GM[1] may be the most optimal medium.

3.3.3 β-MET did not affect cell proliferation and morphology in the IMDM based growth medium

Cells cultured in GM[1] and GM[2] did not display significant difference in proliferation rate, diameter of soma, length of process or the ratio of process/soma. As indicated above β-MET was the only the difference between GM[1] and GM[2] (Table 2-3). Functionally β-MET provides a similar antioxidant effect as selenium to cells. However, as IMDM already included the antioxidant components, the effect of β-MET may not induce a sufficient influence to the cells. However, besides the antioxidant effect β-MET also promotes the uptake of cysteine from the medium and facilitates immune system function, like T lymphocyte-dependent immune response (Heidrick *et al.*, 1984). As microglia belong to the monocytes/macrophages lineage and in previous studies the GM[1] was the most commonly used recipe for N9 cell culture *in vitro* (Table 2-2) (Meng *et al.*, 2008; Wu *et al.*, 2007; Hou *et al.*, 2006; Bi *et al.*, 2005; Cavaliere *et al.*, 2005), GM[1] was used as our growth medium for N9 murine microglia.

3.3.4 There was a minimum seeding density of N9 to trigger abundant NO release

Results indicated that when the seeding density was over 2.5×10^4 cells/well on a 24 well plate NO_2^- concentration in the supernatant was significantly increased (Figure 3-5). This means there was a threshold of cell density over which abundant NO will be released and detected in our assay. Such density-dependent LPS-induced microglial activation may be due to cell to cell communication through gap junctions (Newman, 2001). Microglia form gap junctions (Dobrenis *et al.*, 2005) and inositol trisphosphate ($InsP_3$) may pass through to induce the release of Ca^{2+} from endoplasmic reticulum (ER) stores (Newman, 2001; Scemes & Giaume, 2006). The elevated intracellular Ca^{2+} concentration ($[Ca^{2+}]_i$) may then regulate Ca^{2+}-dependent phosphorylation pathways, regulate activity of nuclear factor kappa-light-chain-enhancer of activated B cells (NFκB), produce inducible nitric oxide synthase (iNOS) and NO.

Above the threshold density it was a near linear relationship between NO release and cell density at least in the range between 2.5×10^4~2×10^5 cells/well on 24 well plate. By normalizing cell amount to the area of 24 well which is $1.9cm^2$ (Table 2-1), the suitable seeding density for LPS-induced microglial NO release was from $1.3\times10^4/cm^2$ to $1.1\times10^5/cm^2$.

3.3.5 Time- and dose-dependent effect of LPS-induced NO release

Activated microglial NO release displayed a time- (Figure 3-6) and dose-dependent (Figure 3-7) manner to LPS treatment. The time course of LPS-induced NO release did not display a linear relationship. However, there was an increasing phase at around 12hr of culture, a plateau at around 24~36hr before a decreasing phase beginning at around 36hr of culture (Figure 3-6). The mechanism why the NO_2^- concentration began to drop at longer culture durations with LPS was not clear.

Similar phenomenon indicated that LPS-induced pro-inflammatory mRNA expression, including iNOS mRNA, decreased at around 48hr (Nikodemova & Watters, 2011) and NFκB has a time-dependent inactivation phenomenon which was supposed to the decreased binding activity of the transcription factor (Granado-Serrano *et al.*, 2010). In addition, LPS-induced microglial activation may desensitize over a long periods (Nörenberg *et al.*, 1992).

Microglial activation displayed a dose-dependent of LPS application at least within the range of 10ng/ml~1μg/ml. Similar phenomenon was observed in previous studies as well (Chang *et al.*, 2008). Here 1μg/ml for either 24hr or 36hr of LPS induced most abundant NO release. As 36hr may be included in the decreasing phase (Figure 3-6), 1μg/ml for 24hr was chosen as the LPS activation for the subsequent N9 microglial *in vitro* studies here.

3.3.6 Conclusion

Here the optimal growth medium for N9 cell *in vitro* culture was determined which consists of IMDM (including 4mM GLX), 5% FCS, 100μg/ml STREP, 100U/ml PEN, and 50μM β-MET. In addition, the optimal cell seeding density, LPS concentration and LPS challenge duration for N9 cell activation were systematically examined. Thus the activation protocol for subsequent assays on N9 cells was: Seeding density was 1.3×10^4~$1.1\times10^5/cm^2$ for 24hr before the application of 1μg/ml LPS and culture with LPS for another 24hr. This provided a reliable and efficient microglial activation model for the following experiment.

CHAPTER FOUR

Potassium Channel mRNA Expression in N9 Microglial Cell Line

4.1 Chapter introduction

4.1.1 Ion channels expressed in microglia

Microglia have been reported to express a variety of ion channels including calcium (Ca^{2+}) channels, potassium (K^+) channels, proton (H^+) channels, sodium (Na^+) channels, chloride (Cl^-) channels as well as a variety of ion pumps (Färber & Kettenmann, 2005; Eder, 2005; Kettenmann *et al.*, 2011). Ions play important roles in regulating cellular functions like maintaining the resting membrane potential, cellular migration, proliferation, intracellular phosphorylation pathways and intercellular signal transduction. The expression of ion channels was believed to be associating with the microglial status (Kotecha & Schlichter, 1999; Boucsein *et al.*, 2000; Kettenmann *et al.*, 1990; Nörenberg *et al.*, 1992; Nörenberg *et al.*, 1994; Chung *et al.*, 1999; Boucsein *et al.*, 2003; Schilling & Eder, 2007; Boucsein *et al.*, 2003; Kettenmann *et al.*, 1990; Ducharme *et al.*, 2007; X. Jiang *et al.*, 2003) which can be modulated by exposure to various agents like lipopolysaccharide (LPS), lysophosphatidylcholine (LPC), tumor necrosis factor alpha (TNFα) or adenosine triphosphate (ATP). Thus studies on the expression pattern of ion channels may provide insight into microglial activation.

4.1.2 K^+ channels play important roles in regulating cellular properties

As one of the largest families of ion channels, K^+ channels include four major types including calcium-activated K^+ channels (K_{Ca}), inwardly rectifying K^+ channels (K_{ir}), tandem pore domain K^+ channels (K_{2p}) and voltage-gated K^+ channels (K_v). K^+ channels set the resting membrane potential, regulate neuronal action potentials, modulate physiological functions of cardiac muscle, maintain vascular tone and regulate the secretion of hormone. They also play important roles in the immune system (Mullen *et al.*, 2006; Cahalan *et al.*, 2001; Koo *et al.*, 1997; Ahluwalia *et al.*, 2004), central nervous system (CNS) inflammation and neuronal degenerative

diseases (Judge *et al.*, 2006). Thus investigation of microglial K^+ channel functions may provide new pathways for treatment of CNS-related diseases.

4.1.3 Microglial K^+ channel expression in the published data

Microglia are very sensitive to the extracellular K^+ (Gehrmann *et al.*, 1995) as they express K^+ channels which regulate homeostasis of the intracellular and extracellular K^+. K^+ channels found in microglia include $K_v1.1$ (Wu *et al.*, 2009), $K_v1.2$ (Li *et al.*, 2008b; Fordyce *et al.*, 2005; Kotecha & Schlichter, 1999), $K_v1.3$ (Küst *et al.*, 1999; Kotecha & Schlichter, 1999; Khanna *et al.*, 2001; Fordyce *et al.*, 2005; Pannasch *et al.*, 2006), $K_v1.5$ (Pannasch *et al.*, 2006; Khanna *et al.*, 2001; Fordyce *et al.*, 2005; Kotecha & Schlichter, 1999), $K_v1.6$ (Kotecha & Schlichter, 1999), G protein-coupled inwardly-rectifying K^+ channels (GIRKs) (Ilschner *et al.*, 1996; Ilschner *et al.*, 1995), human ether-a-go-go-related gene (HERG) channels (Zhou *et al.*, 1998), large conductance Ca^{2+}-sensitive and voltage-activated K^+ channels (BK) (McLarnon *et al.*, 1997; McLarnon *et al.*, 1995; Schilling *et al.*, 2002), small conductance Ca^{2+}-activated K^+ channels (SK) family members (Khanna *et al.*, 2001; Kaushal *et al.*, 2007; Eder, Klee & Heinemann, 1997b; Khanna *et al.*, 2001), intermediate conductance Ca^{2+}-activated K^+ channels (IK) (Kaushal *et al.*, 2007; Khanna *et al.*, 2001; Schilling *et al.*, 2002; Schilling, Stock, *et al.*, 2004b; Schilling, Lehmann, *et al.*, 2004a; Eder, Klee & Heinemann, 1997a), $K_{ir}1.1$ (Küst *et al.*, 1999), $K_{ir}2.1$ (Schilling *et al.*, 2000), $K_{ir}6.1$ (Ortega *et al.*, 2012) and $K_{ir}6.2$ (Ortega *et al.*, 2012). The expression of these K^+ channels was based on analysis at gene level, protein level or functional characterization of ionic currents (Table 4-1). The ionic currents of both $K_v1.5$ and $K_v1.3$ can be enhanced by LPS treatment (Pannasch *et al.*, 2006) while $K_v1.3$ expression, but not $K_v1.5$ was increased by external TGFβ (Schilling *et al.*, 2000). Change in gene expression may not link to the expression change of protein for example mRNA of $K_v1.3$ was upregulated by external LPS which did not change the protein expression (Fordyce *et al.*, 2005). Findings on gene expression of K^+ channels were controversial. For example, expression of $K_v1.1$ was found in

Channels	Species preparation	Reference
$K_v1.1$	mice: BV-2 cell line rat: brain slice	(Wu *et al.*, 2009)
$K_v1.2$	mice: BV-2 cell line rat: cultured primary cells brain slice	(Li *et al.*, 2008a; Fordyce *et al.*, 2005; Kotecha & Schlichter, 1999)
$K_v1.3$	rat: cultured primary cells mice: brain slice cultured primary cells BV-2 cell line	(Cayabyab *et al.*, 2000; Visentin *et al.*, 2001; Chung *et al.*, 2001a; Schilling & Eder, 2007; Kotecha & Schlichter, 1999; Fordyce *et al.*, 2005; Khanna *et al.*, 2001; Pannasch *et al.*, 2006; Küst *et al.*, 1999; Schilling *et al.*, 2000)
$K_v1.5$	mice: cultured primary cells rat: cultured primary cells	(Pannasch *et al.*, 2006; Jou *et al.*, 1998; Khanna *et al.*, 2001; Chung *et al.*, 2001a; Fordyce *et al.*, 2005; Kotecha & Schlichter, 1999)
$K_v1.6$	rat: cultured primary cells	(Kotecha & Schlichter, 1999)
$K_v11.1$	rat: MSL-9 cell line	(Zhou *et al.*, 1998)
BK	human: cultured primary cells bovine: cultured primary cells mice: brain slice BV-2 cell line cultured primary cells	(McLarnon *et al.*, 1995; Schilling & Eder, 2007; McLarnon *et al.*, 1997; Schilling *et al.*, 2002)
SK2	rat: cultured primary cells	(Khanna *et al.*, 2001)
SK3	rat: cultured primary cells	(Khanna *et al.*, 2001; Schlichter *et al.*, 2010)
SK1~3	mice: cultured primary cells rat: cultured primary cells	(Eder, Klee & Heinemann, 1997b; Khanna *et al.*, 2001)
SK4	rat: cultured primary cells mice: cultured primary cells	(Khanna *et al.*, 2001; Schilling *et al.*, 2002; Schilling, Stock, *et al.*, 2004b; Schilling, Lehmann, *et al.*, 2004a; Kaushal *et al.*, 2007)
$K_{ir}1.1$	rat: cultured primary cells	(Küst *et al.*, 1999)
$K_{ir}2.1$	mice: BV-2 cell line	(Schilling *et al.*, 2000)
GIRKs	mice: cultured primary cells	(Ilschner *et al.*, 1996; Ilschner *et al.*, 1995)
$K_{ir}6.1$	mice: BV-2 cell line	(Ortega *et al.*, 2012)
$K_{ir}6.2$	mice: BV-2 cell line rat: brain slice	(Ortega *et al.*, 2012)
SUR1	mice: BV-2 cell line rat: brain slice	(Ortega *et al.*, 2012)
SUR2B	rat: brain slice	(Ortega *et al.*, 2012)

Table 4-1

Table 4-1. Microglial K^+ channel expression in previous studies. Evidence for K^+ channel expression in primary or microglial cell lines. Data are based on gene, protein or current detection of K^+ channels. K_v: voltage-gated potassium channel; K_{ir}: inwardly rectifying potassium channel; SK: small-conductance calcium-activated K^+ channels; BK: large conductance calcium-sensitive and voltage-activated K^+ channels; GIRKs: G protein-coupled inwardly-rectifying potassium channels; SUR: sulfonylurea receptor.

microglia in brain slices from rat of postnatal day (P)1~P10 (Wu *et al.*, 2009), but in cultured rat primary microglia from P5~P14, the $K_v1.1$ mRNA was not detectable (Kotecha & Schlichter, 1999).

4.1.4 K^+ channel expression in microglia needs systematic examination

As shown before, expression of several K^+ channels has been found in microglia, but a systematic screen of all K^+ channels, which includes four families and >80 members, has not been addressed. In addition the expression of several K^+ channels remains controversial such as $K_v1.1$, $K_v1.3$ which were described previously. The discrepancies may result from the differences of cellular preparation as microglia are very sensitive to their environment which lead to changes in trafficking and expression of channels (Kotecha & Schlichter, 1999). Thus, to investigate K^+ channels in microglia, it becomes necessary and important to screen the expression of K^+ channels using a systematic and unified cellular preparation method. This will offer a huge benefit on the understanding of K^+ expression in microglia and facilitate the investigation in the future.

4.1.5 Working hypothesis

In this chapter, the mRNA expression pattern of K^+ channels in the N9 microglial cell line will be examined under control conditions and the LPS treatment.

4.1.6 Aims to be addressed in this chapter

4.1.6.1 What is the expression pattern of K^+ channels in resting microglia?

Based on the optimized cellular preparation described in Chapter 3, mRNA expression of >80 K^+ channel subunits in resting N9 microglia were examined using quantitative reverse transcription polymerase chain reaction (qRT-PCR). Subunits included the pore-forming subunits and regulatory subunits of four K^+ families. The four families included K_v, K_{ir}, K_{Ca} and K_{2p}. Primers for qRT-PCR were listed in Chapter 2 (Table 2-4 to Table 2-9).

4.1.6.2 The effect of LPS on K^+ channel expression.

Beside the K^+ channel expression in resting N9 microglia, changes in mRNA expression in activated microglia by LPS (1μg/ml, 24hr) were examined as well. The cellular preparation was identical to resting microglia in an attempt to have a standardized experiment model to generate comparable conditions for the expression of different K^+ channels in resting and activated microglia.

4.2 Results

4.2.1 Stability of β-actin expression in microglia

Due to the MIQE guidelines regarding the general procedure of qRT-PCR experiments (Bustin *et al.*, 2009), use of a housekeeping gene for normalization in the experiment requires that its expression is not influenced by the condition of the experiments.

Thus before detecting the K^+ channel expression, it was necessary to make sure the housekeeping gene, β-actin, did not change before and after LPS treatment. Its mRNA expression was tested in the resting N9 cells and LPS-activated N9 cells. Ct value of β-actin of each sample was normalised to the relative input cDNA concentration. The expression of β-actin was not influenced by LPS stimulation (Figure 4-1A) and during every round of qRT-PCR experiments the stability of β-actin expression was confirmed as well.

4.2.2 Confirmation of LPS-induced N9 microglial activation

For every qRT-PCR experiment, microglial activation and control (resting) condition was confirmed using Griess reagent assay. It was confirmed that cells treated with LPS (1μg/ml, 24hr) were activated as nitrite (NO_2^-) was detected in the supernatant while cells without LPS treatment did not release detectable nitric oxide (NO) (Figure 4-1B).

4.2.3 Overview of K^+ channel expression in microglia

As the expression of β-actin was stable with or without LPS treatment, the K^+ channel expression in both resting microglia and LPS-activated microglia was

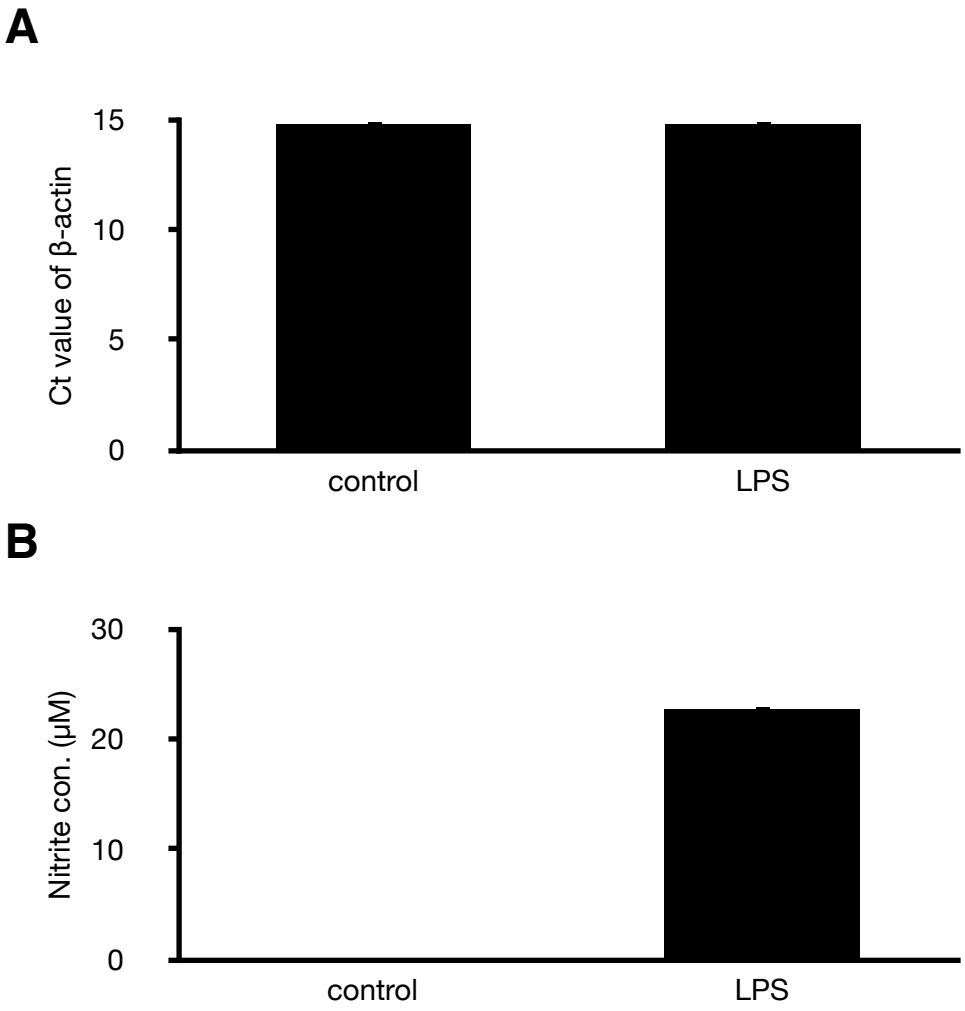

Figure 4-1. Effect of LPS on the expression of β-actin and N9 microglial activation. During each qRT-PCR assay, N9 cells were either activated by lipopolysaccharide (LPS) or treated by vehicle as a control. (**A**) β-actin expression was not significantly regulated by LPS treatment. The data presented is the Ct value of β-actin normalised to input cDNA concentration. There was no significant difference between the expression of β-actin in LPS treated microglia and resting microglia. (**B**) With Griess reagent assay, it was confirmed that LPS is able to activate N9 microglia while resting microglia (control) did not release NO. Data are given as mean±SEM. (n_A=24, n_B=3)

normalised to the relative β-actin expression.

4.2.3.1 Expression pattern of K^+ channels in N9 cells

Totally 82 subunits were examined including the pore-forming subunits of the K_v family, K_{2p} family, K_{Ca} family, K_{2p} family and the regulatory subunits of K^+ channels (Figure 4-2). There were 17 out of the 82 subunits whose mRNA expression was not detectable. These subunits included Kcna2 (K_v1.2), Kcnb2 (K_v2.2), Kcnq2 (K_v7.2), Kcnq4 (K_v7.4), Kcnq5 (K_v7.5), Kcns1 (K_v9.1), Kcnh2 (K_v11.1), Kcnk13 (K_{2p}13.1), Kcnj5 (K_{ir}3.4), Kcnj10 (K_{ir}4.1), Kcnj16 (K_{ir}5.1), Kcnj8 (K_{ir}6.1), Kcnj11 (K_{ir}6.2), Kcnn2 (K_{Ca}2.2), Kcnt1 (K_{Ca}4.1), Kcnmb3 (sloβ3) and Abcc9 (SUR2) (Table 4-2). Among the 65 expressed subunits, only Kcnk6 (K_{2p}6.1) was significantly decreased to 68.8% of control by LPS treatment. The detail of expression for each K^+ family is described in the following sections.

4.2.3.2 Most abundantly expressed K^+ channel subunits mRNAs

Among the 82 subunits, the mRNA encoding Kcnma1 (K_{Ca}1.1), Kcnk6 (K_{2p}6.1), Kcnc3 (K_v3.3), Abcc8 (SUR1), Kcnj2 (K_{ir}2.1), Kcnn4 (K_{Ca}3.1) were the most abundantly expressed in resting microglia. Expression of Kcnk6 (K_{2p}6.1) was significantly reduced by LPS treatment (Figure 4-3).

4.2.4. mRNA expression of K_v pore-forming subunits in N9 cells

In total 33 pore-forming subunits of this K_v family were examined which included members of K_v1.x, K_v2.x, K_v3.x, K_v4.x, K_v5.x, K_v7.x, K_v8.x, K_v9.x, K_v10.x, K_v11.x and K_v12.x excepted for subunits of K_v1.8, K_v6.x, K_v10.2 and K_v12.3 (Figure 4-4). Seven of the examined subunits were not detectable and they were Kcna2 (K_v1.2),

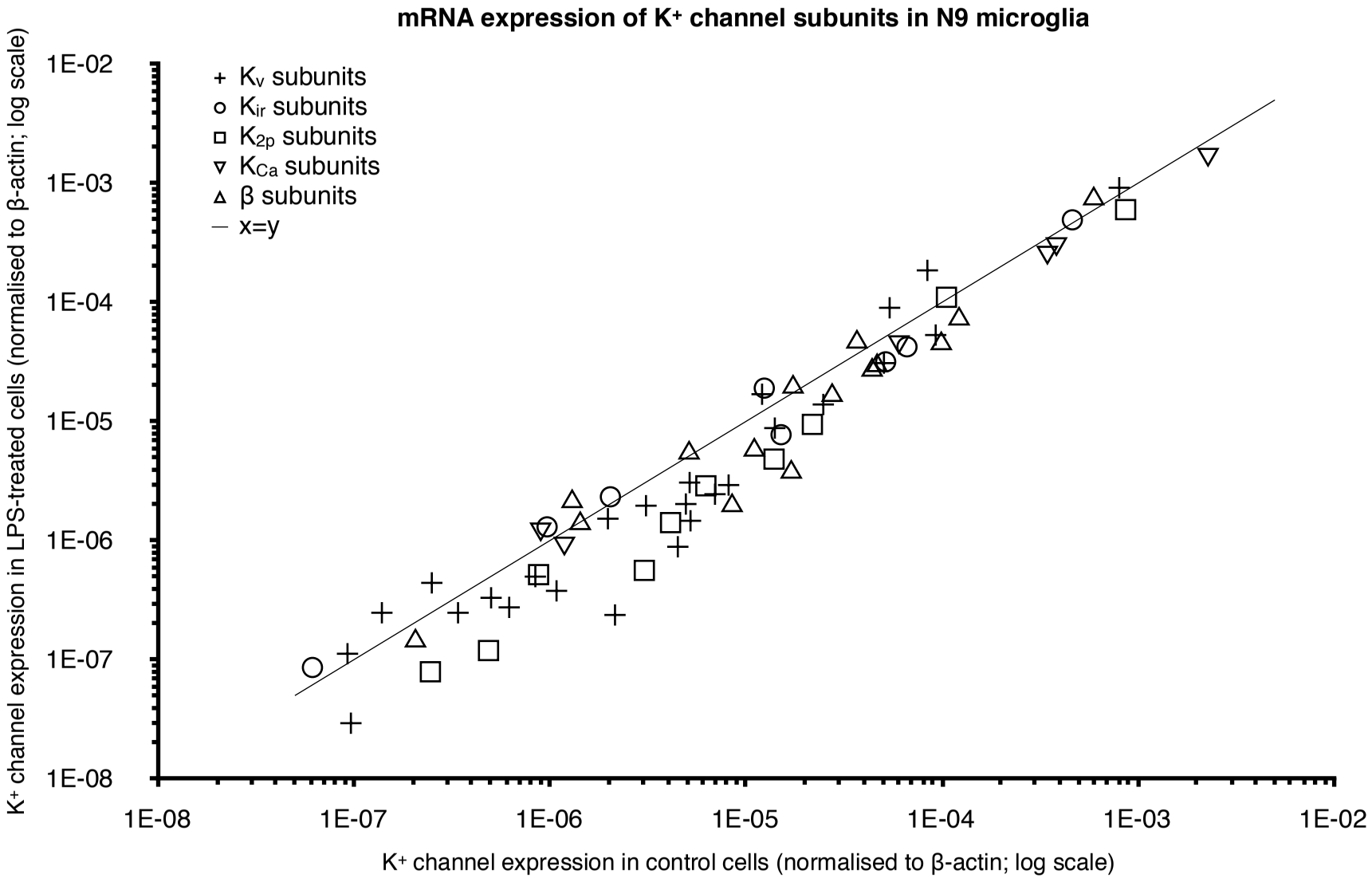
mRNA expression of K+ channel subunits in N9 microglia
Kv subunits
Kir subunits
K2p subunits
KCa subunits
β subunits
x=y
K+ channel expression in LPS-treated cells (normalised to β-actin; log scale)
K+ channel expression in control cells (normalised to β-actin; log scale)
1E-02
1E-03
1E-04
1E-05
1E-06
1E-07
1E-08

Figure 4-2

Figure 4-2. The expression pattern of K^+ channel subunit mRNAs in N9 cells before and after LPS treatment. X axis represents the K^+ channel expression in resting N9 cells while Y axis represents the K^+ channel expression in LPS activated N9 cells. Totally 82 subunits including pore-forming subunits and regulatory subunits tested. 65 subunits were detectable which were represented in the chart. 17 subunits were not detectable (Table 4-2). Data are given as mean. ($n \geq 3$)

Pore-forming subunits				Regulatory subunits
K_v family	**K_{2p} family**	**K_{ir} family**	**K_{Ca} family**	
Kcna2 (K_v1.2)	Kcnk13 (K_{2p}13.1)	Kcnj5 (K_{ir}3.4)	Kcnn2 (K_{Ca}2.2)	Kcnmb3 (sloβ3)
Kcnb2 (K_v2.2)		Kcnj10 (K_{ir}4.1)	Kcnt1 (K_{Ca}4.1)	Abcc9 (SUR2)
Kcnq2 (K_v7.2)		Kcnj16 (K_{ir}5.1)		
Kcnq4 (K_v7.4)		Kcnj8 (K_{ir}6.1)		
Kcnq5 (K_v7.5)		Kcnj11 (K_{ir}6.2)		
Kcns1 (K_v9.1)				
Kcnh2 (K_v11.1)				

Table 4-2. Subunits that were not detectable. Totally 17 subunits were not detectable which are from all four K^+ families.

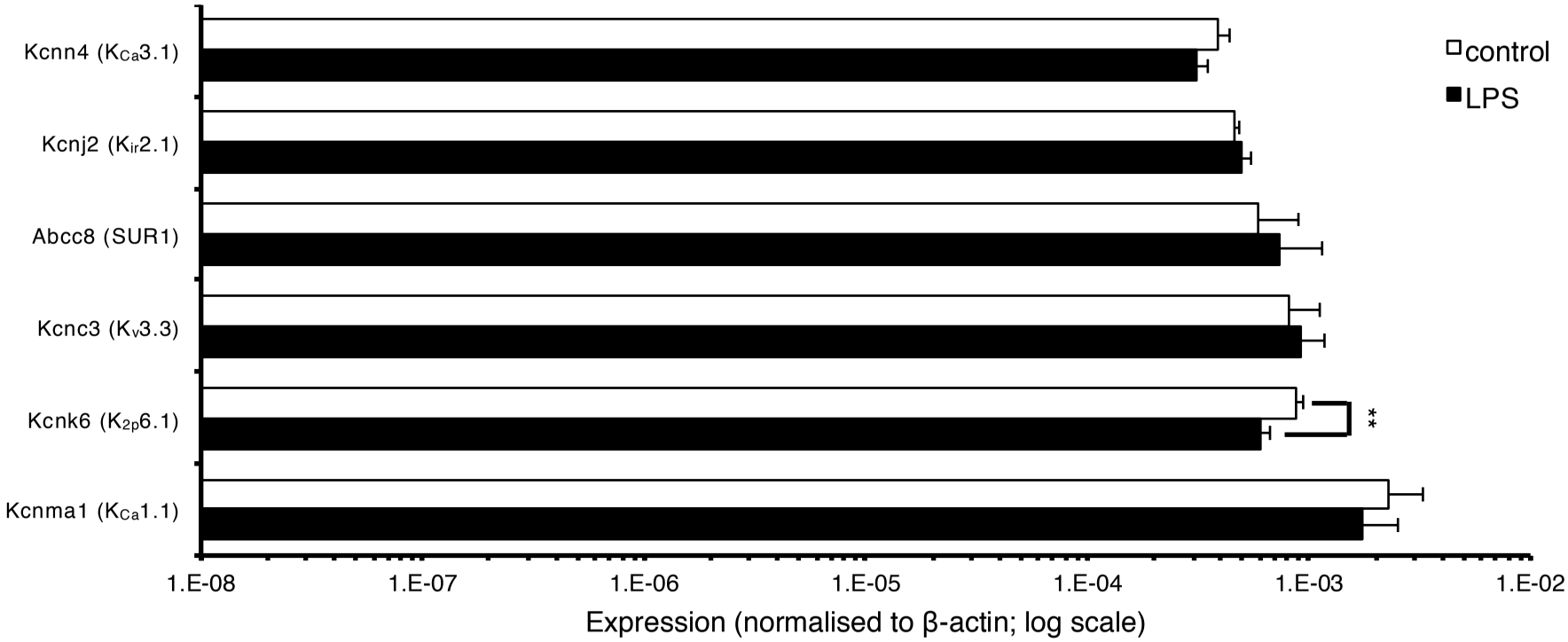

Figure 4-3. Most abundantly expressed subunits before and after LPS treatment. The most abundantly expressed subunits in N9 microglia compared to other subunits included Kcnma1 ($K_{Ca}1.1$), Kcnk6 ($K_{2p}6.1$), Kcnc3 ($K_v3.3$), Abcc8 (SUR1), Kcnj2 (Kir2.1) and Kcnn4 ($K_{Ca}3.1$) in which there were five pore-forming subunits and one regulatory subunit. The expression of Kcnk6 ($K_{2p}6.1$) was significantly decreased by LPS treatment. **$p<0.01$, by Student's t-test. Data are given as mean±SEM. (n=9)

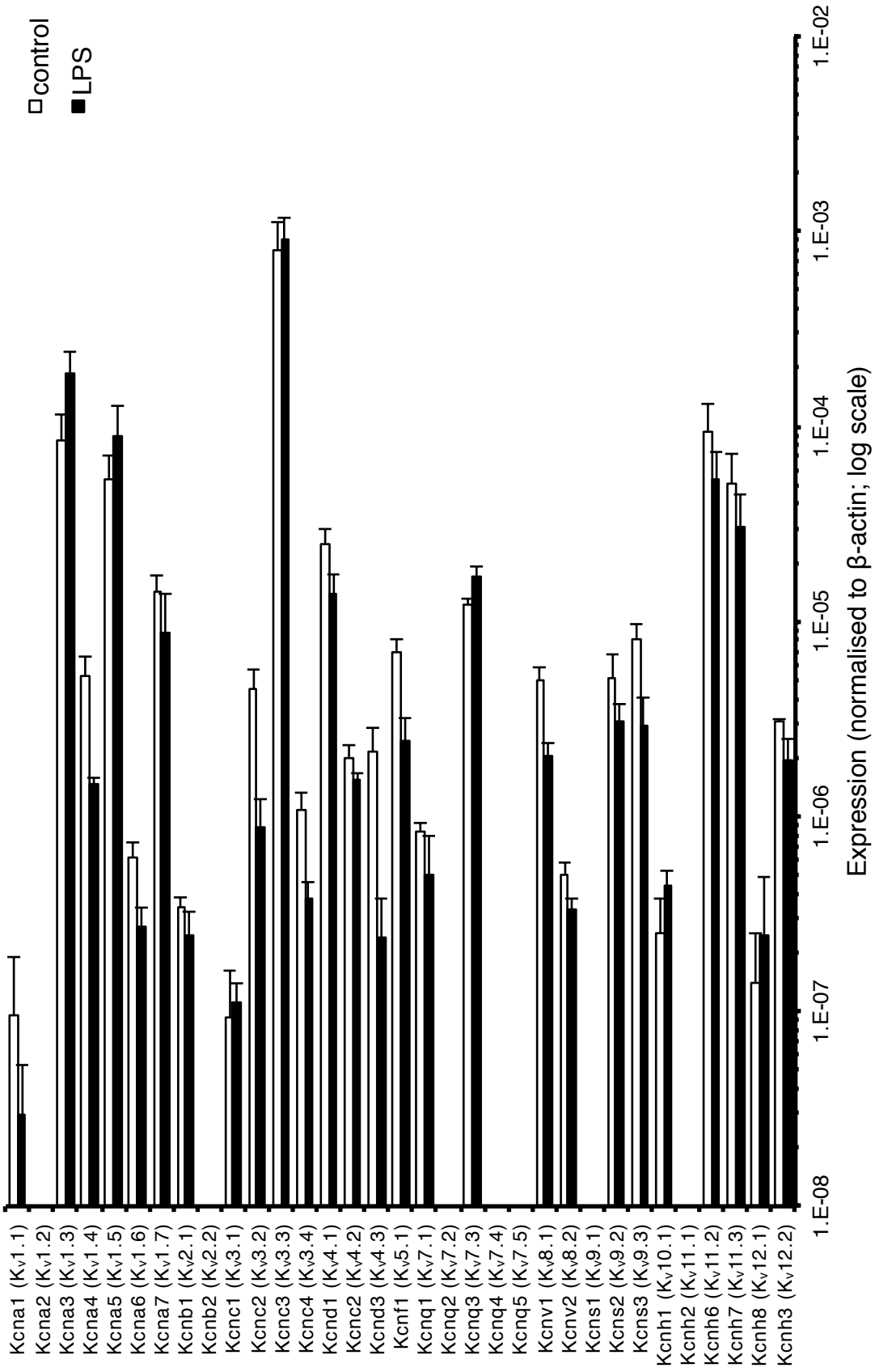
control
LPS
Expression (normalised to β-actin; log scale)
1.E-02
1.E-03
1.E-04
1.E-05
1.E-06
1.E-07
1.E-08
Kcna1 (Kv1.1)
Kcna2 (Kv1.2)
Kcna3 (Kv1.3)
Kcna4 (Kv1.4)
Kcna5 (Kv1.5)
Kcna6 (Kv1.6)
Kcna7 (Kv1.7)
Kcnb1 (Kv2.1)
Kcnb2 (Kv2.2)
Kcnc1 (Kv3.1)
Kcnc2 (Kv3.2)
Kcnc3 (Kv3.3)
Kcnc4 (Kv3.4)
Kcnd1 (Kv4.1)
Kcnc2 (Kv4.2)
Kcnd3 (Kv4.3)
Kcnf1 (Kv5.1)
Kcnq1 (Kv7.1)
Kcnq2 (Kv7.2)
Kcnq3 (Kv7.3)
Kcnq4 (Kv7.4)
Kcnq5 (Kv7.5)
Kcnv1 (Kv8.1)
Kcnv2 (Kv8.2)
Kcns1 (Kv9.1)
Kcns2 (Kv9.2)
Kcns3 (Kv9.3)
Kcnh1 (Kv10.1)
Kcnh2 (Kv11.1)
Kcnh6 (Kv11.2)
Kcnh7 (Kv11.3)
Kcnh8 (Kv12.1)
Kcnh3 (Kv12.2)

Figure 4-4

Figure 4-4. mRNA expression of pore-forming subunits of K_v family before and after LPS treatment. Seven subunits were not detectable which were Kcna2 (K_v1.2), Kcnb2 (K_v2.2), Kcnq2 (K_v7.2), Kcnq4 (K_v7.4), Kcnq5 (K_v7.5), Kcns1 (K_v9.1) and Kcnh2 (K_v11.1). The most abundantly expressed subunits in the resting N9 microglia included Kcnc3 (K_v3.3), Kcnh6 (K_v11.2), Kcna3 (K_v1.3), Kcna5 (K_v1.5) and Kcnh7 (K_v11.3). Data are given as mean ±SEM. (n≥3)

Kcnb2 (K_v2.2), Kcnq2 (K_v7.2), Kcnq4 (K_v7.4), Kcnq5 (K_v7.5), Kcns1 (K_v9.1) and Kcnh2 (K_v11.1). In the resting N9 microglia, the most abundantly expressed subunits of this family included Kcnc3 (K_v3.3), Kcnh6 (K_v11.2), Kcna3 (K_v1.3), Kcna5 (K_v1.5) and Kcnh7 (K_v11.3).

For the fold change of K_v pore-forming subunits, there was no subunit significantly regulated by LPS treatment (Figure 4-5).

4.2.5 mRNA expression of K_{ir} pore-forming subunits in N9 cells

Totally 13 pore-forming subunits of this K_{ir} family were examined which included members of K_{ir}1.x, K_{ir}2.x, K_{ir}3.x, K_{ir}4.x, K_{ir}5.x and K_{ir}6.x except for subunits of K_{ir}2.2 and K_{ir}7.1 (Figure 4-6). Five of the examined subunits were not detectable and they were Kcnj5 (K_{ir}3.4), Kcnj10 (K_{ir}4.1), Kcnj16 (K_{ir}5.1), Kcnj8 (K_{ir}6.1) and Kcnj11 (K_{ir}6.2). In the resting N9 microglia, the most abundantly expressed subunits of this family included Kcnj2 (K_{ir}2.1), Kcnj4 (K_{ir}2.3), Kcnj1 (K_{ir}1.1), Kvnj14 (K_{ir}2.4) and Kcnj3 (K_{ir}3.1).

For the fold change of K_{ir} pore-forming subunits, there was no subunit significantly regulated by LPS treatment (Figure 4-7).

4.2.6 mRNA expression of K_{2p} pore-forming subunits in N9 cells

Totally 11 pore-forming subunits of this K_{2p} family were examined which included members of K_{2p}1.x, K_{2p}2.x, K_{2p}3.x, K_{2p}4.x, K_{2p}5.x, K_{2p}6.x, K_{2p}7.x, K_{2p}9.x, K_{2p}12.x, K_{2p}13.x and K_{2p}18.x except for subunits of K_{2p}10.1, K_{2p}15.1, K_{2p}16.1 and K_{2p}17.1 (Figure 4-8). One of the examined subunits was not detectable and it was Kcnk13 (K_{2p}13.1). In the resting N9 microglia, the most abundantly expressed subunits of this family included Kcnk6 (K_{2p}6.1), Kcnk7 (K_{2p}7.1), Kcnk18 (K_{2p}18.1), Kcnk9

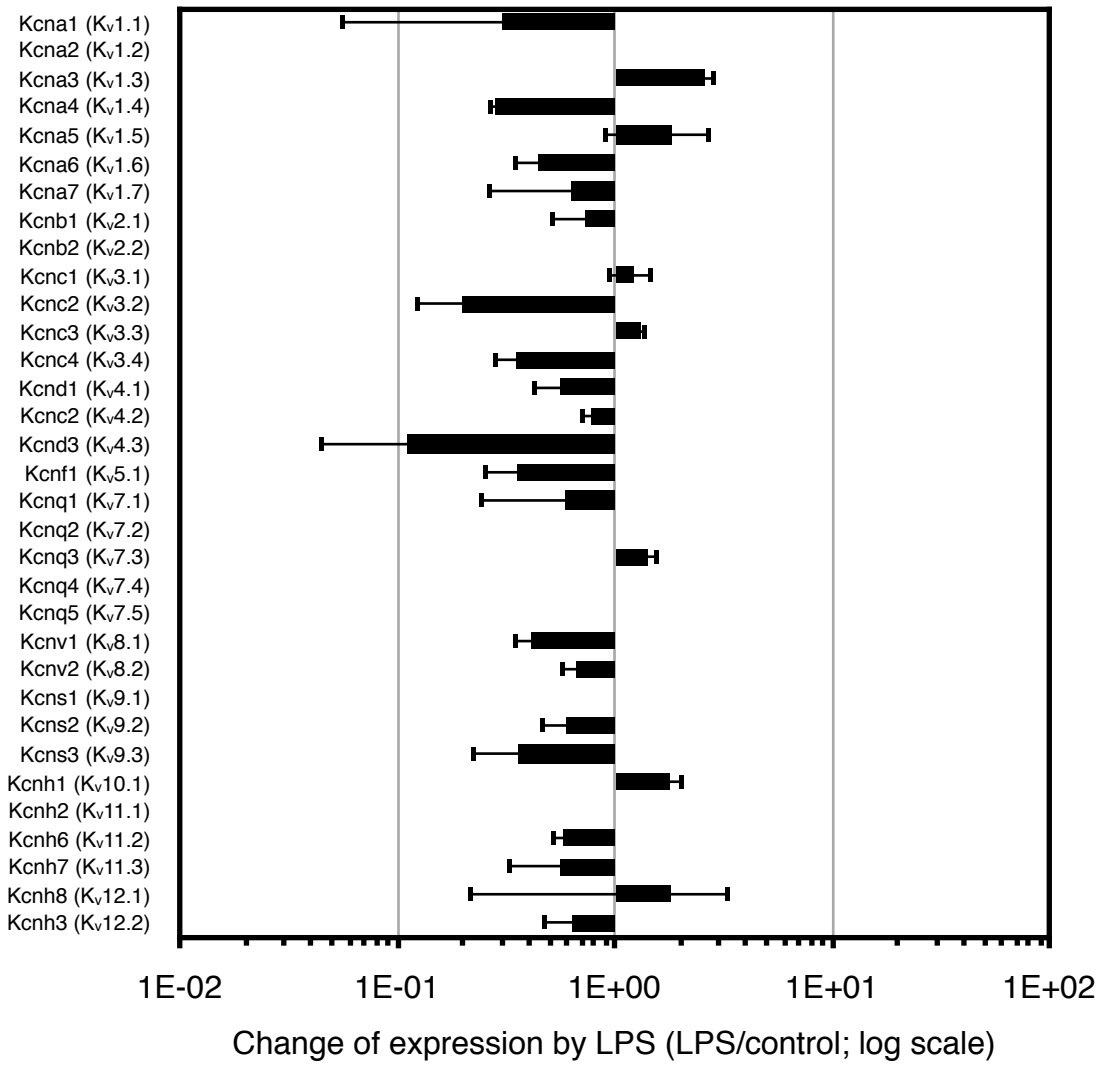

Figure 4-5. Fold change of K_v pore-forming subunits after LPS treatment. For the fold change of K_v pore-forming subunits, there was no subunit significantly regulated by LPS treatment. Data are given as mean ±SEM. (n≥3)

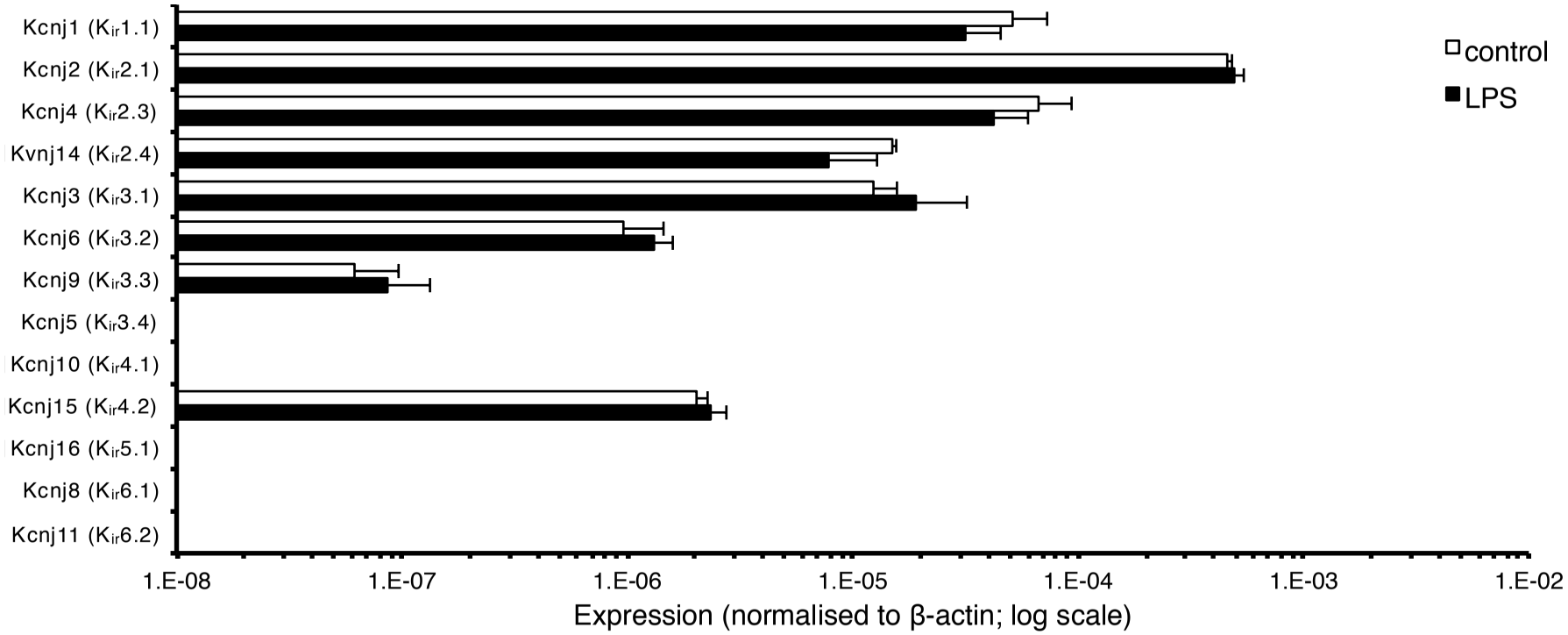

Figure 4-6. mRNA expression of pore-forming subunits of K_{ir} family before and after LPS treatment. Five subunits were not detectable which were Kcnj5 (K_{ir}3.4), Kcnj10 (K_{ir}4.1), Kcnj16 (K_{ir}5.1), Kcnj8 (K_{ir}6.1) and Kcnj11 (K_{ir}6.2). The most abundantly expressed subunits in the resting N9 microglia included Kcnj2 (K_{ir}2.1), Kcnj4 (K_{ir}2.3), Kcnj1 (K_{ir}1.1), Kvnj14 (K_{ir}2.4) and Kcnj3 (K_{ir}3.1). Data are given as mean±SEM. (n≥3)

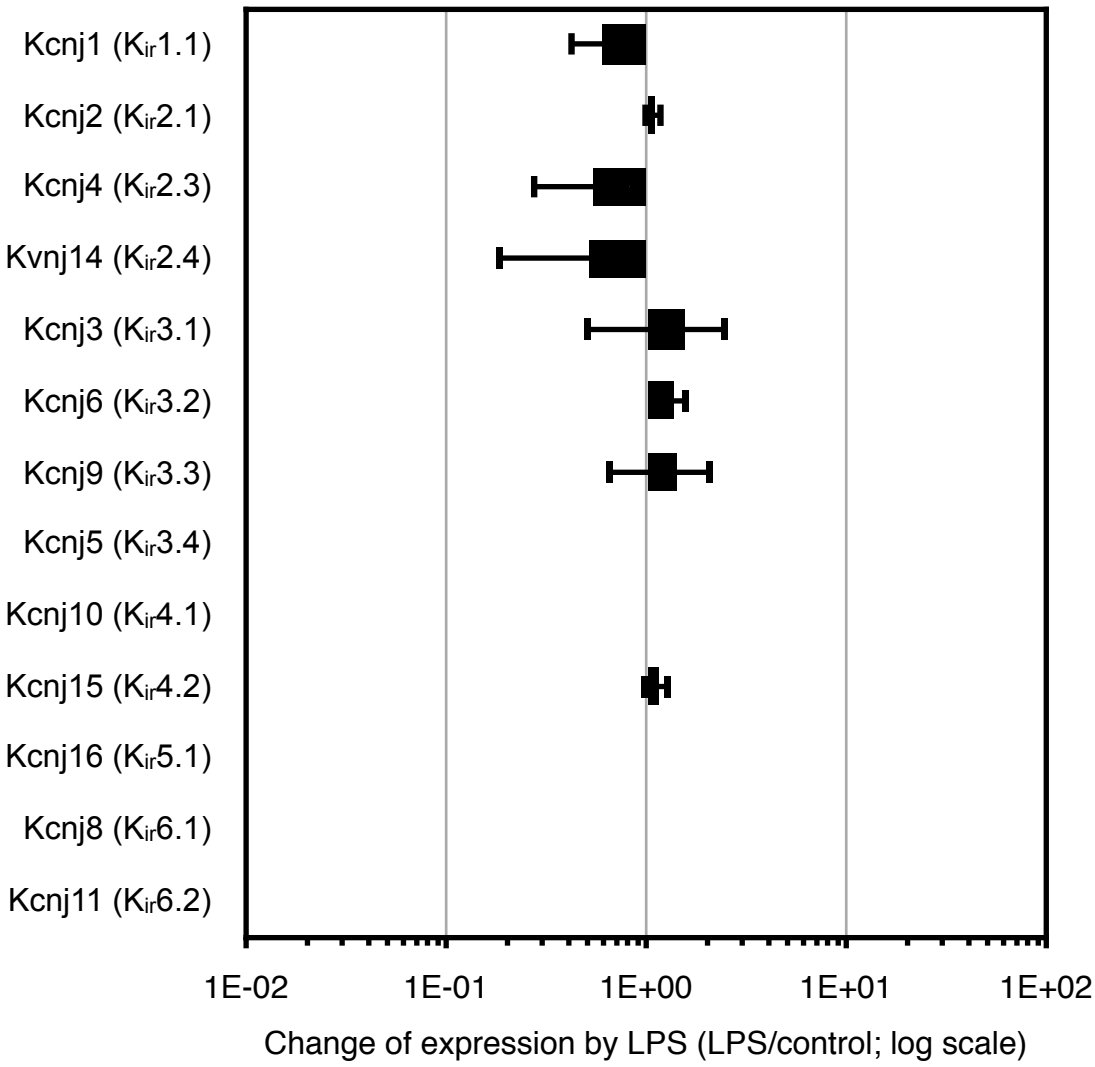

Figure 4-7. Fold change of K_{ir} pore-forming subunits after LPS treatment. For the fold change of K_{ir} pore-forming subunits, there was no subunit significantly regulated by LPS treatment. Data are given as mean ±SEM. (n≥3)

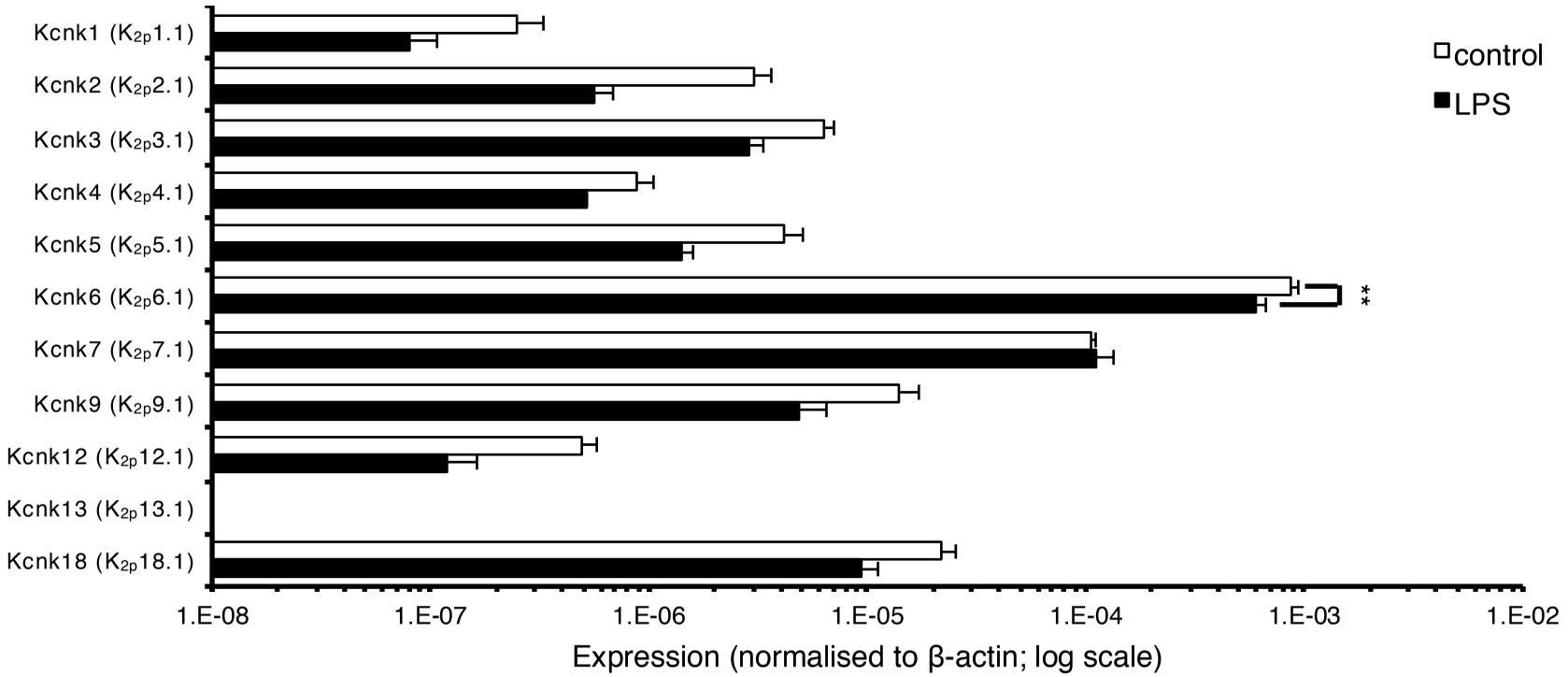

Figure 4-8. mRNA expression of pore-forming subunits of K_{2p} family before and after LPS treatment. Kcnk13 (K_{2p}13.1) was not detectable. The most abundantly expressed subunits in the resting N9 microglia included Kcnk6 (K_{2p}6.1), Kcnk7 (K_{2p}7.1), Kcnk18 (K_{2p}18.1), Kcnk9 (K_{2p}9.1) and Kcnk3 (K_{2p}3.1). The expression of Kcnk6 (K_{2p}6.1) was significantly decreased by LPS treatment. **$p<0.01$, by Student's t-test. Data are given as mean±SEM.

(K_{2p}9.1) and Kcnk3 (K_{2p}3.1).

For the fold change of K_{2p} pore-forming subunits, Kcnk6 (K_{2p}6.1) was significantly decreased by 31.2% by LPS treatment (Figure 4-9).

4.2.7 mRNA expression of K_{Ca} pore-forming subunits in N9 cells

Totally eight pore-forming subunits of this K_{Ca} family were examined which included members of K_{Ca}1.x, K_{Ca}2.x, K_{Ca}3.x, K_{Ca}4.x and K_{Ca}5.x (Figure 4-10). Two of the examined subunits were not detectable and they were Kcnn2 (K_{Ca}2.2) and Kcnt1 (K_{Ca}4.1). In the resting N9 microglia, the most abundantly expressed subunits of this family included Kcnma1 (K_{Ca}1.1), Kcnn4 (K_{Ca}3.1) and Kcnn1 (K_{Ca}2.1).

For the fold change of K_{Ca} pore-forming subunits, there was no subunit significantly regulated by LPS treatment (Figure 4-11).

4.2.8 mRNA expression of regulatory subunits in N9 cells

Totally 17 regulatory subunits for K_v, K_{ir} and K_{Ca} channels were examined which included members of K_vβ, MiRP, KChIP, SUR and sloβ families (Figure 4-12). Two subunits were not detectable and they were Abcc9 (SUR2) and Kcnmb3 (sloβ3). In the resting N9 microglia, the most abundantly expressed subunits of this family included Abcc8 (SUR1), Kcnmb4 (sloβ4), Kcne3 (MiRP2), Kcnmb2 (sloβ2) and Kcnab3 (K_vβ3).

For the fold change of regulatory subunits, there was no subunit significantly regulated by LPS treatment (Figure 4-13).

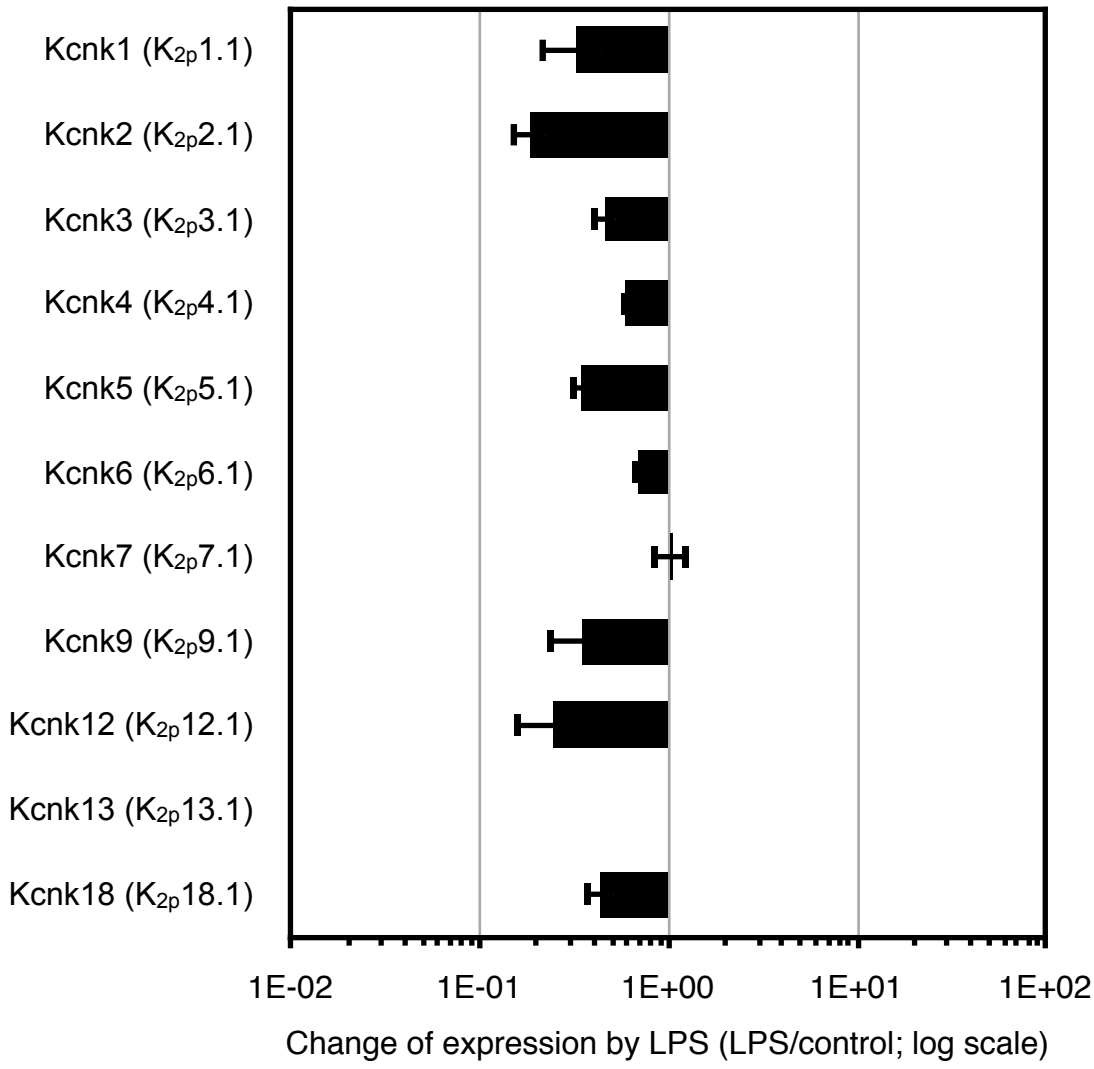

Figure 4-9. Fold change of K_{2p} pore-forming subunits after LPS treatment. For the fold change of K_{2p} pore-forming subunits the expression of Kcnk6 (K_{2p}6.1) was significantly decreased to 68.8% by LPS treatment. Data are given as mean±SEM. (n≥3)

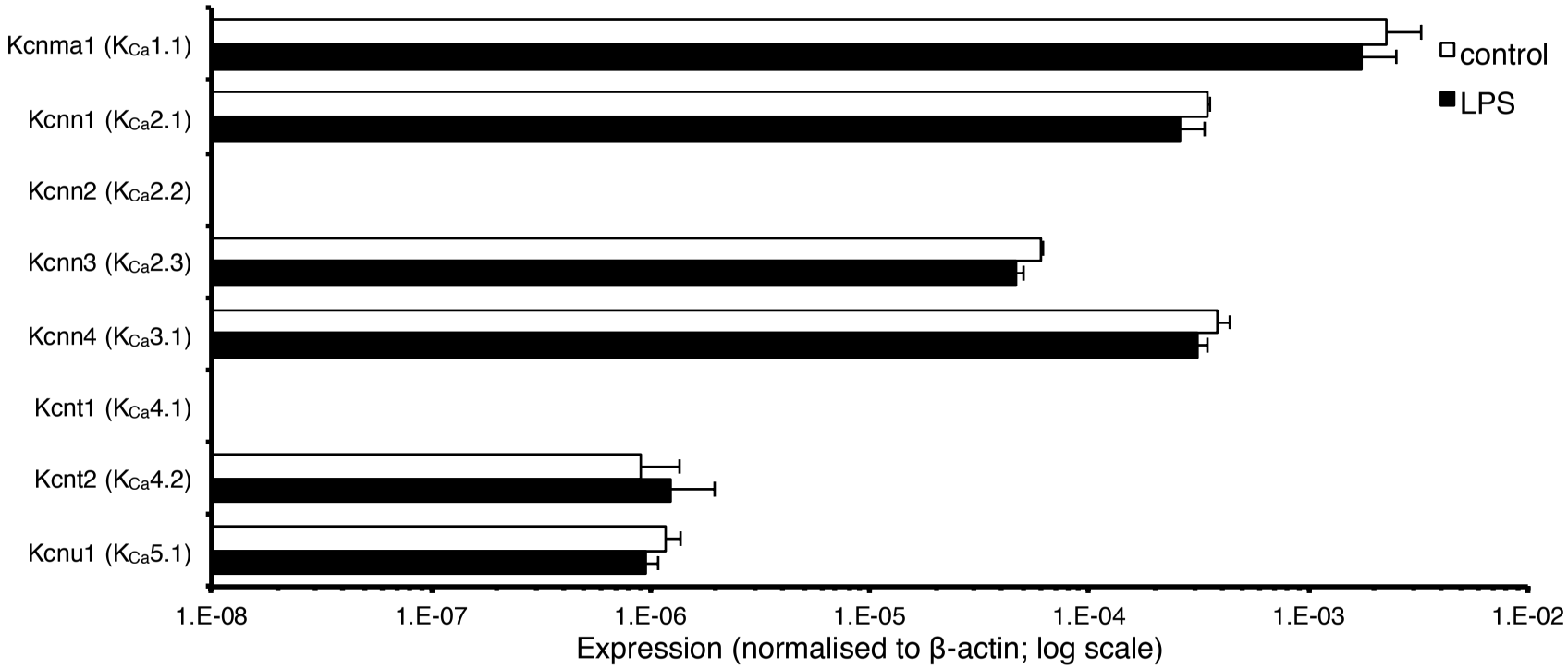

Figure 4-10. mRNA expression of pore-forming subunits of K_{Ca} family before and after LPS treatment. Two subunits Kcnn2 (K_{Ca}2.2) and Kcnt1 (K_{Ca}4.1) were not detectable. The most abundantly expressed subunits in the resting N9 microglia included Kcnma1 (K_{Ca}1.1), Kcnn4 (K_{Ca}3.1) and Kcnn1 (K_{Ca}2.1). Data are given as mean±SEM. (n≥3)

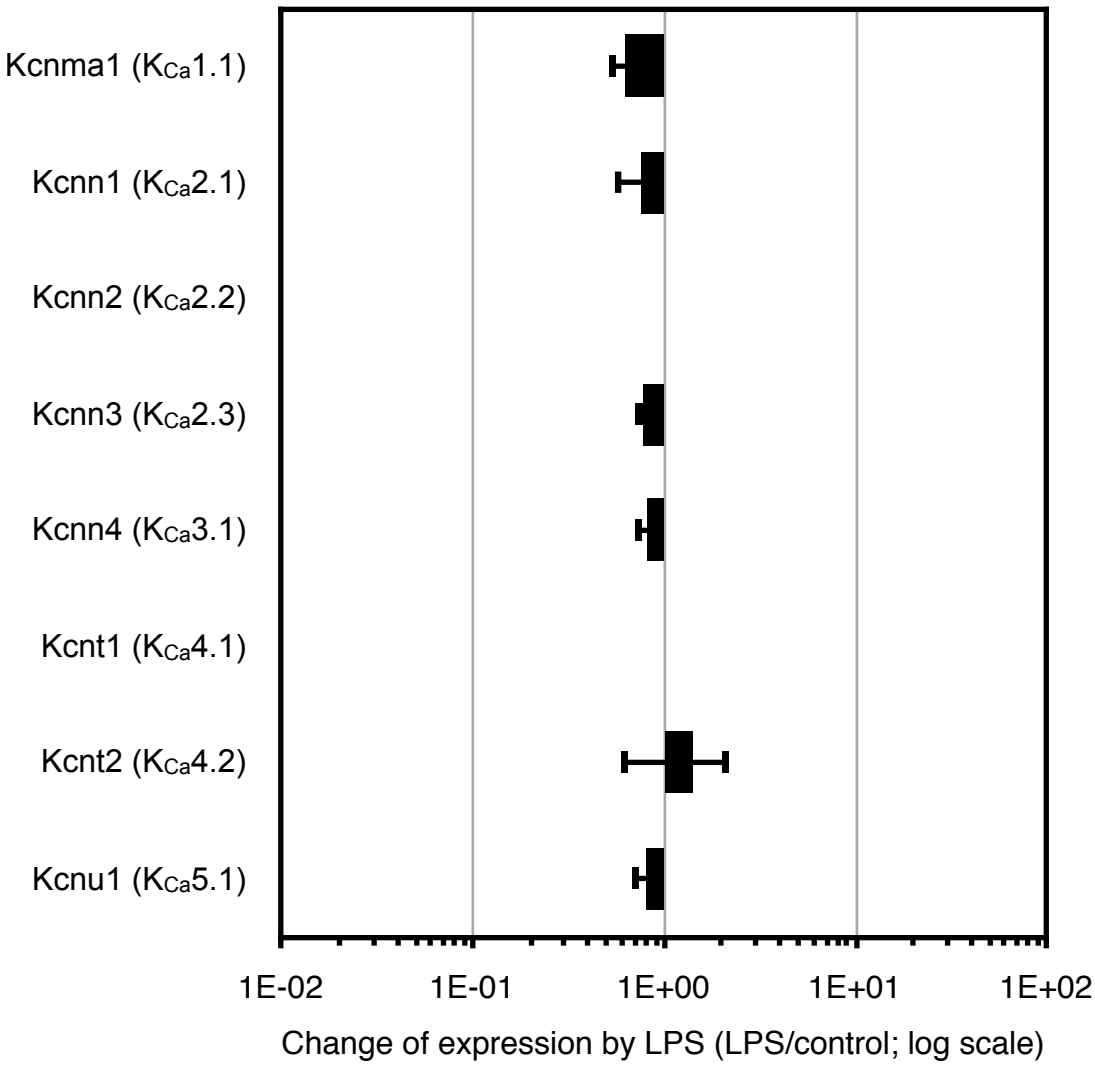

Figure 4-11. Fold change of K_{Ca} pore-forming subunits after LPS treatment. For the fold change of K_{Ca} pore-forming subunits, there was no subunit significantly regulated by LPS treatment. Data are given as mean ±SEM. (n≥3)

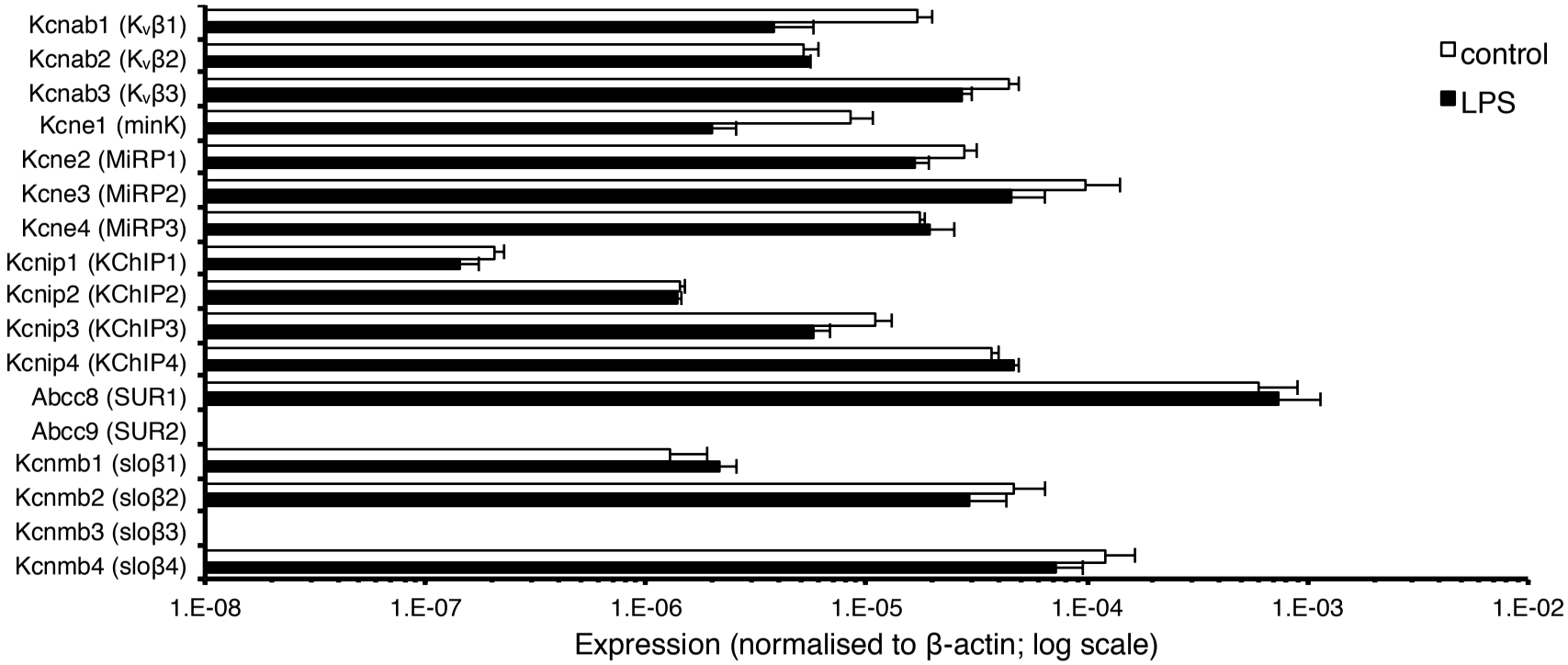

Figure 4-12. mRNA expression of regulatory subunits before and after LPS treatment. As described in the result, totally 17 subunits was examined. Two subunits were not detectable which were Abcc9 (SUR2) and Kcnmb3 (sloβ3). The most abundantly expressed subunits in the resting N9 microglia included Abcc8 (SUR1), Kcnmb4 (sloβ4), Kcne3 (MiRP2), Kcnmb2 (sloβ2) and Kcnab3 ($K_v\beta3$). Data are given as mean±SEM. (n≥3)

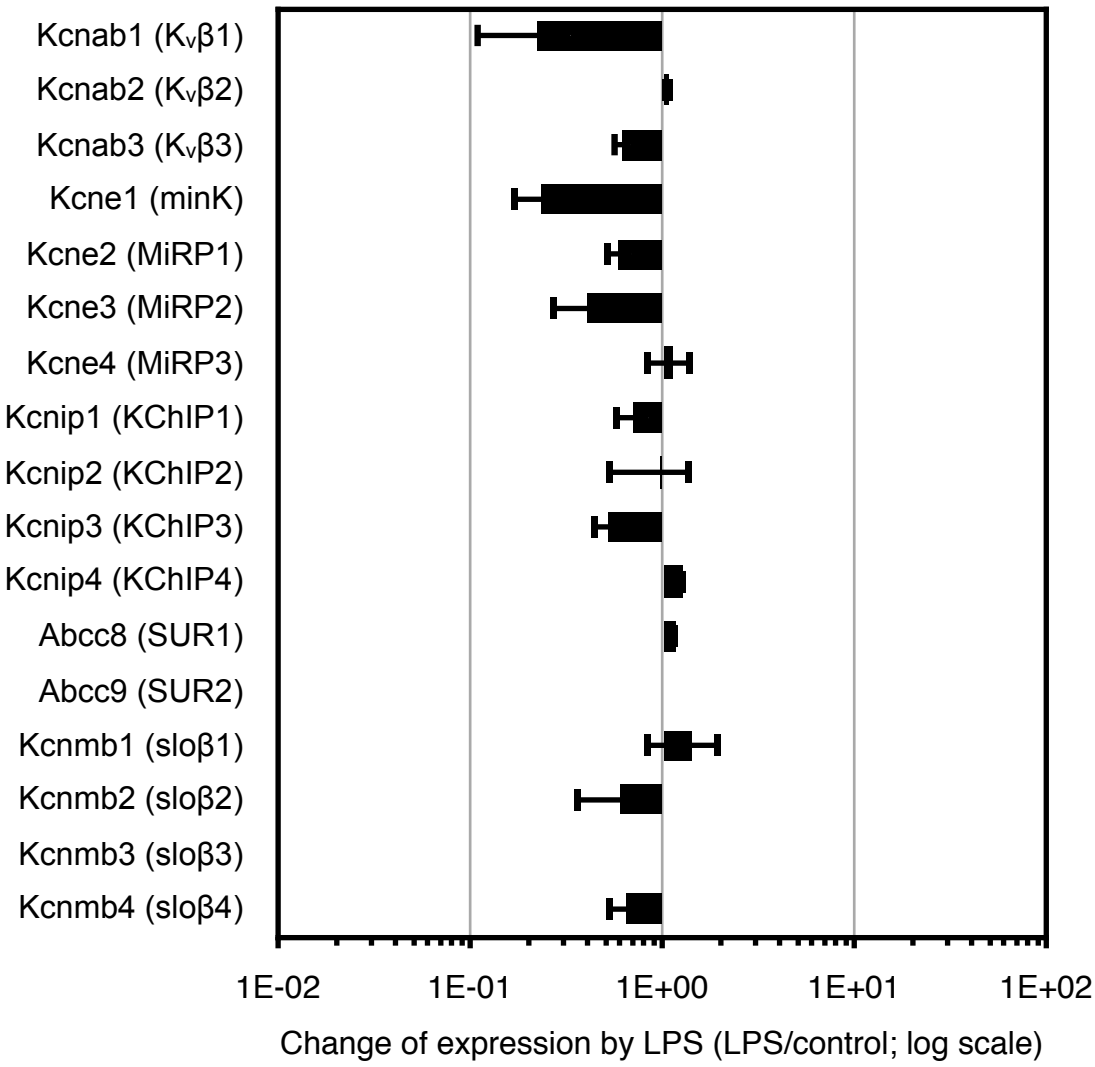

Figure 4-13. Fold change of regulatory subunits after LPS treatment. For the fold change of regulatory subunits, there was no subunit significantly regulated by LPS treatment. Data are given as mean±SEM. (n≥3)

4.3 Discussion

4.3.1 General conclusion of the result

In this chapter, the mRNA expression pattern of K^+ channels was examined in resting N9 microglial cell line and their change in expression after microglial activation by LPS treatment was examined. This is the first time systematic screening of K^+ channel gene expression using the qRT-PCR technique in N9 cells by comparing the expression in both resting and LPS-activated status. Based on the limited numbers (around 15~20) of K^+ channel members previously reported in microglia (Table 4-1), the detection of >60 subunits dramatically expands the understanding of K^+ expression in microglia.

The expression of K^+ channel subunits displayed a low level compared to the reference gene as only 14% (9 out of 65 detected) of subunit expression was over 0.01% of β-actin with the most abundant subunit mRNA expressed at less than 1% of β-actin. The reason may be that β-actin in N9 cells is expressed at a high level. As microglia have the ability to change their morphology according to cellular status or to keep moving their processes to survey the environment, it may require high β-actin expression.

As described in section 4.2.3.1, 65 subunits were expressed, but only the expression of Kcnk6 ($K_{2p}6.1$) was significantly reduced by LPS treatment. The different effects of LPS on K^+ channel expression may result from the different gene regulating pathways activated by LPS. As described in section 1.2.4, LPS binds to the Toll-like receptor (TLR)4/cluster of differentiation molecule (CD)14 receptor which leads to the activation of various transcription factors including ETS-like transcription factor 1 (Elk1), cAMP response element-binding protein (CREB), c-jun, nuclear factor kappa-light-chain-enhancer of activated B cells (NFκB), interferon regulatory factor (IRF)5 and IRF3 (Lu *et al.*, 2008; Bjørkøy *et al.*, 1995; Mas *et al.*, 2003; Dauphinee & Karsan, 2006; Fenton & Golenbock, 1998; Tamemoto *et al.*, 1992; Cobb &

Goldsmith, 1995; Meja *et al.*, 2000; Chan *et al.*, 2001). Thus K^+ channel expression by LPS may be controlled by a complex rather than an unified pathway. In addition, in pituitary cells the mRNA expression of $K_v1.5$ was downregulated by membrane depolarization which was Ca^{2+}- and Na^+-independent (Levitan *et al.*, 1995). Thus, it may be possible the transcription level of K^+ channels is regulated by membrane potential (Lee *et al.*, 2007; Kiefer & Schulze, 1982) and may be independent of the Ca^{2+}-dependent phosphorylation pathways, such as Ca^{2+}/calmodulin-dependent protein kinase II (CaMKII) or calcineurin.

4.3.2 Integration of results with published data

4.3.2.1 K_{ir} channels

Kcnj1 ($K_{ir}1.1$) was detected in our study which supported the finding in previous work (Küst *et al.*, 1999). Kcnj1 ($K_{ir}1.1$) was not significantly regulated by LPS treatment. In isolated rat microglia, study investigating the relationship between cyclic adenosine monophosphate (cAMP) and Kcnj1 ($K_{ir}1.1$) gene expression indicated the elevation of cAMP decreased Kcnj1 ($K_{ir}1.1$) gene expression (Küst *et al.*, 1999). It was known that elevation of cAMP can be induced by LPS in human monocytes (Mengozzi *et al.*, 1993). Perhaps the regulation of $K_{ir}1.1$ channel mRNA expression may not only be through the LPS-induced cAMP pathway. For example, protein kinase C (PKC) has been postulated playing a role in expression of $K_{ir}1.1$ channels (Küst *et al.*, 1999).

From the same K_{ir} family, Kcnj2 ($K_{ir}2.1$) was abundantly expressed in resting N9 cells compared to most other channels. Here the finding of Kcnj2 ($K_{ir}2.1$) in N9 cell line is inline with previous studies in BV-2 cells (Schilling *et al.*, 2000). In addition, it was further discovered that mRNA expression of Kcnj2 ($K_{ir}2.1$) was not significantly affected by LPS stimulation.

In previous studies, the gene of Kcnj8 (K_{ir}6.1), Kcnj11 (K_{ir}6.2) and Abcc8 (SUR1) have been found expressed in BV-2 cells but at a very low level. Their expression was increased after microglial activation by LPS+interferon gama (IFN-γ) (100ng/ml +0.05ng/ml, 48hr) (Ortega *et al.*, 2012) despite that the elevated gene expression was still low. Of these subunits only Abcc8 (SUR1) was expressed in N9 microglia suggesting that N9 and BV-2 share different expression properties on these type of channel subunits. The reason may be: (1) The difference expression pattern of these two cell lines as well as the difference between other cell lines (Horvath *et al.*, 2008). (2) The different cell preparation and stimulation used to induce different microglial responses. In the previous study, BV-2 cells were treated by LPS+IFN-γ while here N9 was treated by LPS only. In addition, the concentration and duration of LPS treatment was different either 100ng/ml for 48hr for BV-2 cells or 1μg/ml for 24hr here. Neither N9 nor BV-2 cells express high level of Abcc9 (SUR2) subunit mRNA (Ortega *et al.*, 2012).

4.3.2.2 K_v channels

The changes in mRNA expression of K_v channels between resting and activated N9 microglia were compared to the previous studies. N9 cells express Kcna1 (K_v1.1) but this was not significantly influenced by LPS activation. This was similar to BV-2 cells in which both mRNA and protein of Kcna1 (K_v1.1) were discovered (Wu *et al.*, 2009). However, in BV-2 cells LPS elevated both its gene and protein expression (Wu *et al.*, 2009). Such discrepancy may result from: (1) BV-2 was treated by 1μg/ml of LPS for 6hr but here 1μg/ml of LPS for 24hr was applied. LPS-regulated microglial current expression was indicated a time-dependent manner (Nörenberg *et al.*, 1992). It may be possible the duration of LPS challenge played a role in the transcription of K^+ channels. (2) In previous studies the protein expression of Kcna1 (K_v1.1) was found in microglia in rat brain slices (C. Y. Wu *et al.*, 2009) while Kcna1 (K_v1.1) was not detected in isolated primary microglia of the same species (Kotecha & Schlichter, 1999). This suggested that the culture environment may play a role in

regulating the expression of microglial $K_v1.1$ channels. (3) For both microglia prepared in *in vitro* culture, BV-2 cells expressed Kcna1 ($K_v1.1$) (Wu *et al.*, 2009) while primary rat microglia did not (Kotecha & Schlichter, 1999). This suggested that different cell types may display different properties (Horvath *et al.*, 2008).

Kcna2 ($K_v1.2$) channel mRNA was not detectable in N9 cells. This may go some way towards explaining the different phenomenon with previous studies. There was one previous study indicating Kcna2 ($K_v1.2$) expression in rat microglia in brain slices (Li *et al.*, 2008a), one study detecting Kcna2 ($K_v1.2$) expression in BV-2 murine microglia cell line (Li *et al.*, 2008a) and two studies detecting Kcna2 ($K_v1.2$) expression in cultured primary rat microglia (Kotecha & Schlichter, 1999; Fordyce *et al.*, 2005). However, comparing the details of these studies may give an explanation for the different results: (1) The study on microglia in brain slices indicated the expression of Kcna2 ($K_v1.2$) is an age-dependent phenomenon during which Kcna2 ($K_v1.2$) expression disappeared when rats were older than P21 (Li *et al.*, 2008a). Thus it was possible that N9 cells represent a similar expression property on Kcna2 ($K_v1.2$) to more mature primary microglia. (2) Another study using cultured primary rat microglia indicated that Kcna2 ($K_v1.2$) gene expression was not changed in activated microglia by LPS or phorbol 12-myristate 13-acetate (PMA) (Fordyce *et al.*, 2005) while Kcna2 ($K_v1.2$) expression in activated microglia in brain slices of same species increased under hypoxia exposure. These different responses may be due to the different activation and maintenance methods which may change Kcna2 ($K_v1.2$) expression. (3) It was indicated that different microglial cell lines had different physiological properties (Horvath *et al.*, 2008). It may be possible the N9 microglial cell line differs from other cell types in the expression of Kcna2 ($K_v1.2$).

In primary rat microglia, Kcna3 ($K_v1.3$) gene was increased to 2~2.5 fold by LPS (Fordyce *et al.*, 2005). In addition, increasing cAMP, one of the downstream mediators of LPS, elevated gene expression of $K_v1.3$ by about 50%~100% (Küst *et al.*, 1999). mRNA expression of Kcna3 ($K_v1.3$) in N9 cells here was not significantly

increased by LPS (1μg/ml, 24hr) although there was a trend to increase after activation which was about a 2.6 fold change. This was similar to the 2~2.5 fold change in cultured rat microglia (Fordyce *et al.*, 2005). Such discrepancies may be from the different activation methods in which 10ng/ml of LPS for overnight was used previously (Fordyce *et al.*, 2005) and 1μg/ml of LPS for 24hr was applied here. As the LPS-induced microglial activation is a dose- and time-dependent process which was confirmed in Chapter 3, it is reasonable to assume different concentration and duration of LPS application may affect on Kcna3 (K_v1.3) gene expression.

In vivo work in rat brain indicated K_v1.5 protein expression in microglia and its upregulation by LPS (2μg) injection in the hippocampus (Jou *et al.*, 1998). Expression of Kcna5 (K_v1.5) was detected in N9 here although its expression was not significantly regulated by LPS. The expression of K_v1.5 channels is still controversial. Besides the upregulation of K_v1.5 protein by LPS in *in vivo* study, neither the gene nor protein was changed in isolated primary rat microglia *in vitro* culture by LPS (10ng/ml, overnight) treatment (Fordyce *et al.*, 2005). What is more interesting, gene expression of K_v1.5 was decreased by LPS (10ng/ml, 24hr) in isolated primary mouse microglia *in vitro* culture (Pannasch *et al.*, 2006). The reason for the different results may be due to species differences and it also can not be neglected that the LPS activation method was different in each study. For example, the LPS injection to the brain may generate a very high concentration of LPS at the injection point. In addition, as shown in Chapter 3, microglial response to LPS treatment was time- and dose-dependent, 10ng/ml of LPS may lead to a different channel expression pattern compared to the 1μg/ml used here.

One more K_v channel published before was Kcna6 (K_v1.6) (Kotecha & Schlichter, 1999). Our work confirmed its expression in N9 microglia and indicated no significant influence by LPS treatment on its gene expression.

4.3.2.3 K_{Ca} channels

BK-type current was recorded in the human, fetal and mouse microglia (McLarnon *et al.*, 1997; McLarnon *et al.*, 1995; Schilling & Eder, 2007). In addition, the expression of BK channel mRNA was found in the BV-2 microglial cell line (Schilling *et al.*, 2002). However, whether BK mRNA expression changes under microglial activation by LPS has not been determined yet. It was shown here that Kcnma1 (K_{Ca}1.1) subunit mRNA was abundantly expressed compared to other subunits in N9 microglia and its expression was not significantly influenced by LPS. In addition, its β subunit mRNA was also examined in which Kcnmb3 (sloβ3) was not detectable and the gene of Kcnmb4 (sloβ4) was higher than Kcnmb1 (sloβ1) and Kcnmb2 (sloβ2). The work here extended the knowledge regarding BK gene expression in microglia. However as a complete BK channel is a tetramer of α subunits and may include four different β subunits, the distribution, proportion and function of both pore-forming subunits and β subunits in microglia still need to be further studied.

The mRNA of Kcnn1 (K_{Ca}2.1), Kcnn3 (K_{Ca}2.3), Kcnn4 (K_{Ca}3.1) were all expressed in N9 cells as well as other rodent microglia in previous studies (Kaushal *et al.*, 2007; Schlichter *et al.*, 2010; Khanna *et al.*, 2001) except for Kcnn2 (K_{Ca}2.2) which was not detectable in N9 cells. In previous studies, two publications (Khanna *et al.*, 2001; Schlichter *et al.*, 2010) identifying Kcnn2 (K_{Ca}2.2) were both from cultured primary rat microglia, thus Kcnn2 (K_{Ca}2.2) expression may be species-dependent. Gene expression of Kcnn1 (K_{Ca}2.1) and Kcnn4 (K_{Ca}3.1) were decreased while gene of Kcnn3 (K_{Ca}2.3) was increased by LPS (100ng/ml, 24hr) in rat microglia. Here LPS (1μg/ml, 24hr) did not significantly influence the expression of these subunits in N9 cells. The reason for such discrepancy may be from either the difference of species or that LPS-induced gene expression of K_{Ca} channels occurs in a dose-dependent manner.

4.3.2.4 Kcnk6 (K_{2p}6.1) channels

Kcnk6 (K_{2p}6.1) is one of the most abundantly expressed subunits in N9 microglia cell line (Figure 4-3). However, in previous studies there was very limited understanding on microglial K_{2p}6.1, including both its expression and function. In addition, Kcnk6 (K_{2p}6.1) was the only subunit significantly downregulated by LPS treatment in N9 microglia. It is then questioned whether its activity may in turn regulate LPS-induced microglial activation.

4.3.3 Conclusion and future work

Here screening for the mRNAs encoding of most K^+ channel subunits was performed in the resting N9 microglial cell line. In addition, using the optimized LPS activation method, the expression pattern of K^+ channel mRNA was also examined in the activated microglia. The generated expression pattern extends the understanding of K^+ channels in microglia which may facilitate the research in the future.

Most K^+ channel mRNA expression was not significantly affected by LPS treatment. As there was evidence indicating that whole cell current expression induced by LPS is time-dependent (Nörenberg *et al.*, 1992), it may be possible that at shorter or longer culture exposure to 1μg/ml LPS the K^+ channel mRNA may display a different expression pattern.

From previous studies, it is clear that the change of gene expression may not be associated with change of protein. For example, K_v1.3 gene expression in the isolated rat primary microglia was upregulated by extracellular PMA or LPS treatment but their protein was not affected by either of these two stimulations (Fordyce *et al.*, 2005). Thus it will be important to screen the protein and current expression of K^+ channels and their change following the LPS application. This would facilitate the understanding of how LPS-induced gene and protein expression

was associated in microglia. In addition, investigations should also examine K^+ channel mRNA expression in different species as mice and rats may potentially display different expression properties. What is more, an important question is to ask what role K^+ channels play in microglia. For example, the blockade of IK channels attenuated microglial respiratory burst and neuronal toxicity (Khanna *et al.*, 2001). As channels are sensitive the to various blockers, a pharmacological approach would be a good way to detect channel function in N9 cells.

Finally, in this thesis most of the 65 subunits detected were expressed at low level (Figure 4-2). Thus it is reasonable to focus on the most abundantly expressed subunits (Figure 4-3) which included Kcnma1 ($K_{Ca}1.1$), Kcnk6 ($K_{2p}6.1$), Kcnc3 ($K_v3.3$), Abcc8 (SUR1), Kcnj2 ($K_{ir}2.1$) and Kcnn4 ($K_{Ca}3.1$) with $K_{2p}6.1$ significantly decreased by LPS treatment. For these channels, roles of $K_{2p}6.1$, $K_v3.3$ and $K_{ir}2.1$ in microglia have not been extensively examined. In addition, it is also important to examine ion channels like BK whose current and gene were discovered before but not their function. Besides abundantly expressed channels, further research on the channels, such as $K_v1.3$ and $K_v1.5$ which were well examined in other types of microglia but not N9 microglia, will extend the understanding of their role in microglia as well.

CHAPTER FIVE

The Functional Role of K^+ Channels in N9 Microglia

5.1 Chapter introduction

Activated microglia release nitric oxide (NO) that plays an important role in neuronal death. As described in Chapter 1, blocking potassium (K^+) channel currents either attenuated (Fordyce *et al.*, 2005) or facilitated (Ortega *et al.*, 2012) microglial activation which further regulated microglial neuronal toxicity. Thus, based on the mRNA expression pattern of K^+ channels examined in Chapter 4, it is aimed to determine how the functional role of K^+ channels is in N9 microglial NO release. In addition, examination of expression of K^+ current would facilitate the understanding of their role in microglial NO release. However, although the N9 microglial cell line has been commonly used for investigation of microglial activation and microglial NO release (Zhao *et al.*, 2011; Chang *et al.*, 2008; Meng *et al.*, 2008; Wu *et al.*, 2007; Hou *et al.*, 2006; Bi *et al.*, 2005; Suuronen *et al.*, 2006; Nuutinen *et al.*, 2005; Suuronen *et al.*, 2003), little electrophysiological work has been done on it. In addition, it was reported the expression of K^+ current varies depending on microglial activation (Boucsein *et al.*, 2000; Kettenmann *et al.*, 1990; Nörenberg *et al.*, 1992; Draheim *et al.*, 1999). Thus, electrophysiological analysis will not only facilitate the investigation of the role of K^+ channels in microglial NO release but also extend the understanding of N9 microglial current properties.

5.1.1 Channels and subunits to be examined

N9 microglia expressed a variety of K^+ channel mRNAs as examined in Chapter 4. Because the majority of their expression was at low level, the focus was then on the most abundantly expressed channels and subunits which included: large conductance Ca^{2+}-sensitive and voltage-activated K^+ channels (BK), tandem pore domain K^+ channel (K_{2p})6.1 channels, voltage-gated K^+ channel (K_v)3.3 channels, sulfonylurea receptor (SUR)1 subunit, inwardly rectifying K^+ channel (K_{ir})2.1 channels and intermediate conductance Ca^{2+}-activated of K^+ ions channels (IK) (Figure 4-3). However, considering the availability of pharmacology, K_v3.3 can not be examined

at this step as there was no specific activator or blocker for it. Besides these abundantly expressed K^+ channel subunits, $K_v1.3$ and $K_v1.5$ channels which are expressed in N9 cell and play important roles in microglia in previous studies were also examined here.

5.1.2 Pharmacological blockers and activators

For BK channels, IK channels, $K_v1.3$ and SUR1 subunits, the well characterized antagonists paxilline, Tram34, margatoxin (MgTX) and glibenclamide (GBC) (Gutman *et al.*, 2005; Kubo *et al.*, 2005; Wei *et al.*, 2005; Lovasz *et al.*, 2011; Ortega *et al.*, 2012) were used. Agonists for BK and IK, NS1619 and NS309, were also used (Wei *et al.*, 2005). NS309 is an activator for both small conductance Ca^{2+}-activated K^+ channels (SK) (half maximal effective concentration (EC_{50})=30nM) and IK (EC_{50}=10nM) channels (Wei *et al.*, 2005; Mannhold *et al.*, 2006; Strøbaek *et al.*, 2004). Due to the lack of an IK channel selective activator, NS309 was applied during the experiment. GBC blocks ATP-sensitive K^+ channel (K_{ATP}) current via binding to either SUR1 or SUR2 subunits (Lovasz *et al.*, 2011). However, as SUR2 was not detectable in N9 cells (Table 4-2), GBC may reveal a role for SUR1 in N9 cells. For $K_v1.5$ channels, the inhibitor propafenone (PPF) was used. Although extracellular PPF is not a potent selective blocker for $K_v1.5$ channels as it is able to block $K_v1.5$, K_{ATP} and human ether-a-go-go-related gene (HERG) currents (Grissmer *et al.*, 1994; Franqueza *et al.*, 1997; Malayev *et al.*, 1995; Franqueza *et al.*, 1998; Seki *et al.*, 1999; Christé *et al.*, 1999; Arias *et al.*, 2003), based on the gene expression described in Chapter 4 the pore-forming subunits of Kcnj8 ($K_{ir}6.1$), Kcnj11 ($K_{ir}6.2$) and Kcnh2 ($K_v11.1$) were not detectable in N9 cells. In addition, previous reports also indicated that $K_v1.2$ current is sensitive to PPF as well, but this was only seen with intracellular application of PPF (Madeja *et al.*, 2003) and Kcna2 ($K_v1.2$) was not detectable in N9 cells, either (Table 4-2). Thus the effect of PPF may be mainly through the $K_v1.5$ in N9 cells. Similar to $K_v1.5$ channels, there was no selective blocker for $K_{2p}6.1$ and $K_{ir}2.1$ channels, but they are both sensitive to

external barium (Ba^{2+}). $K_{ir}2.1$ has half-maximal inhibition concentration (IC_{50}) of 15.9±2.5μM at -120mV or IC_{50} of <45μM at -90mV for external Ba^{2+} (Schram *et al.*, 2002). Its IC_{50} value decreased dramatically if $K_{ir}2.1$ was co-expressed with $K_{ir}2.3$ (about 6.3μM) (Kubo *et al.*, 2005) or $K_{ir}2.4$ (about 3.7μM) (Schram *et al.*, 2002). $K_{2p}6.1$ has IC_{50} of 100μM for external Ba^{2+} (Patel *et al.*, 2000; Goldstein *et al.*, 2005). What is more important, based on the K^+ channel mRNAs expressed in resting N9 microglia, there were potentially >10 channels that are sensitive to external Ba^{2+} (100μM) (Figure 5-1A) (Kubo *et al.*, 2005; Goldstein *et al.*, 2005; Gutman *et al.*, 2005). Kcnk6 ($K_{2p}6.1$) and Kcnj2 ($K_{ir}2.1$) were abundantly expressed which represented over 80% of these channels (Figure 5-1B). Thus effect of low B^{2+} may mainly represent the function of $K_{2p}6.1$ and $K_{ir}2.1$ channels. The applied blockers and activators with commonly used concentrations are listed in Table 5-1.

5.1.3 Working hypothesis

In this chapter, the hypothesis that N9 microglia express multiple K^+ current and the blockade of K^+ channel current regulates N9 microglial NO release will be examined.

5.1.4 Aims to be addressed in this chapter

5.1.4.1 Do the selected K^+ channels regulate LPS-induced microglial NO release?

Under the application of PPF, MgTX, Tram34, paxilline, $BaCl_2$, NS1619 and NS309, their effect on lipopolysaccharide (LPS)-induced N9 microglial NO release will be examined. Because LPS-induced NO release is also dependent on cellular viability, nitrite (NO_2^-) concentration in the supernatant will be normalised to relative cell number.

A

Kcnj1 (K_{ir}1.1)	Kcnj2 (K_{ir}2.1)	Kcnj4 (K_{ir}2.3)	Kcnj14 (K_{ir}2.4)	Kcnj3 (K_{ir}3.1)	Kcnj6 (K_{ir}3.2)	Kcnj15 (K_{ir}4.2)
Kcnk12 (K_{2p}2.1)	Kcnk3 (K_{2p}3.1)	Kcnk6 (K_{2p}6.1)	Kcnk18 (K_{2p}18.1)			
Kcna3 (K_v1.3)	Kcna5 (K_v1.5)	Kcnb1 (K_v2.1)	Kcnh8 (K_v12.1)			

B

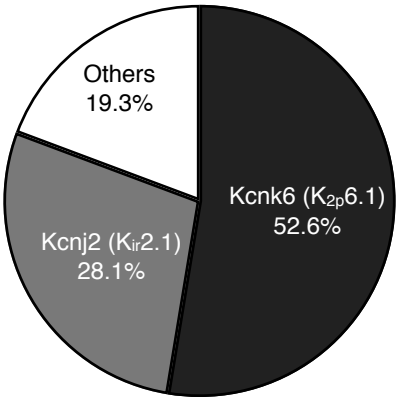

Figure 5-1. K^+ channels expressed in N9 cells that can be blocked by extracellular Ba^{2+}. (**A**) Based on the gene expression described in Chapter 4, in resting N9 microglia there were >10 potassium (K^+) channels reported sensitive to extracellular barium (Ba^{2+}). Kcnj1 (K_{ir}1.1): IC_{50}=NE [10]; Kcnj2 (K_{ir}2.1): IC_{50}<50μM, if co-expressed with either K_{ir}2.4 or K_{ir}2.3 IC_{50}<10μM [1] [4]; Kcnj4 (K_{ir}2.3): IC_{50}=10.3μM [1]; Kcnj14 (K_{ir}2.4): IC_{50}≤116μM [1][4]; Kcnj3 (K_{ir}3.1): IC_{50}=~3.5nM [5]; Kcnj6 (K_{ir}3.2): IC_{50}=NE [1][10]; Kcnj15 (K_{ir}4.2): IC_{50}=NE [10]; Kcnk12 (K_{2p}2.1): IC_{50}=1mM [2]; Kcnk3 (K_{2p}3.1): IC_{50}=500mM [2]; Kcnk6 (K_{2p}6.1): IC_{50}=100μM [2][6]; Kcnk18 (K_{2p}18.1): IC_{50}=3mM [2]; Kcna3 (K_v1.3): IC_{50}=NE, pH-dependent [9][10]; Kcna5 (K_v1.5): IC_{50}=~20μM (0.003Hz), or IC_{50}=~1mM (0.7Hz), depolarization from -80mV to +50mV (ph7.4), frequency- & pH-dependent [8]; Kcnb1 (K_v2.1): IC_{50}=30mM [3]; Kcnh8 (K_v12.1): IC_{50}=180μM [7]. (**B**) Of these K^+ channels, Kcnk6 (K_{2P}6.1) channels occupied 52.6% and Kcnj2 (K_{ir}2.1) occupied 28.1% of these K^+ channel mRNAs expression. K_{ir}: inwardly rectifying K^+ channel; K_{2p}: tandem pore domain K^+ channel; K_v: voltage-gated K^+ channel; IC_{50}: half-maximal inhibition concentration; NE: not established.

References: [1]: (Kubo *et al.*, 2005); [2]: (Goldstein *et al.*, 2005); [3]: (Gutman *et al.*, 2005); [4]: (Schram *et al.*, 2002); [5]: (Ehrlich *et al.*, 2004; Jin & Z. Lu, 1999); [6]: (Patel *et al.*, 2000); [7]: (Zou *et al.*, 2003); [8]: (Cheng *et al.*, 2008); [9]: (Somodi *et al.*, 2004); [10]: (Wulff & Zhorov, 2008).

Name	Regular concentration or IC_{50}	Target	References
PPF	(1) 10μM (2) IC_{50}=4.4μM	K_v1.5 in N9 cells	(1) (Gutman *et al.*, 2005) (2) (Franqueza *et al.*, 1998; Gutman *et al.*, 2005)
MgTX	(1)1nM (2) 230 pM	K_v1.3	(1) (Gutman *et al.*, 2005) (2) (Carrisoza-Gaytán *et al.*, 2010)
GBC	(1) 10^{-5}nM to 10μM (2) IC_{50}=5μM (SUR1+K_{ir}6.1) IC_{50}=8nM (SUR1+K_{ir}6.2)	SUR	(1) (Lovasz *et al.*, 2011; Ortega *et al.*, 2012; Mikhailov *et al.*, 2001; Tan *et al.*, 2007) (2) (Kew & Davies, 2009)
$BaCl_2$	0.1~1mM	see Figure 5-1	(Goldstein *et al.*, 2005; Preisig-Müller *et al.*, 2002; Young *et al.*, 2009; Patel *et al.*, 2000)
Tram34	(1) 1μM (2) IC_{50}=18nM	IK	(1) (Wei *et al.*, 2005) (2) (Toyama *et al.*, 2008)
NS1619	EC_{50}=1μM	BK	(Skalska *et al.*, 2008)
paxilline	(1) 1μM (2) IC_{50}=17nM	BK	(1) (Wei *et al.*, 2005) (2) (Ahluwalia *et al.*, 2004)
NS309	(1) 1μM (2) EC_{50}=10nM (IK) EC_{50}=30nM (SK)	SK/IK	(1) (Sones *et al.*, 2009) (2) (Mannhold *et al.*, 2006; Strøbaek *et al.*, 2004)

Table 5-1. Pharmacological blockers and activators used in this thesis and their regular concentrations used in previous studies. Here includes six K^+ channel blockers (PPF, MgTX, GBC, $BaCl_2$, Tram34 and paxilline) and two K^+ channels activator (NS309 and NS1619). Their target (channels or subunit), regular pharmacological concentration or IC_{50} value are indicated in the table. PPF: propafenone; MgTX: margatoxin; GBC: glibenclamide; BK: large conductance Ca^{2+}-sensitive and voltage-activated K^+ channels; SK: small conductance Ca^{2+}-activated K^+ channels; IK: intermediate conductance Ca^{2+}-activated K^+ channels; SUR: sulfonylurea receptor; IC_{50}: half-maximal inhibition concentration; EC_{50}: half maximal effective concentration.

5.1.4.2 Do N9 microglia express K^+ channel current?

Using whole-cell voltage clamp and current clamp, the electrophysiological properties of resting N9 microglia will be examined including: (1) The membrane potential. (2) Cell capacitance. (3) The whole-cell current of N9 microglia. (4) The sensitivity of N9 microglial whole-cell current to K^+ channels blockers. Both 1μM intracellular Ca^{2+} concentration ($[Ca^{2+}]_i$) and 10nM $[Ca^{2+}]_i$ would be applied to examine any potential calcium-activated K^+ channel (K_{Ca})-type current. As it was reported microglia *in vitro* express large inward K^+ current with low outward K^+ current, the hypothesis is N9 microglia may display similar phenomenon.

5.1.4.3 Is N9 microglial whole-cell current regulated by LPS treatment?

After activation, N9 microglial whole-cell current may be regulated by LPS treatment. The difference between LPS-induced and resting microglial whole-cell current will be compared including current density, membrane potential and cell capacitance. As LPS was reported to regulate the expression of K^+ channel current (Kettenmann *et al.*, 1990; Draheim *et al.*, 1999), whether in N9 microglia different K^+ current will be induced by LPS was examined. The morphology of all activated microglia patched was amoeboid and the morphology of all resting microglia patched was ramified.

5.2 Results

5.2.1 Role of K^+ channels in LPS-induced NO release

The roles of K^+ channels in N9 microglial NO release was examined by culturing N9 microglia with the respective pharmacological blockers or activators. Some channels play a role in regulating LPS-induced NO release while some did not. Here, how each channel regulates N9 microglial activation is introduced below.

5.2.1.1 The effect of $K_v1.3$ channel inhibition on N9 microglial viability and NO release

MgTX, a commonly used $K_v1.3$ blocker (Kazama *et al.*, 2012; Jang *et al.*, 2011), was used to test the role of $K_v1.3$ in LPS-induced NO release. N9 cells were either treated using LPS with MgTX or using LPS with vehicle as control following the optimized activation method generated in Chapter 3. The NO_2^- concentration in the supernatant was normalised to cell number to avoid pharmacological effect on cell viability. Application of MgTX (0.1nM to 10nM) had no significant effect on either cell viability or LPS-induced NO release (Figure 5-2).

5.2.1.2 The effect of $K_v1.5$ channel inhibition on N9 microglial viability and NO release

As described in section 5.1.2, PPF was applied to investigate the function of $K_v1.5$ channels in N9 microglia. PPF at concentrations from 0.1μM to 10μM displayed no significant effect on cellular viability, but at 100μM PPF was toxic to N9 cells (Figure 5-3A). Thus the NO_2^- in the supernatant was not detectable in the sample treated by 100μM PPF. PPF at 0.1μM and 1μM did not regulate LPS-induced microglial NO release, but 10μM PPF significantly attenuated the NO release by about 13.4% (Figure 5-3B).

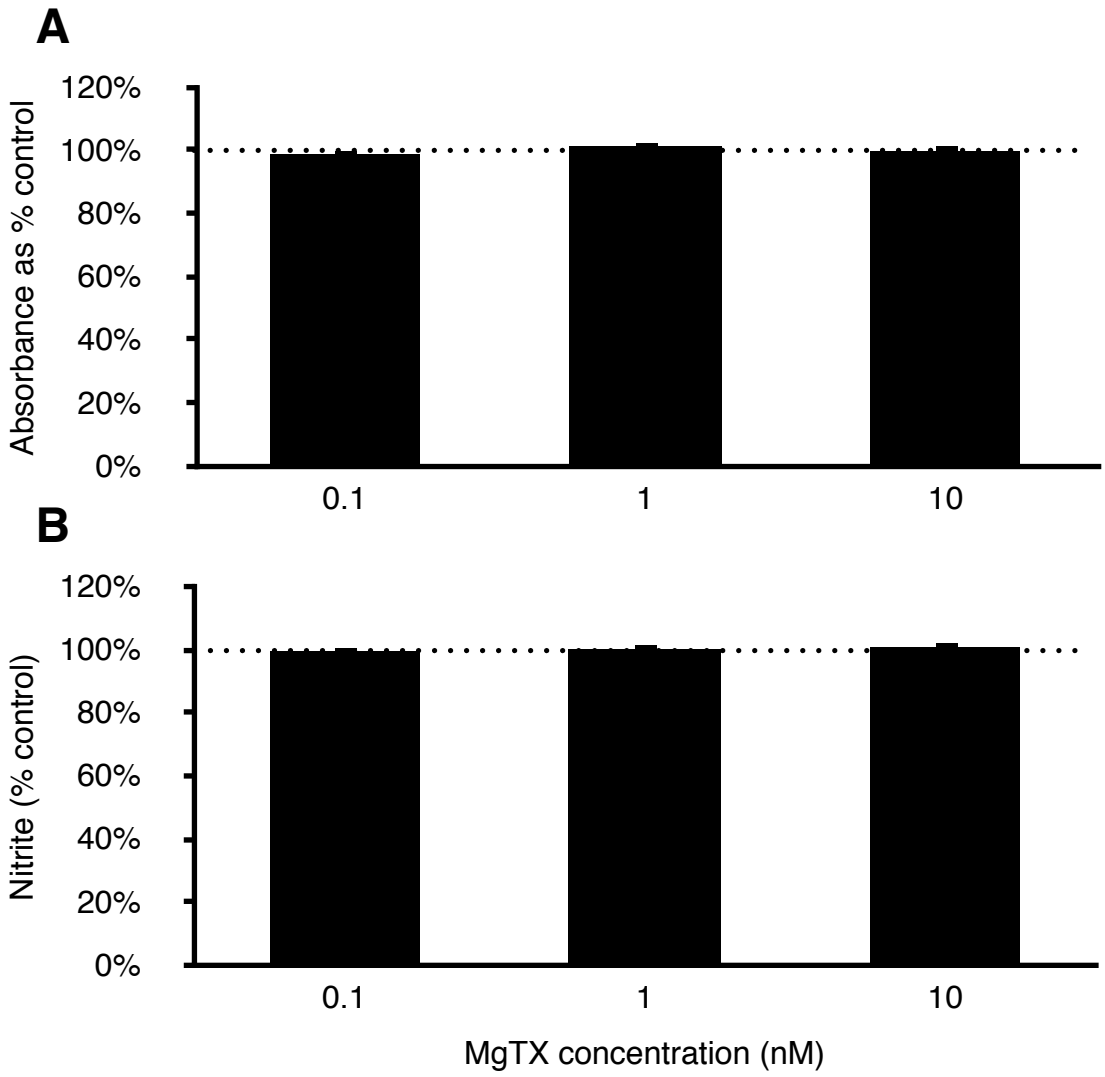

Figure 5-2. Dose-dependence of MgTX on N9 microglial viability and LPS-induced microglial NO. MgTX is a commonly used blocker for $K_v1.3$ channels. N9 cells were activated following the optimized method described in section 2.1.1.5.2 in the presence of MgTX. Nitrite (NO_2^-) concentrations were normalised by cell number and data are presented as percentage of control, lipopolysaccharide (LPS) with respective vehicle (dotted line). (**A**) MgTX ranging from 0.1nM to 10nM did not display any cytotoxicity to N9 cells. Cell number was determined by measuring the absorbance in the MTS assay as described in section 2.1.1.7. (**B**) MgTX ranging form 0.1nM to 10nM did not influence LPS-induced nitric oxide (NO) release. Data are given as mean±SEM. (n=6)

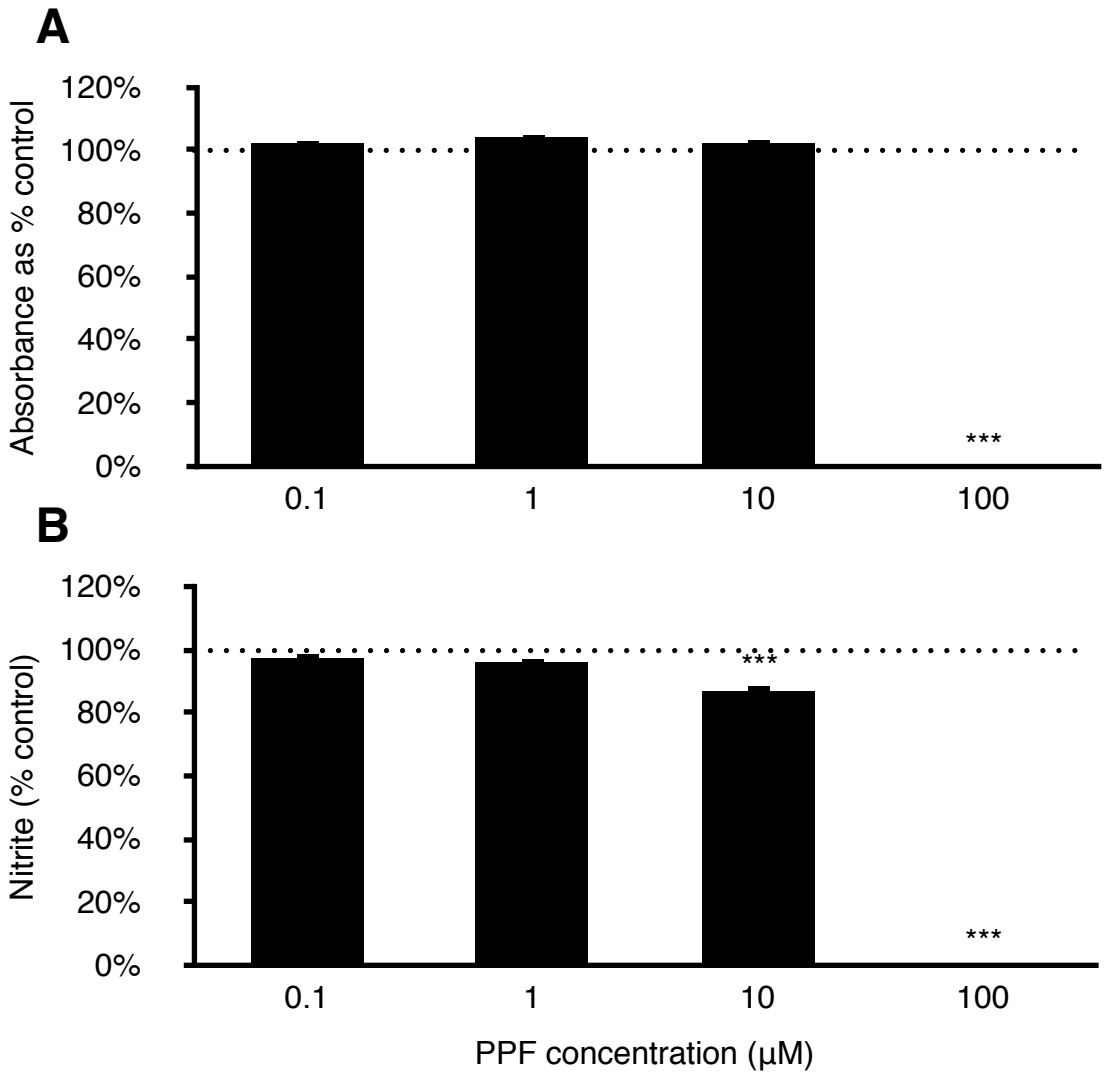

Figure 5-3. Dose-dependence of PPF on N9 microglial viability and LPS-induced microglial NO. NO_2^- concentrations were normalised by cell number and data are presented as percentage of control, LPS with respective vehicle (dotted line). (**A**) PPF at 100µM displayed cytotoxicity to N9 cells which killed 100% of the cells in the sample. (**B**) At 10µM, PPF significantly decreased LPS-induced microglial NO release to about 86.6% of control. No nitrite was detectable in the presence of 100µM PPF. Data are given as mean±SEM. ***$p<0.001$ vs. control, by ANOVA with Tukey post hoc test. (n=6)

5.2.1.3 The effect of Ba^{2+} on N9 microglial viability and NO release

As indicated at the beginning of this chapter there are no selective blockers for $K_{2p}6.1$ or $K_{ir}2.1$ channels. However, as their mRNA expression represents >80% of the mRNA expression of channels that can be blocked by external Ba^{2+} (Figure 5-1). Thus Ba^{2+} was applied to examine the function of these two channels.

$BaCl_2$ at concentration from 10μM to 1mM was not toxic to N9 cells, but 10mM of $BaCl_2$ reduced cell number by about 8.1% (Figure 5-4A). Ba^{2+} at 10μM and 100μM had no effect on LPS-induced NO release. However, at 1mM and 10mM it significantly attenuated LPS-induced NO release by by about 21.6% and 34.4% respectively (Figure 5-4B).

5.2.1.4 The effect of SUR1-associated channels inhibition on N9 microglial viability and NO release

N9 cells were cultured with LPS and GBC (0.1nM to 10μM) which blocks K_{ATP} current by binding to their SUR subunits. As SUR2 mRNA was not detectable in N9 cells (Table 4-2), GBC was assumed to only bind to SUR1 in N9 microglia. However, GBC had no effect on cell viability or LPS-induced NO release (Figure 5-5).

5.2.1.5 The role of IK channels on N9 microglial viability and NO release

To investigate the role of IK channels in microglia, the IK channel selective blocker, Tram34, and activator, NS309, were applied to N9 cells. Tram34 (0.01μM to 10μM) was not toxic to N9 cells (Figure 5-6A). However, Tram34 at 0.01μM and 1μM attenuated LPS-induced microglial NO release by about 9.4% while 10μM Tram34 attenuated microglial NO release by about 50.6% (Figure 5-6B). At the latter concentration Tram34 may nonspecifically block K^+ current (Wei *et al.*, 2005;

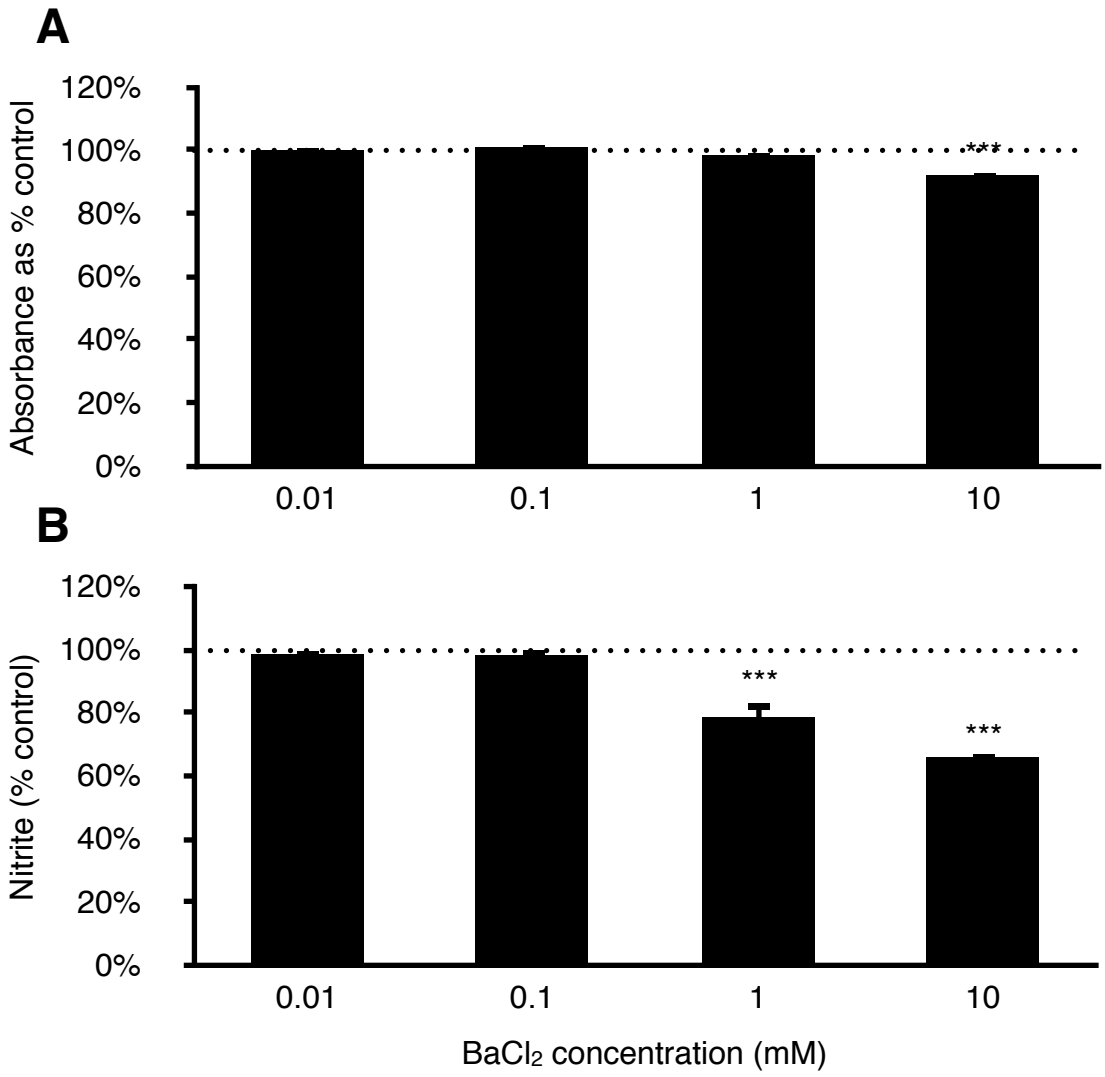

Figure 5-4. Dose-dependence of $BaCl_2$ on N9 microglial viability and LPS-induced microglial NO. $BaCl_2$ is supposed mainly blocking $K_{ir}2.1$ and $K_{2p}6.1$ channels in N9 microglia. NO_2^- concentrations were normalised by cell number and data are presented as percentage of control, LPS with respective vehicle (dotted line). (**A**) $BaCl_2$ only at 10mM displayed cytotoxicity to N9 cells which killed 8.1% of the N9 cells in the sample. (**B**) At 1mM, $BaCl_2$ significantly decreased LPS-induced microglial NO release to about 78.4% of control. At 10mM, $BaCl_2$ significantly decreased microglial NO release to about 65.6%. Data are given as mean±SEM. ***$p<0.001$ vs. control, by ANOVA with Tukey post hoc test. (n=6)

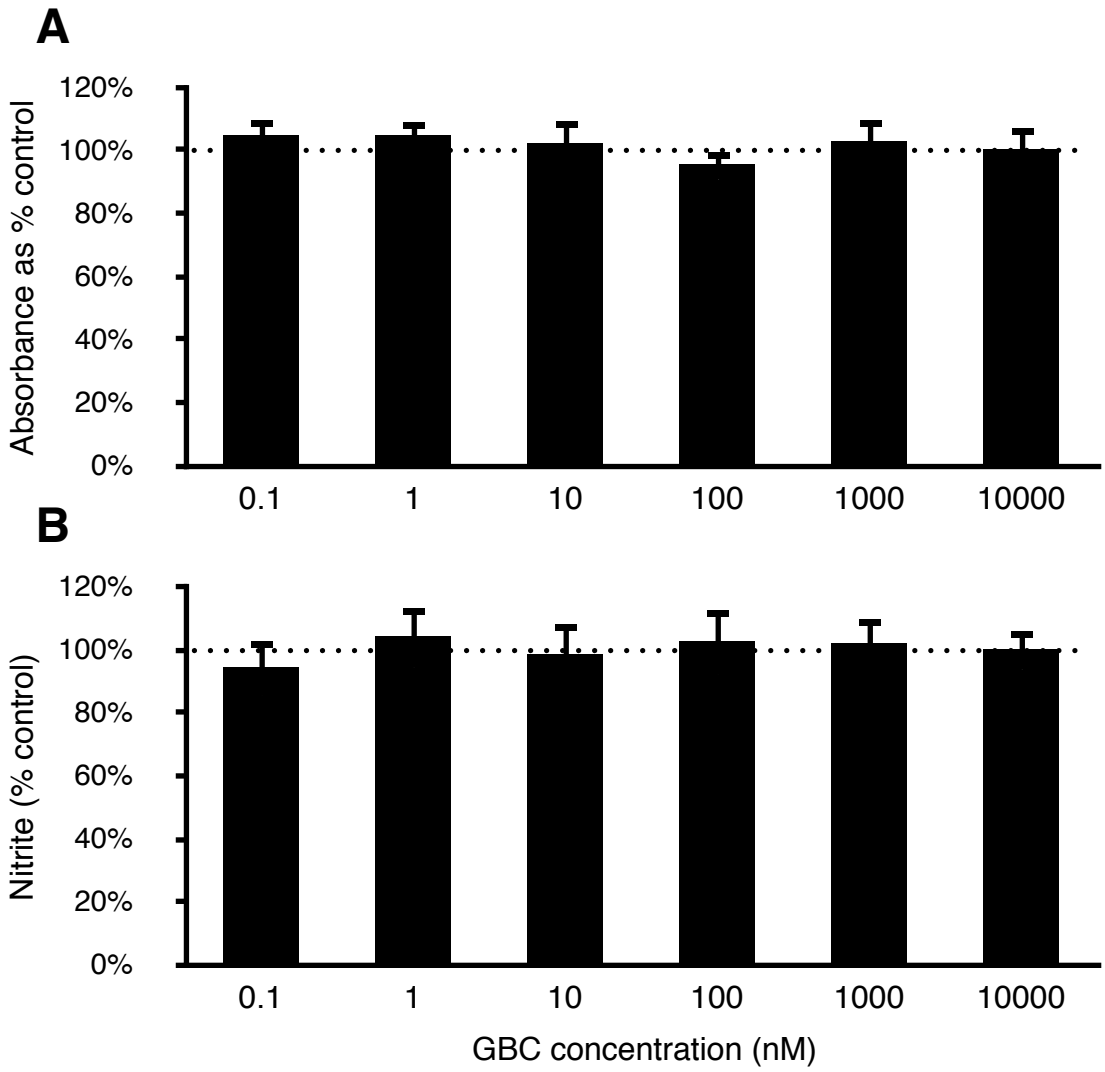

Figure 5-5. Dose-dependence of GBC on N9 microglial viability and LPS-induced microglial NO. GBC is a selective blocker for K_{ATP} current and it was supposed to mainly bind SUR1 subunit in N9 cells. NO_2^- concentrations were normalised by cell number and data are presented as percentage of control, LPS with respective vehicle (dotted line). (**A**) GBC ranging from 0.1nM to 10μM did not display any cytotoxicity to N9 cells. (**B**) GBC did not affect the LPS-induced microglial NO release. Data are given as mean±SEM. (n=4)

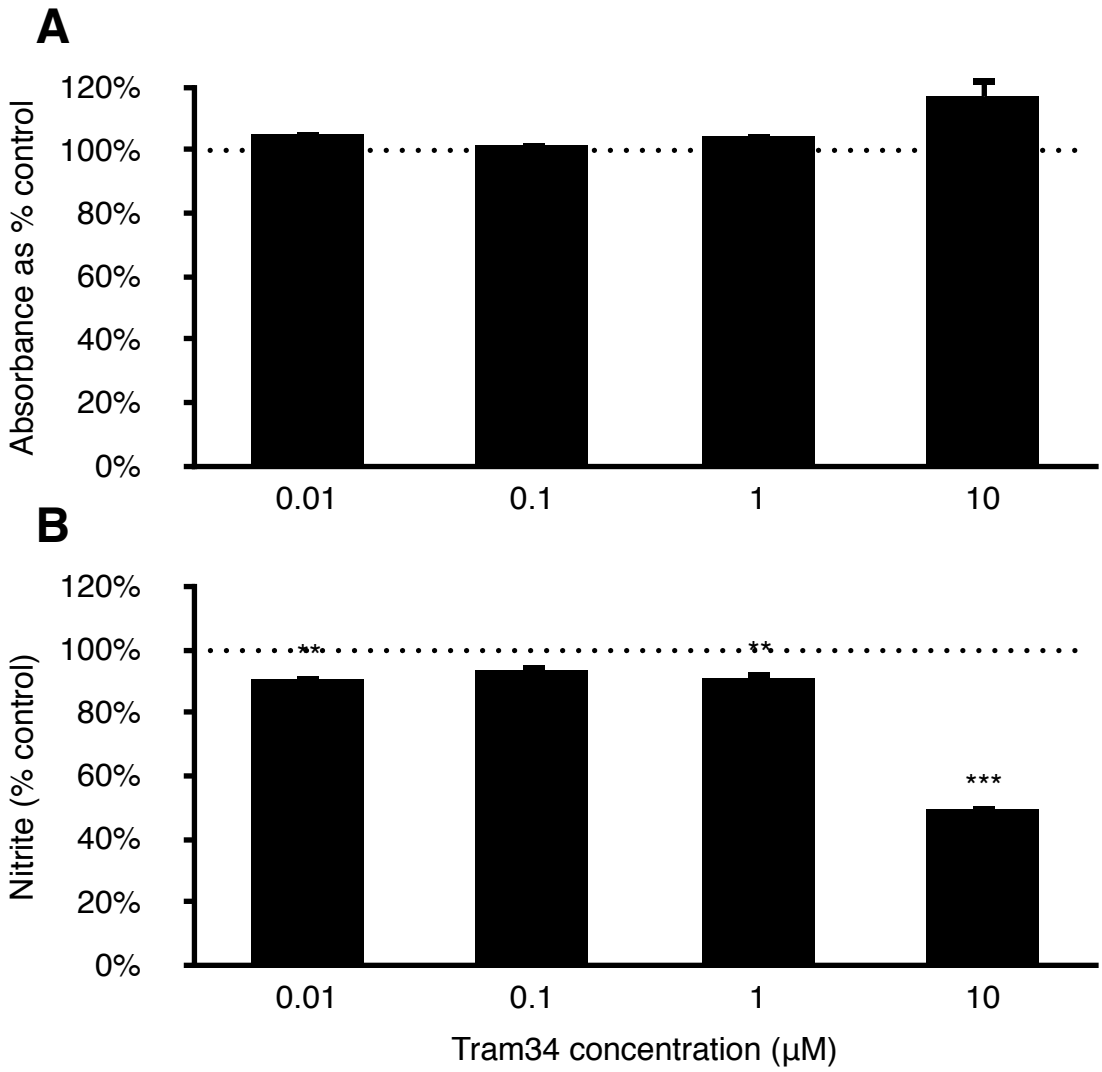

Figure 5-6. Dose-dependence of Tram34 on N9 microglial viability and LPS-induced microglial NO. Tram34 is a selective blocker for IK channels. NO_2^- concentrations were normalised by cell number and data are presented as percentage of control, LPS with respective vehicle (dotted line). (**A**) Tram34 (0.1μM to 10μM) did not display any cytotoxicity to N9 cells. (**B**) At 0.01μM, 1μM and 10μM, Tram34 significantly decreased LPS-induced microglial NO release. Data are given as mean±SEM. **p<0.01, ***p<0.001 vs. control, by ANOVA with Tukey post hoc test. (n=6)

Toyama *et al.*, 2008).

In addition, the activator of IK channels, NS309, (0.1μM to 10μM) had no effect on N9 cell proliferation (Figure 5-7A) or LPS-induced N9 microglial NO release (Figure 5-7B).

5.2.1.6 The role of BK channels on N9 microglial viability and NO release

The BK channel blocker, paxilline, at concentrations from 0.01μM to 10μM (Yaghi *et al.*, 2002; Raffaelli *et al.*, 2004) did not display toxicity to N9 cells (Figure 5-8A) only at 10μM did paxilline significantly decrease LPS-induced NO release by about 43.0% (Figure 5-8B) at which concentration paxilline may nonspecifically block K^+ channels (Wei *et al.*, 2005; Ahluwalia *et al.*, 2004). Meanwhile, the BK activator NS1619 at concentration 1μM and 10μM did not influence N9 cell proliferation but 100μM of NS1619 reduced N9 cells number by about 33.8% (Figure 5-9A). In addition, 100μM NS1619 significantly reduced LPS-induced NO release by about 81.8% while 1μM and 10μM of NS1619 had no effect (Figure 5-9B).

5.2.1.7 Role of BK channels on LPS-induced NO release in the presence of another channel blocker

Paxilline and NS1619 at concentrations 1μM or less (Table 5-1) that are specific for BK channels had no significant effect on LPS-induced NO release. However, BK channels may interact with other K^+ channels, such as IK channels (Thompson & Begenisich, 2009). Thus, it was questioned whether either paxilline or NS1619 may affect the inhibitory effect of Tram34, PPF or $BaCl_2$ on LPS-induced NO release.

Interestingly, paxilline prevented the inhibitory effect of Tram34, $BaCl_2$ and PPF on LPS-induced microglial NO release (Figure 5-10).

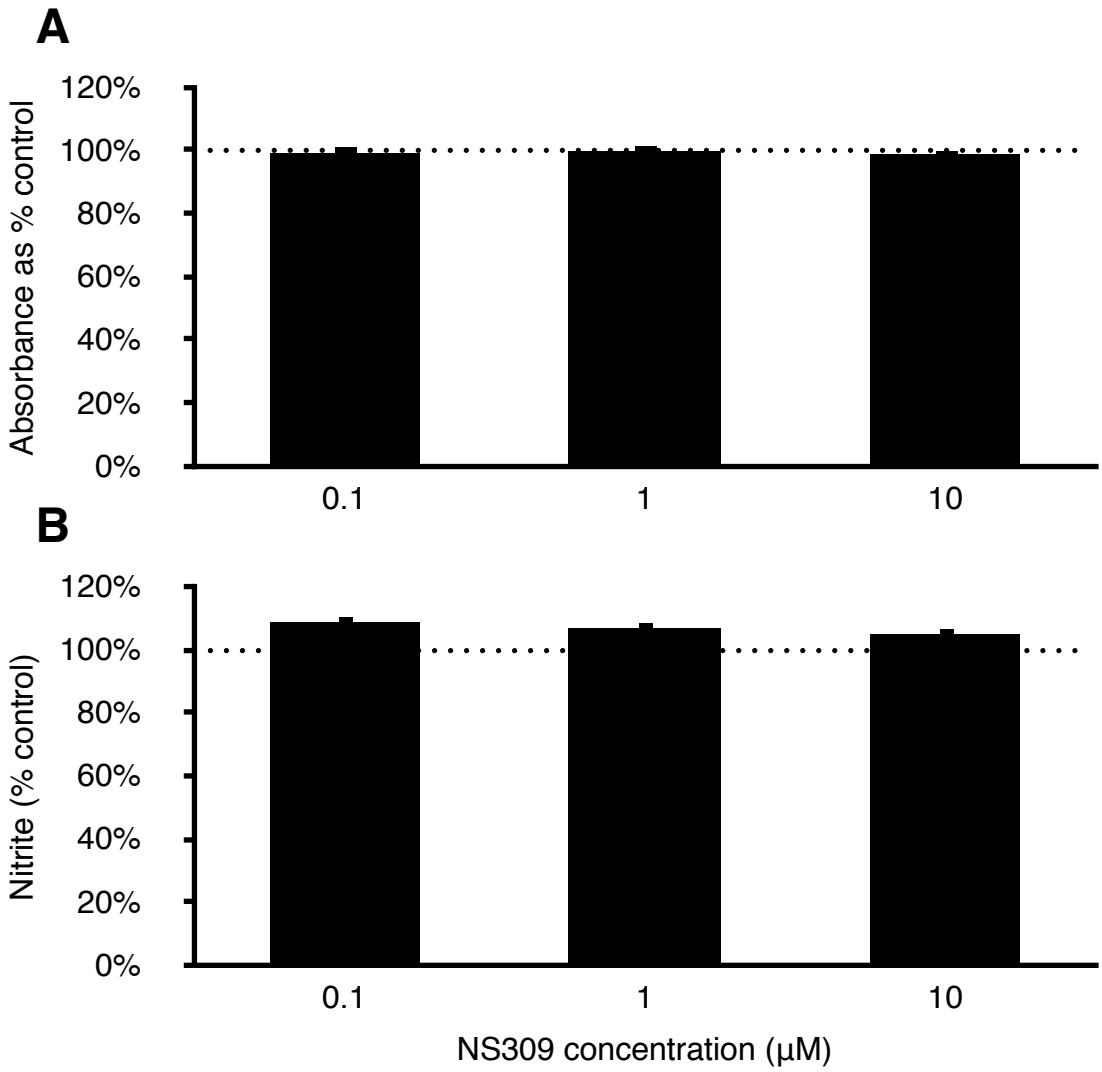

Figure 5-7. Dose-dependence of NS309 on N9 microglial viability and LPS-induced microglial NO. NS309 is able to activate IK channels. NO_2^- concentrations were normalised by cell number and data are presented as percentage of control, LPS with respective vehicle (dotted line). (**A**) NS309 ranging from 0.1µM to 10µM did not display any cytotoxicity to N9 cells. (**B**) NS309 ranging from 0.1µM to 10µM did not affect the LPS-induced microglial NO release. Data are given as mean±SEM. (n=8)

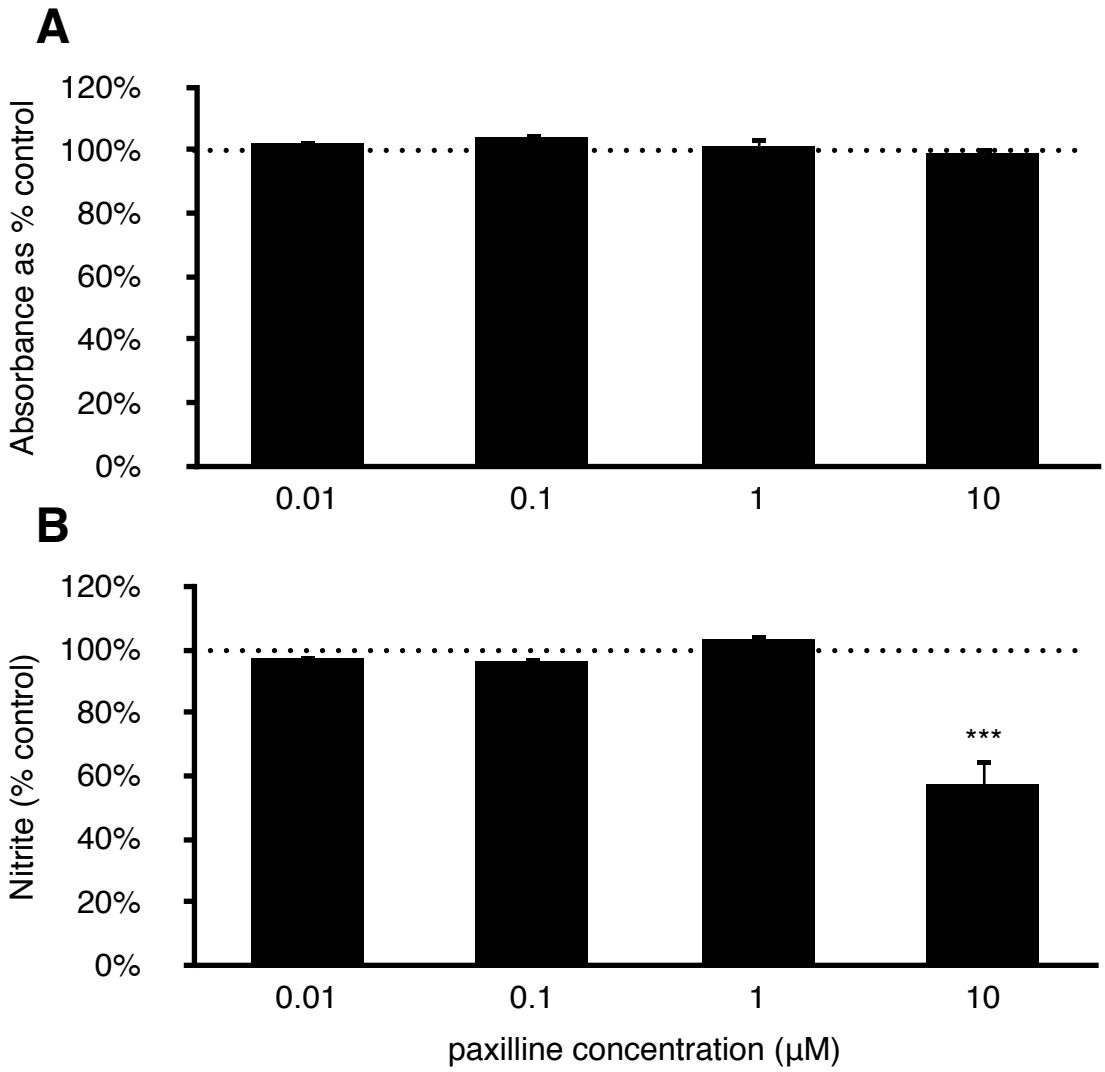

Figure 5-8. Dose-dependence of paxilline on N9 microglial viability and LPS-induced microglial NO. Paxilline is the selective blocker for BK channels. NO_2^- concentrations were normalised by cell number and data are presented as percentage of control, LPS with respective vehicle (dotted line). (**A**) Paxilline ranging from 0.01μM to 10μM did not display any cytotoxicity to N9 cells. (**B**) At 10μM, paxilline significantly decreased LPS-induced microglial NO release to about 57.0%. Data are given as mean±SEM. ***p<0.001 vs. control, by ANOVA with Tukey post hoc test. (n=6)

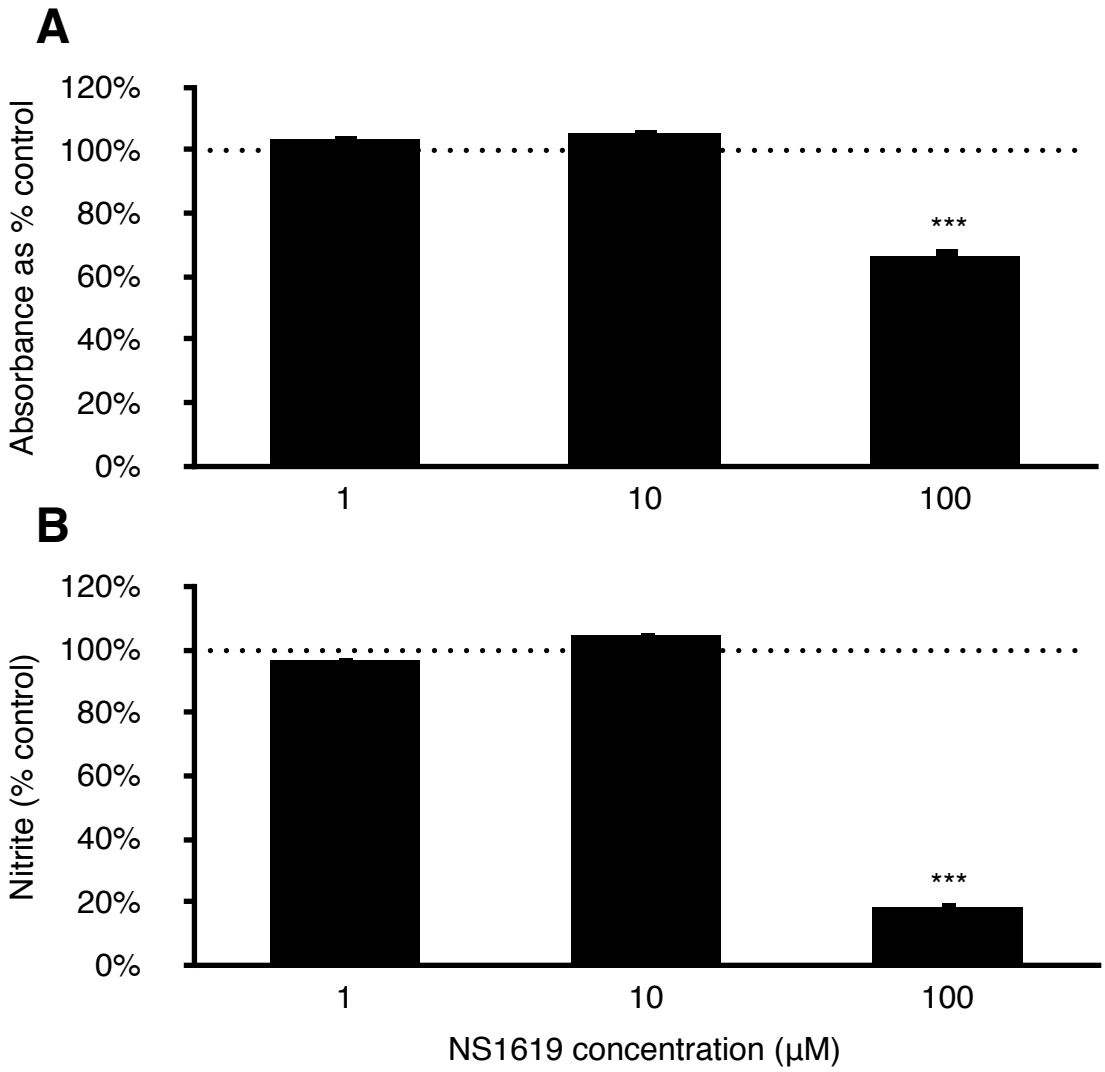

Figure 5-9. Dose-dependence of NS1619 on N9 microglial viability and LPS-induced microglial NO. NS1619 is a selective activator for BK channels. NO_2^- concentrations were normalised by cell number and data are presented as percentage of control, LPS with respective vehicle (dotted line). (**A**) NS1619 only at 100μM inhibited N9 microglial proliferation rate to about 66.2%. (**B**) At 100μM, NS1619 significantly decreased LPS-induced microglial NO release to about 18.2%. Data are given as mean±SEM. ***p<0.001 vs. control, by ANOVA with Tukey post hoc test. (n=12)

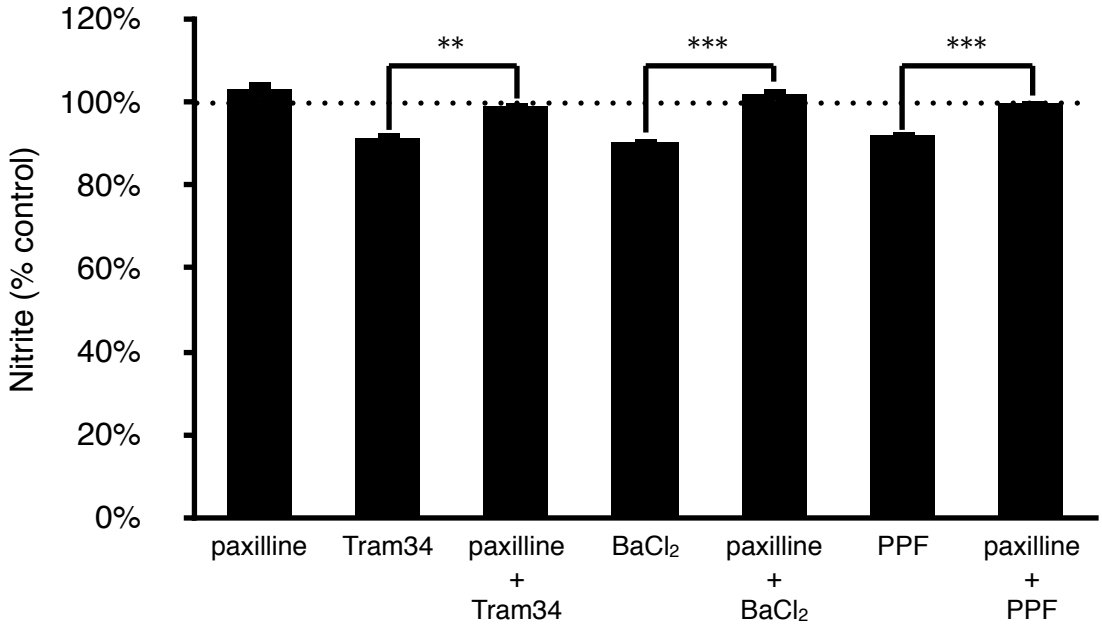

Figure 5-10. Paxilline attenuated the effect of Tram34, $BaCl_2$ and PPF on LPS-induced NO release. Paxilline (1µM), Tram34 (1µM), $BaCl_2$ (1mM) and PPF (10µM) were applied. All NO_2^- concentrations were normalised by cell number and data are presented as percentage of control, LPS with respective vehicle (dotted line). Paxilline attenuated the inhibition effect of Tram34, $BaCl_2$ and PPF on LPS-induced NO release. Data are given as mean±SEM. **p<0.01, ***p<0.001, by ANOVA with Tukey post hoc test. (n=12)

As inhibiting BK channel attenuated the effect of other K^+ channel blockers, it was hypothesized that activating BK using NS1619 might have an opposite effect. NS1619 facilitated the effect of Tram34 and PPF, but not $BaCl_2$, on the N9 microglial NO release by about 5.9% and 13.4% respectively (Figure 5-11).

5.2.1.8 Tram34 is additive with PPF to inhibit LPS-induced NO release

As the examination on BK channels indicated the interaction between channels, it was questioned whether combination of other channel blockers had an additive effect or not. Tram34 was additive with PPF to inhibit LPS-induced N9 microglial NO release (Figure 5-12A). However, $BaCl_2$ had no additive effect with either Tram34 or PPF on LPS-induced NO release (Figure 5-12B&C).

5.2.2 Electrophysiological characterization of N9 cells

It was questioned (1) Whether paxilline, Tram34, PPF, $BaCl_2$ affects N9 microglial whole-cell current. (2) Whether and how LPS affects the whole-cell current and K^+ current expression in N9 microglia. As MgTX (Pannasch *et al.*, 2006; Fordyce *et al.*, 2005) and GBC did not have effect on N9 microglial NO release, they were not examined in these experiments.

5.2.2.1 The whole-cell current of resting N9 cells

By using conventional whole-cell voltage clamp, the whole-cell current of resting N9 cells was examined. Cells were voltage clamped at -50mV and whole-cell current was evoked (200ms) by steps from -140mV to +100mV in 10mV increments (Figure 5-13A) in the physiological K^+ gradient as described in section 2.1.3.2. Intracellular

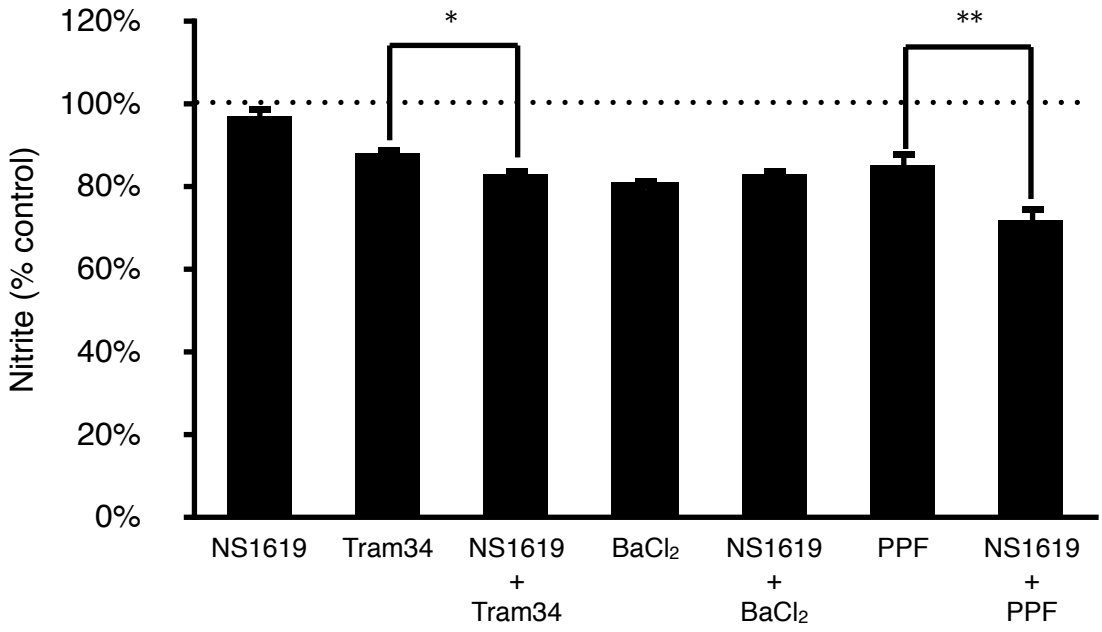

Figure 5-11. NS1619 facilitated the effect of Tram34 and PPF, but not $BaCl_2$ on LPS-induced NO release. NS1619 (10µM), Tram34 (1µM), $BaCl_2$ (1mM) and PPF (10µM) were applied. All NO_2^- concentrations were normalised by cell number and data are presented as percentage of control, LPS with respective vehicle (dotted line). NS1619 facilitated the inhibiting effect of Tram34 and PPF on LPS-induced NO release. However, the effect of $BaCl_2$ on NO release was not significantly regulated by NS1619 treatment. Data are given as mean±SEM. *$p<0.05$, **$p<0.01$, by ANOVA with Tukey post hoc test. (n=8)

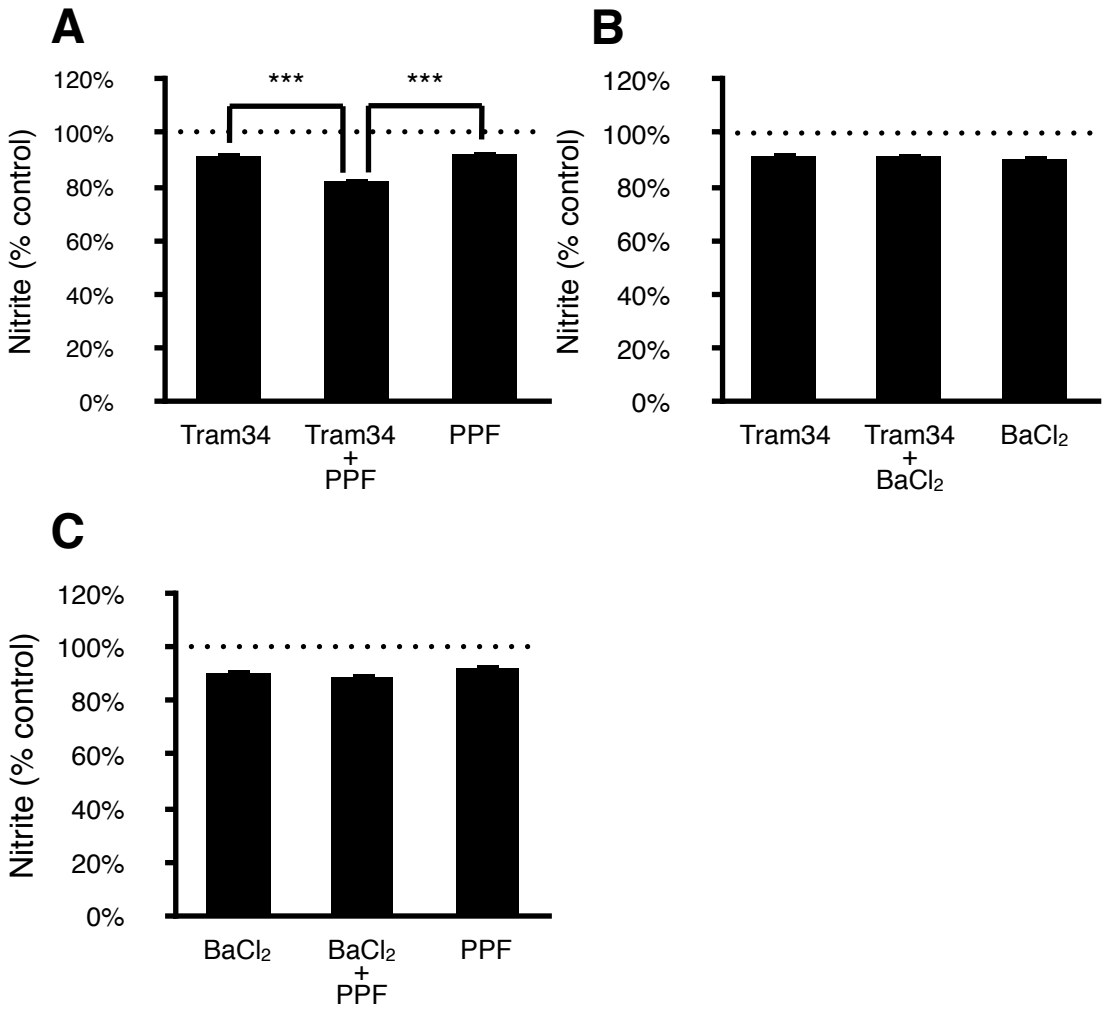

Figure 5-12. Tram34 was additive with the effect of PPF, but not $BaCl_2$ on LPS-induced NO release. Tram34 (1µM), $BaCl_2$ (1mM) and PPF (10µM) were applied. All NO_2^- concentrations were normalised by cell number and data are presented as percentage of control, LPS with respective vehicle (dotted line). (**A**) Only Tram34 with PPF displayed an accumulative effect on the microglial NO release which facilitated their inhibiting effect from 91.3% (Tram34) and 91.9% (PPF) to 81.8%. (**B**) & (**C**) However, $BaCl_2$ was not addictive with the effect of Tram34 or PPF. Data are given as mean±SEM. *p<0.05, **p<0.01, by ANOVA with Tukey post hoc test. (n=12)

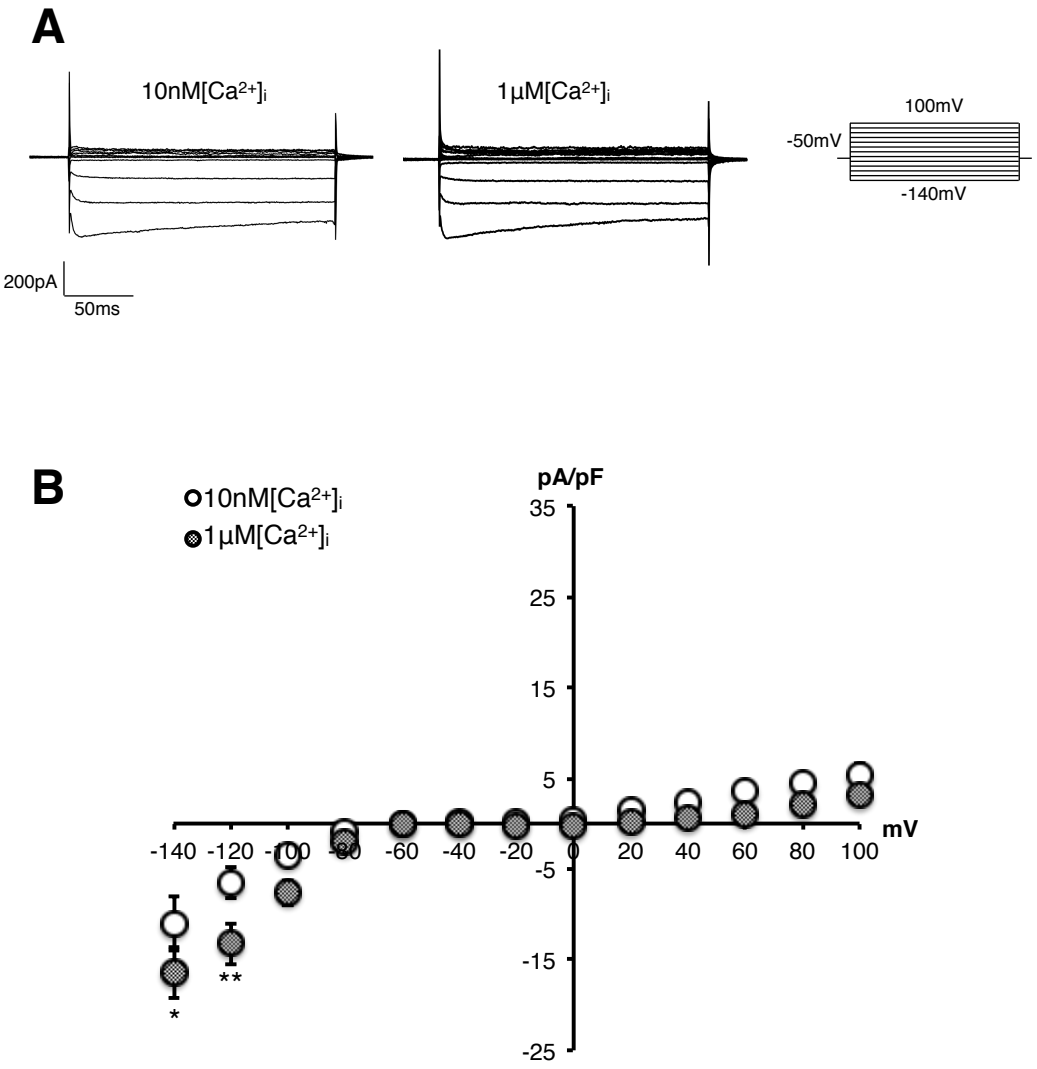

Figure 5-13. N9 microglial whole-cell current with 10nM and 1μM $[Ca^{2+}]_i$. The holding potential was -50mV. Currents were evoked by voltage steps from -140mV to +100mV in 20mV increments (200ms). (**A**) Representative traces of N9 microglial whole-cell current conditioned in physiological ion gradients with intracellular free Ca^{2+} buffered to 10nM and 1μM. On the right side it is the stimulation protocol associating with the traces. (**B**) The current density (pA/pF) vs. voltage (mV) plots for untreated N9 cells with 10nM $[Ca^{2+}]_i$ and 1μM $[Ca^{2+}]_i$. There was no significant difference in the outward current density but 1μM $[Ca^{2+}]_i$ displayed a higher inward current density than 10nM $[Ca^{2+}]_i$. Data are given as mean±SEM. *$p<0.05$, **$p<0.01$ vs. 10nM $[Ca^{2+}]_i$, by ANOVA with Bonferroni post hoc test. Error bars are within the symbol unless otherwise shown. ($N_{10nM[Ca2+]i}=17$, $N_{1\mu M[Ca2+]i}=39$) $[Ca^{2+}]_i$: intracellular Ca^{2+} concentration.

free Ca^{2+} was buffered to 10nM or 1μM to allow examination of the Ca^{2+}-sensitive current. Resting N9 microglia displayed inward current at negative potential but with very low outward current at positive potential (Figure 5-13A). The I-V curve of resting N9 cells with different $[Ca^{2+}]_i$ revealed no significant difference in the outward current density (Figure 5-13B). This suggested there was very little outward K_{Ca}-type current expressed in the resting N9 microglia. However, the inward current density in 1μM $[Ca^{2+}]_i$ was increased compared to 10nM $[Ca^{2+}]_i$ (Figure 5-13B) suggesting a Ca^{2+}-sensitive inward current was generated.

5.2.2.2 The sensitivity of resting N9 microglial whole-cell current to paxilline, Tram34, PPF and Ba^{2+}.

The effects of pharmacological blockers paxilline, Tram34, PPF and Ba^{2+} on N9 microglial whole-cell currents were examined. Each blocker was applied to the cell for >5min before recordings. To reveal a possible K_{Ca} current, 1μM $[Ca^{2+}]_i$ was used in the pipette solution through out this experiment. Compared to the control, there was no significant effect of paxilline (1μM), Tram34 (1μM) or PPF (10μM) on the outward current density (Figure 5-14). However, surprisingly Tram34 attenuated the inward current density significantly compared to the control (Figure 5-14A). $BaCl_2$ (100μM) did not affect the outward current density (data not shown), but it dramatically blocked the inward current (Figure 5-15A) from -16.4±2.9pA/pF to -1.5±0.7pA/pF recorded at -140mV (Figure 5-15B).

5.2.2.3 LPS triggered a Ca^{2+}-sensitive outward current in N9 cells

As LPS has been reported to modify K^+ currents in some microglia, the effect of LPS (1μg/ml, 24hr) on the whole-cell current of N9 cells was examined. LPS significantly elevated the outward current with 1μM $[Ca^{2+}]_i$ (Figure 5-16A). For example, at depolarization from -50 to 100mV the current density of resting microglia was 9.0±3.7pA/pF while in activated microglia it was 23.9±7.0pA/pF. However, LPS-had

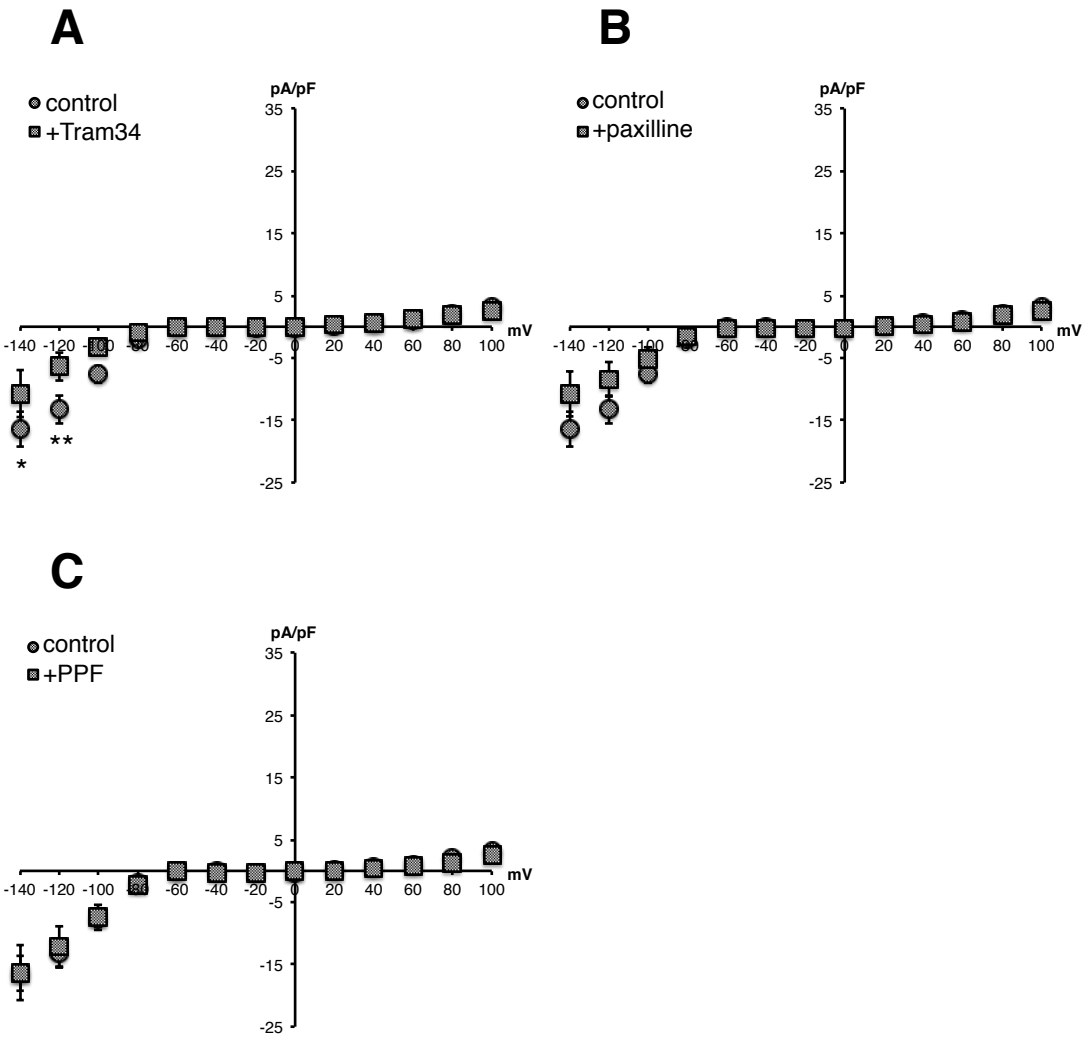

Figure 5-14. The effect of Tram34, paxilline and PPF on the whole-cell current of resting N9 microglia with 1μM $[Ca^{2+}]_i$. Cells were patched after being exposed to extracellular (**A**) Tram34 (1μM), (**B**) paxilline (1μM) or (**C**) PPF (10μM) for >5min. Cells in the absence of blockers were used as control. The holding potential was -50mV. Currents were evoked by voltage steps from -140mV to +100mV in 20mV increments (200ms). Whole cell current were recorded in the presence of 1μM $[Ca^{2+}]_i$. There was no significant effect of these drugs on the whole-cell current except for (**A**) Tram34 which significantly decreased the inward current density at negative potentials. Data are given as mean±SEM. *p<0.05, **p<0.01 vs. control, by ANOVA with Bonferroni post hoc test. Error bars are within the symbol unless otherwise shown. ($N_{control}$=39, $N_{+Tram34}$=22, $N_{+paxiiline}$=14, N_{+PPF}=14)

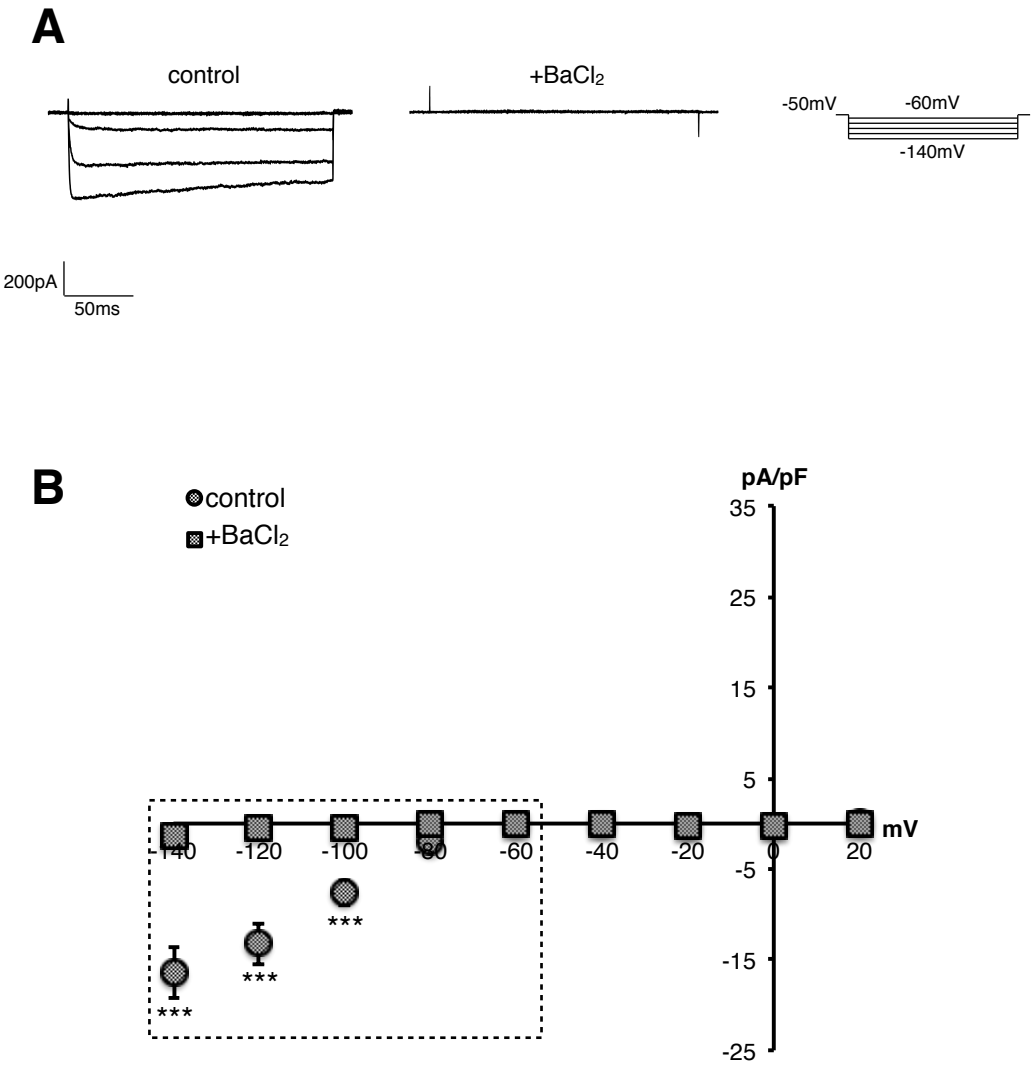

Figure 5-15. The effect of Ba^{2+} on the whole-cell inward current of resting N9 microglia with 1μM $[Ca^{2+}]_i$. Cells were patched after being exposed to extracellular Ba^{2+} (100μM) for >5min while cells in the absence of blocker were used as control. (**A**) Representative traces associated with the plots within the dotted rectangle. On the right side it is the stimulation protocol associating with the traces. (**B**) The current density (pA/pF) vs. voltage (mV) plots of the inward current. The inward current recorded at -140mV to -80mV was completely blocked by extracellular Ba^{2+}. Data are given as mean±SEM. ***p<0.001 vs. control, by ANOVA with Bonferroni post hoc test. Error bars are within the symbol unless otherwise shown. (N_{+BaCl2}=23, $N_{control}$=39)

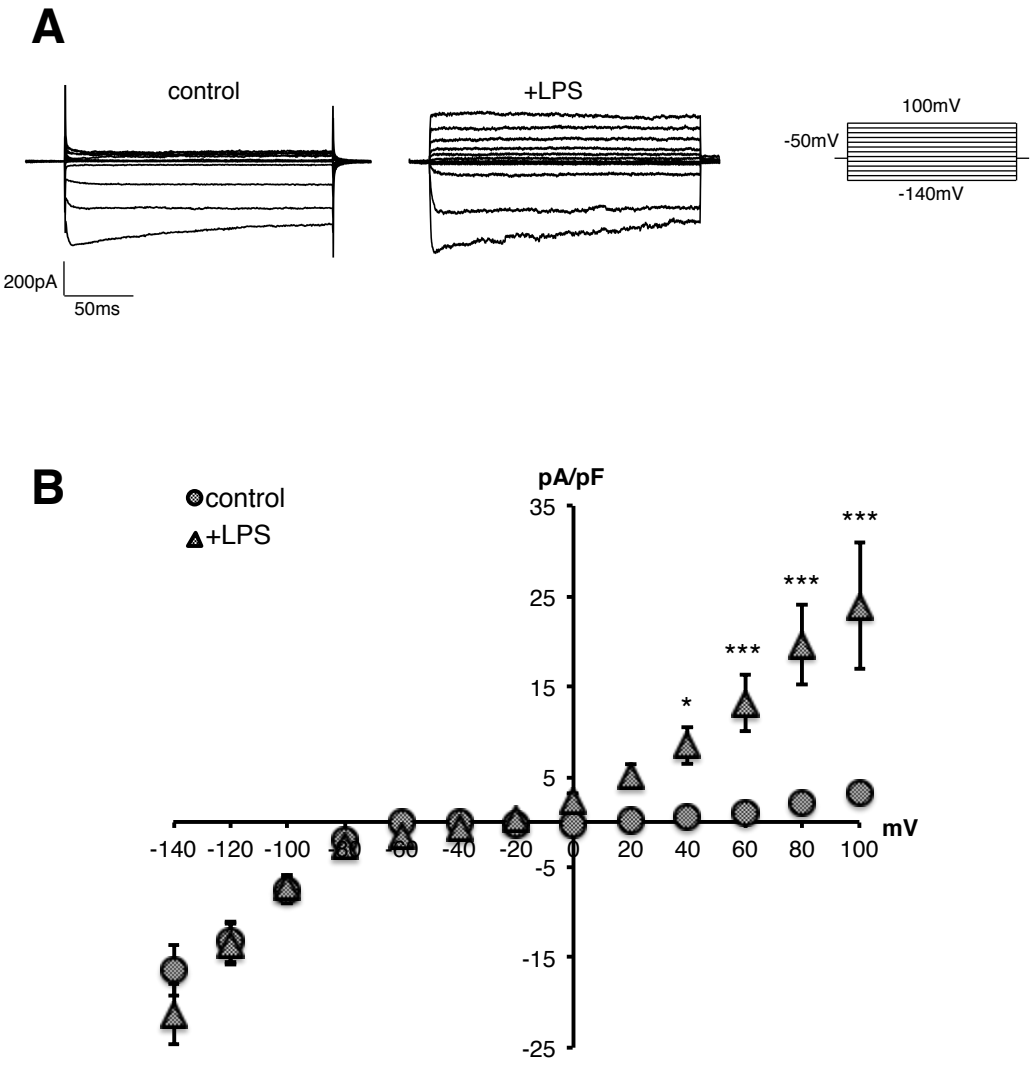

Figure 5-16. LPS-induced whole-cell current of resting N9 microglia with 1μM $[Ca^{2+}]_i$. Cells were treated with LPS (1mg/ml, 24hr) before being patched. The holding potential was -50mV. Currents were evoked by voltage steps from -140mV to +100mV in 20mV increments (200ms). (**A**) Representative traces of resting and LPS-activated N9 microglial whole-cell current under with $[Ca^{2+}]_i$ buffered to 1μM. On the right side is the stimulation protocol associated with the traces. (**B**) The current density (pA/pF) vs. voltage (mV) plots indicated that LPS significantly elevated the outward current density. Data are given as mean±SEM. *p<0.05, ***p<0.001 vs. control, by ANOVA with Bonferroni post hoc test. Error bars are within the symbol unless otherwise shown. (N_{+LPS}=10, $N_{control}$=39)

no significant effect on the outward current with 10nM $[Ca^{2+}]_i$ (Figure 5-17A). These results suggest that LPS induced a Ca^{2+}-sensitive outward current.

Interestingly, LPS in 10nM $[Ca^{2+}]_i$ promoted the inward current density significantly compared to control (Figure 5-17B). This inward current density was -21.3±3.1pA/pF (at -140mV) which was very similar to control or LPS-treated microglia with 1μM $[Ca^{2+}]_i$ which were -16.4±2.9pA/pF and -21.3±3.4pA/pF (at -140mV) respectively (Figure 5-16B).

5.2.2.4 The effect of paxilline and Tram34 on the LPS triggered outward current

As Tram34 and paxilline are selective blockers for K_{Ca} current and the previous results indicated LPS was able to trigger a Ca^{2+}-sensitive outward current in N9 microglia, the focus was on the LPS-induced microglial outward current to examine whether it was mediated by BK or IK channels.

LPS-induced outward current was significantly inhibited by paxilline (1μM) with current density reduced from 23.9±7.0pA/pF to 7.0±1.5pA/pF (at 100mV) (Figure 5-18B). This suggests that LPS induced expression of BK channels on the N9 microglial membrane at the time of current examination.

In contrast, application of Tram34 (1μM) had no significant effect on the LPS-induced outward current (Figure 5-19). The current density of activated N9 microglia was 23.9±7.0pA/pF while it was 19.1±4.1pA/pF (at 100mV) after exposure to external Tram34 (Figure 5-19B).

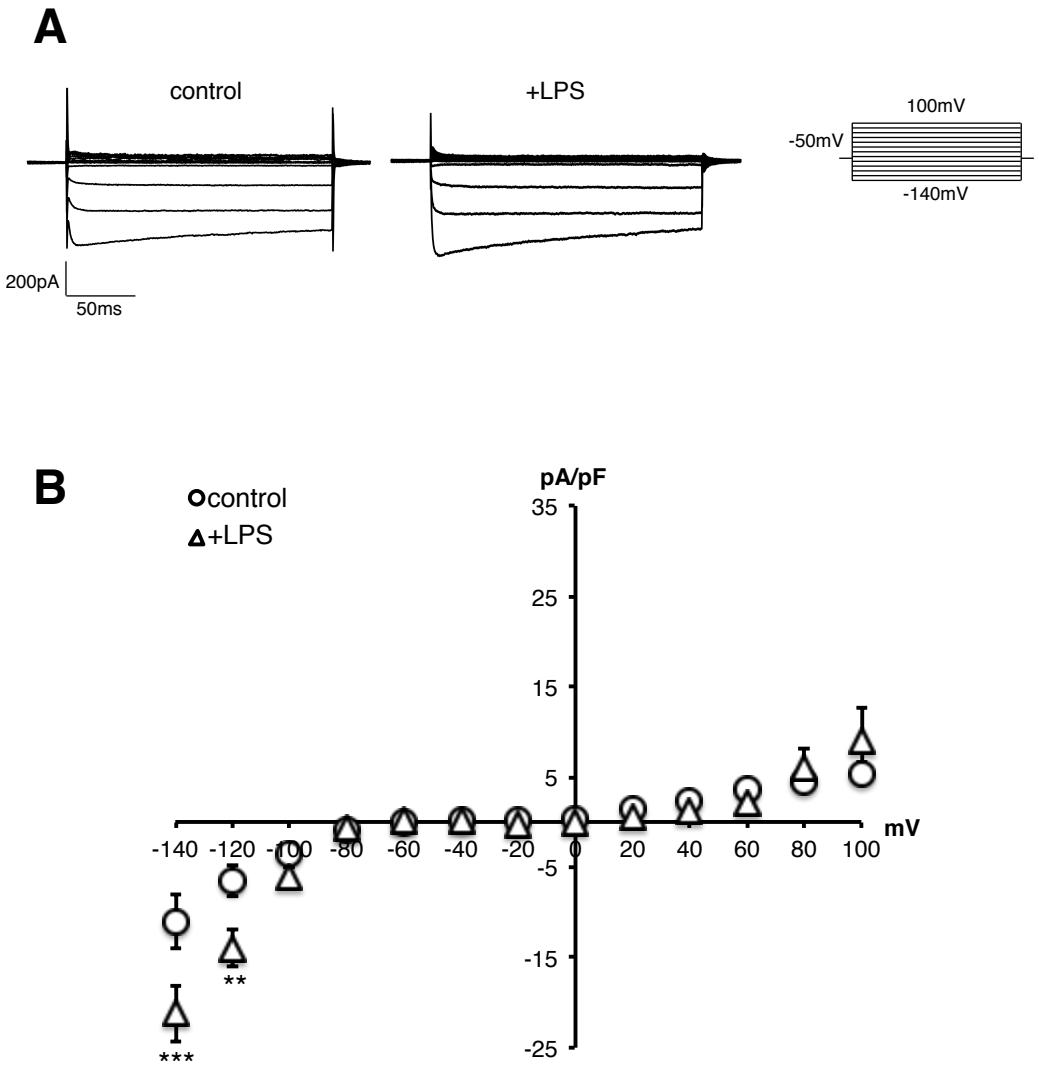

Figure 5-17. LPS-induced whole-cell current of resting N9 microglia with 10nM $[Ca^{2+}]_i$. Cells were treated by LPS (1mg/ml, 24hr) before being patched. The holding potential was -50mV. Currents were evoked by voltage steps from -140mV to +100mV in 20mV increments (200ms). (**A**) Representative traces of resting and activated N9 microglial whole-cell current with $[Ca^{2+}]_i$ buffered to 10nM. On the right side is the stimulation protocol associated with the traces. (**B**) The current density (pA/pF) vs. voltage (mV) plots indicated that LPS had no significant effect on the outward current density of N9 microglia but it significantly improved the inward current density at negative potentials which had no difference to the one of resting microglia with 1μM $[Ca^{2+}]_i$ (Figure 5-16B). Data are given as mean±SEM. **p<0.01, ***p<0.001 vs. control, by ANOVA with Bonferroni post hoc test. Error bars are within the symbol unless otherwise shown. ($N_{control}$=17, N_{+LPS}=9)

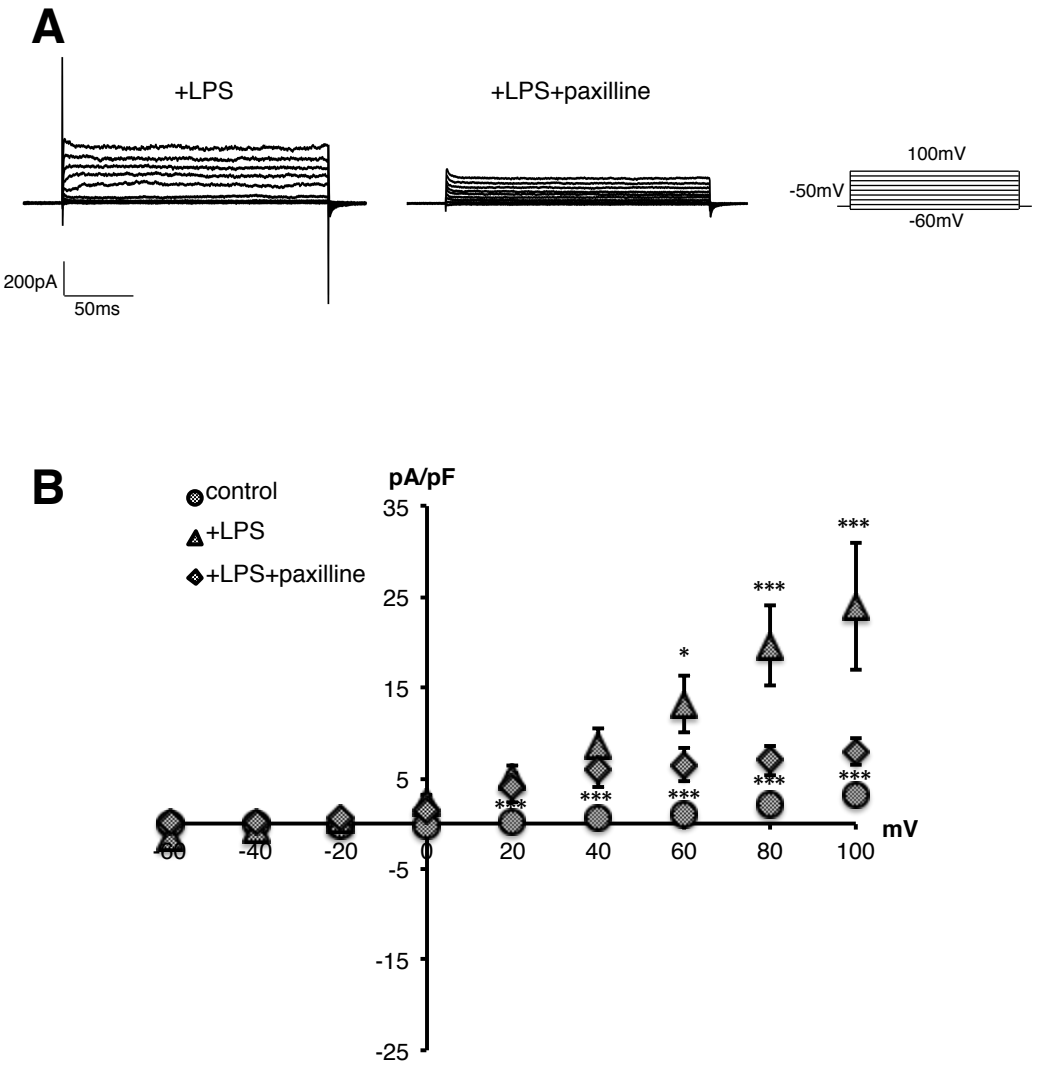

Figure 5-18. Paxilline reduced LPS-induced whole-cell outward current with 1μM $[Ca^{2+}]_i$. LPS-activated microglia were patched after being exposed to extracellular paxilline (1μM) for >5min. The holding potential was -50mV. Currents were evoked by voltage steps from -60mV to +100mV in 20mV increments (200ms). (**A**) Representative traces of whole-cell outward current of activated N9 cells with or without extracellular paxilline treatment. On the right side is the stimulation protocol associating with the traces. (**B**) The current density (pA/pF) vs. voltage (mV) plots revealed that the outward current density was significantly decreased by paxilline. Data are given as mean±SEM. *p<0.01, ***p<0.001 vs. +LPS+paxilline, by ANOVA with Bonferroni post hoc test. Error bars are within the symbol unless otherwise shown. ($N_{control}$=39, N_{+LPS}=10, $N_{+LPS+paxilline}$=5)

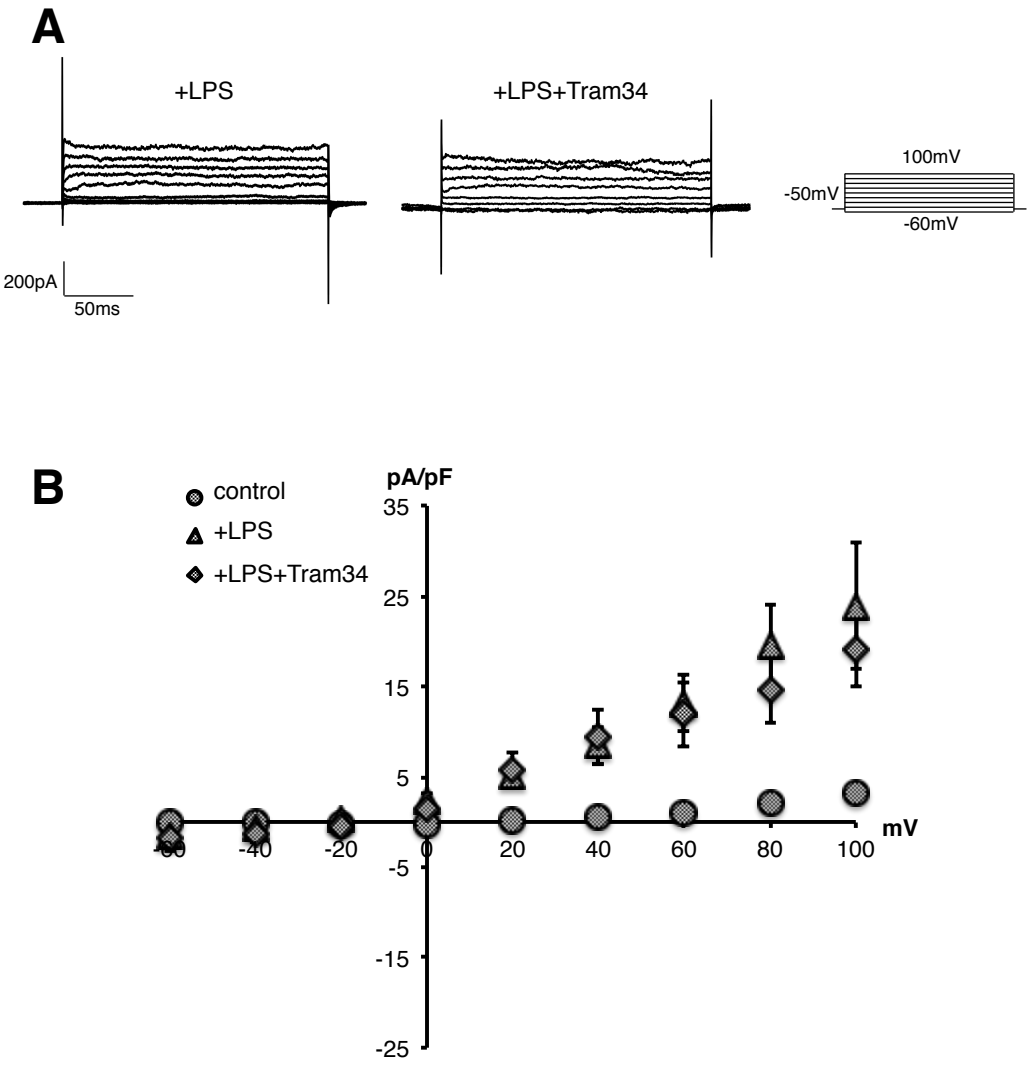

Figure 5-19. Tram34 did not attenuate LPS-induced whole-cell outward current with 1μM $[Ca^{2+}]_i$. LPS-activated microglia were patched after being exposed to extracellular Tram34 (1μM) for >5min. The holding potential was -50mV. Currents were evoked by voltage steps from -60mV to +100mV in 20mV increments (200ms). (**A**) Representative traces of whole-cell outward current of activated N9 cells with or without extracellular Tram34 treatment. On the right side is the stimulation protocol associating with the traces. (**B**) The current density (pA/pF) vs. voltage (mV) plots revealed that the outward current density was not significantly influenced by the Tram34 treatment. Data are given as mean±SEM. Error bars are within the symbol unless otherwise shown. ($N_{control}$=39, N_{+LPS}=10, $N_{+LPS+Tram34}$=4)

5.2.2.5 Resting membrane potential and capacitance of N9 microglia

The resting membrane potential and capacitance of N9 cells under different conditions was also examined. Under the four different conditions: LPS-activated N9 microglia with either 1μM $[Ca^{2+}]_i$ or 10nM $[Ca^{2+}]_i$ and resting N9 microglia with either 1μM $[Ca^{2+}]_i$ or 10nM $[Ca^{2+}]_i$, there was no significant difference in resting membrane potential using current clamp (I=0). The mean resting membrane potential was within the range of -40mV to -60mV (Figure 5-20B). In addition, there was no action potential generation during the current clamp recording (Figure 5-20A).

LPS-activated microglia patched were all amoeboid while resting microglia patched were all ramified. This was to make sure N9 microglia recorded in the desired status. LPS did not significantly change the capacitance of N9 cells compared to control (Figure 5-20C).

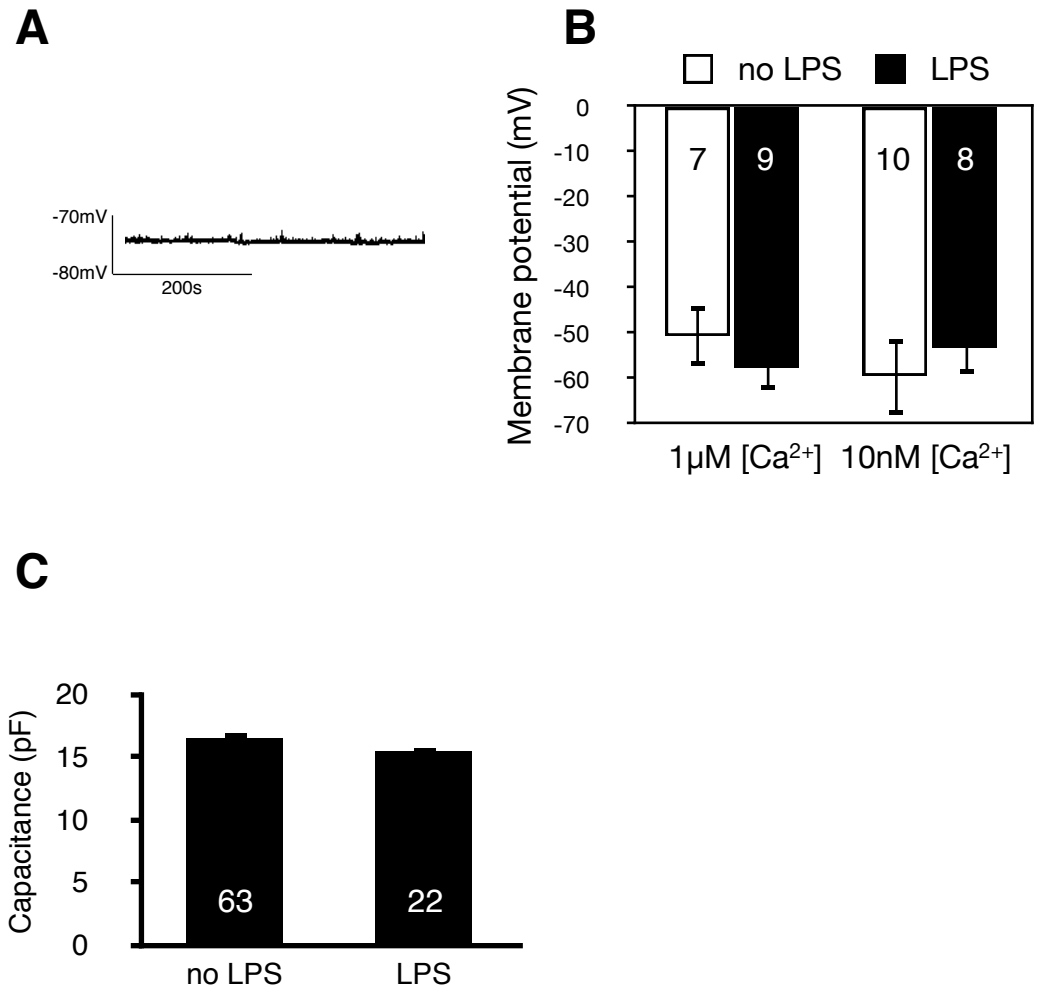

Figure 5-20. LPS had no significant effect on resting membrane potential or capacitance of N9 microglia. Cells were patched using whole-cell current clamp (I=0) and stabilized for >5min before the recording of membrane potential. (**A**) Representative trace of membrane potential from resting N9 microglia with $[Ca^{2+}]_i$ buffered to 10nM. (**B**) Bar chart of resting membrane potential under control and LPS-activated conditions with $[Ca^{2+}]_i$ buffered to 10nM or 1μM. There was no significant difference between any two conditions. (**C**) Activated and resting microglia had no significant difference in the cellular capacitance. Data are given as mean±SEM. (N value was indicated in each bar)

5.3 Discussion

5.3.1 Whole-cell current of resting N9 microglia

The whole-cell current of resting N9 cells displayed a low outward current at positive potentials and large inward current at negative potentials. This was similar to other microglial models in *in vitro* culture in previous studies (Boucsein *et al.*, 2000; Kettenmann *et al.*, 1990; Schilling *et al.*, 2000).

The resting outward current was not significantly different with low or high $[Ca^{2+}]_i$ suggesting little K_{Ca}-type current was expressed. In addition, external PPF (10μM), Tram34 (1μM) or paxilline (1μM) did not significantly block the resting outward current, either (Figure 5-14).

However, the resting microglial whole-cell current displayed a $[Ca^{2+}]_i$-dependent increase of inward current density (Figure 5-13). The reason may be the inward current induced by the intracellular Ca^{2+} such as inward sodium (Na^+)/Ca^{2+} exchanger current (Janvier *et al.*, 1997), inward chloride (Cl^-) current (Korn & Weight, 1987), Ca^{2+}-activated non-specific cationic current (Kramer & Zucker, 1985; Yamashita & Isa, 2003a; Yamashita & Isa, 2003b). In addition, Tram34 (1μM) unexpectedly decreased the inward current density of resting microglia (Figure 5-14A) displaying no significant difference to resting inward whole-cell current with 10nM $[Ca^{2+}]_i$. Previous evidence indicated that IK channels play an important role in maintaining the entry of Ca^{2+} into immune cells, such as in T cells (Fanger *et al.*, 2001; Jensen *et al.*, 2001). Thus, blocking IK channels by Tram34 may lower $[Ca^{2+}]_i$ but this needs to be tested by Ca^{2+} imaging. As the outward current was not significantly sensitive to external Tram34, this suggests that low membrane expression of IK channels was sufficient to regulate $[Ca^{2+}]_i$. A further immunostaining analysis is required to confirm IK protein expression and localization in the cells. Finally, the application of external Ba^{2+} (100μM) fully blocked the inward current as well as previously reported (Figure 5-15).

5.3.2 Effect of LPS on the whole-cell current of N9 microglia

Compared to resting N9 microglia, LPS treatment (1μg/ml, 24hr) affected both the inward and outward whole-cell current.

LPS elevated outward current density at positive potentials (Figure 5-16) similar to previous findings (Boucsein *et al.*, 2000; Nörenberg *et al.*, 1992; Draheim *et al.*, 1999). Because the LPS-induced outward whole-cell current only occurred at high (1μM) $[Ca^{2+}]_i$ (Figure 5-16) but not low (10nM) $[Ca^{2+}]_i$ (Figure 5-17), Tram34 and paxilline were applied to block it. Here, the LPS-induced outward current was significantly blocked by external paxilline (1μM) (Figure 5-18B) but not Tram34 (Figure 5-19B). In addition, because after exposure to paxilline the remaining outward current density was still significantly higher than control (Figure 5-18B) and the LPS-induced outward current was not significantly sensitive to Tram34, it is possible the remaining $[Ca^{2+}]_i$ sensitive outward current is composed of SK-type current. To examine this apamin should be applied which is a SK1~3 channel blocker.

In addition, LPS increased the inward current density at negative potentials (Figure 5-17) as reported previously (Nörenberg *et al.*, 1992). This may be a $[Ca^{2+}]_i$-dependent process, because the LPS-induced inward current density with 10nM $[Ca^{2+}]_i$ had no significant difference to the resting inward current density of N9 microglia with 1μM $[Ca^{2+}]_i$. Reasons may be: (1) LPS can release the Ca^{2+} stores from the endoplasmic reticulum (ER) by activating the inositol trisphosphate ($InsP_3$)-dependent channels (Wheeler & Thurman, 1999; Drysdale *et al.*, 1987; Prpic *et al.*, 1987; Liu *et al.*, 2008). This further induced Ca^{2+} influx through the Ca^{2+} release-activated Ca^{2+} channels (Hoth & Penner, 1993). (2) LPS may also increase $[Ca^{2+}]_i$ via the activation of protein kinase C (PKC) (Wen *et al.*, 2011). PKC can activate the Na^+/Ca^{2+} exchanger (Kettenmann *et al.*, 2011) elevating the $[Ca^{2+}]_i$.

Finally, as previously reported, a morphology-dependent outward Cl^- current was activated by microglial swelling (Schlichter *et al.*, 2011). Thus, it was possible the LPS-regulated N9 microglial whole-cell current may depend on cell morphology.

5.3.3 LPS effect on capacitance and resting membrane potential of N9 microglia

LPS did not significantly affect the capacitance of N9 microglia (Figure 5-20C) as reported elsewhere (Kozlowski & Weimer, 2012). In addition, resting N9 microglia had a resting membrane potential with mean value at about -55mV and they displayed no difference with either 10nM or 1μM $[Ca^{2+}]_i$. LPS here did not significantly change microglial resting membrane potential, either (Figure 5-20B). Due to the low sealing success rate indicated in section 2.1.3.3, there was insufficient data to examine whether the resting membrane potential displayed a bimodal distribution or whether LPS hyperpolarized the higher peak value of the distribution as previously reported (Chung *et al.*, 1999).

5.3.4 The functional role of outward K^+ current in N9 microglia

5.3.4.1 The functional role of BK channels

Previous studies have revealed BK-type current in human, bovine and mouse microglia (McLarnon *et al.*, 1995; McLarnon *et al.*, 1997; Schilling *et al.*, 2002; Schilling & Eder, 2007). In this thesis LPS induced a Ca^{2+}-dependent and paxilline-sensitive outward current (Figure 5-18B) while there was no significant BK current in resting N9 cells. This is similar to previous findings of a BK-type current in activated mouse microglia in brain slices and *in vitro* cultured cells (Schilling & Eder, 2007; Schilling *et al.*, 2002).

In Chapter 4 it was demonstrated that the mRNA expression of Kcnma1 ($K_{Ca}1.1$) was not significantly regulated by LPS treatment (Figure 4-10), but functional studies demonstrated that LPS elevated a BK-type current. There may be several reasons for this apparent discrepancy: (1) LPS elevated BK channel expression at a post-transcriptional level, as protein expression may not be associated with mRNA expression (Ortega *et al.*, 2012). In addition, LPS may regulate BK current through the NO-regulated pathway, as NO was reported to upregulate the protein expression of BK channels (Kadekaro *et al.*, 2006) and directly activate BK current (Zhu & Huizinga, 2008). (2) LPS may induce more BK channels to localize on the plasma membrane. In this case, total protein of BK channels may not be significantly changed, rather LPS may promote channel membrane expression. (3) In the case that membrane expression of BK channels is not changed by LPS, BK channel activity may be elevated by LPS-induced regulation of signaling pathways or $[Ca^{2+}]_i$. For example, the activity of BK channels can be regulated by phosphorylation (Widmer *et al.*, 2003) and LPS is able to activate PKC, protein kinase A (PKA), Ca^{2+}/ calmodulin-dependent protein kinase II (CaMKII) and calcineurin. Thus LPS may regulate BK activity through phosphorylation pathways. To further confirm this hypothesis, it could be possible to examine the LPS-induced BK current after blocking the activity or knocking down the expression of these downstream mediators.

In this chapter, blocking BK channels using paxilline (≤1μM) or activating BK channels using NS1619 (≤10μM) on their own did not display any significant effect on LPS-induced microglial NO release while at higher concentration paxilline (10μM) or NS1619 (100μM) attenuated either microglial NO release or cell numbers. However, at these concentrations these compounds are not selective for BK channels. Although LPS-induced paxilline (1μM) sensitive outward current, blocking BK channels with paxilline (1μM) did not regulate LPS-induced microglial NO release. This suggested that the LPS-induced activation of BK channel current may not be required for NO release. Furthermore, activating BK channels with NS1619

alone or in the presence of LPS did not affect NO release. However, alternative mechanisms may explain the difference. For example, membrane expression of BK channels may be time-dependent as discovered for other types of K^+ channels in microglia (Kotecha & Schlichter, 1999). Although LPS-induced NO release was measured at 24hr, the NO release was already increasing before the time point while LPS-induced outward current was analyzed at 24hr. In this case the effect of LPS on NO release may precede the expression of BK channel current. Thus, blocking BK channels alone may not be able to have an effect on NO release.

5.3.4.2 The functional role of IK channels

Tram34 decreased LPS-induced microglial NO release while it was not toxic to N9 cells in the culture. These results were not only consistent with the previous studies on IK channel function in isolated primary rat microglia (Kaushal *et al.*, 2007) but also extended the role of IK to mouse microglia. In previous work, LPS-induced microglial NO release was attenuated by the blockade of IK channels which was proposed to be via the p38 mitogen-activated protein kinases (MAPKs) pathway but not nuclear factor kappa-light-chain-enhancer of activated B cells (NFκB) (Kaushal *et al.*, 2007). This could explain the role of IK blockade in N9 cells, but it has not been tested. In addition, as described before blocking IK inhibits Ca^{2+} influx (Fanger *et al.*, 2001; Jensen *et al.*, 2001) and in N9 microglia Tram34 induced a similar inward whole-cell current to the low $[Ca^{2+}]_i$ conditions (Figure 5-14A). It is questioned whether the Tram34-induced inhibitory effect on LPS-induced NO release may rely on the Ca^{2+}-dependent phosphorylation pathways, such as CaMKII, and further examinations are required. However, the IK activator NS309 did not display any effect on either N9 microglial viability or NO release after activation. It is postulated that under the experimental activation process most IK channels (or even SK channels) were activated, thus NS309 would not give any further effect.

However, in the LPS-induced Ca^{2+}-dependent outward current, there was no significant Tram34-sensitive outward current detected. In isolated rat primary microglia, the whole-cell currents displayed only a small current component which was sensitive to Tram34 (1μM) (Kaushal *et al.*, 2007). It is possible the proportion of IK current in N9 cells was very small compared to the LPS-induced outward current (Figure 5-19) and then it was not detected by examining cell population data here. Thus, a discrete single cell recording before and after Tram34 exposure is required to examine the existence of a small IK-type current. In addition, in rat microglia the outward current induced by 100ng/ml LPS was time-dependent displaying a plateau at 24hr (Nörenberg *et al.*, 1992). As we used 1μg/ml LPS, this time course may change and IK current may be evoked at different treatment duration. For example, IK channels may sufficiently express at the plasma membrane but internalize after 24hr of culture. What is more, the activity of IK channels can be inhibited by PKA phosphorylation (Regenhard *et al.*, 2001) and LPS is known to activate PKA. Thus this may inhibit the activity of IK channels at the time the current was examined. Intriguingly, a recent study indicated that to fully activate the IK current in microglia, riluzole, a neuroprotective drug, was a necessary modulator while the application of 1μM $[Ca^{2+}]_i$ on its own was not sufficient to trigger the K_{Ca} current (Liu *et al.*, 2012).

5.3.4.3 The functional role of $K_v1.3$ or $K_v1.5$ channels

In previous studies $K_v1.3$ channels have been shown to regulate rat microglial neurotoxicity induced by LPS (Fordyce *et al.*, 2005) which was proposed to be through regulation of the respiratory burst pathway (Fordyce *et al.*, 2005; Khanna *et al.*, 2001; Schilling & Eder, 2011). However, $K_v1.3$ channels did not regulate the LPS-induced NO release as antisense deoxyoligonucleotides knockdown of $K_v1.3$ (Pannasch *et al.*, 2006) or agitoxin-2 (AgTX-2) blockade (Fordyce *et al.*, 2005) displayed no effect in rat microglia. Here it confirmed a similar result that $K_v1.3$ inhibition had no effect on LPS-induced N9 microglial NO release.

In previous studies, LPS-induced NO release was almost abolished from the $K_v1.5^{-/-}$ mouse and it was decreased by around 50% by the AO knockdown of $K_v1.5$ (Pannasch *et al.*, 2006). Here, LPS-induced N9 microglial NO release was decreased by about 10~14% in the presence of PPF (10μM) (Figure 5-3 & Figure 5-11). This data suggests a role of $K_v1.5$ on N9 microglial NO release using a pharmacological approach. However, the attenuation effect (10~14%) by pharmacological blockade was much less than the 50~100% inhibition of NO release by genetic deletion of $K_v1.5$ (Pannasch *et al.*, 2006). It has been postulated previously that $K_v1.5$ may regulate microglial NO release through intracellular pathways rather than regulating ion transport (Pannasch *et al.*, 2006). If this was true, pharmacological interference of $K_v1.5$ channels may not fully abolish their functions in microglia. In addition, PPF at 100μM displayed a high toxicity to N9 cells. As the IC_{50} of PPF for $K_v1.5$ channels is around 4.4μM (Franqueza *et al.*, 1998; Gutman *et al.*, 2005), it is possible 100μM of PPF began to block other channels rather than specifically blocking $K_v1.5$ which led to an abnormal metabolism of N9 cells.

However, the mRNA expression of Kcna5 ($K_v1.5$) was not significantly regulated by LPS although the mean expression increased by 80% (Figure 4-5). In addition, there was no significant PPF (10μM)-sensitive current detected in resting microglia (Figure 5-14B) and the LPS-elevated outward current was shown mainly composed of K_{Ca}-type current as with 10nM $[Ca^{2+}]_i$ LPS-induced outward current was not significantly different to control (Figure 5-17B). First it is questioned why mRNA of Kcna5 ($K_v1.5$) was detected while there was no PPF-sensitive current. Similar to explanations before, protein expression of $K_v1.5$ may not be associated with its mRNA expression. LPS may induce more $K_v1.5$ channels to localize in the cytosol. Besides these possibilities, the current of $K_v1.5$ channels can be inactivated by PKC-phosphorylated intracellular $K_v\beta1.3$ (Kwak *et al.*, 1999; Sewing *et al.*, 1996) whose mRNA (Kcnab1) expression was detected in N9 microglia (Figure 4-12). In addition, LPS was able to activate the PKC family (Comalada *et al.*, 2003; Wen *et al.*, 2011; Lee *et al.*, 2008). Thus it is possible even if $K_v1.5$ channels were expressed on the

plasma membrane their current was inhibited by such mechanisms. Second it is questioned while there was no PPF-sensitive current detected why blockade of $K_v1.5$ channels attenuated LPS-induced NO release. As previously reported expression of $K_v1.5$ channels on microglial plasma membrane depended on the *in vitro* culture duration (Kotecha & Schlichter, 1999). Thus, it is possible $K_v1.5$ channels may express sufficiently on the plasma membrane during the 24hr of culture but at the time of current analysis their membrane expression reduced dramatically or even their activity is blocked by $K_v\beta1.3$ subunit as described before.

5.3.5 The functional role of inward K^+ current in N9 microglia

As discussed at the beginning of this chapter, the effect of Ba^{2+} in N9 cells is thought likely to be mainly through the blockade of $K_{2p}6.1$ and $K_{ir}2.1$ as mRNA expression of Kcnk6 ($K_{2p}6.1$) together with Kcnj2 ($K_{ir}2.1$) was over 80% among the detected K^+ channel subunits which were sensitive to extracellular Ba^{2+} (Figure 5-1).

$K_{ir}2.1$ has been supposed as the major component of inward K^+ current of microglia (Schilling *et al.*, 2000). Here the N9 microglial inward current was completely blocked by 100μM Ba^{2+} (Figure 5-15B) which was similar to previous reports (Kettenmann *et al.*, 1990; Schilling *et al.*, 2000). Activated $K_{2p}6.1$ channels generate both outward current at positive potentials and inward currents at negative potentials and they exhibit a weak outward rectification under physiological K^+ gradients (Patel *et al.*, 2000). Ba^{2+} can block both the inward and outward current generated by $K_{2p}6.1$ (Patel *et al.*, 2000) and as LPS significantly downregulated expression of Kcnk6 ($K_{2p}6.1$), there would be more $K_{2p}6.1$ current generated in resting N9 microglia if its protein expression was associated with mRNA expression. However, as the current generated by $K_{2p}6.1$ is inactivated by depolarization (Patel *et al.*, 2000), this may explain why Ba^{2+} (100μM) did not significantly decrease the whole-cell outward current of resting N9 microglia. Thus immunostaining could be applied

to detect the expression of $K_{2p}6.1$ channels and gene knockdown to examine the function.

Although Ba^{2+} (100μM) fully blocked the whole-cell inward current (Figure 5-15), it did not affect LPS-induced microglial NO release while higher concentrations (1mM) significantly decreased it by 21.6% with out significant affect on cell viability (Figure 5-4). Based on the IC_{50} values of $K_{ir}2.1$ for Ba^{2+}, 100μM Ba^{2+} is sufficient to fully block current generated by $K_{ir}2.1$ (Kubo *et al.*, 2005; Schram *et al.*, 2002). This suggests that the inward Ba^{2+}-sensitive K^+ current may not be involved in LPS-induced NO release. In addition, 100μM Ba^{2+} is able to block about 50% current of $K_{2p}6.1$ (Patel *et al.*, 2000; Goldstein *et al.*, 2005; Lloyd *et al.*, 2009), thus 1mM Ba^{2+} may fully block $K_{2p}6.1$ current in N9 microglia. It is then questioned whether $K_{2p}6.1$ play a role in LPS-induced NO release. Alternative techniques are required to examine the role of $K_{2p}6.1$ channels in LPS-induced NO release, such as siRNA knockdown. Besides $K_{2p}6.1$ channels, 1mM Ba^{2+} is able to block other outward K^+ current (Shi *et al.*, 2000), for example $K_{2p}2.1$ (IC_{50}=1mM for external Ba^{2+}) or $K_v12.1$ (IC_{50}=180μM for external Ba^{2+}) (Figure 5-1) whose mRNAs were detected in N9 microglia. Thus, other K^+ channels may be implicated in LPS-induced NO release even if expressed at a low level. In addition, external Ba^{2+} depolarizes the resting membrane potential (Chung *et al.*, 1999). Depolarization is able to regulate activity of transcription factors via Ca^{2+} signaling pathways (Bernal-Mizrachi *et al.*, 2002). This provides a possible mechanism how K^+ channels regulate the NO release. What is more, during the 24hr culture, Ba^{2+} may diffuse into the cytosol such as through the voltage-dependent Ca^{2+} channels (Heldman *et al.*, 1989). Intracellular Ba^{2+} would either activate or block different K^+ channels leading to a more complex interaction between K^+ channels. Finally Ba^{2+} at 10mM inhibited both N9 microglial proliferation by 8.1% and microglial NO release by 34.4% (Figure 5-4). The additional osmolarity induced by 10mM of Ba^{2+} in the environment may be one reason leading to microglial cell death and attenuated NO release. In addition, there are several channels sensitive to such high concentration of external Ba^{2+}, for

example $K_v2.1$ (IC_{50}=30mM for external Ba^{2+}). Blockade of these channels may play a role in N9 microglia viability and LPS-induced NO release.

GBC blocks K_{ATP} channels by binding to sites on the SUR subunit (Ortega *et al.*, 2012; Mikhailov *et al.*, 2001). In the presence of $K_{ir}6.1$ the IC_{50} of SUR1 is 5μM for GBC while in the presence of $K_{ir}6.2$ the IC_{50} of SUR1 is 8nM for GBC (Kew & Davies, 2009). Up to 10μM GBC was applied to N9 microglia here. However, no concentration affected either N9 microglial proliferation or NO release (Figure 5-5). As previously reported, GBC induced microglial activation and tumor necrosis factor alfa (TNFα) release preventing neuronal death in hypoxic conditions (Ortega *et al.*, 2012). Thus, similar to $K_v1.3$, GBC may participate in microglial activation but not regulate NO release. What is more, it may be possible there was no pore-forming subunits expressed in N9 microglia, because the mRNA expression of Kcnj8 ($K_{ir}6.1$) and Kcnj11 ($K_{ir}6.2$) were not detectable in N9 microglia.

5.3.6 Functional role of interactions between K^+ currents in N9 microglia

5.3.6.1 BK channels regulate LPS-induced NO release in the presence of another K^+ channel blocker

Although paxilline or NS1619 did not affect LPS-induced N9 microglial NO release on their own, interestingly in the presence of other K^+ channel blockers, paxilline significantly attenuated the inhibitory effect of Tram34, PPF and Ba^{2+} to inhibit LPS-induced NO release while NS1619 significantly facilitated the inhibitory effect of Tram34 and PPF (Figure 5-10 and Figure 5-11).

How might BK channel regulate the effect of IK channels on LPS-induced NO release? As previously described in other immune cells, blocking IK depolarizes membrane potential and inhibits Ca^{2+} influx through nonselective cation channels (Fanger *et al.*, 2001; Jensen *et al.*, 2001) while blockade of BK channel induces

membrane depolarization (Semenov *et al.*, 2011) and depolarization is able to activate voltage-dependent Ca^{2+} channels and induce Ca^{2+} influx (Fukushima & Hagiwara, 1983). In addition, microglia express both voltage-gated Ca^{2+} channels (Eder, 1998) and nonselective cation channels (Schilling & Eder, 2009). Thus, if in N9 microglia IK channels were colocalized with non-selective cation channels while BK channels were colocalized with voltage-dependent Ca^{2+} channels, the net effect of blocking BK and IK on $[Ca^{2+}]_i$ may be cancelled out. Conversely, activating BK by NS1619 may decrease the activity of voltage-dependent Ca^{2+} channels which is then additive to the effect of blocking IK channels. As described before, the change of $[Ca^{2+}]_i$ may activate phosphorylation pathways, such as CaMKII and calcineurin. These pathways can further regulate the activity of transcription factors such as NFκB which induce the synthesis of inducible nitric oxide synthase (iNOS) and NO release. However, such an hypothesis is based on one precondition. Because Ca^{2+}-dependent phosphorylation pathways display different sensitivity to various Ca^{2+} stimulations (Dupont *et al.*, 2003; Saucerman & Bers, 2008). It is thus supposed that in N9 microglia activity of BK channel on its own can not induce a sufficient change of pattern of $[Ca^{2+}]_i$ to further regulate these pathways. Finally, to examine this hypothesis immunostaining is required to localize the channels expression. Ca^{2+}-imaging is required to confirm the BK or IK channel-regulated change of $[Ca^{2+}]_i$. Blockade of Ca^{2+} channels can be applied to investigate the role of Ca^{2+} under this phenomenon. What is more, siRNA knockdown can be applied. Another mechanism may involve the activation of IK channels that blocked BK channels as reported in salivary gland acinar cells. Activated IK channels insert their N termini into the intracellular portals of BK channels and this process is voltage independent (Thompson & Begenisich, 2009). It is thus possible blocking IK by Tram34 changed the structure of IK channels and led to less BK channels blocked by IK N termini. The blockade of BK channels by paxilline becomes a competitive process to the blockade of IK channels meanwhile the activation of BK by NS1619 assists it, but such mechanism would require BK and IK channels locate closely enough.

Secondly, the mechanisms underlying the interactions among BK and $K_v1.5$ channels are not clear. $K_v1.5$ is a voltage-activated K^+ channels which is opened by membrane depolarization. Blocking BK can depolarize the membrane potential (Semenov *et al.*, 2011). Thus it is possible that blocking BK leads to activation of $K_v1.5$ channels and thus opposes the effect of blocking $K_v1.5$. The activation of BK using NS1619 may display an additive effect.

In addition, because neither the Tram34- nor PPF-sensitive current was observed in N9 microglia, it was assumed that channels of IK and $K_v1.5$ may have moved onto the membrane during the 24hr culture while at the time of whole-cell current examination, there were no or little channels left on the plasma membrane. In such case, one can not exclude that BK, IK and $K_v1.5$ channels may not simultaneously express on the plasma membrane during the 24hr of culture.

Thirdly, BK channels are Ca^{2+}-sensitive and voltage-activated K^+ channels which would be activated under this condition. External Ba^{2+} is able to depolarize cellular membrane potential (Pappas & Ransom, 1994). In addition, as described in section 5.3.2 LPS is able to elevate $[Ca^{2+}]_i$ by releasing Ca^{2+} from the ER (Wheeler & Thurman, 1999; Drysdale *et al.*, 1987; Prpic *et al.*, 1987; Liu *et al.*, 2008) or by activating Na^+/Ca^{2+} exchanger (Kettenmann *et al.*, 2011) and the Ca^{2+} release-activated Ca^{2+} channels (Hoth & Penner, 1993). However, external Ba^{2+} was also reported to decrease $[Ca^{2+}]_i$ (Franchini *et al.*, 2004). The net effect may still lead to sufficient elevation of $[Ca^{2+}]_i$ to activate BK channels. Thus, blockade of BK channels may oppose the effect of Ba^{2+}. What is more, during the 24hr of culture, Ba^{2+} may enter the N9 microglia. Intracellular Ba^{2+} was recently reported to selectively activate BK channels by binding to the Ca^{2+} bowl at the regulator of conductance for K^+ 2 (RCK2) domain (Zhou *et al.*, 2012). However, NS1619 did not facilitate the inhibitory effect of Ba^{2+}. After LPS treatment, BK channels may be mostly activated so that further activation by NS1619 would not have any significant effect.

5.3.6.2 The inhibitory effect of Tram34 and PPF, but not Ba^{2+}, on LPS-induced NO release was additive

The inhibitory effect of Tram34 (1μM) was additive with PPF (10μM) displaying a further attenuation on NO release (Figure 5-12A). The mechanism is not clear yet. As indicated in the section 5.3.6.1, IK and $K_v1.5$ channels may not simultaneously express on the plasma membrane which may be one possibility why their inhibitory effect on LPS-induced NO release is additive. In the case IK and $K_v1.5$ simultaneously express on the plasma membrane, blocking either of them may depolarize membrane potential. Although $K_v1.5$ can be activated by depolarization, the net effect of blocking both channels may still lead to more depolarization than blockade of either IK or $K_v1.5$ channels on its own.

However, Ba^{2+} did not display any additive inhibitory effect on LPS-induced NO release with either Tram34 or PPF (Figure 5-12B&C). As described in before, the blockade of either inward K^+ current (Pappas & Ransom, 1994) or outward K^+ current (Chung *et al.*, 1998) of microglia induced membrane depolarization, but blocking both of these currents at the same time may display less regulation on ionic homeostasis. In this case the net effect may not induce more membrane depolarization. What is more, as described before, external Ba^{2+} decreases $[Ca^{2+}]_i$ (Franchini *et al.*, 2004). Although LPS is known to elevate $[Ca^{2+}]_i$, it is questioned during the period that IK channels express on the plasma membrane, whether the net effect of Ba^{2+} and LPS led to less $[Ca^{2+}]_i$ which was not sufficient to activate IK. In such case, additional blocker of IK would not offer a significant effect. In addition, although the IC_{50} of $K_v1.5$ for extracellular Ba^{2+} varies depending on the different conditions, such as pH (Cheng *et al.*, 2008), it can be in the range of 20μM~1mM (Figure 5-1). Thus, 1mM Ba^{2+} may block $K_v1.5$ current on its own, so additional application of PPF would not give any significant effect.

5.3.7 Summary

The work presented here demonstrated the functional roles of selected K^+ channels in the N9 microglia including their effect on cell viability, LPS-induced NO release and the sensitivity of whole-cell current to their pharmacological blockers. External PPF (10μM), Tram34 (1μM) and Ba^{2+} (1mM) inhibited LPS-induced N9 microglial NO release. What is more, LPS elevated a significant paxilline-sensitive outward current from N9 microglia. BK channels play a role in modulating the effect of other K^+ channels on LPS-induced NO release.

It is hard to determine whether the effects of pharmacological manipulation are additive or display summation. Further study acquiring a wider range of combined pharmacological reagents is required to fix this issue. The membrane expression of K^+ channels during LPS challenge may be a time-dependent manner which plays an important role in modulating LPS-induced NO release. A time-course study on the localization of K^+ channels is thus required. $[Ca^{2+}]_i$ may play an important role in mediating the K^+ channel-regulated LPS-induced NO release. Investigations on the role of Ca^{2+} channels, cytosolic Ca^{2+}, and Ca^{2+}-dependent phosphorylation pathways need to be further performed to understand the role of these K^+ channels in N9 microglial cell function.

CHAPTER SIX

General Discussion

6.1 General discussion

6.1.1 Hypothesis and aims of the Thesis

The overall hypothesis to be tested was that: N9 murine microglia express multiple K^+ channels and that potassium (K^+) channels regulate lipopolysaccharide (LPS)-induced microglial nitric oxide (NO) release. The major aims to address these were: (1) Optimizing maintenance of N9 microglial cell line and LPS-induced N9 microglial activation. (2) To investigate what K^+ channel mRNAs express in resting N9 microglia and how they are regulated by LPS. (3) Functional role of K^+ channels in N9 microglia including LPS-induced NO release and current expression.

6.1.2 Optimized maintenance of resting and LPS-activated N9 microglia

By comparing morphology and proliferation of N9 microglia cultured in different growth media, microglia cultured in Iscove's modified Dulbecco's medium (IMDM) display higher proliferation rate and increased ramified morphology than ones in Dulbecco's Modified Eagle Medium (DMEM). Thus, as described in Chapter 3, the optimal growth media for N9 microglia maintenance in the resting state contains IMDM (including 4mM glutamine (GLX)) with 5% fetal calf serum (FCS), 100U/ml penicillin (PEN), 100μg/ml streptomycin (STREP) and 50μM β-mercaptoethanol (β-MET).

What media components promote the resting state of N9 microglia? Compared to DMEM, IMDM contains extra antioxidant components, such as selenium and sodium pyruvate, which may protect cells from oxidative damage from peroxides in the growth medium (Giandomenico *et al.*, 1997). In addition, this growth media provides components that mimic the central nervous system (CNS) environment to the microglia culture *in vitro*, such as GLX (Reeds, 2000). Thus these may provide

N9 microglia an environment more similar to the one *in vivo* and with less oxidative stress.

As determined using the Griess assay, N9 microglia cultured at the optimized seeding density (1.3×10^4~1.1×10^5/cm^2) were able to release abundant NO in response to LPS (Figure 3-5). In addition, LPS-induced microglial NO release reached a plateau during 24~36hr with a decreasing phase beginning from around 36hr (Figure 3-6) and displayed a dose-dependence of LPS application (10ng/ml~1μg/ml) over this time course (Figure 3-7). Thus, LPS at 1μg/ml for 24hr was used as the activation method.

The optimized maintenance and activation methods for N9 microglia provided a reliable cell preparation and efficient microglial activation model for the subsequent assays, including K^+ channel expression and their functional role in resting and LPS-activated microglia.

6.1.3 N9 microglia express a variety of K^+ channel mRNAs

Using quantitative reverse transcription polymerase chain reaction (qRT-PCR), expression of 82 K^+ channels subunits was systematically examined in resting and LPS-activated N9 microglia. There were 17 subunits not detected (Table 4-2) and 65 subunits were detected. The most abundantly expressed subunits were Kcnma1 ($K_{Ca}1.1$), Kcnk6 ($K_{2p}6.1$), Kcnc3 ($K_v3.3$), Abcc8 (SUR1), Kcnj2 ($K_{ir}2.1$), Kcnn4 ($K_{Ca}3.1$) (Figure 4-3). Surprisingly, Kcnk6 ($K_{2p}6.1$) was the only subunit mRNA significantly regulated by LPS treatment and was decreased to 68.8% compared to resting N9 cells. Further experiments need to be performed to investigate how LPS regulates the expression of Kcnk6 ($K_{2p}6.1$).

The systematic examination extended the understanding of K^+ channel gene expression in microglia and provided an important result for future investigations on

microglial K^+ channels. Importantly, whether the LPS-regulated K^+ channel expression in N9 microglia is temporally regulated needs to be determined. Thus, future experiments are required to address which K^+ channel proteins are expressed, the time course of channel expression and the sub-cellular distribution of microglial K^+ channels.

6.1.4 Functional role of K^+ channels in N9 microglia

6.1.4.1 LPS elevated paxilline-sensitive outward current in N9 microglia

Using whole-cell voltage clamp, the whole-cell current of resting N9 microglia had a small outward current with a large inward current which is similar to previous reports on microglia *in vitro*. Importantly, LPS induced a calcium (Ca^{2+})-dependent outward current which was significantly blocked by paxilline suggesting a large conductance Ca^{2+}-sensitive and voltage-activated K^+ (BK) channel current was elevated by LPS. However, LPS did not change BK channel mRNA expression suggesting the effect of LPS is post-transcriptional. Future work needs to address whether the elevation of BK current results from increased protein expression or the activation of BK channels on the plasma membrane.

External barium (Ba^{2+}) fully blocked the inward current as reported in previous studies. Tram34 and propafenone (PPF) did not significantly block the outward current in either resting or LPS-activated N9 microglia. In addition, paxilline had no effect on the outward current of resting N9 microglia. Due to the limitation of analysis on cell population data performed here, there could be a very small proportion of each relative type of current expressed. To confirm this hypothesis, discrete single cell recordings before and after blocker exposure is required. As previously reported, both K^+ channel expression on the microglial plasma membrane (Kotecha & Schlichter, 1999) and LPS-induced outward current (Nörenberg *et al.*, 1992) may display a time-dependence. Thus, a more systematic time course

examination of LPS-regulated K^+ channel protein location and ionic current is required in N9 microglia.

6.1.4.2 BK channels modulate the effect of other K^+ channels on LPS-induced microglial NO release

The external application of K^+ channel blockers, PPF (10μM), Tram34 (1μM) and Ba^{2+} (1mM), attenuated LPS-induced N9 microglial NO release. Inhibiting or activating BK channels on their own did not significantly affect LPS-induced NO release. However, blocking BK channel activity attenuated the inhibitory effect of PPF, Tram34 and Ba^{2+} while activating BK channels significantly facilitated the effect of Tram34 and PPF on LPS-induced NO release.

Is there a common mechanism for how blocking K^+ channels using PPF, Tram34 or Ba^{2+} may inhibit LPS-induced NO release? The mechanism is not clear yet. As described before, blocking K^+ channels likely depolarizes the membrane potential which would decrease the driving force for Ca^{2+} influx through non-selective cation channels, such as transient receptor potential channel (TRP), in microglia. Decreased intracellular Ca^{2+} concentration ($[Ca^{2+}]_i$) may result in reduced inducible nitric oxide synthase (iNOS)/NO synthesis (Figure 6-1).

How might BK channels modulate the effect of other K^+ channels in LPS-induced NO release? A working hypothesis is that BK channels may potentially locate with voltage-gated Ca^{2+} channels which are known to be expressed by microglia. Thus, blocking BK channels might induce depolarization which would activate voltage-gated Ca^{2+} channels and increase $[Ca^{2+}]_i$. This increased $[Ca^{2+}]_i$ would oppose the effect of blocking other K^+ channels, which decrease $[Ca^{2+}]_i$ through the interactions with non-selective cation channels. Thus, blocking BK may prevent the inhibitory effect of blocking other K^+ channels on LPS-induced NO release.

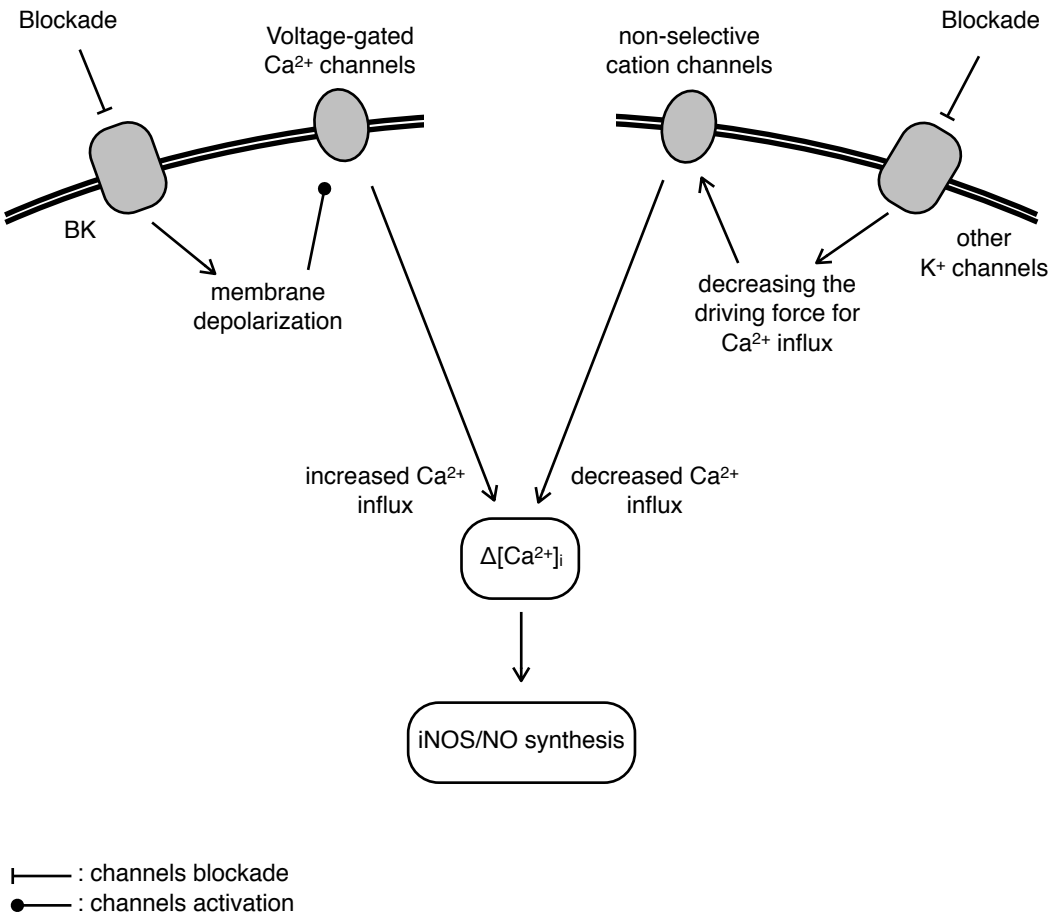

Figure 6-1. Working hypothesis to explain how BK channels may modulate the effect of blocking other K^+ channels on $[Ca^{2+}]_i$ and LPS-induced NO release. The hypothesis is based on BK channels locating with voltage-gated Ca^{2+} channels while other K^+ channels locating with non-selective cation channels. Blockade of other K^+ channels, such as IK, reduces the Ca^{2+} influx through the non-selective cation channels by decreasing the driving force for Ca^{2+} influx. However, blockade of BK channel induces membrane depolarization and activates voltage-gated Ca^{2+} channels inducing Ca^{2+} influx. The net effect may result in no significant change in $[Ca^{2+}]_i$ and thus blocking BK prevents the inhibitory effect of blocking other K^+ channels on LPS-induced NO release. BK: large conductance Ca^{2+}-sensitive and voltage-activated K^+ channels; IK: intermediate conductance Ca^{2+}-activated K^+ channels; K^+: potassium; $[Ca^{2+}]_i$: intracellular Ca^{2+} concentration; iNOS: inducible nitric oxide synthase; NO: nitric oxide.

To address this hypothesis, experiments are required to examine the $[Ca^{2+}]_i$ regulated by blocking these K^+ channels, the colocalization of Ca^{2+} channels and K^+ channels, the activity of Ca^{2+}-dependent phosphorylation pathways and iNOS/NO synthesis. Furthermore whether BK channel may modulate LPS-induced NO release in native mouse microglia via similar mechanism needs to be investigated.

6.1.5 Final overview

The work here extends the understanding of K^+ channel expression in resting and activated microglia and their role in LPS-induced NO release. Intriguingly it provides the first evidence of the functional role of BK channels in modulating the effect of other K^+ channels in LPS-induced N9 microglial NO release. However, the regulation of K^+ channels and NO release by LPS may involve a more complex interaction of pathways (Figure 6-2). Thus, further examination is required to address the potential mechanisms.

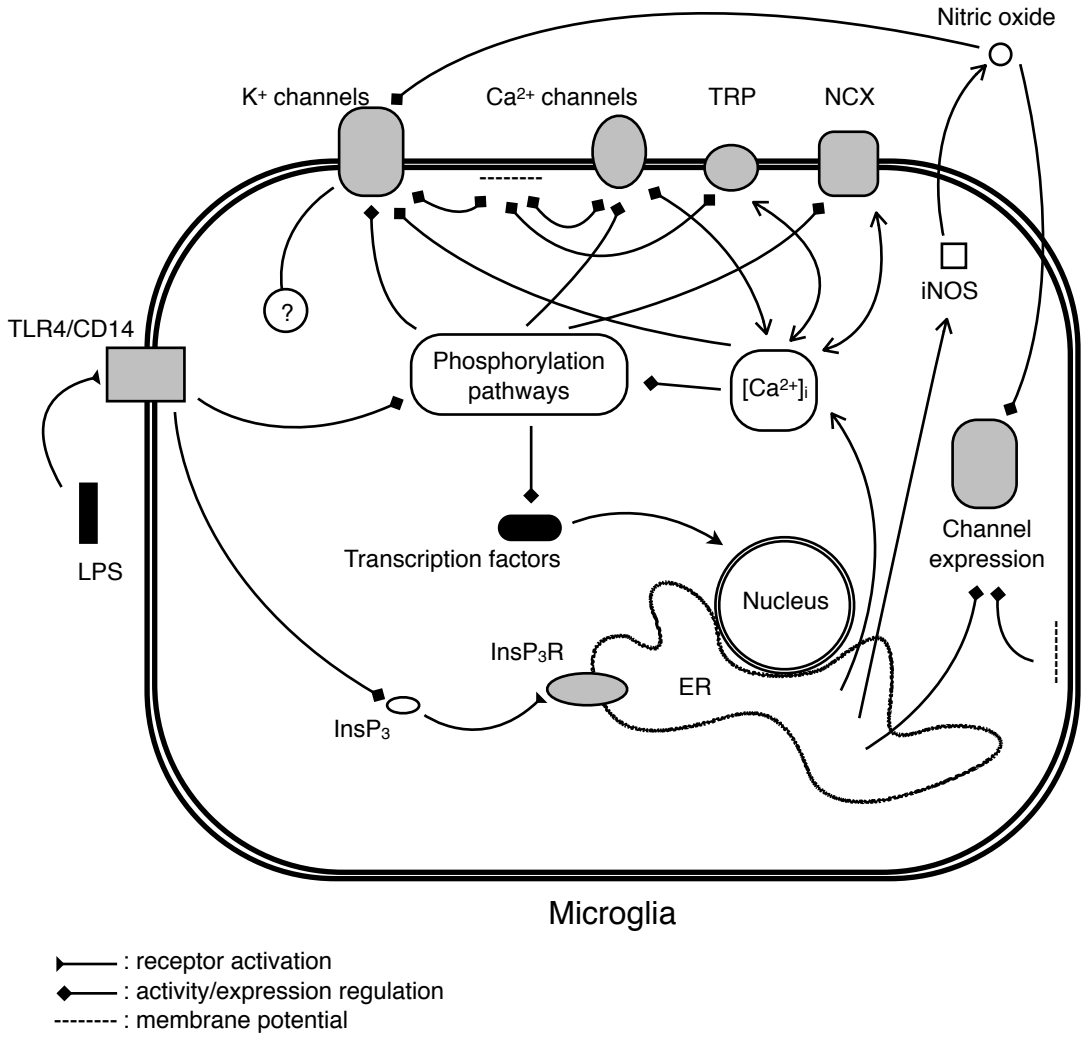

Figure 6-2. Schematic of LPS-induced regulation of K^+ channel function and NO release in microglia. LPS induces microglial NO release by activating TLR4/CD14 receptors which regulates the activity of downstream phosphorylation pathways and induction of iNOS expression via the regulation of transcription factors. Then iNOS produces NO from L-arginine (Hobbs *et al.*, 1994). As Ca^{2+} is able to regulate the phosphorylation pathways, K^+ channels may thus regulate LPS-induced NO release by regulating membrane potential and $[Ca^{2+}]_i$. This process includes interaction between K^+ channels and other channels, such as Ca^{2+} channels, TRP channels and NCX which are expressed by microglia (Eder, 1998). Additionally, expression and activities of K^+ channels can be regulated by NO (Zhu & Huizinga, 2008) and membrane potential (Levitan *et al.*, 1995). TRP: transient receptor potential channel; ER: endoplasmic reticulum; NCX: Na^+/Ca^{2+} exchanger; $InsP_3$(R): inositol trisphosphate (receptor).

References

References

Agulhon C, Fiacco TA and McCarthy KD (2010) Hippocampal short- and long-term plasticity are not modulated by astrocyte Ca^{2+} signaling. *Science (New York, NY)*. 327 (5970), 1250–1254.

Ahluwalia J, Tinker A, Clapp LH, Duchen MR, Abramov AY, Pope S, Nobles M and Segal AW (2004) The large-conductance Ca^{2+}-activated K^{+} channel is essential for innate immunity. *Nature*. 427 (6977), 853–858.

Ajami B, Bennett JL, Krieger C, Tetzlaff W and Rossi FMV (2007) Local self-renewal can sustain CNS microglia maintenance and function throughout adult life. *Nature Neuroscience*. 10 (12), 1538–1543.

Allen NJ and Barres BA (2009) Neuroscience: Glia - more than just brain glue. *Nature*. 457 (7230), 675–677.

Aloisi F (2001) Immune function of microglia. *Glia*. 36 (2), 165–179.

Araque A, Parpura V, Sanzgiri RP and Haydon PG (1999) Tripartite synapses: glia, the unacknowledged partner. *Trends in Neurosciences*. 22 (5), 208–215.

Arias C, González T, Moreno I, Caballero R, Delpon E, Tamargo J and Valenzuela C (2003) Effects of propafenone and its main metabolite, 5-hydroxypropafenone, on *HERG* channels. *Cardiovascular Research*. 57 (3), 660–669.

Ashwell K (1991) The distribution of microglia and cell death in the fetal rat forebrain. *Developmental Brain Research*. 58 (1), 1–12.

Azevedo FAC, Carvalho LRB, Grinberg LT, Farfel JM, Ferretti REL, Leite REP, Jacob Filho W, Lent R and Herculano-Houzel S (2009) Equal numbers of neuronal and nonneuronal cells make the human brain an isometrically scaled-up primate brain. *The Journal of Comparative Neurology*. 513 (5), 532–541.

Banks WA and Kastin AJ (1996) Passage of peptides across the blood-brain barrier: pathophysiological perspectives. *Life Sciences*. 59 (23), 1923–1943.

Barbas CF, Burton DR, Scott JK and Silverman GJ (2007) Quantitation of DNA and RNA. *CSH Protocols*. 2007, doi: 10.1101/pdb.ip47.

Baumann N and Pham-Dinh D (2001) Biology of oligodendrocyte and myelin in the mammalian central nervous system. *Physiological Reviews*. 81 (2), 871–927.

Beam TR and Allen JC (1977) Blood, brain, and cerebrospinal fluid concentrations of several antibiotics in rabbits with intact and inflamed meninges. *Antimicrobial Agents and Chemotherapy*. 12 (6), 710–716.

Becher B, Dodelet V, Fedorowicz V and Antel JP (1996) Soluble tumor necrosis factor receptor inhibits interleukin 12 production by stimulated human adult microglial cells *in vitro*. *Journal of Clinical Investigation*. 98 (7), 1539–1543.

Bechmann I, Mor G, Nilsen J, Eliza M, Nitsch R and Naftolin F (1999) FasL (CD95L, Apo1L) is expressed in the normal rat and human brain: evidence for the existence of an immunological brain barrier. *Glia*. 27 (1), 62–74.

Beers DR, Henkel JS, Xiao Q, Zhao W, Wang J, Yen AA, Siklos L, McKercher SR and Appel SH (2006) Wild-type microglia extend survival in PU.1 knockout mice with familial amyotrophic lateral sclerosis. *Proceedings of the National Academy of Sciences of the United States of America*. 103 (43), 16021–16026.

Benzie IFF (2003) Evolution of dietary antioxidants. *Comparative Biochemistry and Physiology-Part A: Molecular & Integrative Physiology*. 136 (1), 113–126.

Bernal-Mizrachi E, Wen W, Shornick M and Permutt MA (2002) Activation of nuclear factor-κB by depolarization and Ca^{2+} influx in MIN6 insulinoma cells. *Diabetes*. 51 Suppl 3, S484–8.

Bi XL, Yang JY, Dong YX, Wang JM, Cui YH, Ikeshima T, Zhao YQ and Wu CF (2005) Resveratrol inhibits nitric oxide and TNF-α production by lipopolysaccharide-activated microglia. *International Immunopharmacology*. 5 (1), 185–193.

Bianco F, Fumagalli M, Pravettoni E, D'Ambrosi N, Volonte C, Matteoli M, Abbracchio MP and Verderio C (2005) Pathophysiological roles of extracellular nucleotides in glial cells: differential expression of purinergic receptors in resting and activated microglia. *Brain Research Reviews*. 48 (2), 144–156.

Bjørkøy G, Overvatn A, Diaz-Meco MT, Moscat J and Johansen T (1995) Evidence for a bifurcation of the mitogenic signaling pathway activated by Ras and phosphatidylcholine-hydrolyzing phospholipase C. *The Journal of Biological Chemistry*. 270 (36), 21299–21306.

Blasi E, Barluzzi R, Bocchini V, Mazzolla R and Bistoni F (1990) Immortalization of murine microglial cells by a v-raf/v-myc carrying retrovirus. *Journal of Neuroimmunology*. 27 (2-3), 229–237.

Block ML, Zecca L and Hong JS (2007) Microglia-mediated neurotoxicity: uncovering the molecular mechanisms. *Nature Reviews Neuroscience*. 8 (1), 57–69.

Bocchini V, Mazzolla R, Barluzzi R, Blasi E, Sick P and Kettenmann H (1992) An immortalized cell line expresses properties of activated microglial cells. *Journal of Neuroscience Research*. 31 (4), 616–621.

Bonaiuto C, McDonald PP, Rossi F and Cassatella MA (1997) Activation of nuclear factor-κB by β-amyloid peptides and interferon-γ in murine microglia. *Journal of Neuroimmunology*. 77 (1), 51–56.

Boucsein C, Kettenmann H and Nolte C (2000) Electrophysiological properties of microglial cells in normal and pathologic rat brain slices. *The European Journal of Neuroscience*. 12 (6), 2049–2058.

Boucsein C, Zacharias R, Färber K, Pavlovic S, Hanisch UK and Kettenmann H (2003) Purinergic receptors on microglial cells: functional expression in acute brain slices and modulation of microglial activation *in vitro*. *The European Journal of Neuroscience*. 17 (11), 2267–2276.

Boya J, Calvo J and Prado A (1979) The origin of microglial cells. *Journal of Anatomy*. 129 (Pt 1), 177.

Brockhaus J, Ilschner S, Banati RB and Kettenmann H (1993) Membrane properties of ameboid microglial cells in the corpus callosum slice from early postnatal mice. *The Journal of Neuroscience : the Official Journal of the Society for Neuroscience*. 13 (10), 4412–4421.

Broom L, Marinova-Mutafchieva L, Sadeghian M, Davis JB, Medhurst AD and Dexter DT (2011) Neuroprotection by the selective iNOS inhibitor GW274150 in a model of Parkinson disease. *Free Radical Biology & Medicine*. 50 (5), 633–640.

Bruce-Keller AJ, Barger SW, Moss NI, Pham JT, Keller JN and Nath A (2001) Pro-inflammatory and pro-oxidant properties of the HIV protein Tat in a microglial cell line: attenuation by 17 β-estradiol. *Journal of Neurochemistry*. 78 (6), 1315–1324.

Buster BL, Weintrob AC, Townsend GC and Scheld WM (1995) Potential role of nitric oxide in the pathophysiology of experimental bacterial meningitis in rats. *Infection and Immunity*. 63 (10), 3835–3839.

Bustin SA, Benes V, Garson JA, Hellemans J, Huggett J, Kubista M, Mueller R, Nolan T, Pfaffl MW, Shipley GL, Vandesompele J and Wittwer CT (2009) The

MIQE guidelines: minimum information for publication of quantitative real-time PCR experiments. *Clinical Chemistry*. 55 (4), 611–622.

Cahalan MD, Wulff H and Chandy KG (2001) Molecular properties and physiological roles of ion channels in the immune system. *Journal of Clinical Immunology*. 21 (4), 235–252.

Calderón-Garcidueñas L, Mora-Tiscareño A, Gómez-Garza G, Carrasco-Portugal MDC, Pérez-Guillé B, Flores-Murrieta FJ, Pérez-Guillé G, Osnaya N, Juárez-Olguín H, Monroy ME, Monroy S, González-Maciel A, Reynoso-Robles R, Villarreal-Calderon R, Patel SA, Kumarathasan P, Vincent R, Henríquez-Roldán C, Torres-Jardón R and Maronpot RR (2009) Effects of a cyclooxygenase-2 preferential inhibitor in young healthy dogs exposed to air pollution: a pilot study. *Toxicologic Pathology*. 37 (5), 644–660.

Campbell K and Götz M (2002) Radial glia: multi-purpose cells for vertebrate brain development. *Trends in Neurosciences*. 25 (5), 235–238.

Carrisoza-Gaytán R, Salvador C, Satlin LM, Liu W, Zavilowitz B, Bobadilla NA, Trujillo J and Escobar LI (2010) Potassium secretion by voltage-gated potassium channel $K_v1.3$ in the rat kidney. *American Journal of Physiology. Renal Physiology*. 299 (1), F255–64.

Cavaliere F, Dinkel K and Reymann K (2005) Microglia response and P2 receptor participation in oxygen/glucose deprivation-induced cortical damage. *Neuroscience*. 136 (3), 615–623.

Cayabyab FS, Khanna R, Jones OT and Schlichter LC (2000) Suppression of the rat microglia $K_v1.3$ current by src-family tyrosine kinases and oxygen/glucose deprivation. *The European Journal of Neuroscience*. 12 (6), 1949–1960.

Chan ED, Morris KR, Belisle JT, Hill P, Remigio LK, Brennan PJ and Riches DW (2001) Induction of inducible nitric oxide synthase-NO by lipoarabinomannan of *Mycobacterium tuberculosis* is mediated by MEK1-ERK, MKK7-JNK, and NF-κB signaling pathways. *Infection and Immunity*. 69 (4), 2001–2010.

Chan WY, Kohsaka S and Rezaie P (2007) The origin and cell lineage of microglia: new concepts. *Brain Research Reviews*. 53 (2), 344–354.

Chang LC, Tsao LT, Chang CS, Chen CJ, Huang LJ, Kuo SC, Lin RH and Wang JP (2008) Inhibition of nitric oxide production by the carbazole compound LCY-2-CHO via blockade of activator protein-1 and CCAAT/enhancer-binding protein activation in microglia. *Biochemical Pharmacology*. 76 (4), 507–519.

Chatton JY, Pellerin L and Magistretti PJ (2003) GABA uptake into astrocytes is not associated with significant metabolic cost: implications for brain imaging of

inhibitory transmission. *Proceedings of the National Academy of Sciences of the United States of America*. 100 (21), 12456–12461.

Chen G and Goeddel DV (2002) TNF-R1 signaling: a beautiful pathway. *Science (New York, NY)*. 296 (5573), 1634–1635.

Cheng YM, Fedida D and Kehl SJ (2008) External Ba^{2+} block of human $K_v1.5$ at neutral and acidic pH: evidence for H_o^+-induced constriction of the outer pore mouth at rest. *Biophysical Journal*. 95 (9), 4456–4468.

Christensen RN, Ha BK, Sun F, Bresnahan JC and Beattie MS (2006) Kainate induces rapid redistribution of the actin cytoskeleton in ameboid microglia. *Journal of Neuroscience Research*. 84 (1), 170–181.

Christé G, Tebbakh H, Simurdová M, Forrat R and Simurda J (1999) Propafenone blocks ATP-sensitive K^+ channels in rabbit atrial and ventricular cardiomyocytes. *European Journal of Pharmacology*. 373 (2-3), 223–232.

Chung S, Joe E, Soh H, Lee MY and Bang HW (1998) Delayed rectifier potassium currents induced in activated rat microglia set the resting membrane potential. *Neuroscience Letters*. 242 (2), 73–76.

Chung S, Jung W and Lee MY (1999) Inward and outward rectifying potassium currents set membrane potentials in activated rat microglia. *Neuroscience Letters*. 262 (2), 121–124.

Chung S, Lee J, Joe EH and Uhm DY (2001a) β-amyloid peptide induces the expression of voltage dependent outward rectifying K^+ channels in rat microglia. *Neuroscience Letters*. 300 (2), 67–70.

Chung YH, Shin CM, Kim MJ, Lee BK and Cha CI (2001b) Age-related changes in the distribution of $K_v1.1$ and $K_v1.2$ channel subunits in the rat cerebellum. *Brain Research*. 897 (1-2), 193–198.

Ciccarelli R, Ballerini P, Sabatino G, Rathbone MP, D'Onofrio M, Caciagli F and Di Iorio P (2001) Involvement of astrocytes in purine-mediated reparative processes in the brain. *International Journal of Developmental Neuroscience : the Official Journal of the International Society for Developmental Neuroscience*. 19 (4), 395–414.

Cobb MH and Goldsmith EJ (1995) How MAP kinases are regulated. *The Journal of Biological Chemistry*. 270 (25), 14843–14846.

Colton CA, Keri JE, Chen WT and Monsky WL (1993) Protease production by cultured microglia: substrate gel analysis and immobilized matrix degradation. *Journal of Neuroscience Research*. 35 (3), 297–304.

Comalada M, Xaus J, Valledor AF, López-López C, Pennington DJ and Celada A (2003) PKCε is involved in JNK activation that mediates LPS-induced TNF-α, which induces apoptosis in macrophages. *American Journal of Physiology Cell Physiology*. 285 (5), C1235–45.

Conner GE, Salathe M and Forteza R (2002) Lactoperoxidase and hydrogen peroxide metabolism in the airway. *American Journal of Respiratory and Critical Care Medicine*. 166 (12 Pt 2), S57–61.

Conrad AH, Albrecht M, Pettit-Scott M and Conrad GW (2009) Embryonic corneal Schwann cells express some Schwann cell marker mRNAs, but no mature Schwann cell marker proteins. *Investigative Ophthalmology & Visual Science*. 50 (9), 4173–4184.

Constam DB, Philipp J, Malipiero UV, Dijke Ten P, Schachner M and Fontana A (1992) Differential expression of transforming growth factor-β1, -β2, and -β3 by glioblastoma cells, astrocytes, and microglia. *Journal of Immunology (Baltimore, Md : 1950)*. 148 (5), 1404–1410.

Conti B, Park LC, Calingasan NY, Kim Y, Kim H, Bae Y, Gibson GE and Joh TH (1999) Cultures of astrocytes and microglia express interleukin 18. *Brain Research Molecular Brain Research*. 67 (1), 46–52.

Corey S, Krapivinsky G, Krapivinsky L and Clapham DE (1998) Number and stoichiometry of subunits in the native atrial G-protein-gated K^+ channel, I_{KACh}. *The Journal of Biological Chemistry*. 273 (9), 5271–5278.

Corradin SB, Mauël J, Donini SD, Quattrocchi E and Ricciardi-Castagnoli P (1993) Inducible nitric oxide synthase activity of cloned murine microglial cells. *Glia*. 7 (3), 255–262.

Crocker SJ, Frausto RF, Whitton JL and Milner R (2008) A novel method to establish microglia-free astrocyte cultures: comparison of matrix metalloproteinase expression profiles in pure cultures of astrocytes and microglia. *Glia*. 56 (11), 1187–1198.

Cross AK and Woodroofe MN (1999) Chemokine modulation of matrix metalloproteinase and TIMP production in adult rat brain microglia and a human microglial cell line *in vitro*. *Glia*. 28 (3), 183–189.

Dauphinee SM and Karsan A (2006) Lipopolysaccharide signaling in endothelial cells. *Laboratory Investigation; a Journal of Technical Methods and Pathology*. 86 (1), 9–22.

Davalos D, Grutzendler J, Yang G, Kim JV, Zuo Y, Jung S, Littman DR, Dustin ML and Gan W-B (2005) ATP mediates rapid microglial response to local brain injury *in vivo*. *Nature Neuroscience*. 8 (6), 752–758.

DeCoursey TE, Kim SY, Silver MR and Quandt FN (1996) Ion channel expression in PMA-differentiated human THP-1 macrophages. *The Journal of Membrane Biology*. 152 (2), 141–157.

Defarias FP, Stevens SP and Leonard RJ (1995) Stable expression of human $K_v1.3$ potassium channels resets the resting membrane potential of cultured mammalian cells. *Receptors & Channels*. 3 (4), 273–281.

Devasagayam TPA, Tilak JC, Boloor KK, Sane KS, Ghaskadbi SS and Lele RD (2004) Free radicals and antioxidants in human health: current status and future prospects. *The Journal of the Association of Physicians of India*. 52, 794–804.

Dheen ST, Kaur C and Ling EA (2007) Microglial activation and its implications in the brain diseases. *Current Medicinal Chemistry*. 14 (11), 1189–1197.

Dobrenis K, Chang HY, Pina-Benabou MH, Woodroffe A, Lee SC, Rozental R, Spray DC and Scemes E (2005) Human and mouse microglia express connexin36, and functional gap junctions are formed between rodent microglia and neurons. *Journal of Neuroscience Research*. 82 (3), 306–315.

Doetsch F (2003) The glial identity of neural stem cells. *Nature Neuroscience*. 6 (11), 1127–1134.

Dowling P, Shang G, Raval S, Menonna J, Cook S and Husar W (1996) Involvement of the CD95 (APO-1/Fas) receptor/ligand system in multiple sclerosis brain. *The Journal of Experimental Medicine*. 184 (4), 1513–1518.

Draheim HJ, Prinz M, Weber JR, Weiser T, Kettenmann H and Hanisch UK (1999) Induction of potassium channels in mouse brain microglia: cells acquire responsiveness to pneumococcal cell wall components during late development. *Neuroscience*. 89 (4), 1379–1390.

Drysdale BE, Yapundich RA, Shin ML and Shin HS (1987) Lipopolysaccharide-mediated macrophage activation: the role of calcium in the generation of tumoricidal activity. *Journal of Immunology (Baltimore, Md : 1950)*. 138 (3), 951–956.

Ducharme G, Newell EW, Pinto C and Schlichter LC (2007) Small-conductance Cl^- channels contribute to volume regulation and phagocytosis in microglia. *The European Journal of Neuroscience*. 26 (8), 2119–2130.

Dupont G, Houart G and De Koninck P (2003) Sensitivity of CaM kinase II to the frequency of Ca^{2+} oscillations: a simple model. *Cell Calcium*. 34 (6), 485–497.

Eder C (1998) Ion channels in microglia (brain macrophages). *The American Journal of Physiology*. 275 (2 Pt 1), C327–42.

Eder C (2005) Regulation of microglial behavior by ion channel activity. *Journal of Neuroscience Research*. 81 (3), 314–321.

Eder C and Heinemann U (1996) Proton modulation of outward K^+ currents in interferon-γ-activated microglia. *Neuroscience Letters*. 206 (2-3), 101–104.

Eder C, Fischer HG, Hadding U and Heinemann U (1995) Properties of voltage-gated currents of microglia developed using macrophage colony-stimulating factor. *Pflügers Archiv : European Journal of Physiology*. 430 (4), 526–533.

Eder C, Klee R and Heinemann U (1997a) Distinct soluble astrocytic factors induce expression of outward K^+ currents and ramification of brain macrophages. *Neuroscience Letters*. 226 (3), 147–150.

Eder C, Klee R and Heinemann U (1997b) Pharmacological properties of Ca^{2+}-activated K^+ currents of ramified murine brain macrophages. *Naunyn-Schmiedeberg's Archives of Pharmacology*. 356 (2), 233–239.

Eglitis MA and Mezey E (1997) Hematopoietic cells differentiate into both microglia and macroglia in the brains of adult mice. *Proceedings of the National Academy of Sciences of the United States of America*. 94 (8), 4080–4085.

Ehlers MR (2000) CR3: a general purpose adhesion-recognition receptor essential for innate immunity. *Microbes and Infection / Institut Pasteur*. 2 (3), 289–294.

Ehrlich JR, Cha TJ, Zhang L, Chartier D, Villeneuve L, Hébert TE and Nattel S (2004) Characterization of a hyperpolarization-activated time-dependent potassium current in canine cardiomyocytes from pulmonary vein myocardial sleeves and left atrium. *The Journal of Physiology*. 557 (Pt 2), 583–597.

El-Benna J, Dang PMC and Gougerot-Pocidalo MA (2008) Priming of the neutrophil NADPH oxidase activation: role of p47phox phosphorylation and NOX2 mobilization to the plasma membrane. *Seminars in Immunopathology*. 30 (3), 279–289.

Fanger CM, Rauer H, Neben AL, Miller MJ, Rauer H, Wulff H, Rosa JC, Ganellin CR, Chandy KG and Cahalan MD (2001) Calcium-activated potassium channels sustain calcium signaling in T lymphocytes. Selective blockers and manipulated channel expression levels. *The Journal of Biological Chemistry*. 276 (15), 12249–12256.

Färber K and Kettenmann H (2005) Physiology of microglial cells. *Brain Research Reviews*. 48 (2), 133–143.

Fellin T and Carmignoto G (2004) Neurone-to-astrocyte signalling in the brain represents a distinct multifunctional unit. *The Journal of Physiology*. 559 (Pt 1), 3–15.

Fenton MJ and Golenbock DT (1998) LPS-binding proteins and receptors. *Journal of Leukocyte Biology*. 64 (1), 25–32.

Ferrer I, Bernet E, Soriano E, del Rio T and Fonseca M (1990) Naturally occurring cell death in the cerebral cortex of the rat and removal of dead cells by transitory phagocytes. *Neuroscience*. 39 (2), 451–458.

Fiacco TA, Agulhon C and McCarthy KD (2009) Sorting out astrocyte physiology from pharmacology. *Annual Review of Pharmacology and Toxicology*. 49, 151–174.

Fischer HG, Eder C, Hadding U and Heinemann U (1995) Cytokine-dependent K^+ channel profile of microglia at immunologically defined functional states. *Neuroscience*. 64 (1), 183–191.

Fordyce CB, Jagasia R, Zhu X and Schlichter LC (2005) Microglia $K_v1.3$ channels contribute to their ability to kill neurons. *Journal of Neuroscience*. 25 (31), 7139–7149.

Franchini L, Levi G and Visentin S (2004) Inwardly rectifying K^+ channels influence Ca^{2+} entry due to nucleotide receptor activation in microglia. *Cell Calcium*. 35 (5), 449–459.

Franqueza L, Longobardo M, Vicente J, Delpón E, Tamkun MM, Tamargo J, Snyders DJ and Valenzuela C (1997) Molecular determinants of stereoselective bupivacaine block of $hK_v1.5$ channels. *Circulation Research*. 81 (6), 1053–1064.

Franqueza L, Valenzuela C, Delpón E, Longobardo M, Caballero R and Tamargo J (1998) Effects of propafenone and 5-hydroxy-propafenone on $hK_v1.5$ channels. *British Journal of Pharmacology*. 125 (5), 969–978.

Frigerio S, Silei V, Ciusani E, Massa G, Lauro GM and Salmaggi A (2000) Modulation of fas-ligand (Fas-L) on human microglial cells: an *in vitro* study. *Journal of Neuroimmunology*. 105 (2), 109–114.

Fukushima Y and Hagiwara S (1983) Voltage-gated Ca^{2+} channel in mouse myeloma cells. *Proceedings of the National Academy of Sciences of the United States of America*. 80 (8), 2240–2242.

Furuse M, Fujita K, Hiiragi T, Fujimoto K and Tsukita S (1998) Claudin-1 and -2: novel integral membrane proteins localizing at tight junctions with no sequence similarity to occludin. *The Journal of Cell Biology*. 141 (7), 1539–1550.

Furuse M, Hirase T, Itoh M, Nagafuchi A, Yonemura S, Tsukita S and Tsukita S (1993) Occludin: a novel integral membrane protein localizing at tight junctions. *The Journal of Cell Biology*. 123 (6 Pt 2), 1777–1788.

Fürst P and Stehle P (2004) What are the essential elements needed for the determination of amino acid requirements in humans? *The Journal of Nutrition*. 134 (6 Suppl), 1558S–1565S.

Gan L, Ye S, Chu A, Anton K, Yi S, Vincent VA, Schack von D, Chin D, Murray J, Lohr S, Patthy L, Gonzalez-Zulueta M, Nikolich K and Urfer R (2004) Identification of cathepsin B as a mediator of neuronal death induced by Aβ-activated microglial cells using a functional genomics approach. *The Journal of Biological Chemistry*. 279 (7), 5565–5572.

Garg TK and Chang JY (2006) Methylmercury causes oxidative stress and cytotoxicity in microglia: attenuation by 15-deoxy-delta 12, 14-prostaglandin J_2. *Journal of Neuroimmunology*. 171 (1-2), 17–28.

Gehrmann J, Matsumoto Y and Kreutzberg GW (1995) Microglia: intrinsic immuneffector cell of the brain. *Brain Research Reviews*. 20 (3), 269–287.

Gehrmann J, Schoen SW and Kreutzberg GW (1991) Lesion of the rat entorhinal cortex leads to a rapid microglial reaction in the dentate gyrus. A light and electron microscopical study. *Acta Neuropathologica*. 82 (6), 442–455.

Giandomenico AR, Cerniglia GE, Biaglow JE, Stevens CW and Koch CJ (1997) The importance of sodium pyruvate in assessing damage produced by hydrogen peroxide. *Free Radical Biology & Medicine*. 23 (3), 426–434.

Gibbons HM and Dragunow M (2006) Microglia induce neural cell death via a proximity-dependent mechanism involving nitric oxide. *Brain Research*. 1084 (1), 1–15.

Ginhoux F, Greter M, Leboeuf M, Nandi S, See P, Gokhan S, Mehler MF, Conway SJ, Ng LG, Stanley ER, Samokhvalov IM and Merad M (2010) Fate mapping analysis reveals that adult microglia derive from primitive macrophages. *Science (New York, NY)*. 330 (6005), 841–845.

Giulian D, Corpuz M, Richmond B, Wendt E and Hall ER (1996) Activated microglia are the principal glial source of thromboxane in the central nervous system. *Neurochemistry International*. 29 (1), 65–76.

Goldstein SAN, Bayliss DA, Kim D, Lesage F, Plant LD and Rajan S (2005) International Union of Pharmacology. LV. Nomenclature and molecular relationships of two-P potassium channels. *Pharmacological Reviews*. 57 (4), 527–540.

Granado-Serrano AB, Martín MA, Bravo L, Goya L and Ramos S (2010) Quercetin modulates NF-κB and AP-1/JNK pathways to induce cell death in human hepatoma cells. *Nutrition and Cancer*. 62 (3), 390–401.

Green LC, Wagner DA, Glogowski J, Skipper PL, Wishnok JS and Tannenbaum SR (1982) Analysis of nitrate, nitrite, and [^{15}N]nitrate in biological fluids. *Analytical Biochemistry*. 126 (1), 131–138.

Grissmer S, Nguyen AN, Aiyar J, Hanson DC, Mather RJ, Gutman GA, Karmilowicz MJ, Auperin DD and Chandy KG (1994) Pharmacological characterization of five cloned voltage-gated K^+ channels, types K_v1.1, 1.2, 1.3, 1.5, and 3.1, stably expressed in mammalian cell lines. *Molecular Pharmacology*. 45 (6), 1227–1234.

Groemping Y and Rittinger K (2005) Activation and assembly of the NADPH oxidase: a structural perspective. *The Biochemical Journal*. 386 (Pt 3), 401–416.

Gutman GA, Chandy KG, Grissmer S, Lazdunski M, McKinnon D, Pardo LA, Robertson GA, Rudy B, Sanguinetti MC, Stühmer W and Wang X (2005) International Union of Pharmacology. LIII. Nomenclature and molecular relationships of voltage-gated potassium channels. *Pharmacological Reviews*. 57 (4), 473–508.

Hanisch UK (2002) Microglia as a source and target of cytokines. *Glia*. 40 (2), 140–155.

Hanisch UK and Kettenmann H (2007) Microglia: active sensor and versatile effector cells in the normal and pathologic brain. *Nature Neuroscience*. 10 (11), 1387–1394.

Hanisch UK, Lyons SA, Prinz M, Nolte C, Weber JR, Kettenmann H and Kirchhoff F (1997) Mouse brain microglia express interleukin-15 and its multimeric receptor complex functionally coupled to Janus kinase activity. *The Journal of Biological Chemistry*. 272 (46), 28853–28860.

Hatai S (1902) *On the origin of neuroglia tissue from the mesoblast*. J Comp Neurol

Hawkins A and Olszewski J (1957) Glia/nerve cell index for cortex of the whale. *Science (New York, NY)*. 126 (3263), 76–77.

Haydon PG (2001) GLIA: listening and talking to the synapse. *Nature Reviews Neuroscience*. 2 (3), 185–193.

Haydon PG and Carmignoto G (2006) Astrocyte control of synaptic transmission and neurovascular coupling. *Physiological Reviews*. 86 (3), 1009–1031.

Haziot A, Ferrero E, Köntgen F, Hijiya N, Yamamoto S, Silver J, Stewart CL and Goyert SM (1996) Resistance to endotoxin shock and reduced dissemination of gram-negative bacteria in CD14-deficient mice. *Immunity*. 4 (4), 407–414.

Heidrick ML, Hendricks LC and Cook DE (1984) Effect of dietary 2-mercaptoethanol on the life span, immune system, tumor incidence and lipid peroxidation damage in spleen lymphocytes of aging $BC3F_1$ mice. *Mechanisms of Ageing and Development*. 27 (3), 341–358.

Heldman E, Levine M, Raveh L and Pollard HB (1989) Barium ions enter chromaffin cells via voltage-dependent calcium channels and induce secretion by a mechanism independent of calcium. *The Journal of Biological Chemistry*. 264 (14), 7914–7920.

Hemmi H, Takeuchi O, Kawai T, Kaisho T, Sato S, Sanjo H, Matsumoto M, Hoshino K, Wagner H, Takeda K and Akira S (2000) A Toll-like Receptor Recognizes Bacterial DNA. *Nature*. 408 (6813), 740–745.

Henderson B, Poole S and Wilson M (1996) Bacterial modulins: a novel class of virulence factors which cause host tissue pathology by inducing cytokine synthesis. *Microbiological Reviews*. 60 (2), 316–341.

Hickey WF and Kimura H (1988) Perivascular microglial cells of the CNS are bone marrow-derived and present antigen *in vivo*. *Science (New York, NY)*. 239 (4837), 290–292.

Hobbs AJ, Fukuto JM and Ignarro LJ (1994) Formation of free nitric oxide from l-arginine by nitric oxide synthase: direct enhancement of generation by superoxide dismutase. *Proceedings of the National Academy of Sciences of the United States of America*. 91 (23), 10992–10996.

Honda S, Sasaki Y, Ohsawa K, Imai Y, Nakamura Y, Inoue K and Kohsaka S (2001) Extracellular ATP or ADP induce chemotaxis of cultured microglia through $G_{i/o}$-coupled P2Y receptors. *Journal of Neuroscience*. 21 (6), 1975–1982.

Hoozemans JJM, Veerhuis R, Janssen I, van Elk EJ, Rozemuller AJM and Eikelenboom P (2002) The role of cyclo-oxygenase 1 and 2 activity in prostaglandin E_2 secretion by cultured human adult microglia: implications for Alzheimer's disease. *Brain Research*. 951 (2), 218–226.

Horvath RJ, Nutile-McMenemy N, Alkaitis MS and Deleo JA (2008) Differential migration, LPS-induced cytokine, chemokine, and NO expression in immortalized BV-2 and HAPI cell lines and primary microglial cultures. *Journal of Neurochemistry*. 107 (2), 557–569.

Hoth M and Penner R (1993) Calcium release-activated calcium current in rat mast cells. *The Journal of Physiology*. 465, 359–386.

Huo Y, Wu CF, Yang JY, He X, Bi XL, Yu L and Guo T (2006) Effects of clozapine, olanzapine and haloperidol on nitric oxide production by lipopolysaccharide-activated N9 cells. *Progress in Neuro-psychopharmacology & Biological Psychiatry*. 30 (8), 1523–1528.

Huo Y, Rangarajan P, Ling EA and Dheen ST (2011) Dexamethasone inhibits the Nox-dependent ROS production via suppression of MKP-1-dependent MAPK pathways in activated microglia. *BMC Neuroscience*. 12, 49.

Ilschner S, Nolte C and Kettenmann H (1996) Complement factor C5a and epidermal growth factor trigger the activation of outward potassium currents in cultured murine microglia. *Neuroscience*. 73 (4), 1109–1120.

Ilschner S, Ohlemeyer C, Gimpl G and Kettenmann H (1995) Modulation of potassium currents in cultured murine microglial cells by receptor activation and intracellular pathways. *Neuroscience*. 66 (4), 983–1000.

Imamoto K and Leblond CP (1978) Radioautographic investigation of gliogenesis in the corpus callosum of young rats. II. Origin of microglial cells. *The Journal of Comparative Neurology*. 180 (1), 139–163.

Inoue K (2002) Microglial activation by purines and pyrimidines. *Glia*. 40 (2), 156–163.

Iscove NN and Melchers F (1978) Complete replacement of serum by albumin, transferrin, and soybean lipid in cultures of lipopolysaccharide-reactive B lymphocytes. *The Journal of Experimental Medicine*. 147 (3), 923–933.

Jang SH, Choi SY, Ryu PD and Lee SY (2011) Anti-proliferative effect of $K_v1.3$ blockers in A549 human lung adenocarcinoma *in vitro* and *in vivo*. *European Journal of Pharmacology*. 651 (1-3), 26–32.

Janvier NC, Harrison SM and Boyett MR (1997) The role of inward Na^+-Ca^{2+} exchange current in the ferret ventricular action potential. *The Journal of Physiology*. 498 (Pt 3), 611–625.

Jensen BS, Strøbaek D, Olesen SP and Christophersen P (2001) The Ca^{2+}-activated K^+ channel of intermediate conductance: a molecular target for novel treatments? *Current Drug Targets*. 2 (4), 401–422.

Jerison HJ (1973) *Evolution of the brain and intelligence*. Academic Pr

Jiang FX, Yurke B, Firestein BL and Langrana NA (2008) Neurite outgrowth on a DNA crosslinked hydrogel with tunable stiffnesses. *Annals of Biomedical Engineering*. 36 (9), 1565–1579.

Jiang X, Newell EW and Schlichter LC (2003) Regulation of a TRPM7-like current in rat brain microglia. *The Journal of Biological Chemistry*. 278 (44), 42867–42876.

Jin W and Lu Z (1999) Synthesis of a stable form of tertiapin: a high-affinity inhibitor for inward-rectifier K^+ channels. *Biochemistry*. 38 (43), 14286–14293.

Jou I, Pyo H, Chung S, Jung SY and Gwag B (1998) Expression of $K_v1.5$ K^+ channels in activated microglia *in vivo*. *Glia*. 24, 408–414

Judge SIV, Lee JM, Bever CT and Hoffman PM (2006) Voltage-gated potassium channels in multiple sclerosis: Overview and new implications for treatment of central nervous system inflammation and degeneration. *Journal of Rehabilitation Research and Development*. 43 (1), 111–122.

Kadekaro M, Su G, Chu R, Lei Y, Li J and Fang L (2006) Nitric oxide up-regulates the expression of calcium-dependent potassium channels in the supraoptic nuclei and neural lobe of rats following dehydration. *Neuroscience Letters*. 404 (1-2), 50–55.

Kastin AJ, Pan W, Maness LM and Banks WA (1999) Peptides crossing the blood-brain barrier: some unusual observations. *Brain Research*. 848 (1-2), 96–100.

Kauppinen TM and Swanson RA (2005) Poly(ADP-ribose) polymerase-1 promotes microglial activation, proliferation, and matrix metalloproteinase-9-mediated neuron death. *Journal of Immunology (Baltimore, Md : 1950)*. 174 (4), 2288–2296.

Kaur C, Hao AJ, Wu CH and Ling EA (2001) Origin of microglia. *Microscopy Research and Technique*. 54 (1), 2–9.

Kaushal V and Schlichter LC (2008) Mechanisms of microglia-mediated neurotoxicity in a new model of the stroke penumbra. *Journal of Neuroscience*. 28 (9), 2221–2230.

Kaushal V, Koeberle PD, Wang Y and Schlichter LC (2007) The Ca^{2+}-activated K^+ channel KCNN4/$K_{Ca}3.1$ contributes to microglia activation and nitric oxide-dependent neurodegeneration. *Journal of Neuroscience*. 27 (1), 234–244.

Kawahara K, Oyadomari S, Gotoh T, Kohsaka S, Nakayama H and Mori M (2001) Induction of CHOP and apoptosis by nitric oxide in p53-deficient microglial cells. *FEBS Letters*. 506 (2), 135–139.

Kazama I, Maruyama Y, Endo Y, Toyama H, Ejima Y, Matsubara M and Kurosawa S (2012) Overexpression of delayed rectifier K^+ channels promotes *in situ* proliferation of leukocytes in rat kidneys with advanced chronic renal failure. *International Journal of Nephrology*. 2012, 581581.

Kettenmann H and Ransom BR (2005) *Neuroglia*. Oxford University Press, USA

Kettenmann H, Banati R and Walz W (1993) Electrophysiological behavior of microglia. *Glia*. 7 (1), 93–101.

Kettenmann H, Hanisch UK, Noda M and Verkhratsky A (2011) Physiology of microglia. *Physiological Reviews*. 91 (2), 461–553.

Kettenmann H, Hoppe D, Gottmann K, Banati R and Kreutzberg G (1990) Cultured microglial cells have a distinct pattern of membrane channels different from peritoneal macrophages. *Journal of Neuroscience Research*. 26 (3), 278–287.

Kew J and Davies C (2009) *Ion Channels: From Structure to Function* (1st edition). Oxford University Press, USA.

Khanna R, Roy L, Zhu X and Schlichter LC (2001) K^+ channels and the microglial respiratory burst. *American Journal of Physiology Cell Physiology*. 280 (4), C796–806.

Kiefer H and Schulze R (1982) The membrane potential of lymphocytes changes only in response to specific stimulation. *Bioscience Reports*. 2 (8), 583–588.

Kim B, Lee JH, Yang MS, Jou I and Joe EH (2008) Retinoic acid enhances prostaglandin E_2 production through increased expression of cyclooxygenase-2 and microsomal prostaglandin E synthase-1 in rat brain microglia. *Journal of Neuroscience Research*. 86 (6), 1353–1360.

Kim S, Ock J, Kim AK, Lee HW, Cho JY, Kim DR, Park JY and Suk K (2007) Neurotoxicity of microglial cathepsin D revealed by secretome analysis. *Journal of Neurochemistry*. 103 (6), 2640–2650.

King IL, Dickendesher TL and Segal BM (2009) Circulating Ly-$6C^+$ myeloid precursors migrate to the CNS and play a pathogenic role during autoimmune demyelinating disease. *Blood*. 113 (14), 3190–3197.

Kingham PJ and Pocock JM (2001) Microglial secreted cathepsin B induces neuronal apoptosis. *Journal of Neurochemistry*. 76 (5), 1475–1484.

Kitamura Y, Taniguchi T, Kimura H, Nomura Y and Gebicke-Haerter PJ (2000) Interleukin-4-inhibited mRNA expression in mixed rat glial and in isolated microglial cultures. *Journal of Neuroimmunology*. 106 (1-2), 95–104.

Koeberle PD and Schlichter LC (2010) Targeting K_v channels rescues retinal ganglion cells *in vivo* directly and by reducing inflammation. *Channels (Austin, Tex)*. 4 (5), 337–346.

Koo GC, Blake JT, Talento A, Nguyen M, Lin S, Sirotina A, Shah K, Mulvany K, Hora D, Cunningham P, Wunderler DL, McManus OB, Slaughter R, Bugianesi R, Felix J, Garcia M, Williamson J, Kaczorowski G, Sigal NH, Springer MS and Feeney W (1997) Blockade of the voltage-gated potassium channel $K_v1.3$ inhibits immune responses *in vivo*. *Journal of Immunology (Baltimore, Md : 1950)*. 158 (11), 5120–5128.

Korn SJ and Weight FF (1987) Patch-clamp study of the calcium-dependent chloride current in AtT-20 pituitary cells. *Journal of Neurophysiology*. 58 (6), 1431–1451.

Korotzer AR and Cotman CW (1992) Voltage-gated currents expressed by rat microglia in culture. *Glia*. 6 (2), 81–88.

Kotecha SA and Schlichter LC (1999) A $K_v1.5$ to $K_v1.3$ switch in endogenous hippocampal microglia and a role in proliferation. *Journal of Neuroscience*. 19 (24), 10680–10693.

Kozlowski C and Weimer RM (2012) An automated method to quantify microglia morphology and application to monitor activation state longitudinally *in vivo*. *PLoS ONE*. 7 (2), e31814.

Kramer RH and Zucker RS (1985) Calcium-dependent inward current in *Aplysia* bursting pace-maker neurones. *The Journal of Physiology*. 362, 107–130.

Krapivinsky G, Gordon EA, Wickman K, Velimirović B, Krapivinsky L and Clapham DE (1995) The G-protein-gated atrial K^+ channel I_{KACh} is a heteromultimer of two inwardly rectifying K^+-channel proteins. *Nature*. 374 (6518), 135–141.

Kreutzberg GW (1996) Microglia: a sensor for pathological events in the CNS. *Trends in Neurosciences*. 19 (8), 312–318.

Kubo Y, Adelman JP, Clapham DE, Jan LY, Karschin A, Kurachi Y, Lazdunski M, Nichols CG, Seino S and Vandenberg CA (2005) International Union of Pharmacology. LIV. Nomenclature and molecular relationships of inwardly rectifying potassium channels. *Pharmacological Reviews*. 57 (4), 509–526.

Kubo Y, Baldwin TJ, Jan YN and Jan LY (1993) Primary structure and functional expression of a mouse inward rectifier potassium channel. *Nature*. 362 (6416), 127–133.

Küst BM, Biber K, van Calker D and Gebicke-Haerter PJ (1999) Regulation of K^+ channel mRNA expression by stimulation of adenosine A_{2a}-receptors in cultured rat microglia. *Glia*. 25 (2), 120–130.

Kwak YG, Navarro-Polanco RA, Grobaski T, Gallagher DJ and Tamkun MM (1999) Phosphorylation is required for alteration of $K_v1.5$ K^+ channel function by the $K_v\beta1.3$ subunit. *The Journal of Biological Chemistry*. 274 (36), 25355–25361.

Launay P, Fleig A, Perraud AL, Scharenberg AM, Penner R and Kinet JP (2002) TRPM4 is a Ca^{2+}-activated nonselective cation channel mediating cell membrane depolarization. *Cell*. 109 (3), 397–407.

Lawson LJ, Perry VH, Dri P and Gordon S (1990) Heterogeneity in the distribution and morphology of microglia in the normal adult mouse brain. *Neuroscience*. 39 (1), 151–170.

Lee MC, Wei SC, Tsai-Wu JJ, Wu CHH and Tsao PN (2008) Novel PKC signaling is required for LPS-induced soluble Flt-1 expression in macrophages. *Journal of Leukocyte Biology*. 84 (3), 835–841.

Lee SC, Liu W, Dickson DW, Brosnan CF and Berman JW (1993) Cytokine production by human fetal microglia and astrocytes. Differential induction by lipopolysaccharide and IL-1β. *Journal of Immunology (Baltimore, Md : 1950)*. 150 (7), 2659–2667.

Lee YK, Kim K, Kim HL, Sacket SJ, Han M, Jo JY and Im DS (2007) Lysophosphatidylserine increases membrane potentials in rat C6 glioma cells. *Archives of Pharmacal Research*. 30 (9), 1096–1101.

Levitan ES, Gealy R, Trimmer JS and Takimoto K (1995) Membrane depolarization inhibits $K_v1.5$ voltage-gated K^+ channel gene transcription and protein expression in pituitary cells. *The Journal of Biological Chemistry*. 270 (11), 6036–6041.

Li F, Lu J, Wu CY, Kaur C, Sivakumar V, Sun J, Li S and Ling EA (2008a) Expression of $K_v1.2$ in microglia and its putative roles in modulating production of proinflammatory cytokines and reactive oxygen species. *Journal of Neurochemistry*. 106 (5), 2093–2105.

Li JJ, Lu J, Kaur C, Sivakumar V, Wu CY and Ling EA (2008b) Effects of hypoxia on expression of transforming growth factor-β1 and its receptors I and II in the amoeboid microglial cells and murine BV-2 cells. *Neuroscience*. 156 (3), 662–672.

Linehan SA, Martínez-Pomares L and Gordon S (2000) Macrophage lectins in host defence. *Microbes and Infection / Institut Pasteur*. 2 (3), 279–288.

Liu BS, Ferreira R, Lively S and Schlichter LC (2012) Microglial SK3 and SK4 Currents and Activation State are Modulated by the Neuroprotective Drug, Riluzole. *Journal of Neuroimmune Pharmacology : the Official Journal of the Society on NeuroImmune Pharmacology*.

Liu HT, Du YG, He JL, Chen WJ, Li WM, Yang Z, Wang YX and Yu C (2010) Tetramethylpyrazine inhibits production of nitric oxide and inducible nitric oxide synthase in lipopolysaccharide-induced N9 microglial cells through blockade of MAPK and PI3K/Akt signaling pathways, and suppression of intracellular reactive oxygen species. *Journal of Ethnopharmacology*. 129 (3), 335–343.

Liu X, Yao M, Li N, Wang C, Zheng Y and Cao X (2008) CaMKII promotes TLR-triggered proinflammatory cytokine and type I interferon production by directly binding and activating TAK1 and IRF3 in macrophages. *Blood*. 112 (13), 4961–4970.

Liuzzi GM, Latronico T, Rossano R, Viggiani S, Fasano A and Riccio P (2007) Inhibitory effect of polyunsaturated fatty acids on MMP-9 release from microglial cells-implications for complementary multiple sclerosis treatment. *Neurochemical Research*. 32 (12), 2184–2193.

Liuzzo JP, Petanceska SS, Moscatelli D and Devi LA (1999) Inflammatory mediators regulate cathepsin S in macrophages and microglia: A role in attenuating heparan sulfate interactions. *Molecular Medicine (Cambridge, Mass.)*. 5 (5), 320–333.

Lloyd EE, Marrelli SP, Namiranian K and Bryan RM (2009) Characterization of TWIK-2, a two-pore domain K^+ channel, cloned from the rat middle cerebral artery. *Experimental Biology and Medicine (Maywood, N.J.)*. 234 (12), 1493–1502.

Lovasz N, Ducza E, Gaspar R and Falkay G (2011) Ontogeny of sulfonylurea-binding regulatory subunits of K_{ATP} channels in the pregnant rat myometrium. *Reproduction (Cambridge, England)*. 142 (1), 175–181.

Lu DY, Liou HC, Tang CH and Fu WM (2006) Hypoxia-induced iNOS expression in microglia is regulated by the PI3-kinase/Akt/mTOR signaling pathway and activation of hypoxia inducible factor-1α. *Biochemical Pharmacology*. 72 (8), 992–1000.

Lu YC, Yeh WC and Ohashi PS (2008) LPS/TLR4 signal transduction pathway. *Cytokine*. 42 (2), 145–151.

Lund S, Christensen KV, Hedtjärn M, Mortensen AL, Hagberg H, Falsig J, Hasseldam H, Schrattenholz A, Pörzgen P and Leist M (2006) The dynamics of

the LPS triggered inflammatory response of murine microglia under different culture and *in vivo* conditions. *Journal of Neuroimmunology*. 180 (1-2), 71–87.

Lyons SA, Pastor A, Ohlemeyer C, Kann O, Wiegand F, Prass K, Knapp F, Kettenmann H and Dirnagl U (2000) Distinct physiologic properties of microglia and blood-borne cells in rat brain slices after permanent middle cerebral artery occlusion. *Journal of Cerebral Blood Flow and Metabolism : Official Journal of the International Society of Cerebral Blood Flow and Metabolism*. 20 (11), 1537–1549.

Madeja M, Leicher T, Friederich P, Punke MA, Haverkamp W, Musshoff U, Breithardt G and Speckmann E-J (2003) Molecular site of action of the antiarrhythmic drug propafenone at the voltage-operated potassium channel K_v2.1. *Molecular Pharmacology*. 63 (3), 547–556.

Malayev AA, Nelson DJ and Philipson LH (1995) Mechanism of clofilium block of the human K_v1.5 delayed rectifier potassium channel. *Molecular Pharmacology*. 47 (1), 198–205.

Mannhold R, Kubinyi H and Folkers G (2006) *Voltage-Gated Ion Channels as Drug Targets (Methods and Principles in Medicinal Chemistry)* (1st edition). Wiley-VCH

Marino L (1998) A comparison of encephalization between odontocete cetaceans and anthropoid primates. *Brain, Behavior and Evolution*. 51 (4), 230–238.

Marletta MA, Yoon PS, Iyengar R, Leaf CD and Wishnok JS (1988) Macrophage oxidation of L-arginine to nitrite and nitrate: nitric oxide is an intermediate. *Biochemistry*. 27 (24), 8706–8711.

Martìn-Padura I, Lostaglio S, Schneemann M, Williams L, Romano M, Fruscella P, Panzeri C, Stoppacciaro A, Ruco L, Villa A, Simmons D and Dejana E (1998) Junctional adhesion molecule, a novel member of the immunoglobulin superfamily that distributes at intercellular junctions and modulates monocyte transmigration. *The Journal of Cell Biology*. 142 (1), 117–127.

Mas VMD, Hernandez H, Plo I, Bezombes C, Maestre N, Quillet-Mary A, Filomenko R, Demur C, Jaffrézou J-P and Laurent G (2003) Protein kinase Cζ mediated Raf-1/extracellular-regulated kinase activation by daunorubicin. *Blood*. 101 (4), 1543–1550.

Maton A (1993) *Human Biology and Health*. Pearson Prentice Hall

McKimmie CS and Fazakerley JK (2005) In response to pathogens, glial cells dynamically and differentially regulate Toll-like receptor gene expression. *Journal of Neuroimmunology*. 169 (1-2), 116–125.

McLarnon JG, Sawyer D and Kim SU (1995) Cation and anion unitary ion channel currents in cultured bovine microglia. *Brain Research*. 693 (1-2), 8–20.

McLarnon JG, Xu R, Lee YB and Kim SU (1997) Ion channels of human microglia in culture. *Neuroscience*. 78 (4), 1217–1228.

McLarnon JG, Zhang L, Goghari V, Lee YB, Walz W, Krieger C and Kim SU (1999) Effects of ATP and elevated K^+ on K^+ currents and intracellular Ca^{2+} in human microglia. *Neuroscience*. 91 (1), 343–352.

Meda L, Cassatella MA, Szendrei GI, Otvos L, Baron P, Villalba M, Ferrari D and Rossi F (1995) Activation of microglial cells by β-amyloid protein and interferon-γ. *Nature*. 374 (6523), 647–650.

Medzhitov R and Janeway C (2000) Innate immune recognition: mechanisms and pathways. *Immunological Reviews*. 173, 89–97.

Meja KK, Seldon PM, Nasuhara Y, Ito K, Barnes PJ, Lindsay MA and Giembycz MA (2000) p38 MAP kinase and MKK-1 co-operate in the generation of GM-CSF from LPS-stimulated human monocytes by an NF-κB-independent mechanism. *British Journal of Pharmacology*. 131 (6), 1143–1153.

Meng XL, Yang JY, Chen GL, Zhang LJ, Wang LH, Li J, Wang JM and Wu CF (2008) RV09, a novel resveratrol analogue, inhibits NO and TNF-α production by LPS-activated microglia. *International Immunopharmacology*. 8 (8), 1074–1082.

Mengozzi M, Fantuzzi G, Sironi M, Bianchi M, Fratelli M, Peri G, Bernasconi S and Ghezzi P (1993) Early down-regulation of TNF production by LPS tolerance in human monocytes: comparison with IL-1β, IL-6, and IL-8. *Lymphokine and Cytokine Research*. 12 (4), 231–236.

Merkle FT, Tramontin AD, García-Verdugo JM and Alvarez-Buylla A (2004) Radial glia give rise to adult neural stem cells in the subventricular zone. *Proceedings of the National Academy of Sciences of the United States of America*. 101 (50), 17528–17532.

Middeldorp J, Boer K, Sluijs JA, De Filippis L, Encha-Razavi F, Vescovi AL, Swaab DF, Aronica E and Hol EM (2010) GFAPδ in radial glia and subventricular zone progenitors in the developing human cortex. *Development*. 137 (2), 313–321.

Mikhailov MV, Mikhailova EA and Ashcroft SJ (2001) Molecular structure of the glibenclamide binding site of the β-cell K_{ATP} channel. *FEBS Letters*. 499 (1-2), 154–160.

Mildner A, Mack M, Schmidt H, Brück W, Djukic M, Zabel MD, Hille A, Priller J and Prinz M (2009) CCR2^{+}Ly-6C^{hi} monocytes are crucial for the effector phase of autoimmunity in the central nervous system. *Brain*. 132 (Pt 9), 2487–2500.

Mildner A, Schlevogt B, Kierdorf K, Böttcher C, Erny D, Kummer MP, Quinn M, Brück W, Bechmann I, Heneka MT, Priller J and Prinz M (2011) Distinct and non-redundant roles of microglia and myeloid subsets in mouse models of Alzheimer's disease. *Journal of Neuroscience*. 31 (31), 11159–11171.

Mildner A, Schmidt H, Nitsche M, Merkler D, Hanisch UK, Mack M, Heikenwalder M, Brück W, Priller J and Prinz M (2007) Microglia in the adult brain arise from Ly-6C^{hi}CCR2^{+} monocytes only under defined host conditions. *Nature Neuroscience*. 10 (12), 1544–1553.

Milner R, Crocker SJ, Hung S, Wang X, Frausto RF and del Zoppo GJ (2007) Fibronectin- and vitronectin-induced microglial activation and matrix metalloproteinase-9 expression is mediated by integrins $\alpha_5\beta_1$ and $\alpha_v\beta_5$. *Journal of Immunology (Baltimore, Md : 1950)*. 178 (12), 8158–8167.

Minghetti L and Levi G (1995) Induction of prostanoid biosynthesis by bacterial lipopolysaccharide and isoproterenol in rat microglial cultures. *Journal of Neurochemistry*. 65 (6), 2690–2698.

Mohri I, Taniike M, Taniguchi H, Kanekiyo T, Aritake K, Inui T, Fukumoto N, Eguchi N, Kushi A, Sasai H, Kanaoka Y, Ozono K, Narumiya S, Suzuki K and Urade Y (2006) Prostaglandin D_2-mediated microglia/astrocyte interaction enhances astrogliosis and demyelination in *twitcher*. *Journal of Neuroscience*. 26 (16), 4383–4393.

Moncada S, Palmer RM and Higgs EA (1989) Biosynthesis of nitric oxide from L-arginine. A pathway for the regulation of cell function and communication. *Biochemical Pharmacology*. 38 (11), 1709–1715.

Monif M, Reid CA, Powell KL, Smart ML and Williams DA (2009) The $P2X_7$ receptor drives microglial activation and proliferation: a trophic role for $P2X_7R$ pore. *Journal of Neuroscience*. 29 (12), 3781–3791.

Morioka T, Kalehua AN and Streit WJ (1992) Progressive expression of immunomolecules on microglial cells in rat dorsal hippocampus following transient forebrain ischemia. *Acta neuropathologica*. 83 (2), 149–157.

Mrak RE and Griffin WST (2005) Glia and their cytokines in progression of neurodegeneration. *Neurobiology of Aging*. 26 (3), 349–354.

Mullen KM, Rozycka M, Rus H, Hu L, Cudrici C, Zafranskaia E, Pennington MW, Johns DC, Judge SIV and Calabresi PA (2006) Potassium channels $K_v1.3$ and

$K_v1.5$ are expressed on blood-derived dendritic cells in the central nervous system. *Annals of Neurology*. 60 (1), 118–127.

Murugan M, Sivakumar V, Lu J, Ling EA and Kaur C (2011) Expression of N-methyl D-aspartate receptor subunits in amoeboid microglia mediates production of nitric oxide via NF-κB signaling pathway and oligodendrocyte cell death in hypoxic postnatal rats. *Glia*. 59 (4), 521–539.

Newman EA (2001) Propagation of intercellular calcium waves in retinal astrocytes and Müller cells. *Journal of Neuroscience*. 21 (7), 2215–2223.

Nikodemova M and Watters JJ (2011) Outbred ICR/CD1 mice display more severe neuroinflammation mediated by microglial TLR4/CD14 activation than inbred C57Bl/6 mice. *Neuroscience*. 190, 67–74.

Nishiyama A, Yang Z and Butt A (2005) Astrocytes and NG2-glia: what's in a name? *Journal of Anatomy*. 207 (6), 687–693.

Noctor SC, Flint AC, Weissman TA, Dammerman RS and Kriegstein AR (2001) Neurons derived from radial glial cells establish radial units in neocortex. *Nature*. 409 (6821), 714–720.

Nörenberg W, Appel K, Bauer J, Gebicke-Haerter PJ and Illes P (1993) Expression of an outwardly rectifying K^+ channel in rat microglia cultivated on teflon. *Neuroscience Letters*. 160 (1), 69–72.

Nörenberg W, Gebicke-Haerter PJ and Illes P (1992) Inflammatory stimuli induce a new K^+ outward current in cultured rat microglia. *Neuroscience Letters*. 147 (2), 171–174.

Nörenberg W, Gebicke-Haerter PJ and Illes P (1994) Voltage-dependent potassium channels in activated rat microglia. *The Journal of Physiology*. 475 (1), 15–32.

Nuutinen T, Suuronen T, Kyrylenko S, Huuskonen J and Salminen A (2005) Induction of clusterin/apoJ expression by histone deacetylase inhibitors in neural cells. *Neurochemistry International*. 47 (8), 528–538.

Oh YT, Lee JY, Lee J, Lee JH, Kim J-E, Ha J and Kang I (2010) Oleamide suppresses lipopolysaccharide-induced expression of iNOS and COX-2 through inhibition of NF-κB activation in BV2 murine microglial cells. *Neuroscience Letters*. 474 (3), 148–153.

Or TCT, Yang CLH, Law AHY, Li JCB and Lau ASY (2011) Isolation and identification of anti-inflammatory constituents from *Ligusticum chuanxiong* and their underlying mechanisms of action on microglia. *Neuropharmacology*. 60 (6), 823–831.

Ortega FJ, Gimeno-Bayon J, Espinosa-Parrilla JF, Carrasco JL, Batlle M, Pugliese M, Mahy N and Rodríguez MJ (2012) ATP-dependent potassium channel blockade strengthens microglial neuroprotection after hypoxia-ischemia in rats. *Experimental Neurology*. 235 (1), 282-296.

Paintlia MK, Paintlia AS, Khan M, Singh I and Singh AK (2008) Modulation of peroxisome proliferator-activated receptor-α activity by N-acetyl cysteine attenuates inhibition of oligodendrocyte development in lipopolysaccharide stimulated mixed glial cultures. *Journal of Neurochemistry*. 105 (3), 956–970.

Pannasch U, Färber K, Nolte C, Blonski M, Yan Chiu S, Messing A and Kettenmann H (2006) The potassium channels $K_v1.5$ and $K_v1.3$ modulate distinct functions of microglia. *Molecular and Cellular Neurosciences*. 33 (4), 401–411.

Pappas CA and Ransom BR (1994) Depolarization-induced alkalinization (DIA) in rat hippocampal astrocytes. *Journal of Neurophysiology*. 72 (6), 2816–2826.

Parri R and Crunelli V (2003) An astrocyte bridge from synapse to blood flow. *Nature Neuroscience*. 6 (1), 5–6.

Patel AJ, Maingret F, Magnone V, Fosset M, Lazdunski M and Honoré E (2000) TWIK-2, an inactivating 2P domain K^+ channel. *The Journal of Biological Chemistry*. 275 (37), 28722–28730.

Pelvig DP, Pakkenberg H, Stark AK and Pakkenberg B (2008) Neocortical glial cell numbers in human brains. *Neurobiology of Aging*. 29 (11), 1754–1762.

Penfield W (1965) *Cytology and Cellular Pathology of the Nervous System* (1932nd edition). Hafner Publishing Co Ltd

Petanceska S, Canoll P and Devi LA (1996) Expression of rat cathepsin S in phagocytic cells. *The Journal of Biological Chemistry*. 271 (8), 4403–4409.

Pfrieger FW and Barres BA (1995) What the fly's glia tell the fly's brain. *Cell*. 83 (5), 671–674.

Poltorak A, He X, Smirnova I, Liu MY, Van Huffel C, Du X, Birdwell D, Alejos E, Silva M, Galanos C, Freudenberg M, Ricciardi-Castagnoli P, Layton B and Beutler B (1998) Defective LPS signaling in C3H/HeJ and C57BL/10ScCr mice: mutations in *Tlr4* gene. *Science (New York, NY)*. 282 (5396), 2085–2088.

Preisig-Müller R, Schlichthörl G, Goerge T, Heinen S, Brüggemann A, Rajan S, Derst C, Veh RW and Daut J (2002) Heteromerization of $K_{ir}2.x$ potassium channels contributes to the phenotype of Andersen's syndrome. *Proceedings of the National Academy of Sciences of the United States of America*. 99 (11), 7774–7779.

Priller J, Flügel A, Wehner T, Boentert M, Haas CA, Prinz M, Fernández-Klett F, Prass K, Bechmann I, de Boer BA, Frotscher M, Kreutzberg GW, Persons DA and Dirnagl U (2001) Targeting gene-modified hematopoietic cells to the central nervous system: use of green fluorescent protein uncovers microglial engraftment. *Nature Medicine*. 7 (12), 1356–1361.

Prinz M and Hanisch UK (1999) Murine microglial cells produce and respond to interleukin-18. *Journal of Neurochemistry*. 72 (5), 2215–2218.

Prpic V, Weiel JE, Somers SD, DiGuiseppi J, Gonias SL, Pizzo SV, Hamilton TA, Herman B and Adams DO (1987) Effects of bacterial lipopolysaccharide on the hydrolysis of phosphatidylinositol-4,5-bisphosphate in murine peritoneal macrophages. *Journal of Immunology (Baltimore, Md : 1950)*. 139 (2), 526–533.

Pyo H, Chung S, Jou I, Gwag B and Joe EH (1997) Expression and function of outward K^+ channels induced by lipopolysaccharide in microglia. *Molecules and Cells*. 7 (5), 610–614.

Qin L, Li G, Qian X, Liu Y, Wu X, Liu B, Hong JS and Block ML (2005) Interactive role of the toll-like receptor 4 and reactive oxygen species in LPS-induced microglia activation. *Glia*. 52 (1), 78–84.

Qin L, Liu Y, Wang T, Wei SJ, Block ML, Wilson B, Liu B and Hong JS (2004) NADPH oxidase mediates lipopolysaccharide-induced neurotoxicity and proinflammatory gene expression in activated microglia. *The Journal of Biological Chemistry*. 279 (2), 1415–1421.

Quinn MT and Gauss KA (2004) Structure and regulation of the neutrophil respiratory burst oxidase: comparison with nonphagocyte oxidases. *Journal of Leukocyte Biology*. 76 (4), 760–781.

Qureshi ST, Larivière L, Leveque G, Clermont S, Moore KJ, Gros P and Malo D (1999) Endotoxin-tolerant mice have mutations in Toll-like receptor 4 (*Tlr4*). *The Journal of Experimental Medicine*. 189 (4), 615–625.

Rada B and Leto TL (2008) Oxidative innate immune defenses by Nox/Duox family NADPH oxidases. *Contributions to Microbiology*. 15, 164–187.

Raffaelli G, Saviane C, Mohajerani MH, Pedarzani P and Cherubini E (2004) BK potassium channels control transmitter release at CA3-CA3 synapses in the rat hippocampus. *The Journal of Physiology*. 557 (Pt 1), 147–157.

Ransohoff RM (2007) Microgliosis: the questions shape the answers. *Nature Neuroscience*. 10 (12), 1507–1509.

Reeds PJ (2000) Dispensable and indispensable amino acids for humans. *The Journal of Nutrition*. 130 (7), 1835S–40S.

Regenhard P, Goethe R and Phi-van L (2001) Involvement of PKA, PKC, and Ca^{2+} in LPS-activated expression of the chicken lysozyme gene. *Journal of Leukocyte Biology*. 69 (4), 651–658.

Rezaie P and Male D (2002) Mesoglia & microglia-a historical review of the concept of mononuclear phagocytes within the central nervous system. *Journal of the History of the Neurosciences*. 11 (4), 325–374.

Rieske E, Graeber MB, Tetzlaff W, Czlonkowska A, Streit WJ and Kreutzberg GW (1989) Microglia and microglia-derived brain macrophages in culture: generation from axotomized rat facial nuclei, identification and characterization *in vitro*. *Brain Research*. 492 (1-2), 1–14.

Rietschel ET, Kirikae T, Schade FU, Mamat U, Schmidt G, Loppnow H, Ulmer AJ, Zähringer U, Seydel U and Di Padova F (1994) Bacterial endotoxin: molecular relationships of structure to activity and function. *The FASEB Journal : Official Publication of the Federation of American Societies for Experimental Biology*. 8 (2), 217–225.

Righi M, Mori L, De Libero G, Sironi M, Biondi A, Mantovani A, Donini SD and Ricciardi-Castagnoli P (1989) Monokine production by microglial cell clones. *European Journal of Immunology*. 19 (8), 1443–1448.

Ritter MR, Banin E, Moreno SK, Aguilar E, Dorrell MI and Friedlander M (2006) Myeloid progenitors differentiate into microglia and promote vascular repair in a model of ischemic retinopathy. *Journal of Clinical Investigation*. 116 (12), 3266–3276.

Rock RB, Gekker G, Hu S, Sheng WS, Cheeran M, Lokensgard JR and Peterson PK (2004) Role of microglia in central nervous system infections. *Clinical microbiology reviews*. 17 (4), 942–64, table of contents.

Roessmann U, Velasco ME, Sindely SD and Gambetti P (1980) Glial fibrillary acidic protein (GFAP) in ependymal cells during development. An immunocytochemical study. *Brain Research*. 200 (1), 13–21.

Roy A, Jana A, Yatish K, Freidt MB, Fung YK, Martinson JA and Pahan K (2008) Reactive oxygen species up-regulate CD11b in microglia via nitric oxide: Implications for neurodegenerative diseases. *Free radical biology & medicine*. 45 (5), 686–699.

Saijo K and Glass CK (2011) Microglial cell origin and phenotypes in health and disease. *Nature Reviews Immunology*. 11 (11), 775–787.

Sakamoto M, Miyamoto K-I, Wu Z and Nakanishi H (2008) Possible involvement of cathepsin B released by microglia in methylmercury-induced cerebellar pathological changes in the adult rat. *Neuroscience Letters*. 442 (3), 292–296.

Santello M and Volterra A (2009) Synaptic modulation by astrocytes via Ca^{2+}-dependent glutamate release. *Neuroscience*. 158 (1), 253–259.

Sanz JM and Di Virgilio F (2000) Kinetics and mechanism of ATP-dependent IL-1β release from microglial cells. *Journal of Immunology (Baltimore, Md : 1950)*. 164 (9), 4893–4898.

Saucerman JJ and Bers DM (2008) Calmodulin mediates differential sensitivity of CaMKII and calcineurin to local Ca^{2+} in cardiac myocytes. *Biophysical Journal*. 95 (10), 4597–4612.

Scemes E and Giaume C (2006) Astrocyte calcium waves: what they are and what they do. *Glia*. 54 (7), 716–725.

Schilling T and Eder C (2011) Amyloid-β-induced reactive oxygen species production and priming are differentially regulated by ion channels in microglia. *Journal of Cellular Physiology*.

Schilling T and Eder C (2009) Importance of the non-selective cation channel TRPV1 for microglial reactive oxygen species generation. *Journal of Neuroimmunology*. 216 (1-2), 118–121.

Schilling T and Eder C (2007) Ion channel expression in resting and activated microglia of hippocampal slices from juvenile mice. *Brain Research*. 1186, 21–28.

Schilling T, Lehmann F, Rückert B and Eder C (2004a) Physiological mechanisms of lysophosphatidylcholine-induced de-ramification of murine microglia. *The Journal of Physiology*. 557 (Pt 1), 105–120.

Schilling T, Quandt FN, Cherny VV, Zhou W, Heinemann U, DeCoursey TE and Eder C (2000) Upregulation of $K_v1.3$ K^+ channels in microglia deactivated by TGF-β. *American journal of physiology Cell Physiology*. 279 (4), C1123–34.

Schilling T, Repp H, Richter H, Koschinski A, Heinemann U, Dreyer F and Eder C (2002) Lysophospholipids induce membrane hyperpolarization in microglia by activation of IKCa1 Ca^{2+}-dependent K^+ channels. *Neuroscience*. 109 (4), 827–835.

Schilling T, Stock C, Schwab A and Eder C (2004b) Functional importance of Ca^{2+}-activated K^+ channels for lysophosphatidic acid-induced microglial migration. *The European Journal of Neuroscience*. 19 (6), 1469–1474.

Schlichter LC, Kaushal V, Moxon-Emre I, Sivagnanam V and Vincent C (2010) The Ca^{2+} activated SK3 channel is expressed in microglia in the rat striatum and contributes to microglia-mediated neurotoxicity *in vitro*. *Journal of Neuroinflammation*. 7, 4.

Schlichter LC, Mertens T and Liu B (2011) Swelling activated Cl^- channels in microglia: Biophysics, pharmacology and role in glutamate release. *Channels (Austin, Tex)*. 5 (2), 128–137.

Schlichter LC, Sakellaropoulos G, Ballyk B, Pennefather PS and Phipps DJ (1996) Properties of K^+ and Cl^- channels and their involvement in proliferation of rat microglial cells. *Glia*. 17 (3), 225–236.

Schmidtmayer J, Jacobsen C, Miksch G and Sievers J (1994) Blood monocytes and spleen macrophages differentiate into microglia-like cells on monolayers of astrocytes: membrane currents. *Glia*. 12 (4), 259–267.

Schram G, Melnyk P, Pourrier M, Wang Z and Nattel S (2002) $K_{ir}2.4$ and $K_{ir}2.1$ K^+ channel subunits co-assemble: a potential new contributor to inward rectifier current heterogeneity. *The Journal of Physiology*. 544 (Pt 2), 337–349.

Schumann RR, Leong SR, Flaggs GW, Gray PW, Wright SD, Mathison JC, Tobias PS and Ulevitch RJ (1990) Structure and function of lipopolysaccharide binding protein. *Science (New York, NY)*. 249 (4975), 1429–1431.

Schwandner R, Dziarski R, Wesche H, Rothe M and Kirschning CJ (1999) Peptidoglycan- and lipoteichoic acid-induced cell activation is mediated by toll-like receptor 2. *The Journal of Biological Chemistry*. 274 (25), 17406–17409.

Seki A, Hagiwara N and Kasanuki H (1999) Effects of propafenone on K currents in human atrial myocytes. *British Journal of Pharmacology*. 126 (5), 1153–1162.

Semenov I, Wang B, Herlihy JT and Brenner R (2011) BK channel β1 subunits regulate airway contraction secondary to M2 muscarinic acetylcholine receptor mediated depolarization. *The Journal of Physiology*. 589 (Pt 7), 1803–1817.

Sewing S, Roeper J and Pongs O (1996) $K_v\beta1$ subunit binding specific for *shaker*-related potassium channel α subunits. *Neuron*. 16 (2), 455–463.

Shapiro LA, Korn MJ, Shan Z and Ribak CE (2005) GFAP-expressing radial glia-like cell bodies are involved in a one-to-one relationship with doublecortin-immunolabeled newborn neurons in the adult dentate gyrus. *Brain Research*. 1040 (1-2), 81–91.

Shi H, Wang H, Li D, Nattel S and Wang Z (2004) Differential alterations of receptor densities of three muscarinic acetylcholine receptor subtypes and current

densities of the corresponding K^+ channels in canine atria with atrial fibrillation induced by experimental congestive heart failure. *Cellular Physiology and Biochemistry : International Journal of Experimental Cellular Physiology, Biochemistry, and Pharmacology*. 14 (1-2), 31–40.

Shi H, Wang HZ and Wang Z (2000) Extracellular Ba^{2+} blocks the cardiac transient outward K^+ current. *American Journal of Physiology Heart and Circulatory Physiology*. 278 (1), H295–9.

Shih AY, Fernandes HB, Choi FY, Kozoriz MG, Liu Y, Li P, Cowan CM and Klegeris A (2006) Policing the police: astrocytes modulate microglial activation. *Journal of Neuroscience*. 26 (15), 3887–3888.

Shimazu R, Akashi S, Ogata H, Nagai Y, Fukudome K, Miyake K and Kimoto M (1999) MD-2, a molecule that confers lipopolysaccharide responsiveness on Toll-like receptor 4. *The Journal of Experimental Medicine*. 189 (11), 1777–1782.

Sievers J, Parwaresch R and Wottge HU (1994) Blood monocytes and spleen macrophages differentiate into microglia-like cells on monolayers of astrocytes: morphology. *Glia*. 12 (4), 245–258.

Sivagnanam V, Zhu X and Schlichter LC (2010) Dominance of *E. coli* phagocytosis over LPS in the inflammatory response of microglia. *Journal of Neuroimmunology*. 227 (1-2), 111–119.

Skalska J, Piwońska M, Wyroba E, Surmacz L, Wieczorek R, Koszela-Piotrowska I, Zielińska J, Bednarczyk P, Dołowy K, Wilczynski GM, Szewczyk A and Kunz WS (2008) A novel potassium channel in skeletal muscle mitochondria. *Biochimica et Biophysica Acta*. 1777 (7-8), 651–659.

Somodi S, Varga Z, Hajdu P, Starkus JG, Levy DI, Gáspár R and Panyi G (2004) pH-dependent modulation of $K_v1.3$ inactivation: role of His399. *American Journal of Physiology Cell Physiology*. 287 (4), C1067–76.

Sones WR, Leblanc N and Greenwood IA (2009) Inhibition of vascular calcium-gated chloride currents by blockers of $K_{Ca}1.1$, but not by modulators of $K_{Ca}2.1$ or $K_{Ca}2.3$ channels. *British Journal of Pharmacology*. 158 (2), 521–531.

Spanaus KS, Schlapbach R and Fontana A (1998) TNF-α and IFN-γ render microglia sensitive to Fas ligand-induced apoptosis by induction of Fas expression and down-regulation of Bcl-2 and Bcl-xL. *European Journal of Immunology*. 28 (12), 4398–4408.

Stefano L, Racchetti G, Bianco F, Passini N, Gupta RS, Panina Bordignon P and Meldolesi J (2009) The surface-exposed chaperone, Hsp60, is an agonist of the microglial TREM2 receptor. *Journal of Neurochemistry*. 110 (1), 284–294.

Stock C, Schilling T, Schwab A and Eder C (2006) Lysophosphatidylcholine stimulates IL-1β release from microglia via a $P2X_7$ receptor-independent mechanism. *Journal of Immunology (Baltimore, Md : 1950)*. 177 (12), 8560–8568.

Streit WJ and Kreutzberg GW (1988) Response of endogenous glial cells to motor neuron degeneration induced by toxic ricin. *The Journal of Comparative Neurology*. 268 (2), 248–263.

Streit WJ, Walter SA and Pennell NA (1999) Reactive microgliosis. *Progress in Neurobiology*. 57 (6), 563–581.

Strøbaek D, Teuber L, Jørgensen TD, Ahring PK, Kjaer K, Hansen RS, Olesen SP, Christophersen P and Skaaning-Jensen B (2004) Activation of human IK and SK Ca^{2+}-activated K^+ channels by NS309 (6,7-dichloro-1H-indole-2,3-dione 3-oxime). *Biochimica et Biophysica Acta*. 1665 (1-2), 1–5.

Suuronen T, Huuskonen J, Nuutinen T and Salminen A (2006) Characterization of the pro-inflammatory signaling induced by protein acetylation in microglia. *Neurochemistry International*. 49 (6), 610–618.

Suuronen T, Huuskonen J, Pihlaja R, Kyrylenko S and Salminen A (2003) Regulation of microglial inflammatory response by histone deacetylase inhibitors. *Journal of Neurochemistry*. 87 (2), 407–416.

Suuronen T, Nuutinen T, Huuskonen J, Ojala J, Thornell A and Salminen A (2005) Anti-inflammatory effect of selective estrogen receptor modulators (SERMs) in microglial cells. *Inflammation Research : Official Journal of the European Histamine Research Society*. 54 (5), 194–203.

Suzuki J, Bayna E, Li HL, Molle ED and Lew WYW (2007) Lipopolysaccharide activates calcineurin in ventricular myocytes. *Journal of the American College of Cardiology*. 49 (4), 491–499.

Suzumura A, Sawada M and Takayanagi T (1998) Production of interleukin-12 and expression of its receptors by murine microglia. *Brain Research*. 787 (1), 139–142.

Tamemoto H, Kadowaki T, Tobe K, Ueki K, Izumi T, Chatani Y, Kohno M, Kasuga M, Yazaki Y and Akanuma Y (1992) Biphasic activation of two mitogen-activated protein kinases during the cell cycle in mammalian cells. *The Journal of Biological Chemistry*. 267 (28), 20293–20297.

Tan JH, Abed Al A and Brock JA (2007) Inhibition of K_{ATP} channels in the rat tail artery by neurally released noradrenaline acting on postjunctional α2-adrenoceptors. *The Journal of Physiology*. 581 (Pt 2), 757–765.

Tan W, Haydon PG and Yeung ES (1997) Imaging neurotransmitter uptake and depletion in astrocytes. *Applied Spectroscopy*. 51 (8), 1139–1143.

Tanaka R, Komine-Kobayashi M, Mochizuki H, Yamada M, Furuya T, Migita M, Shimada T, Mizuno Y and Urabe T (2003) Migration of enhanced green fluorescent protein expressing bone marrow-derived microglia/macrophage into the mouse brain following permanent focal ischemia. *Neuroscience*. 117 (3), 531–539.

Taylor DL, Jones F, Kubota ESFCS and Pocock JM (2005) Stimulation of microglial metabotropic glutamate receptor mGlu2 triggers tumor necrosis factor α-induced neurotoxicity in concert with microglial-derived Fas ligand. *Journal of Neuroscience*. 25 (11), 2952–2964.

Terrazzino S, Bauleo A, Baldan A and Leon A (2002) Peripheral LPS administrations up-regulate Fas and FasL on brain microglial cells: a brain protective or pathogenic event? *Journal of Neuroimmunology*. 124 (1-2), 45–53.

Thiel VE and Audus KL (2001) Nitric oxide and blood-brain barrier integrity. *Antioxidants & Redox Signaling*. 3 (2), 273–278.

Thompson J and Begenisich T (2009) Mechanistic details of BK channel inhibition by the intermediate conductance, Ca^{2+}-activated K channel. *Channels (Austin, Tex)*. 3 (3), 194–204.

Tobias PS, Soldau K and Ulevitch RJ (1989) Identification of a lipid A binding site in the acute phase reactant lipopolysaccharide binding protein. *The Journal of Biological Chemistry*. 264 (18), 10867–10871.

Toyama K, Wulff H, Chandy KG, Azam P, Raman G, Saito T, Fujiwara Y, Mattson DL, Das S, Melvin JE, Pratt PF, Hatoum OA, Gutterman DD, Harder DR and Miura H (2008) The intermediate-conductance calcium-activated potassium channel $K_{Ca}3.1$ contributes to atherogenesis in mice and humans. *Journal of Clinical Investigation*. 118 (9), 3025–3037.

Troelstra A, de Graaf-Miltenburg LA, van Bommel T, Verhoef J, Van Kessel KP and Van Strijp JA (1999) Lipopolysaccharide-coated erythrocytes activate human neutrophils via CD14 while subsequent binding is through CD11b/CD18. *Journal of Immunology (Baltimore, Md : 1950)*. 162 (7), 4220–4225.

Tseng CY, Ling EA and Wong WC (1983) Light and electron microscopic and cytochemical identification of amoeboid microglial cells in the brain of prenatal rats. *Journal of Anatomy*. 136 (Pt 4), 837–849.

Tsujimoto H, Gotoh N and Nishino T (1999) Diffusion of macrolide antibiotics through the outer membrane of *Moraxella catarrhalis*. *Journal of Infection and Chemotherapy : Official Journal of the Japan Society of Chemotherapy*. 5 (4), 196–200.

Ullian EM, Sapperstein SK, Christopherson KS and Barres BA (2001) Control of synapse number by glia. *Science (New York, NY)*. 291 (5504), 657–661.

Visentin S and Levi G (1997) Protein kinase C involvement in the resting and interferon-γ-induced K^+ channel profile of microglial cells. *Journal of Neuroscience Research*. 47 (3), 233–241.

Visentin S, Agresti C, Patrizio M and Levi G (1995) Ion channels in rat microglia and their different sensitivity to lipopolysaccharide and interferon-γ. *Journal of Neuroscience Research*. 42 (4), 439–451.

Visentin S, Nuccio CD and Bellenchi GC (2006) Different patterns of Ca^{2+} signals are induced by low compared to high concentrations of P2Y agonists in microglia. *Purinergic Signalling*. 2 (4), 605–617.

Visentin S, Renzi M and Levi G (2001) Altered outward-rectifying K^+ current reveals microglial activation induced by HIV-1 Tat protein. *Glia*. 33 (3), 181–190.

Vitry S, Bertrand JY, Cumano A and Dubois-Dalcq M (2003) Primordial hematopoietic stem cells generate microglia but not myelin-forming cells in a neural environment. *Journal of Neuroscience*. 23 (33), 10724–10731.

Volterra A and Meldolesi J (2005) Astrocytes, from brain glue to communication elements: the revolution continues. *Nature reviews Neuroscience*. 6 (8), 626–640.

Wang H, Kunkel DD, Schwartzkroin PA and Tempel BL (1994) Localization of $K_v1.1$ and $K_v1.2$, two K channel proteins, to synaptic terminals, somata, and dendrites in the mouse brain. *The Journal of Neuroscience : the Official Journal of the Society for Neuroscience*. 14 (8), 4588–4599.

Wang T, Qin L, Liu B, Liu Y, Wilson B, Eling TE, Langenbach R, Taniura S and Hong JS (2004) Role of reactive oxygen species in LPS-induced production of prostaglandin E_2 in microglia. *Journal of Neurochemistry*. 88 (4), 939–947.

Wang X, Li C, Chen Y, Hao Y, Zhou W, Chen C and Yu Z (2008) Hypoxia enhances CXCR4 expression favoring microglia migration via HIF-1α activation. *Biochemical and Biophysical Research Communications*. 371 (2), 283–288.

Wang Y, Lawson MA, Kelley KW and Dantzer R (2010) Primary murine microglia are resistant to nitric oxide inhibition of indoleamine 2,3-dioxygenase. *Brain, Behavior, and Immunity*. 24 (8), 1249–1253.

Wei AD, Gutman GA, Aldrich R, Chandy KG, Grissmer S and Wulff H (2005) International Union of Pharmacology. LII. Nomenclature and molecular relationships of calcium-activated potassium channels. *Pharmacological Reviews*. 57 (4), 463–472.

Wen J, Ribeiro R and Zhang Y (2011) Specific PKC isoforms regulate LPS-stimulated iNOS induction in murine microglial cells. *Journal of Neuroinflammation*. 8, 38.

Wheeler MD and Thurman RG (1999) Production of superoxide and TNF-α from alveolar macrophages is blunted by glycine. *The American Journal of Physiology*. 277 (5 Pt 1), L952–9.

White CA, McCombe PA and Pender MP (1998) Microglia are more susceptible than macrophages to apoptosis in the central nervous system in experimental autoimmune encephalomyelitis through a mechanism not involving Fas (CD95). *International Immunology*. 10 (7), 935–941.

Widmer HA, Rowe ICM and Shipston MJ (2003) Conditional protein phosphorylation regulates BK channel activity in rat cerebellar Purkinje neurons. *The Journal of Physiology*. 552 (Pt 2), 379–391.

Wong D, Dorovini-Zis K and Vincent SR (2004) Cytokines, nitric oxide, and cGMP modulate the permeability of an *in vitro* model of the human blood-brain barrier. *Experimental Neurology*. 190 (2), 446–455.

Wright SD, Ramos RA, Tobias PS, Ulevitch RJ and Mathison JC (1990) CD14, a receptor for complexes of lipopolysaccharide (LPS) and LPS binding protein. *Science (New York, NY)*. 249 (4975), 1431–1433.

Wu CY, Kaur C, Sivakumar V, Lu J and Ling EA (2009) $K_v1.1$ expression in microglia regulates production and release of proinflammatory cytokines, endothelins and nitric oxide. *Neuroscience*. 158 (4), 1500–1508.

Wu CF, Bi XL, Yang JY, Zhan JY, Dong YX, Wang JH, Wang JM, Zhang R and Li X (2007) Differential effects of ginsenosides on NO and TNF-α production by LPS-activated N9 microglia. *International Immunopharmacology*. 7 (3), 313–320.

Wulff H and Zhorov BS (2008) K^+ channel modulators for the treatment of neurological disorders and autoimmune diseases. *Chemical Reviews*. 108 (5), 1744–1773.

Xiang Z and Burnstock G (2005) Expression of P2X receptors on rat microglial cells during early development. *Glia*. 52 (2), 119–126.

Xiang Z, Chen M, Ping J, Dunn P, Lv J, Jiao B and Burnstock G (2006) Microglial morphology and its transformation after challenge by extracellular ATP *in vitro*. *Journal of Neuroscience Research*. 83 (1), 91–101.

Yaghi A, Mehta S and McCormack DG (2002) Delayed rectifier potassium channels contribute to the depressed pulmonary artery contractility in pneumonia. *Journal of Applied Physiology (Bethesda, Md. : 1985)*. 93 (3), 957–965.

Yamamoto M, Yamazaki S, Uematsu S, Sato S, Hemmi H, Hoshino K, Kaisho T, Kuwata H, Takeuchi O, Takeshige K, Saitoh T, Yamaoka S, Yamamoto N, Yamamoto S, Muta T, Takeda K and Akira S (2004) Regulation of Toll/IL-1-receptor-mediated gene expression by the inducible nuclear protein IκBζ. *Nature*. 430 (6996), 218–222.

Yamashita T and Isa T (2003a) Ca^{2+}-dependent inward current induced by nicotinic receptor activation depends on Ca^{2+}/calmodulin-CaMKII pathway in dopamine neurons. *Neuroscience Research*. 47 (2), 225–232.

Yamashita T and Isa T (2003b) Fulfenamic acid sensitive, Ca^{2+}-dependent inward current induced by nicotinic acetylcholine receptors in dopamine neurons. *Neuroscience Research*. 46 (4), 463–473.

Yang Q, Chen SR, Li DP and Pan HL (2007) $K_v1.1/1.2$ channels are downstream effectors of nitric oxide on synaptic GABA release to preautonomic neurons in the paraventricular nucleus. *Neuroscience*. 149 (2), 315–327.

Yoshimura A, Lien E, Ingalls RR, Tuomanen E, Dziarski R and Golenbock D (1999) Cutting edge: recognition of Gram-positive bacterial cell wall components by the innate immune system occurs via Toll-like receptor 2. *Journal of Immunology (Baltimore, Md : 1950)*. 163 (1), 1–5.

Young CC, Stegen M, Bernard R, Müller M, Bischofberger J, Veh RW, Haas CA and Wolfart J (2009) Upregulation of inward rectifier K^+ ($K_{ir}2$) channels in dentate gyrus granule cells in temporal lobe epilepsy. *The Journal of Physiology*. 587 (Pt 17), 4213–4233.

Zahn von J, Möller T, Kettenmann H and Nolte C (1997) Microglial phagocytosis is modulated by pro- and anti-inflammatory cytokines. *Neuroreport*. 8 (18), 3851–3856.

Zech NH (2004) Adult stem cell manipulation and possible clinical perspectives. *J Reproduktionsmed Endokrinol*. 1 (2), 91–99.

Zhang F, Liu J and Shi JS (2010) Anti-inflammatory activities of resveratrol in the brain: role of resveratrol in microglial activation. *European Journal of Pharmacology*. 636 (1-3), 1–7.

Zhang Jian, Fujii S, Wu Z, Hashioka S, Tanaka Y, Shiratsuchi A, Nakanishi Y and Nakanishi H (2006) Involvement of COX-1 and up-regulated prostaglandin E synthases in phosphatidylserine liposome-induced prostaglandin E_2 production by microglia. *Journal of Neuroimmunology*. 172 (1-2), 112–120.

Zhang Jianmin, Geula C, Lu C, Koziel H, Hatcher LM and Roisen FJ (2003) Neurotrophins regulate proliferation and survival of two microglial cell lines *in vitro*. *Experimental Neurology*. 183 (2), 469–481.

Zhao S, Zhang L, Lian G, Wang X, Zhang H, Yao X, Yang J and Wu C (2011) Sildenafil attenuates LPS-induced pro-inflammatory responses through down-regulation of intracellular ROS-related MAPK/NF-κB signaling pathways in N9 microglia. *International Immunopharmacology*. 11 (4), 468–474.

Zhou W, Cayabyab FS, Pennefather PS, Schlichter LC and DeCoursey TE (1998) HERG-like K^+ channels in microglia. *The Journal of General Physiology*. 111 (6), 781–794.

Zhou Y, Zeng XH and Lingle CJ (2012) Barium ions selectively activate BK channels via the Ca^{2+}-bowl site. *Proceedings of the National Academy of Sciences of the United States of America*. 109 (28), 11413–11418.

Zhu Y and Huizinga JD (2008) Nitric oxide decreases the excitability of interstitial cells of Cajal through activation of the BK channel. *Journal of Cellular and Molecular Medicine*. 12 (5A), 1718–1727.

Zou A, Lin Z, Humble M, Creech CD, Wagoner PK, Krafte D, Jegla TJ and Wickenden AD (2003) Distribution and functional properties of human KCNH8 (Elk1) potassium channels. *American Journal of Physiology Cell Physiology*. 285 (6), C1356–66.

Appendices

Appendices

The work of this thesis has been presented as a poster (ID: PC81) in Physiology 2012 with the title:

Potassium channel expression and function in the N9 murine microglial cell line

Geng Pan and Michael J. Shipston